

Synthesis of Tailored Polymer Structures by the Combination of Cationic and Anionic Polymerizations

Dissertation

zur Erlangung des Grades
"Doktor der Naturwissenschaften"

am Fachbereich Chemie und Pharmazie
der Johannes Gutenberg-Universität
in Mainz

Vorgelegt von

Jesper Feldthusen Jensen

geboren in Torsted, Dänemark

Mainz 1998

Summary

A new method for the synthesis of tailored polyisobutylene-based (PIB-based) block copolymers by the combination of controlled/living cationic and controlled/living anionic polymerizations has been developed. In addition, parallel to this subject new synthetic routes for preparation of telechelic PIBs and amphiphilic networks have been investigated.

The PIB precursors used for subsequent controlled/living anionic polymerization of various methacrylates and ethylene oxide were prepared by controlled/living cationic polymerization of isobutylene followed by quenching with 1,1-diphenylethylene (DPE) under selected conditions. Depending on the quenching procedure two different endgroups, either a diphenylmethoxy- or a diphenylvinyl endgroup were obtained.

Since the diphenylmethoxy endgroup can be obtained in quantitative yield by quenching with methanol under carefully selected conditions, quenching experiments involving the diphenyl-cation with different alcohols were performed, e.g. with 2-hydroxyethyl methacrylate (HEMA) leading to *in situ* formation of a macromonomer. However, since the competing reaction between the Lewis acid (TiCl_4) and the alcohol is more pronounced in case of these alcohols only partial functionality was reached (with HEMA \approx 65 % was detected). The side product is the diphenylvinyl endgroup formed as consequence of the reduced Lewis acidity ($\text{TiCl}_4 + x\text{ROH} \rightarrow \text{Ti}(\text{OR})_x\text{Cl}_{4-x}$). Further experiments with these alcohols using different Lewis acids might lead to improvements.

Preliminary model studies involving the transformation from cationic to anionic polymerization with low molecular weight compounds having the same active sites as the corresponding PIB precursors were performed. The compounds used in these experiments were; diphenylmethane (DPM), triphenylmethane (TPM), 3,3,5,5-tetramethyl-1,1-diphenylhex-1-ene (TMP-DPV), and 1-methoxy-3,3,5,5-tetramethyl-1,1-diphenyl (TMP-DPOMe).

With the first two compounds (DPM and TPM) $<$ 85 % conversion was reached under different conditions. Lithiation of TMP-DPV was performed with *n/s*-BuLi. However, in contrast to DPE, the addition of BuLi is not quantitative due to sterical hindrance. Direct metalation of TMP-DPV with K/Na alloy or Cs led to quantitative conversion within 15 min verified by ^1H NMR and UV spectroscopy. Interestingly, coupling was not detected which is the case in a similar reaction with DPE. Under the same conditions metalation of TMP-DPOMe was completed also in 15-20 min. In both experiments the same product was formed after quenching with methanol, 3,3,5,5-tetramethylhexane. By addition of LiCl, the corresponding lithium initiator was achieved. That means that by this procedure (macro)initiators with various counterions; K^+ , Cs^+ , and Li^+ are available in quantitative yield in less than 20 min (metalation with Na-mirror is rather slow). Anionic polymerizations of methacrylates with the synthesized initiator, 3,3,5,5-tetra-methylhexyllithium from TMP-DPV and/or TMP-DPOMe indicate quantitative initiating efficiency.

In order to analyze effects of potential Cl^\dagger -terminated PIB (due to incomplete DPE-capping) metalation experiments were carried out with a sample containing 85 % DPV and 15 % Cl^\dagger endgroups and one with 100 % Cl^\dagger -terminated PIB. With the former sample coupling was observed due to nucleophilic substitution of the Cl^\dagger endgroup with PIB-DPE $^-$. Experiments with the 100 % Cl^\dagger -

terminated PIB led to interesting observations. Metalation with K/Na alloy in *n*-hexane containing N,N,N,N-tetramethylethyldiamine resulted in quantitative formation of isopropenyl capped PIB faster and more selectively than existing methods (instead of the expected generation of a PIB macrocarbanion which is partially formed in pure *n*-hexane together with the isopropenyl endgroup).

Metalation of the resulting DPE-capped PIB precursor with K/Na alloy or Cs led also to quantitative formation of a PIB macrocarbanion within less than 60 min independent of the molecular weight. The independence of the metalation and anionic polymerization on the ratio of the diphenylvinyl and diphenylmethoxy endgroups is an important finding. This means that it is not necessary to consider the chain end composition of the DPE-capped PIB in the course of its preparation by controlled/living cationic polymerization.

Well-defined OH-terminated PIBs with quantitative functionality were synthesized by adding ethylene oxide to the lithium salt of the PIB macroinitiator. Using the corresponding potassium or cesium salt of the PIB macroinitiator tailored amphiphilic i.e. water soluble PIB-*b*-PEO block copolymers were prepared.

Different tailored PIB-based AB, ABA, and (AB)₃ block copolymers of various methacrylates were synthesized in order to obtain materials which can subsequently be characterized. Near to quantitative blocking efficiencies were normally reached proved by SEC analysis (and ¹H NMR).

Thermoplastic elastomers (TPEs) based on linear poly(methyl methacrylate)-*b*-polyisobutylene-*b*-poly(methyl methacrylate) PMMA-*b*-PIB-*b*-PMMA and star-shaped (PIB-*b*-PMMA)₃ block copolymers with tensile strength exceeding 20 MPa have been prepared. The synthesized samples have similar properties compared to corresponding polystyrene-based block copolymers (PSt-*b*-PIB-*b*-PSt). In addition, the morphology was examined by small angle X-ray scattering. Lamellar and cylindrical morphologies were observed.

Amphiphilic polyisobutylene-*b*-poly(methacrylic acid) (PIB-*b*-PMAA) block copolymers have been synthesized and characterized. The characterization of these block copolymers in aqueous media with dynamic and static light scattering, fluorescence correlation spectroscopy, ultracentrifugation, and transmission electron microscopy verified the formation of well-defined micelles with an aggregation number and a hydrodynamic radius which depend primarily on the chain length of the PIB block segment. Compared to other polymer systems, an extremely low CMC was detected for all the PIB-*b*-PMAA samples, about 2-3 orders of magnitude lower than comparable PMMA-*b*-PMAA block copolymers.

Preliminary studies regarding synthesis of amphiphilic networks (APNs) based on block copolymer units have been carried out using different methods: A series of APNs were prepared by adding ethylene glycol dimethacrylate to living block copolymer units. A second curing process involving crosslinking reactions between alcohol groups at the polymer chain ends and isocyanates or acid chlorides was examined, too. Optimization of the curing procedures and systematic characterization of the resulting APNs have to be performed in a future work.

Table of contents

Summary

List of abbreviations and symbols	1
1 Introduction.....	3
1.1 Properties and applications of polyisobutylene, poly(meth)acrylates, block copolymers, and amphiphilic networks	3
1.2 Polymerization methods leading to tailored polymer structures.....	5
1.2.1 Cationic polymerization.....	5
1.2.2 Anionic polymerization.....	12
1.2.3 Alternative polymerization procedures	16
1.2.4 Combination of different polymerization procedures	18
1.3 Tailored polymers	21
1.3.1 (End)-functionalized polymers	21
1.3.2 Polymer structures (topologies and compositions).....	23
2 Motivation	31
3 Strategy	33
4 Experimental.....	35
4.1 Materials.....	35
4.1.1 Cationic polymerization.....	35
4.1.2 Anionic polymerization.....	35
4.1.3 Network synthesis.....	37
4.2 Cationic polymerization.....	37
4.2.1 Synthesis of TMP-DPOMe and TMP-DPV.....	37
4.2.2 Cationic polymerization of isobutylene	37
4.2.3 Synthesis of DPE-capped PIB.....	39
4.2.4 Quenching of living DPE-capped PIB with different alcohols.....	40
4.2.5 Synthesis of OH-functionalized PIB using the isopropenyl-ended PIB.....	40
4.2.6 Synthesis of OH functionalized PIB using ethylene oxide.....	41
4.2.7 Polymerization of vinyl ethers and attempted functionalization.....	41
4.3 Lithiation/metalation experiments with TMP-DPV, DPM, and with Cl ^t -capped PIB	41
4.3.1 Lithiation of TMP-DPV and DPM	41
4.3.2 Metalation of Cl ^t -capped PIB.....	41
4.4 Metalation of TMP-DPV, TMP-DPOMe, and the corresponding PIB precursors.....	41
4.5 Anionic polymerization.....	42
4.5.1 Synthesis of PIB- <i>b</i> -PtBMA and PIB- <i>b</i> -PMAA block copolymers.....	42
4.5.2 Synthesis of PMMA- <i>b</i> -PIB- <i>b</i> -PMMA and PIB- <i>b</i> -(PMMA) ₃ block copolymers	43
4.5.3 Synthesis of homopolymers of <i>N,N</i> -dimethylacrylamide	43
4.5.4 Synthesis of homo- and block copolymers of ethylene oxide.....	43
4.5.5 Hydrolysis experiments with tBMA, TBDMHEMA, TMSHEMA, and DMAA	44
4.5.6 Synthesis of ABC type block copolymers of IB, tBMA/DMAA/TBDMHEMA, and TMSHEMA.....	44
4.6 Synthesis of amphiphilic networks.....	44
4.6.1 Method 1	44

4.6.2 Method 2	45
4.7 Characterization methods.....	46
4.7.1 Size exclusion chromatography (SEC)	46
4.7.2 High Performance Liquid Chromatography (HPLC) under critical conditions.....	46
4.7.3 NMR spectroscopy.....	47
4.7.4 UV spectroscopy	47
4.7.5 Light scattering (dynamic and static)	47
4.7.6 Fluorescence correlation spectroscopy	47
4.7.7 Transmission electron microscopy.....	48
4.7.8 Analytical ultracentrifugation.....	49
4.7.9 Dynamic-mechanical analysis, stress-strain measurements, and small angle X-ray scattering measurements	49
4.7.10 Differential scanning calorimetry measurements	49
5 Results and discussion.....	50
5.1 Cationic polymerization of isobutylene.....	50
5.2 End-functionalized PIBs	53
5.2.1 Vinyl, hydroxy, and tolyl functionalized polyisobutylenes	54
5.2.2 Functionalization of living polyisobutylene with 1,1-diphenylethylene	55
5.2.3 Quenching of the living PIB-DPE ^A with different alcohols.....	60
5.3 Cationic polymerization of vinyl ethers and attempted functionalization with DPE.....	64
5.4 Cross-over from cationic to anionic polymerization.....	65
5.4.1 Screening experiments with different potential initiators for anionic polymerization	65
5.4.2 Metalation of 1-methoxy-3,3,5,5-tetramethyl-1,1-diphenylhexane (TMP-DPOMe) and 3,3,5,5- tetramethyl- 1,1-di-phenylhex-1-ene (TMP-DPV).....	69
5.4.3 Metalation of DPE-ended PIB precursors	75
5.5 Anionic polymerization experiments.....	78
5.5.1 Experiments with ethylene oxide.....	79
5.5.2 Polymerization of N,N-dimethylacrylamide	83
5.5.3 Synthesis of tailored poly(methacrylates).....	84
5.5.4 Synthesis of OH-terminated polymers.....	89
5.6 Linear ABA and star-shaped (AB) ₃ block copolymers (thermoplastic elastomers).....	91
5.6.1 Synthesis and SEC measurements.....	91
5.6.2 Characterization of thermoplastic elastomers.....	97
5.7 Amphiphilic AB block copolymers	106
5.7.1 Synthesis of PIB- <i>b</i> -PMAA and PIB- <i>b</i> -PEO block copolymers and preparation of aqueous polymer solutions	
5.7.2 Characterization of PIB- <i>b</i> -PMAA block copolymers.....	108
5.8 Synthesis and characterization of star polymers and amphiphilic networks.....	114
5.8.1 Method 1: Living block copolymers crosslinked with ethylene glycol dimethacrylate	115
5.8.2 Method 2: Block copolymers crosslinked with polyfunctional curing agents	117
5.8.3 Method 3: End-functionalized PIB/PEO-based block copolymer crosslinked with polyfunctional curing agents.....	123
6 Appendix.....	124
6.1 Titration of BuLi	124
References.....	124

List of abbreviations and symbols

AADCl:	Adipine acid dichloride
APN:	Amphiphilic network
AUC:	Analytical Ultra Centrifugation
Bd:	Butadiene
n-BuLi:	Butyllithium
s/t-BuLi:	<i>sec/tert</i> -Butyllithium
BTCTCl:	1,3,5-Benzenetricarbonyl trichloride
Cl ^t :	<i>tert</i> -Chlorine
CMC:	Critical micelle concentration
CumCl:	(2-Chloro-2-propyl)benzene
DABCO:	1,4-Diazabicyclo[2.2.2]octane
DMA:	N,N-dimethylacetamide
DMAA:	N,N-dimethyl acrylamide
DMF:	Dimethyl formamide
DtBP:	2,6-di- <i>tert</i> -Butyl pyridine
DLS:	Dynamic Light Scattering
DPE:	1,1-Diphenylethylene
DPM:	Diphenylmethane
DSC:	Differential scanning calorimetry
DVB:	Divinyl benzene
EGDMA:	Ethylene glycol dimethacrylate
EO:	Ethylene oxide
FCS:	Fluorescence correlation spectroscopy
GC:	Gas Chromatography
GTP:	Group Transfer Polymerization
HEMA:	2-Hydroxyethyl methacrylate
HMDI:	1,6-Hexamethylene diisocyanate
HPLC:	High Performance Liquid Chromatography
IB:	Isobutylene
IBVE:	Isobutyl vinyl ether
LA ⁻ Pzn:	Controlled/living anionic polymerization
LC ⁺ Pzn:	Controlled/living cationic polymerization
LDA:	Lithium diisopropylamide
LP:	Living polymerization
MAA:	Methacrylic acid
MDI:	Diphenylmethane-4,4'-diisocyanate
MeLi:	Methyl lithium
MMA:	Methyl methacrylate
MVE:	Methyl vinyl ether
MWD:	Molecular weight distribution
NaphK:	Potassium naphthalene
PDI:	Polydispersity index (M_w/M_n)
PIB-DPOMe:	1-Methoxy-1,1-diphenyl ended PIB
PIB-DPV:	1,1-Diphenylvinyl ended PIB
pMeSt:	<i>para</i> -Methylstyrene
RI:	Refractive index

RT:	Room temperature
SAXS:	Small Angle X-ray Scattering
SBS:	Styrene-butadiene thermoplastic elastomer
SEBS:	Styrene-(ethylene-co-butylene) thermoplastic elastomer
SEC:	Size Exclusion Chromatography
SIS:	Styrene-isoprene thermoplastic elastomer
St:	Styrene
tBA:	<i>tert</i> -Butyl acrylate
TBDMHEMA:	2-[(<i>tert</i> -Butyldimethylsilyl)oxy]ethyl methacrylate
TBDM-Cl:	<i>tert</i> -Butyldimethylchlorosilane
tBMA:	<i>tert</i> -Butyl methacrylate
tBuDiCumCl:	1,3-bis(2-Chloro-2-propyl)-5- <i>tert</i> -butylbenzene
tBuDiCumOH:	1,3-bis(2-Hydroxy-2-propyl)-5- <i>tert</i> -butylbenzene
TEM:	Transmission Electron Microscopy
TMPCl:	2-Chloro-2,4,4-trimethylpentane
TMP-DPOMe:	1-Methoxy-3,3,5,5-tetramethyl-1,1-diphenylhexane
TMP-DPH:	3,3,5,5-tetramethyl-1,1-diphenylhexane
TMP-DPV:	3,3,5,5-tetramethyl-1,1-diphenylhex-1-ene
TMSHEMA:	2-[(Trimethylsilyl)oxy]ethyl methacrylate
TMS-Cl:	Trimethylchlorosilane
TPE:	ThermoPlastic Elastomer
TriCumCl:	1,3,5-tris(2-Chloro-2-propyl)benzene
D_m :	Micelle diameter ($D_m = 2R_h$)
DP_n :	Number-average degree of polymerization
δ_A :	The solubility parameter of polymer A
f:	Initiating efficiency
Φ_A :	Volume fraction of component A.
I:	Initiator
k_i :	Rate constant of propagation
k_p :	Rate constant of initiation
M:	Monomer
M_c :	Number average molecular weight between crosslinking points in a network
M_n :	Number average molecular weight
M_w :	Weight average molecular weight
n:	Number of initiating sites on an initiator or of reactive sites on a quenching agent
P_n :	Degree of polymerization
R_g :	Radius of gyration
R_h :	Hydrodynamic radius
r_1 :	Reactivity ratio
R_p :	Rate of propagation
R_i :	Rate of initiation
T_c :	Ceiling temperature
T_g :	Glass-transition temperature
T_m :	Melting temperature
Z:	Aggregation number

1 Introduction

In this chapter a critical review of topics related to the synthesis of tailored polymer structures will be made in order to summarize the major fundamental aspects of the preparation of such polymers. It will include an introduction of different controlled/living polymerization procedures, synthesis of (end)-functionalized polymers, (amphiphilic) block copolymers, and amphiphilic networks with well-defined microstructures.

1.1 Properties and applications of polyisobutylene, poly(meth)acrylates, block copolymers, and amphiphilic networks

Polyisobutylene (PIB) is a widely used polymer in different areas of the industry. Parameters like molecular weight and functional (end)groups should usually be controlled and adjusted for the required application. For instance, low molecular weight PIBs can be used as adhesives, as lubricating oil and fuel additives, or as component in polyolefin blends for improving flexibility, non-slip, and impact resistance at low temperatures, just to mention a few applications of PIBs manufactured by companies like BP and BASF. High molecular weight PIBs are mainly used in the rubber industry, e.g. butyl rubber which is obtained by copolymerizing isobutylene (IB) and a few percent isoprene. Specific products include chewing gums, sealants and a variety of medical products.

Poly(meth)acrylates which include many types of polymers are used in a large number of applications, for example, contact lenses are based on poly(2-hydroxyethyl methacrylate) (PHEMA), poly(methyl methacrylate) (PMMA) is used as construction material in automotive, lighting, advertising, and sanitary ware industries, and butyl acrylates as impact modifier. Again, parameters like T_g , molecular weight, and functionalities should be regulated in order to optimize the properties for each application.

In the following some properties/characteristics of the respective homopolymers are summarized:

Polyisobutylene

- low T_g (-55 °C)
- highly hydrophobic
- thermally, oxidatively, and hydrolytically stable
- large capacity for taking up fillers
- low permeability to gases
- high resistance to chemicals
- good electric insulation
- easily functionalized
- available only by cationic polymerization

Poly(meth)acrylates

- high/low T_g
- hydrophilic or hydrophobic
- oxidatively stable, resistant to weathering
- easily functionalized

e.g. PMMA:

- excellent transparency and brilliance
- unsurpassed resistance to weathering and aging
- high surface hardness and scratch resistance

By combining the properties of the homopolymers into block copolymers or networks, new materials with new and promising properties can be synthesized. These materials might also partially substitute already existing products.

Two classes of materials are of interest among block copolymers. Amphiphilic AB block copolymers, e.g. PIB-*b*-PMAA, can be used as potential emulsifiers, i.e. in wash powders, as additive in emulsion polymerization (in industrial scale), or as dye or pigment vehicles in printing technologies. Moreover, micelles formed by AB block copolymers are also interesting for potential medical and pharmaceutical applications, e.g. as drug carriers.¹

Thermoplastic elastomers (TPE) are the second class which include mainly linear ABA and star-shaped (AB)_n block copolymers, e.g. PMMA-*b*-PBd-*b*-PMMA. The ability of TPEs to become fluid on heating and then solidify on cooling opens the possibility for the production of rubber-like articles by using fast processing equipments (injection molding, extruder, etc.) which are also used for the plastic industry.² At the present time especially SBS and SEBS TPEs dominate the market, and at the same time they replace partially vulcanized rubbers. Due to the fact that one can vary the composition of the hard and rubbery parts, there is a versatile spectrum of application areas, e.g. footwear, wires, cables, adhesives, sealants (soft materials), brake hose, and automobile grease boots (hard materials).² Since one of the aims of this project is to produce PIB-based TPEs, a major advantage has to be pointed out: PIB is a fully saturated polymer leading to materials which will be much more stable than the corresponding polybutadiene (PBd) products. The major drawback concerning the PBd-based block copolymers is the double bonds in the chain which can undergo further reactions during storage, e.g. cleavage of C-C bond by oxidation or network formation, for example, initiated by light.

Amphiphilic networks (APNs) is a new area in polymer science starting in the early 80's.³ Therefore, one can more or less only speculate about their potential applications. One of the important properties of APNs is that they swell in all kinds of solvents. At the present time the research concentrates upon the biomedical field, e.g. drug delivery devices, membranes, implants, wound dressing, artificial organs, etc.⁴ The nature of the surface zone of the material is the most decisive factor, since it is in contact with the biological environment.⁵ In connection to this, biocompatibility of APNs is the major requirement for such applications. It has been published that the roughness or texture is a crucial property, because it is generally accepted that the smoother the surface of a polymer, the less thrombogenic it is.⁶

In order to obtain the desired materials described above, conventional polymerization procedures like free radical polymerization or polycondensation cannot be utilized, since they do not lead to tailored materials. Instead, controlled/living polymerization methods, in this case cationic and anionic polymerizations, are used. In these polymerizations the molecular weight can be regulated through the ratio of initiator to monomer and functional groups, e.g. an OH-group can be introduced by a quenching agent ⁷ or by a monomer containing a protected OH- or NH₂-group.⁸⁻¹¹

1.2 Polymerization methods leading to tailored polymer structures

The polymerization procedures discussed in this section and partially used in this work belong to the category of controlled/living polymerizations. By definition these proceed by a chain growth reaction where under ideal conditions, side reactions like chain transfer and irreversible termination can be excluded and the rate of initiation is faster than that of propagation ($R_i \cong R_p$).

If such side reactions are absent, the following parameters can be controlled:

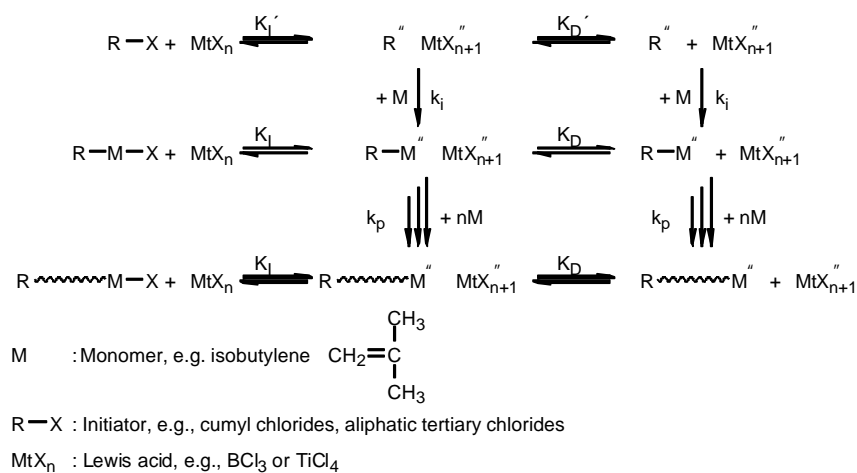
- Molecular weight/degree of polymerization, $DP_n = \Delta[M]/[I]_0 = n \cdot ([M]_0 \cdot x_p)/[I]_0$.
- Molecular weight distribution (MWD) which under ideal conditions is a Poisson distribution. By a good approximation the polydispersity index (PDI) of this distribution can be expressed as, $M_w/M_n \approx 1 + 1/DP_n$.
- Endgroups/degree of functionality.

Besides, under ideal conditions, the synthesis of block copolymers can also be carried out which is an important part of this project. By analyzing the kinetics of these polymerizations as well as the synthesized materials (for example, by SEC and 1H NMR) one can see whether the chosen conditions lead to controlled/living polymerizations. In order to achieve these conditions the influence of all components, i.e. solvent, initiator, and additives, have to be adjusted for each type of monomer.

1.2.1 Cationic polymerization

1.2.1.1 General concepts of controlled/living cationic polymerization

The polymerization of a monomer like IB can be divided into different steps, each having its own characteristic rate constant as shown in Schemes 1.1 and 1.2. As mentioned above, undesired side reactions, such as transfer and termination have to be taken into account in some systems as shown in Scheme 1.2. It is then the relative ratios between rate constants in a system that decide whether or not it is a controlled/living or conventional cationic polymerization.



Scheme 1.1: Elemental reaction steps in cationic polymerization

It is important to know how the polymerization proceeds, i.e. how the chain end incorporates the monomer during propagation if we assume ideal conditions. A living polymerization with a dynamic equilibrium between inactive (dormant) and active species seems to be the most plausible mechanism as represented in Scheme 1.1 taking the fundamental experimental/kinetic facts into consideration.¹² The existence of this equilibrium is a central topic later when influence of coinitiator and solvent is discussed. If we ignore the equilibrium between the active and inactive species, this scheme also includes the "ideal" living polymerization. It is impossible to distinguish between the two ways of living polymerizations (LPs), if the rates of exchange between active and inactive species are much higher than the rate of propagation. The rates of propagation for ideal LP and LP with reversible termination is expressed by the following equations:

$$R_p = k_{app}[M] = k_p[P^*][M],$$

$$\text{in "ideal" case } [P^*] = [I]_0$$

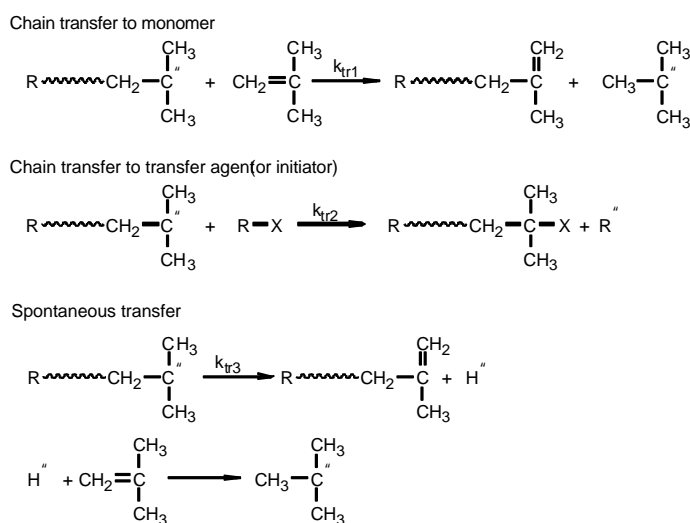
and with reversible termination:

$$P' + C \rightleftharpoons P^* \Rightarrow K_I = P^*/(P' \cdot C), \text{ taking the following assumptions into account;}$$

$$P^* \ll P', P' \approx I_0, \text{ and } C \approx C_0 \approx [MtX_n]_0 \Rightarrow K_I = P^*/(I_0 \cdot C_0),$$

$$[P^*] \approx K_I[MtX_n]_0[I]_0 \text{ (neglecting dissociation of ion pairs),}$$

where $[P^*]$ is the concentration of living chain end, $[P']$ the concentration of dormant i.e. inactive chain ends, $[I]_0$ the initial initiator concentration, $[C]_0 = [MtX_n]_0$ the initial catalyst concentration, and K_I the equilibrium constant of ionization. Since the number of polymer chains does not change during polymerization ($[P] = [I]_0$), DP_n is independent of the way it proceeds. The equilibrium between inactive and active species is usually stronger shifted toward the inactive ones ($K_I \ll 1$). This is indirectly verified by the fact that in polymerization of IB in the presence of electron donors (EDs), quenching with methanol does not give a methoxy but a chlorine endgroup.¹³



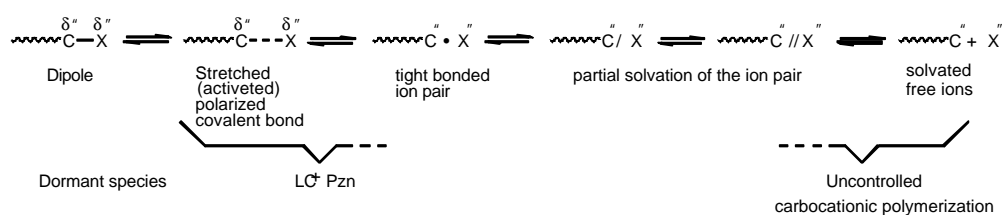
Scheme 1.2: Potential side reactions in living cationic polymerization of isobutylene.

Transfer can take place in three ways as seen in Scheme 1.2, to monomer, to transfer agent or spontaneous transfer due to the elimination of a proton at the chain end. In all cases the ionicity of the

chain end is important, and the latter two types of transfer reactions can be totally suppressed by addition of ED. Transfer to monomer is not as simple as described in Scheme 1.2. Actually one can distinguish between three different transfer reactions with regard to monomer.¹⁴ The purpose of mentioning these reactions is that experiments with IB¹⁴ have proved that temperature has a distinct influence on which kind of reaction dominates. In addition to temperature, parameters like solvent and additives also control the outcome of these reactions.

An important detail which has to be noted here is that quenching/termination of a LC⁺Pzn of IB with methanol can be interpreted as a deactivation of the Lewis acid. Mt(OR)_n is a much weaker acid than MtCl_n. Therefore, after the formation of Mt(OR)_n the degree of ionization of the chain end is very low. Quenching/termination can also be carried out in a controlled way (end-quenching, see section 1.3.1) which gives the possibility to prepare polymers with well-defined endgroups. This is a crucial point since the aim in our study is to use the tailored PIBs for subsequent anionic polymerization. One of the most important undesired reactions when aromatic initiators (or styrene as monomer) are used is the formation of indanyl skeletons.¹⁵ This reaction can be avoided by the use of sterically hindered initiators, e.g. tBuDiCumCl instead of DiCumCl. The parameters which affect this reaction have been investigated with DiCumCl¹⁵ and DiCumOH¹⁶. The results show that low temperature and low polarity of the reaction medium favors the wanted end-product (even at -70°C in pure CH₃Cl solvent as much as 32% mono-indane and 21% di-indane adducts are observed).

An important feature of LC⁺Pzn is the ionicity at the reaction center both in the ion generating and propagating step. The Winstein spectrum (Scheme 1.3) is frequently used to elucidate the different kind of propagating species which can exist in a polymerization system. One important aspect considering the equilibria is that the rates of exchange between the species have a strong effect on MWD of the end product.¹⁷



Scheme 1.3: The Winstein spectrum.

Total control is not achieved until each step is mastered. This means initiation shall only be performed by the added initiator and not by moisture or impurities like phosgene (which can be formed by oxidation of the solvent, such as methylene chloride). If more than one type of initiator is present, Poisson MWD can not be attained, instead a polymodal MWD will appear. Therefore, it is important to work under relatively pure conditions. Furthermore, initiation has to be rapid, at least comparable to propagation, if narrow MWD should be reached.^{13,18-20} The next critical event is propagation (the nature of the propagating chain end) which, considering Scheme 1.3 and the concept introduced in Scheme 1.1 can be guided into the wanted direction by additives like electron donors (ED) (see section 1.2.1.4).

1.2.1.2 Monomers

IB is the most explored monomer which is polymerized by LC^+Pzn , but of course other types of monomers can also be used. The requirement for polymerization is to develop a carbocation which can be sufficiently stabilized (resonance forms/hyperconjugation). The monomer as an element in a polymerization system can possess several functions.²¹ A slow decomposition has been detected when $[M]$ approaches zero, indicating that monomers have some kind of stabilization effect on the growing chain end due to the formation of a monomer/chain end complex. An interesting detail regarding this effect could be the results (e.g. MWD) obtained by a continuous monomer addition (all our experiments are either batch or incremental monomer addition). Some research concerning this topic has been pursued²², but the results are not really satisfactory ($PDI = 1.2-1.4$). However, such process might be important for industrial application in the future.

Two types of monomers, olefins (e.g. IB, indene and different kinds of styrene derivatives) and vinyl ethers can be polymerized by LC^+Pzn . In cationic ring-opening polymerization monomers like THF and ethylene oxide can be polymerized. Since the products prepared in this project are planned to be used in manufacture of thermoplastic ABA block copolymers, amphiphilic AB block copolymers and amphiphilic networks, the second monomer must have high T_g and/or it should be hydrophilic. Styrene has a high T_g and thermoplastic elastomers like PSt-*b*-PIB-*b*-PSt have been synthesized only using LC^+Pzn with sequential monomer addition.^{23,24} Amphiphilic block copolymers of methyl vinyl ether (MVE) (hydrophilic) and IB were also prepared²⁵. However, block copolymers with (meth)acrylates cannot be prepared by cationic polymerization alone, since the ester group of these monomers does not have the ability to stabilize a cation at the chain end. Secondly, the oxygens of the ester group will complex the Lewis acid leading to a deactivated coiniciator and thereby to termination. Particularly the limitation with regard to monomers is a central topic for this project, since block copolymers containing (meth)acrylate segments are of special interest. To overcome this problem, the block copolymers have to be prepared from PIB macroinitiators using either GTP or anionic polymerization for the second monomer (see section 1.3.1).

1.2.1.3 Initiating systems

The initiator and coiniciator are the key elements in a controlled/living cationic polymerization system. As described before, a necessary demand to a system where narrow MWD is wanted ($PDI < 1.2$) is that the rate of initiation is much higher than the rate of propagation. For that reason different types of initiating systems exist depending on the monomer used, i.e. olefins and vinyl ethers.

Figure 1.1 illustrates some of the most used initiators in living cationic polymerization of IB, but they can also be used with other vinyl monomers like styrene derivatives. In the case of the cumyl type initiators, mono-, di- and trifunctional ones are frequently used, which makes it possible to synthesize linear AB and ABA or star-shaped $(AB)_3$ block copolymers¹³ (see also chapter 5). Recently, polyfunctional cumyl type initiators, so-called calix[*n*]arenes ($n = 4-8$), have been used for

the synthesis of PIB-multiarm stars.²⁶ The advantages of star-shaped polymer structures will be discussed in section 1.3.2.

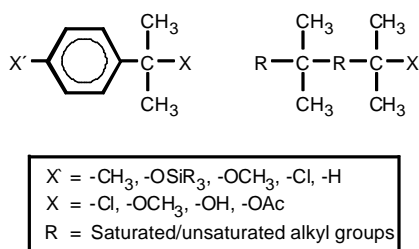


Figure 1.1: Typical initiators used in LC^+Pzn of IB.

The coinitiator which is the second part of an initiating system is a Lewis acid (Friedel-Crafts acid), such as TiCl_4 , BCl_3 , AlCl_3 , SnCl_4 or Zn halides.^{13,27} The right selection of Lewis acids depends on different factors like the monomer, the M_n of the wanted polymer and the solvent(s), since the crucial point is the acidity of these acids which affects the ionization equilibrium between inactive and active species (see Scheme 1.1) and thereby, the kinetic events (Scheme 1.1 and 1.2). In addition to this it is also important to note the influence of these processes, in some quenching reactions of living PIB²⁸⁻³¹ which will be discussed in details in section 1.3.1 and in Chapter 5.

Especially BCl_3 and TiCl_4 are of interest for the polymerization of IB. In this project, some of the precursor polymers should have molecular weights in the range of $M_n = 5,000-7,500$, exactly in the area where most systems fail. The BCl_3 system gives good results in the low M_n range ($M_n = 1,000-3,000$).^{32,33} At higher M_n values precipitation is observed (usually gives broader MWD) because the solvent has to be relatively polar (CH_2Cl_2 or CH_3Cl , in which PIB has a low solubility) in order to obtain a certain degree of ionization (see Scheme 1.1) (BCl_3 is a weaker Lewis acid than TiCl_4). TiCl_4 is normally considered to give the best results for $M_n > 10,000$, where the solvent is a mixture of n-hexane and a polar component normally in the range 60:40 to 40:60 (see below section 1.2.1.5). Some experiments have been made with TiCl_4 ³⁴ where prepolymers having M_n in the wanted range were prepared. However, compared to a two-step procedure using BCl_3 in the first one together with TiCl_4 in the second one^{35,36} the MWD is somewhat broader (details of this two-step procedure can be found in chapter 5).

Actually, BCl_3 does not only function as a coinitiator. In some systems it can also initiate the polymerization itself due to self-ionization ($2\text{BCl}_3 \rightleftharpoons \text{BCl}_2^+ + \text{BCl}_4^-$).^{37,38} The initiator BCl_2^+ is incorporated into the polymer resulting in a functional head group which can undergo further reactions.³⁹ This initiation system can compete with, e.g. $\text{TMPCl}/\text{BCl}_3$ under certain conditions, leading to two initiating species simultaneously present in the polymerization media. Therefore, careful selection of experimental conditions is necessary in order to minimize the direct initiation with BCl_3 , for example, by addition of additives like electron donors (EDs).

1.2.1.4 Solvents

The choice of a solvent or a mixture of solvents is restricted to a few possibilities in LC^+Pzn of IB, namely because of the solubility of the polymer and the influence of the solvent polarity on the ionization equilibrium of the initiator and the living chain end (see Scheme 1.1). Another aspect

which shall be kept in mind is that the solvent as well as any of the other elements can affect the central steps in a polymerization (for instance can cause transfer). CH_2Cl_2 and a mixture of CH_2Cl_2 :*n*-hexane (40:60 v/v %) are often used. The main problem with CH_2Cl_2 is a relatively high concentration of moisture (about 10^{-3} M). This problem is more or less eliminable with the use of a proton trap. The second complication is that PIBs with a $M_n > 2500$ -3000 begin to precipitate in pure CH_2Cl_2 and thereby result in uncontrolled reaction conditions. *n*-Hexane on the other hand dissolves PIB and is therefore used when high molecular weight material is prepared. However, the presence of *n*-hexane shifts the equilibrium between inactive and active species toward the inactive one and that is reason why a strong Lewis acid like TiCl_4 is needed when such a solvent mixture is used. Since *n*-hexane normally is purchased as a technical product special purification is necessary to remove 1-hexene (see Experimental) which acts as termination agent. Other solvents like CH_3Cl and $\text{CH}_2\text{ClCH}_2\text{Cl}$ are also well-known solvents for cationic polymerizations.

In general, the change from a non-polar to a polar solvent or *visa versa* has remarkable effects on the kinetic events due to shifts of the equilibria shown in Scheme 1.1. The rate of propagation as well as the rate of initiation are both proportional to the respective ionization constant ($R_p \propto k_p \cdot K_I$, $R_i \propto k_i \cdot K_I'$). Some experiments with vinyl ethers⁴⁰, show that the apparent rate constant in CH_2Cl_2 is 40 times higher than in CH_2Cl_2 :*n*-hexane (1:9). MWD is also affected by the solvent. Broader MWD is obtained in a non-polar solvent¹⁸ because K_I and K_I' are influenced by the polarity to a different extent in this case. The kinetics can even be totally modified in some cases when the solvent is changed. For instance, with respect to reaction orders in monomer.⁴¹ The reaction order of different vinyl ethers is zeroth order in *n*-hexane and first order in toluene or CH_2Cl_2 . The explanation for these observations is that competitive interactions of the vinyl ether monomer and the solvent with the living chain end exist. In experiments performed with DiCumOH as initiator, problems arise due to termination caused by indanyl ring formation. If the polymerization is made at a fixed temperature, it can be demonstrated that the polarity of the reaction media has a decisive influence on the relative ratio between the three potential structures.¹⁶ From these considerations concerning the influence of solvents on different parameters in LC^+Pzn , it can be concluded that it is very important to choose the right solvent for each specific polymerization system.

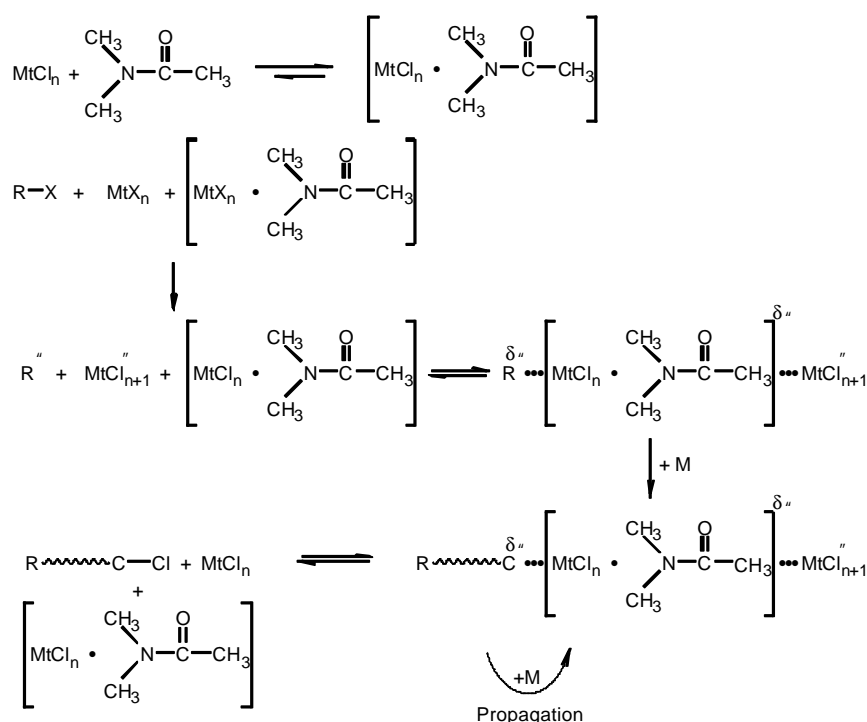
The limitations regarding cationic polymerization are first of all the restricted number of monomers which can be polymerized by this system. Secondly, the experimental setup used in our case is performed in a way where high vacuum-line technique is not necessary, and this caused a limit in regard to M_n ($M_n < 100,000$) due to potential impurities. However, a second problem which may arise at a very high molecular weight is detectable amount of transfer.⁴²

As discussed above, important features of LC^+Pzn are the possibility to obtain materials having a well-defined M_n , narrow MWD, and a versatile number of endgroups in quantitative yield which can be utilized for further reactions. Concerning end-functionalized PIB see below section 1.3.1.

1.2.1.5 Additives

One type of additives are electron donors (EDs). The effect and purpose of using EDs is to reduce the net positive charge of the propagating chain end and thereby reduce the rate of propagation and moreover the rate of transfer/termination. Different categories of EDs systems exist depending on the way they are formed. The external ED system is made by adding the ED intentionally in order to obtain a Lewis acid/ED complex (see below). In the internal ED system the cation stabilization is achieved by EDs formed *in situ* during the initiation process due to initiators containing an oxygen atom e.g., an ether or alcohol group.¹³

The most decisive objective using ED is the narrowing of the MWD and control of the chain ends. Polymerizations with our initiating system have been made with and without ED, N,N-dimethyl acetamide (DMA).^{32,43} The results clearly show the appreciable change in MWD. Without DMA, PDI = 2.0-3.0 while PDI < 1.4 with DMA. EDs suppress the indanyl ring formation, a potential side reaction when DiCumOH/DiCumCl are used, and chain transfer, just to mention the most important beneficial effects of EDs on MWD.¹³ When DMA or other external EDs are used, one shall have in mind the relative proportion between coinitiator and ED. If ED is added in excess $[ED]/[coinitiator] > 1$ the conversion of monomer is equal to zero, whereas $[ED]/[coinitiator] < 1$ gives 100% conversion (normally $[I]:[ED]:[MtCl_n] = 1:1:8-20$).⁴⁴ DMA and DMSO are strong EDs⁴⁵ which means that the electron-pair donating tendency of these compounds is relatively high. The exact nature of the cation modulating effect is still obscure, but the concept of living polymerization with reversible termination (Scheme 1.1) in the presence of EDs, such as DMA or pyridine, is supposed to take place via a complex between the Friedel-Crafts acid and the ED.^{13,34,44,46} The following scheme illustrates the key events when DMA is used as ED.



Scheme 1.4: Polymerization of IB in the presence of an electron donor, e.g., DMA (R: initiator fragment).

In the case of DMA (Scheme 1.4) coordination/complexation to the Lewis acid can take place with lone-pair electrons either from the oxygen or the nitrogen atom. However, the exact complex structure is not known yet.

Proton traps are a second type of additives added to the cationic polymerization system in order to improve the control of the polymerization. Contrary to EDs, the effect is not attributed to stabilization of the propagating species but to scavenging of protons.^{44,46-48} They are strong bases (pyridine derivatives, especially 2,6-di-tert-butyl pyridine (DtBP)) which under ideal circumstances (e.g. homogeneous system) are able only to react with protons and not with other electrophiles. Recently, quantitative results concerning this topic have been published.⁴⁹ The conclusion is that the alkyl groups in the 2- and 6-position have to be tert.-butyl if the rate constant of reaction with other electrophiles shall be suppressed to an acceptable level. DtBP, a sterically hindered pyridine derivative is used in the same concentration which must be expected in regard to adventitious moisture in CH_2Cl_2 ($\approx 10^{-3}$ M).⁵⁰ A simple way to prove whether or not DtBP abstracts a proton from the propagating end (causing a vinylic endgroup) is the use of ^1H NMR (detection of vinyl proton) and SEC. In the SEC trace a shoulder toward high molecular weight (doubled $M_{w,\text{theo}}$) is a direct prove for the interaction between DtBP and the chain end, since the vinyl-capped PIB reacts as a macromonomer with the living chain ends. In the literature the action of proton traps in regard to coupling has been discussed, and there is a pronounced reaction in some cases⁵¹ when DtBP is used in the ratio 1:1 to initiator.

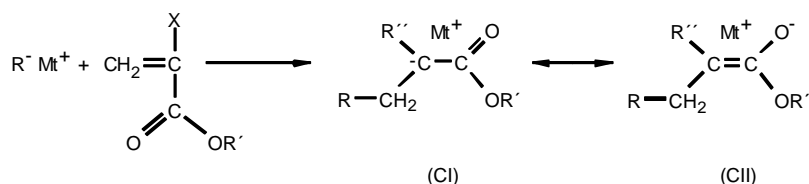
Addition of salts (common ion effect) is a third way to modulate the propagating chain end giving products with narrower MWD, but the concentration has to be in a certain range, or else bimodal MWD is obtained.⁵² The effect of salts is related to shifts in the Winstein spectrum toward the left side, meaning the equilibrium between inactive and active species is shifted to the inactive one lowering the rate of propagating and the rates of side-reactions.^{13,52,53}

1.2.2 Anionic polymerization

1.2.2.1 General concepts of controlled/living anionic polymerization

In contrast to LC^+Pzn , LA^-Pzn has to be performed with high vacuum technique because of the sensitivity toward, e.g., moisture and oxygen. Due to the use of such a technique, high molecular weight materials ($> 100,000$) are attainable. LA^-Pzn can be carried out with many different systems. However, as in LC^+Pzn one has to choose the right conditions: initiator (counterion), solvent(s), additives etc. for each monomer in order to reach ideal conditions.

In Scheme 1.5 the polymerization of a polar monomer containing an electron-withdrawing side-group is shown. The polar side-group makes the monomer highly reactive and stabilizes at the same time the living carbanion by the formation of an ester enolate.



Scheme 1.5: The mesomeric structures CI/CII present in LA⁻Pzn of (meth)acrylates (R'' = CH₃ or H).

Scheme 1.5 represents the two extreme cases (structures (CI) and (CII), since the actual structure is in between with delocalization of the π -electrons. In a similar way as described in Scheme 1.3, the Winstein spectrum, equilibria between ion pair, solvated ion pairs, free anions, and associated ion pairs exist. Since sometimes more than one of these species are present (in equilibrium) it is crucial that a fast exchange takes place compared to the rate of propagation.⁵⁴ If this is not the case, different propagating species would be simultaneously present leading to a broadening of the MWD. Besides, through the addition of additives (e.g. salts, and ligands) the direction of these equilibria can be affected.⁵⁵ At this point it is decisive what kind of systems we are dealing with, i.e. the type of solvent, polar (e.g., THF, DME, THP) or non-polar (e.g., toluene, benzene, hexane) and type of monomer, polar (e.g., (meth)acrylates) or non-polar (e.g., styrene). The choice of solvent has dramatic influence on the stereochemistry of the polymerization, and therefore on the T_g of the resulting material.⁵⁶ In this project the experiments are carried out with polar monomers, e.g., MMA, DMAA, EO etc. (see below) and mainly in THF. For such a system free anions, contact ion-pairs, and aggregates can exist.⁵⁷ The rate of propagation is here much higher for the free anions than for the other two chain ends ($k_p^{(-)} \gg k_p^{(\pm)} \gg k_p^{\text{agg}}$). In case of aggregation, the reaction order regarding the initiator can vary from 1 to 0.5, the latter value corresponding to high extent of dimer aggregation.

An important aspect in controlled/living anionic polymerization is the introduction of functional endgroups which can undergo further reactions. The OH group is here of special interest, e.g. regarding subsequent curing reactions with isocyanates or acid chlorides. The subject, end-functionalized polymers, i.e. quenching of living chain ends in LA⁻Pzn is discussed in section 1.3.1

1.2.2.2 Monomers

Several classes of monomers can be polymerized by LA⁻Pzn.⁵⁸ Non-polar monomers like styrenes and conjugated dienes and polar monomers, e.g., acrylates, methacrylates, vinyl ketones, and vinyl pyridines. Heterocyclic monomers, for example epoxides, lactams etc. can be polymerized by ring opening polymerization. Since LA⁻Pzn cannot be performed with monomers having labile protons (e.g., alcohols, acids, and amines) protected monomers are often utilized for the synthesis of hydrophilic or amphiphilic polymers. The requirement for these protecting groups, e.g., acetals, silyl derivatives, and *tert*-butyl esters^{10,59}, is that they are stable in alkaline solution and easy to hydrolyze/remove in acid solution without destroying the polymer itself. In this work the hydrophilic monomers illustrated in Figure 1.2 are of special interest since they are frequently used in the preparation of biomaterials^{1,60-63}, and the resulting PIB-based block copolymers are expected to be soluble (micelles) or at least swellable in water. By the polymerization of these monomers, one has to be aware of the possible complications, i.e. the presence of termination (see below). Therefore, careful selection of conditions, e.g., size of counterion is necessary in order to have a polymerization

which proceeds in a controlled manner. For instance, the polymerization of N,N-dimethyl acrylamide (DMAA) (structure (II), Figure 1.2) with Li^+ is heterogeneous since the resulting polymer is insoluble in THF (because of the large isotactic content), with K^+ it is nearly homogenous and $\text{PDI} = 1.2\text{-}1.3$, whereas with Cs^+ it is completely homogenous and leads to perfect LA⁻Pzn with a $\text{PDI} < 1.1$.⁶⁴ On the other hand, the best control of the polymerization of MMA and silyl protected HEMAs is obtained with Li^+ (see chapter 5).

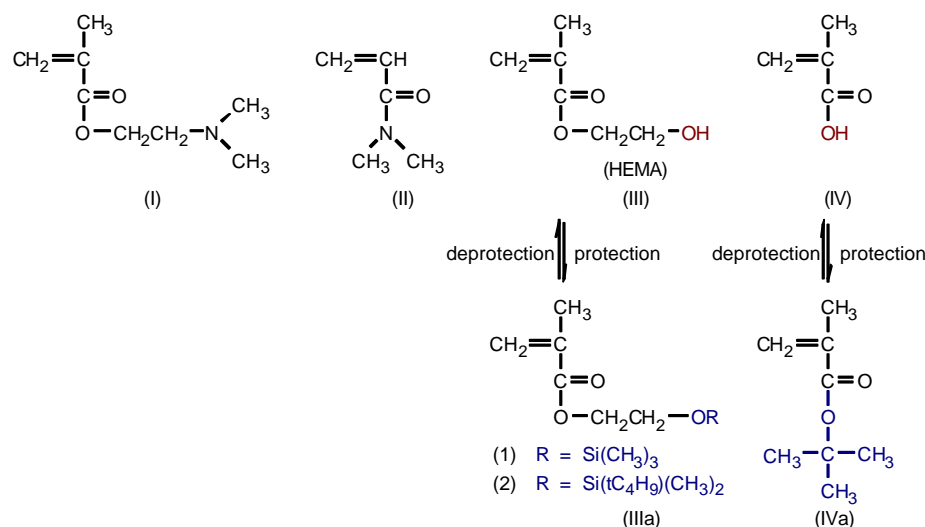


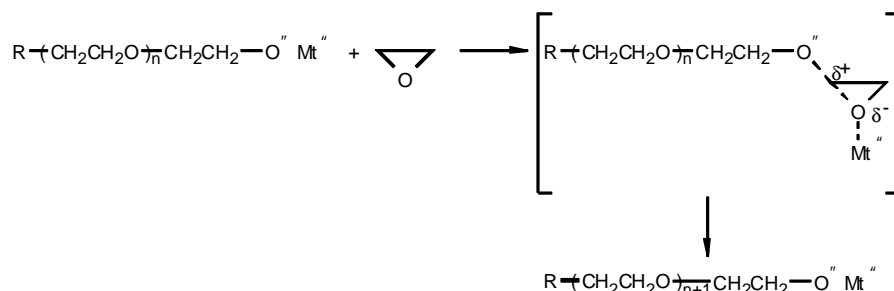
Figure 1.2: Hydrophilic (meth)acrylic monomers which can be used for the synthesis of amphiphilic PIB-based block copolymers or networks

For the synthesis of thermoplastic elastomers, monomers like MMA or isobornyl methacrylate⁶⁵ are interesting since the heat resistance, i.e. service temperature of the resulting polymer segment, is mainly related to the high T_g .

In polymerization of polar monomers, especially in the case of (meth)acrylates, a few potential termination reactions exist depending on the chosen conditions.⁶⁶ Nucleophilic attack at the carbonyl group either on the monomer or the polymer chain is one problem. However, it can be more or less eliminated by careful selection of initiators as discussed below, since attack by the ester enolate anions, i.e. living chain end, has been proved not to be important.^{57,67} Backbiting on the other hand can be a result of several factors, e.g., size of counterion, the polarity of the solvent, monomer concentration, and reaction temperature. Again this side-reaction can be suppressed when the right conditions (e.g. low temperature and large counterion) are found. The consequences of termination, as mentioned before, is poor control of the molecular weight, broad MWD ($\text{PDI} \leq 2$), difficulties in synthesizing block copolymers by sequential monomer addition, and less than quantitative end-functionalization.

A somewhat different, however, important hydrophilic monomer is EO which is often used for biomedical applications.¹ The LA⁻Pzn of EO can be initiated by many different types of initiators: hydroxides, alkoxides, alkali alkyls etc.⁶⁸ However, one has to be aware of the fact that polymerization of EO only works with large counterions like potassium or cesium.⁶⁹ With lithium, polymerization is not possible, only mono-addition is reached due to the strong bonding between lithium and the alkoxide.⁷⁰ The explanation for this difference between the alkali metals is described

in the following Scheme 1.6. It takes into account that the ring-opening reaction passes through an intermediate where an electrophilic activation of the epoxide ring is postulated to take place by the counterion.⁷¹



Scheme 1.6: Insertion mechanism proposed for the polymerization of ethylene oxide.

With potassium as counterion and a concentration of active chain ends in the range $5 \cdot 10^{-3}$ M in THF at RT a deviation from the expected first order kinetics regarding initiator, i.e. potassium alkoxide, has been noticed.⁷² A reaction order of 0.33 was found. This observation is assumed to be related to aggregation, where an equilibrium between an active unimer and a inactive trimer exists analogous to BuLi in THF.⁷³ With sodium a reaction order of 0.25, i.e. an association number of 4 was found.⁷² The counterion is fixed by the negative charge on the alkoxide, but it also interacts with the solvent, monomer, ligands like crown ethers and cryptands, similar to that described above for the (meth)acrylates. By the use of ligands, aggregation can be eliminated leading to straightforward first order kinetics regarding the initiator.⁶⁸ The dilution of the active chain ends to below 10^{-4} M also decreases aggregation.⁶⁸ In the polymerization of EO, problems regarding termination are not important like for the (meth)acrylates.

1.2.2.3 Initiators

The reactivity of an initiator depends on the nucleophilicity of the anion, which roughly correlates with the pK_A value of the non-metallated compound. In Figure 1.3 some initiators are shown starting with BuLi which is the most nucleophilic one and some counterions where Li^+ is the smallest and most strongly bonded one.

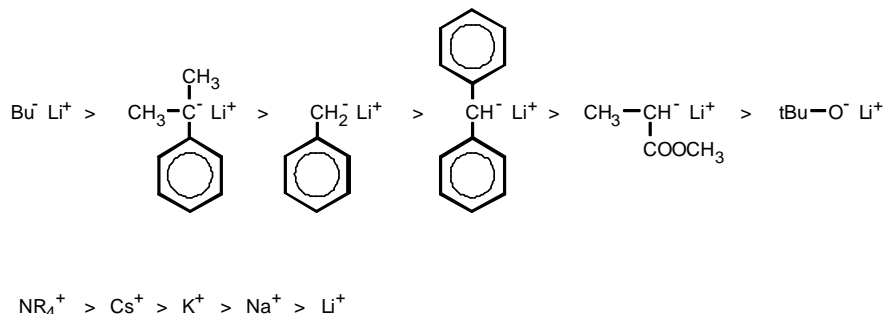
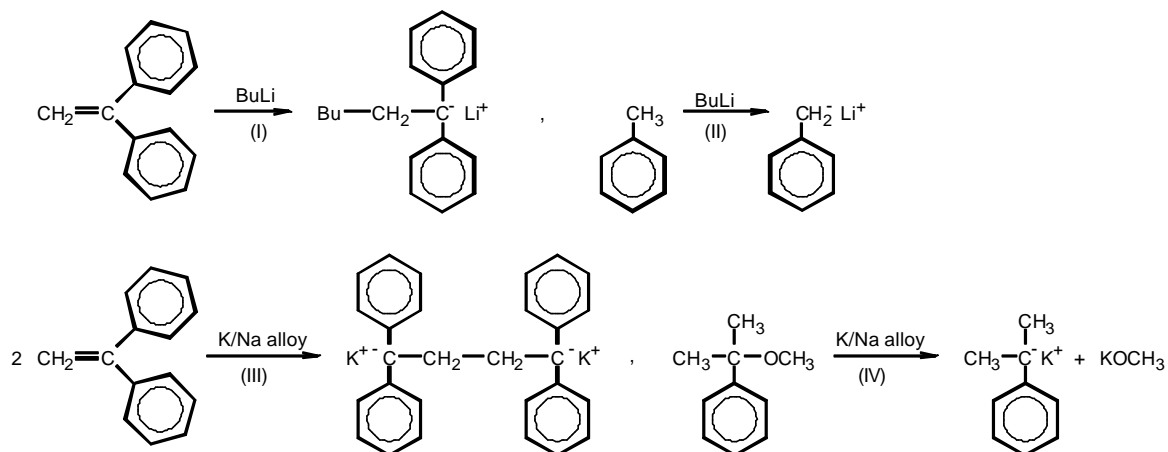


Figure 1.3: Typical initiators and counterions used in LA-Pzn

The initiators used in this work are all alkali metal-based initiators, and since most of the investigated monomers are (meth)acrylates, they have to be sterically hindered (di)phenyl-substituted

carbanions in order to avoid the nucleophilic attack of the initiator on the ester group of the monomer (see above). In case of a non-polar monomer like styrene, BuLi can be used as initiator.

Initiators can be prepared in three different ways (Scheme 1.7). Either by an addition reaction where, e.g. BuLi reacts with a double bond of DPE, by proton abstraction, by electron transfer reactions, e.g. to the double bond in DPE which leads to coupling of two radical anions⁷⁴ or cleavage of an ether bond⁷⁵⁻⁷⁷.



Scheme 1.7: Preparation of anionic initiators by different methods.

1.2.2.4 Additives

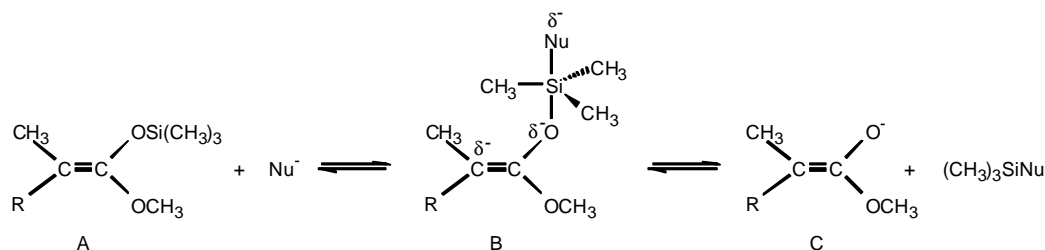
The living chain end can be modified in order to adjust its reactivity (e.g. controllable rate of propagation) by the addition of additives, like LiCl, TMEDA, crown ethers, lithium alkoxides etc.⁷⁸⁻⁸¹ Based on recent improvements gained by adding LiCl to the polymerization system^{55,82-84}, it is used as additive and for counterion exchange in the polymerization of different methacrylates in this project. LiCl affects the polymerization in different respects. It exerts a significant effect on both kinetics and MWD, mainly due to depletion of associated ion pairs.⁸⁴ Different adducts of living chain ends and LiCl can be formed. The 1:1 complex ($[\text{LiCl}]/[\text{I}] \leq 1$) has a rate constant comparable to that of the ion pair and the 2:1 complex ($[\text{LiCl}]/[\text{I}] > 1$) a lower one. Concerning the LiCl to initiator ratio it has been shown that with $[\text{LiCl}]/[\text{I}] > 10$ no changes, e.g. in MWD, could be detected.^{59,85} Therefore, in this project 10 times excess LiCl was used in all experiments. Regarding the tacticity and rate of termination (back-biting), no influence was observed in THF.⁸⁵ However, in a non-polar solvent, toluene/THF (9:1), the syndiotactic placements increase by the addition of LiCl.⁸⁶

1.2.3 Alternative polymerization procedures

1.2.3.1 Group transfer polymerization

In group transfer polymerization (GTP) where the initiating and propagating species are silyl ketene acetals, acrylic monomers can be polymerized.^{87,88} The major differences between GTP and LA-Pzn is the nature of the propagating chain end which is here covalent in character and that GTP can be performed at room temperature. In each propagation step a SiR_3 group is transferred to the

carbonyl oxygen of the incoming monomer. The exact mechanism is not known with certainty but in the case of anionic catalysis it has been proposed that the nucleophilic catalyst activates the silyl group, possibly through a hypervalent silicon intermediate (Scheme 1.8, structure B)⁸⁹, which promotes a Michael-type addition of the initiator to the monomer with a concerted transfer of the silyl group to the carbonyl of the monomer.



Scheme 1.8: The structures of the propagating species in GTP

Another class of catalysts are the electrophilic ones like Lewis acids. Here different mechanisms are proposed involving activation of the initiator and monomer.^{90,91} In general, higher molecular weights and narrower MWDs are realized with anionic catalysts.

An interesting feature related to this method is that well-defined block copolymers with different morphologies (e.g., linear AB/ABA using mono- and difunctional initiators and star-shaped) as well as telechelic polymers can be synthesized.^{91,92} However, block copolymers with non-polar monomers, e.g. styrene cannot be obtained only by GTP. Another important limitation of GTP regarding this work is that silyl protected monomers (e.g., TMSHEMA) cannot be polymerized because of the coordination of the catalyst to each monomer unit. In that case acetal protected monomers might be utilized.

1.2.3.2 Coordinative polymerization

With organo-lanthanide initiators such as $[(C_5(CH_3)_5)_2SmH]$ or $(C_5(CH_3)_5)_2SmCH_3$ in a polar solvent^{93,94} or methyl-(5,10,15,20-tetraphenylporphinato) aluminum in a non-polar solvent⁹⁵ high molecular weight poly(meth)acrylates, polyepoxides, and polylactones with narrow MWD can be obtained. Due to the living nature of the chain end block copolymers have been also synthesized by this procedure.⁹⁶⁻⁹⁹

1.2.3.3 Controlled/living radical polymerization

Recently, new types of controlled/living radical polymerization have been developed. One is the Atom Transfer Radical Polymerization (ATRP), where the inactive chain end contains a halogen atom and the active chain end a radical gained by the oxidation of a metal complex (mainly copper complexes have been investigated).¹⁰⁰⁻¹⁰³ A second one is the nitroxide-based radical polymerization.¹⁰⁴⁻¹⁰⁶ The advantages of these are first of all the ability to prepare polymers with a MWD narrower (< 1.3) than with conventional radical polymerization, and due to the living nature of the chain end block copolymers^{107,108} and polymers with new well-defined topologies, e.g. branched¹⁰⁹ and hyperbranched materials¹⁰⁶ can be prepared. The behavior of the chain ends can in both cases be described in a similar way as in cationic polymerization (Scheme 1.1, section 1.2.1),

namely, by the existence of an equilibrium between inactive and active species which moderates the rate of propagation. As a consequence of that termination can be reduced, due to the fact that the rate of propagation is first order with regard to $[P^{\cdot}]$ and the rate of termination is second order (termination proceeds by combination or disproportionation of two radical chain ends). In contrast to LA-Pzn, unprotected monomers like HEMA can be polymerized by ATRP, and in the literature it is also postulated that highly purified reagents (e.g. absence of H^+) are not necessary.

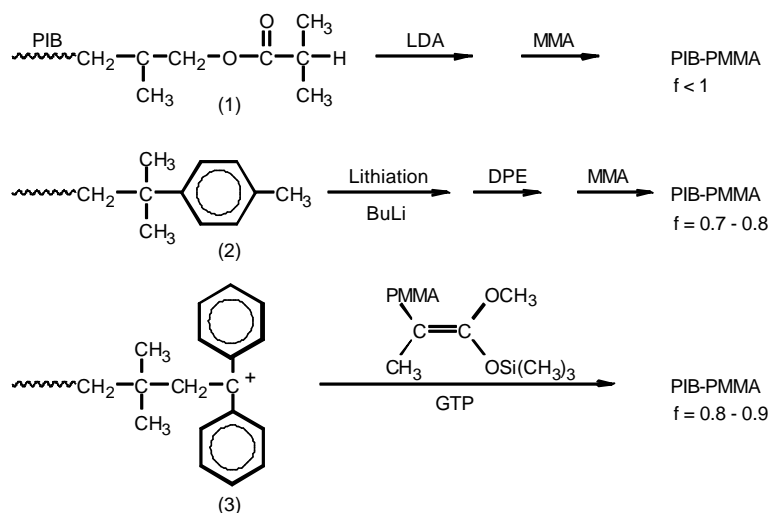
1.2.4 Combination of different polymerization procedures

As already introduced in section 1.2.1 and 1.2.2 specific living polymerization methods (e.g. cationic and anionic polymerizations) are applicable only to a limited number of monomers. Block copolymers with TPE properties or amphiphilic block copolymers have been obtained by cationic as well as by anionic polymerization. In cationic polymerization TPEs like PSt-*b*-PIB-*b*-PSt^{23,48} or amphiphilic block copolymers, e.g. PMVE-*b*-PMTEGVE¹¹⁰, PIB-PIBVE¹¹¹, and PIB-*b*-PMVE²⁵ have been synthesized. In these instances, the desired materials were obtained by sequential addition of the monomers. In a similar way block copolymers, e.g., PMMA-*b*-PBd-*b*-PMMA¹¹² and PMMA-*b*-PAA⁵⁹, PSt-*b*-PAA¹¹³ were synthesized anionically.

The major objective of this project is to find a new procedure to synthesize PIB-based block copolymers containing mainly one or more (meth)acrylate block segments. The combination of different polymerization techniques is expected to lead to new and unique, otherwise unavailable, polymer architectures.

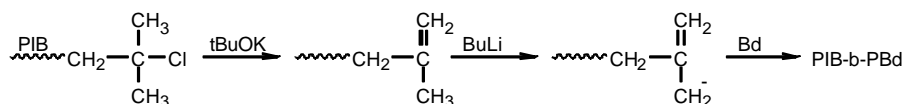
Several attempts have been made for obtaining block copolymers by utilization of end-functionalized PIBs (see section 1.3.1) as macroinitiators for living anionic polymerization in order to synthesize new useful block copolymers. One attempt used isobutyrate-telechelic PIB which was prepared by a multi-step reaction sequence (see section 1.3.1).^{114,115} Lithiation of these isobutyrate-telechelic PIBs with lithium diisopropylamide (LDA)^{114,115} was reported to lead to initiation of methyl methacrylate (MMA) polymerization for the synthesis of PMMA-*b*-PIB-*b*-PMMA block copolymers (Scheme 1.9). The major problem with this method is addition of a stoichiometric amount of LDA. Too much LDA would possibly lead to the formation of homo-PMMA. If less than needed LDA is added, e.g. due to impurities in the PIB samples, then homo-PIB will be present. The isobutyrate endgroups were also converted to silyl ketene acetal chain ends, which subsequently were used to initiate group transfer polymerization of MMA.⁹²

In another approach, lithiation of tolyl-telechelic PIB¹¹⁶ obtained by Friedel-Crafts alkylation of *tert*-chlorine-ended PIB¹¹⁸ and subsequent addition of 1,1-diphenylethylene (DPE) to the metallated chain ends were applied to initiate the polymerization of MMA (Scheme 1.9). Living PMMA chains were also attached to PIB containing short endblocks of poly(*p*-vinylbenzyl-bromide).¹¹⁹ Although detailed characterization of the products is not available, this method is expected to yield PMMA branches at the PIB termini.



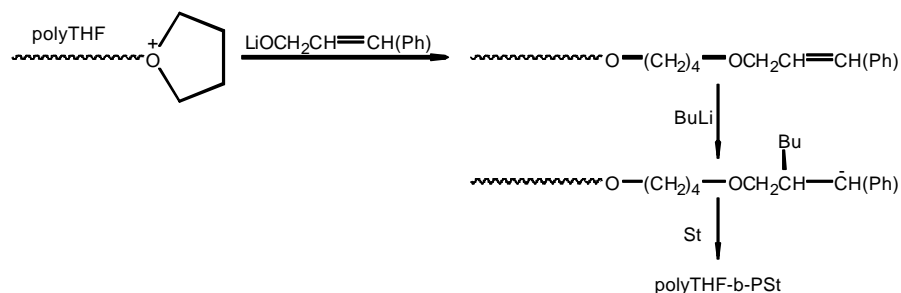
Scheme 1.9: Different approaches used for combining cationic polymerization of IB with anionic polymerization and GTP of MMA, (1)^{114,115}, (2)¹¹⁶, and (3)¹¹⁷.

Metallated PIB, obtained by one-pot dehydrochlorination-metalation of PIB-Cl^t by potassium *tert*-amylate/*n*BuLi and *t*BuOK/*n*-BuLi mixtures was used to initiate the anionic polymerization of butadiene (Bd) resulting PIB-*b*-PBd block copolymers (see Scheme 1.10).¹²⁰ However, the highest blocking efficiency of the PIB-Cl^t was about 80 %, although preliminary studies involving silylation of the gained PIB-macroinitiator verified quantitative metalation. Therefore, fractionation was necessary. In order to use this lithiated PIB for polymerization of (meth)acrylates one has to add, e.g. DPE to the living PIB carbanion leading to a less nucleophilic initiating species (see section 1.2.2.3).



Scheme 1.10: Synthesis of PIB-*b*-PBd block copolymers by the combination of LC⁺Pzn and LA⁻Pzn.

PTHF-*b*-PtBMA block copolymers have been prepared with nearly quantitative yield using a combination of ring-opening cationic polymerization and LA⁻Pzn via two-electron reduction by samarium iodide.¹²¹ However, the samarium chemistry cannot be utilized for similar experiments with PIB. In another example, a PTHF precursor is used for subsequent anionic polymerization of styrene. The first step involves quenching of the living PTHF with a lithium alcoholate possessing a styrene unit.¹²² Successive addition of BuLi then leads to a macroinitiator capable to initiate polymerization of styrene (see Scheme 1.11).



Scheme 1.11: Synthesis of PTHF-*b*-PSt by the combination of ring-opening polymerization and LA⁻Pzn.

The relatively stable, highly ionized cationic chain end formed by 1,1-diphenylethylene (DPE) addition to PIB^+ was reacted with living PMMA chains carrying silyl ketene acetal endgroups obtained by group transfer polymerization resulting in $\text{PIB-}b\text{-PMMA}$ block copolymer (Scheme 1.9).¹¹⁷ However, the major disadvantage of this method is its applicability only under very specific conditions and precise stoichiometry. In addition to this, the titanium compounds (most likely $\text{Ti}(\text{OR})_x\text{Cl}_{4-x}$) present in this system cleave the coupled blocks by forming PMMA with titanium enolate endgroups and thereby decrease the blocking efficiency. Finally, at the linkage point between the two blocks the C-C bond ($\text{R}'(\text{Ph})_2\text{C-C}(\text{CH}_3)(\text{COOCH}_3)\text{R}$) is sterically unfavored, since two tertiary carbons are linked together. Therefore, the formed block copolymer might also be unstable at elevated temperature or if it is exposed to UV light.

The one-pot quenching of LC^+Pzn of IB with DPE, a non-homopolymerizable olefin in cationic polymerization, may yield either 1-methoxy-1,1-diphenylethyl (DPOMe)¹²³ or 2,2-diphenylvinyl (DPV)^{124,125} chain ends depending on the polymerization conditions (see also chapter 5).

Both the 2,2-diphenylvinyl and the 1-methoxy-1,1-diphenylethyl chain ends are potential endgroups for the anionic polymerization of a variety of monomers by metalation (see chapter 5). Preliminary results indicate that quantitative metalation of the 2,2-diphenylvinyl endgroups with alkyllithium cannot be achieved, most likely because of steric hindrance (see chapter 5). In addition, it is difficult to add a stoichiometric amount of BuLi to the PIB precursor. Too much BuLi would lead to formation of homo-PMMA or nucleophilic attack on the carbonyl group of MMA. If less than needed BuLi is added, e.g., due to impurities in the PIB samples, then homo-PIB will be present (similar to reactions in Scheme 1.9).

In conclusion, all these methods have several disadvantages: multistep endgroup derivatizations are required for the synthesis of the telechelic PIB initiator precursor (except those involving quenching with DPE), and lithiation and thus the subsequent initiation of anionic polymerization is not quantitative or it requires extreme conditions. As a consequence of less than 100 % initiating efficiency these methods yielded mixtures of homopolymers and block copolymers. This is indicated by the fact that pure $\text{PMMA-}b\text{-PIB-}b\text{-PMMA}$ was only obtained by selective extraction.^{92,114-116}

The combination of cationic and anionic polymerization procedures for the synthesis of tailored block copolymers (free of homopolymers) seems to implicate considerable problems. Having the above-mentioned approaches (Scheme 1.9) and related problems in mind, the aim in this project is to develop a method where stoichiometric complications might not be present, and if possible to obtain a self-cleaning system in order to remove potential impurities in the polymer (solution). This means, that the initiation by the PIB precursor should proceed with excess metalation agent, which can be removed before the LA^+Pzn proceeds.

In addition to the above-mentioned transformations from cationic into anionic polymerization, several methods have been worked out for transformations from anionic to radical, anionic to cationic, anionic to metathesis, and cationic to radical polymerization. A comprehensive review of these procedures can be found in the literature.¹²⁶

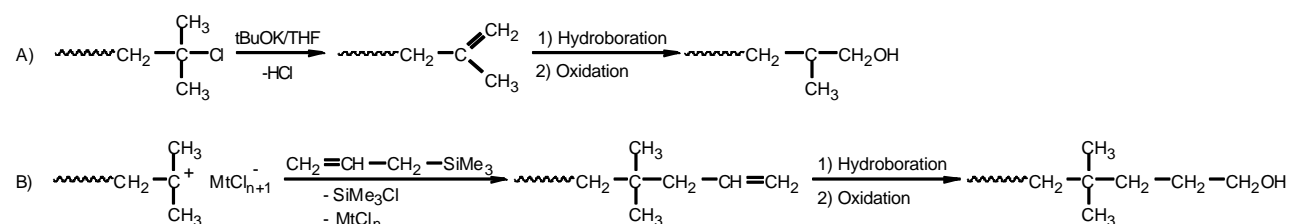
1.3 Tailored polymers

Two classes of tailored macromolecular materials will be discussed in the following section: polymers with one or more functional groups, and polymers with different structures. These well-defined macromolecules are only obtainable by using controlled/living polymerization procedures.

1.3.1 (End)-functionalized polymers

In cationic as well as in anionic polymerizations different kinds of endgroups can be introduced either during quenching or by the use of an initiator having a (protected) functional group. In addition they can be further modified by subsequent organic reactions.

Concerning cationic polymerization, especially PIB chemistry, the $-Cl^t$ endgroup can be obtained by quenching the living polymerization of IB with methanol. This endgroup opens up possibilities for a number of functionalities by quantitative derivatizations.¹³ In Scheme 1.12 two procedures are shown both leading to an OH-terminated PIB.^{28,127,128} Method A is a two-step-procedure where first the isopropenyl chain end is obtained by dehydrochlorination. The problem with this process is that the shown external (exo)-vinyl group needed for subsequent hydroboration/oxidation is not always the only product. Internal (endo)-vinyl groups can also be formed which cannot react with the borane compound 9-BBN (in section 5.4.1 a new dehydrochlorination procedure will be introduced). Method B is in fact a one-step-procedure since the vinyl group is obtained by an *in situ* quenching reaction with allyltrimethylsilane. OH endgroups are especially of interest in respect of synthesis of macromonomers¹²⁹ or for curing/linking reactions, e.g. with isocyanates or acid chlorides (see chapter 5). In this respect one has to notice the following order of reactivity: allyl alcohol > primary alcohol > secondary alcohol > tertiary alcohol. Besides, structure 1 in Scheme 1.9 was obtained from the corresponding PIB-OH, by reacting it with isobutyroyl chloride.¹¹⁴ In addition, OH-terminated PIB might for example also be used directly as precursor for the anionic polymerization of EO leading to PIB-*b*-PEO. In section 5.2.3 and 5.5.3 new procedures for the synthesis of OH-terminated PIB will be introduced.



Scheme 1.12: Synthesis of OH terminated PIB.

Friedel-Crafts alkylation of toluene with PIB- $-Cl^t$ and AlCl_3 was performed previously^{118,130} with high degree of functionality. The benzylic group with relatively acidic protons was used for subsequent anionic polymerization. However, the blocking efficiencies were relatively low, less than 50%.¹³⁰ Since the alkylation reaction proceeds in high yield (> 95%) it might be possible to extend the reaction to diphenyl methane (DPM) or triphenyl methane which contain more acidic protons. In contrast to toluene one has to be aware of the potential coupling reaction, high excess of the phenyl

compound relative to the chain end is needed. However, these PIB were not synthesized because of the results gained in preliminary metalation studies described in section 5.4.1.

A frequently used type of compounds in LC^+Pzn and LA^-Pzn for the synthesis of functionalized polymers are 1,1-diarylethylenes which are non-homopolymerizable monomers. In cationic polymerization DPE has been used for introduction of endgroups¹³¹ or for synthesis of $PIB-b-IBVE$ ¹¹¹ and $PIB-b-PMVE$ ²⁵. In the latter case DPE is added in order to modify the living PIB chain end suitable for subsequent polymerization of a vinyl ether. 2,2-Bis[4-(1-phenylethenyl)phenyl]propane, a compound containing two DPE functionalities has been used as coupling agent in LC^+Pzn ¹³² or as difunctional initiator in LA^-Pzn ¹³³. In LA^-Pzn these compounds are utilized either to reduce the nucleophilicity of the anion for polymerization of (meth)acrylates as discussed in 1.2.2 or for introduction of functionalities (amine, alcohol, carboxylic acid etc.)¹³⁴.

In a normal LA^-Pzn of (meth)acrylates, quenching is achieved by addition of alcohols, acids, or moisture leading to a stable protonated endgroup, i.e. a normal ester endgroup which cannot undergo further reactions. Quenching with functional reagents is the most common way to obtain end-functionalized polymers in LA^-Pzn . Especially OH groups are of significant interest. However, again as noted above, the reactivity of the formed functionality (OH group) has to be taken into account.

In the literature most of the described quenching reactions have been performed with monomers like styrene or butadiene and less with (meth)acrylates. Since it is a nucleophilic reaction one has to be aware of the nucleophilicity of the living chain ends. As intimated in Figure 1.3 the initiators can be ordered with regard to nucleophilicity and the living chain ends in the same way. Therefore, reactions which proceed with living poly(styryl) chain ends do not necessarily work out with living poly((meth)acrylates) because of their lower reactivity. The relative low reactivity of the living poly((meth)acrylates) might be the reason for the rare description of end-functionalization of these polymers.

In principle, all kind of quenching agents which are able to undergo a nucleophilic attack (electrophilic reagents) can be taken into consideration (CO_2 , aldehydes, ketones, acid chlorides, isocyanates, ethylene oxide etc.). With monomers like styrene and butadiene, ethylene oxide¹³⁵ and formaldehyde have been used for synthesis of primary alcohols and other aldehydes for secondary alcohols, and ketones for tertiary alcohols.⁵⁸ Another interesting endgroup, e.g. for isocyanate curing reactions is an amine chain end. For that purpose protected imines were utilized to quench living poly(styryl)lithium.¹³⁶ A third class are carboxylated polymers which have been prepared by reacting poly(styryl)lithium or poly(isoprenyl)lithium with carbon dioxide. However, this reaction is not straightforward due to the formation of dimeric ketones and tertiary alcohols in addition to the desired carboxylated polymer.¹³⁷ Polymerization of EO gives the desired OH group (primary alcohol) directly as previously discussed (section 1.2.2).

In case of acrylates (tBA) benzaldehyde was used for direct preparation of secondary alcohol endgroups, but it was not quantitative.⁷ A primary alcohol endgroup was synthesized by quenching living PMMA with allyl iodide.¹³⁸ The resulting vinyl endgroup was subsequently hydroborated/oxidated leading to the wanted primary alcohol endgroup (100 % functionality was

claimed). Quenching with EO does not work very successfully with PtBA⁻Li⁺.¹³⁹ However, with PtBMA it has been demonstrated that PtBMA-*b*-PEO block copolymer can be prepared from PtBMA⁻K⁺.¹⁴⁰ On the other hand, mono-addition of EO normally achieved with Li as counterion does not proceed with PtBMA⁻Li⁺. Concerning isocyanates (primary isocyanates may homopolymerize), acid chlorides, and anhydrides one can only anticipate that a reaction takes place.

A critical point related to end-functionalized polymers is that only one reactive group is present at each chain end and less than quantitative functionalization is frequently observed at least in LA-Pzn. These complications in curing reactions between OH-terminated polymers and polyfunctional isocyanates will lead to a blend of linked and non-linked polymers and thereby, to materials with impaired properties. In order to overcome this problem we will, in addition to end-functionalized polymers, also look at polymers containing a short segment of monomers with functional groups (see chapter 5). In a similar way functional monomers can be copolymerized together with a second monomer leading to a statistically copolymer. The resulting material can act for example as a precursor for synthesis of comb-shaped polymers or graft copolymers using either the grafting onto or graft from method (see below).

1.3.2 Polymer structures (topologies and compositions)

The structure of a macromolecule includes the topology (Figure 1.4) and the arrangement of different monomers (Figure 1.5). In Figure 1.4 some of the most important topologies are summarized including linear as well as different kinds of branched polymers. All these materials either have industrial applications (section 1.1) or scientifically interesting perspectives as model compounds.

Branched structures like star-shaped, hyperbranched, and comb-shaped polymers exhibit lower intrinsic viscosity compared to the linear polymer analog.¹⁴¹ An interesting feature regarding the hyperbranched polymers is the number of functionalities per molecule which is extremely high.¹⁴² Therefore, these materials have interesting perspectives with regard to subsequent functionalization by attachment of active molecules, e.g. for pharmaceutical applications. Concerning the synthesis of star-shaped polymers different strategies are feasible. One way is to start with a polyfunctional initiator ($n = 3-8$)²⁶ or to quench with a polyfunctional quenching agent, e.g. chlorosilanes resulting a well-defined star with the number of arms equal to the number of initiating or quenching sites. In another method (arm first method) a difunctional monomer like ethylene glycol methacrylate (EGDMA)¹⁴³ or divinyl benzene (DVB)¹⁴⁴ is added to the living polymer chain end first leading to a short segment of this monomer and then to crosslinking reactions. However, this procedure gives a less-defined number of arms (a distribution of arms) since each chain contains a Poisson distributed number of the difunctional monomer units. It is still obscure how this curing process exactly progresses. In a similar way first the core can be prepared by homo-polymerizing, e.g., DVB forming a microgel with many functionalities (core-first method),^{145,146} and then to the living core styrene can be added. A potential problem is network formation/gelation which can be more or less eliminated by working in highly diluted solutions.

The synthesis of comb-shaped polymers can also be performed in different ways. Either by the copolymerization of macromonomers with low molecular weight monomers (grafting through) where the incorporation of the respective monomers depend on the reactivity ratios of the monomer and macromonomer or by the synthesis of a copolymer containing a certain amount of functionalities which can undergo further reactions (grafting from or grafting onto).⁵⁸

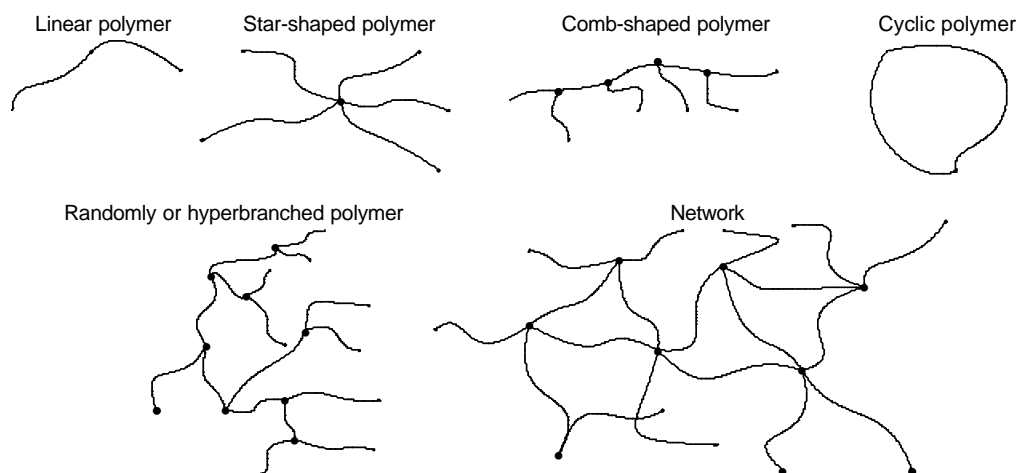


Figure 1.4: Attainable topologies using controlled/living polymerization procedures.

Polymers containing more than one kind of monomer can be categorized as shown in, Figure 1.5. The decisive parameter which determines the structure of the polymer, either block copolymer, random copolymer, or alternating copolymer is the reactivity ratios, r_1 (k_{11}/k_{12}) and r_2 (k_{22}/k_{21}) of the different monomers when these are polymerized simultaneously.¹⁴⁷

- $r_1 r_2 \ll 1$ Tendency to obtain alternating copolymer
- $r_1 r_2 \approx 1$ Tendency to obtain random copolymer
- $r_1 r_2 \gg 1$ Tendency to obtain block or tapered copolymer

If the reactivity ratios of a monomer system do not allow the formation of block copolymers directly, these can be synthesized by sequential monomer addition.

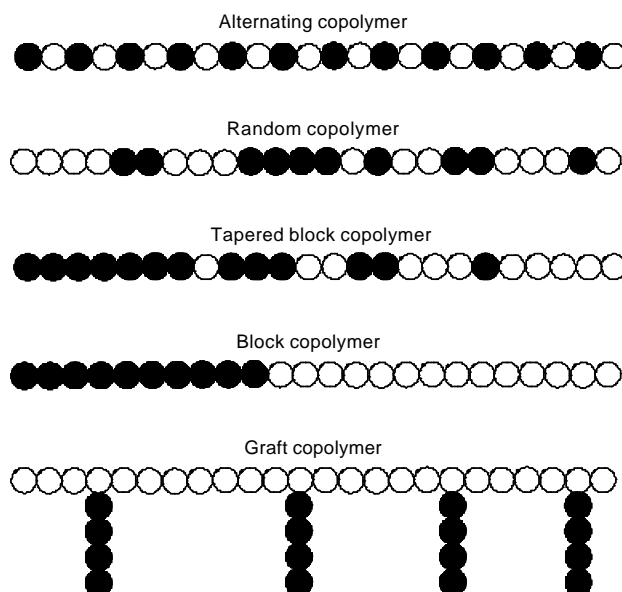


Figure 1.5: Compositions attainable by using two different monomers.

In this project only block copolymers obtained by sequential addition of monomers are treated due the interesting properties related to phase separation. Thermoplastic elastomers, amphiphilic block copolymers, and amphiphilic networks will be discussed more detailed in the next sections.

1.3.2.1 Block copolymers, thermoplastic elastomers

Thermoplastic elastomers are materials which combine the processing characteristics of thermoplastics with the physical properties of vulcanized rubbers. The majority of TPEs are linear or star-shaped block copolymers and graft copolymers. The most important characteristic of block copolymers, which is at the same time the reason for the unique physical properties, is that they undergo phase separation due to the incompatibility of the block segments. Some of these well-defined morphologies for linear ABA and star-shaped $(AB)_3$ block copolymers are presented in Figure 1.6: spheres, cylinders, and lamellae. Additional morphologies (gyroid and ordered bicontinuous double diamond) have been observed for AB (and ABC) systems.² The outer ("hard") segments are below T_g at the application temperature and the T_g of this phase corresponds the upper service temperature. The inner segment is above its T_g (rubbery or "soft") at the application temperature and the T_g of this one is equivalent to the lower service temperature.

The type of morphology obtained with a specific type of block copolymer is mainly dictated by the following parameters:¹⁴⁸

- 1) The degree of polymerization $N = N_A + N_B$
- 2) The composition $x = N_A / (N_A + N_B)$ or volume fraction $\Phi_A, \Phi_B = 1 - \Phi_A$
- 3) The interaction parameter $\chi_{AB} = v_A \cdot (\delta_A - \delta_B)^2 / (k \cdot T)$
(v_A : the volume of one monomer unit; δ : the solubility parameter)

The first two parameters can simply be regulated through the total degree of polymerization and the composition, whereas χ_{AB} is given by the choice of polymer A and B (since it can be correlated to the surface tension of between the two phases which is proportional to the difference between the respective dipole moments) and the temperature. The product $\chi_{AB} \cdot N$ is used as a measure for the phase separation.

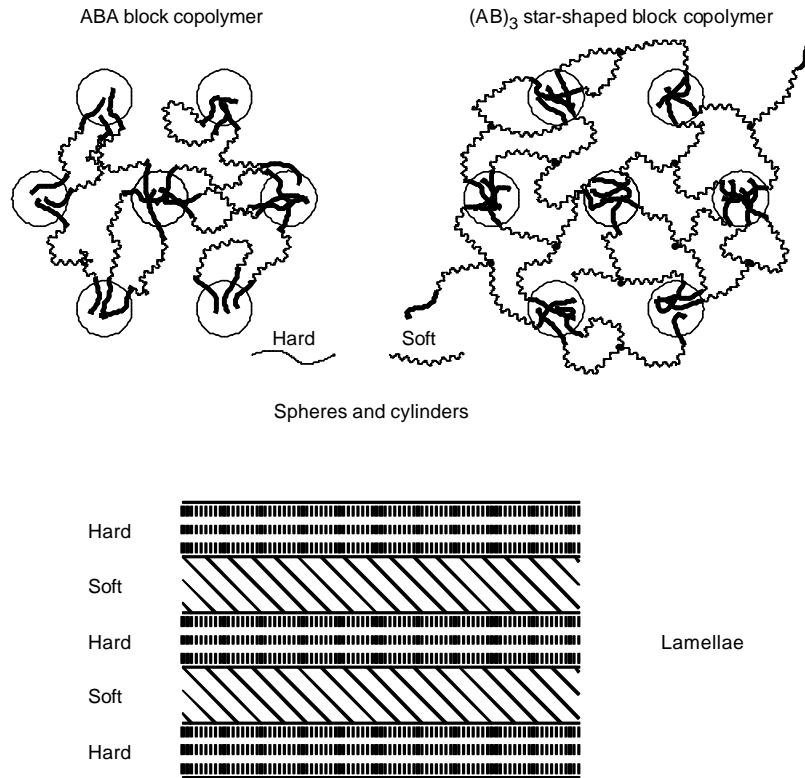


Figure 1.6: Potential morphologies obtained by annealing ABA/(AB)₃ block copolymers.

The Gibbs equation can be used to describe whether mixing or phase separation of two polymer segments occurs:

The conditions for phase separation is $\Delta G_m > 0$ (ΔG_m , the free energy of mixing) i.e.

$$\Delta H_m > T\Delta S_m$$

where, $\Delta H_m = f(\chi_{AB})$.² Based on these considerations several factors favoring the formation of domains can be expected:²

- A high degree of structural difference between the segments
- High segmental molecular weight
- Low temperature

Due to the fact that the morphology, and thereby the TPE properties can be controlled one can develop materials exhibiting predictable and specialized properties by careful choice of A and B, the degree of polymerization, and the composition.

Concerning the spherical and cylindrical structures (Figure 1.6) one has to imagine (in this case where $\Phi_{PIB} > 0.5$) that the hard segments are present as small crosslinking domains in a matrix of the rubbery segment leading to a 3-dimensional (reversible) network. Due to the existence of these morphologies, it might be possible to improve the properties of the resulting TPEs by using an (AB)₃ instead of an ABA, since in this case three outer segments can participate in the formation of a pseudo network. However, with both block copolymers (but especially with ABA) loop formation cannot be excluded (more than one outer segment (A) from one molecule is present in one domain), which might have similar impaired effects on the TPE properties as impurities caused by AB fragment (less than quantitative blocking efficiency). Entanglements of the loops can on the other hand (re)improve the

physical properties if the B segments exceed the entanglement length. It is difficult to predict the fraction of loops, the resulting loss of TPE properties, and the influence of potential entanglements. The reverse situation with small rubbery domains also exists, e.g., if $\Phi_{\text{PMMA}} > 0.5$. The latter type of materials does not have much usage as TPE, since they are very hard/brittle, which means that the tensile strength is very high and do not undergo any elongation, but they can be used as impact modifiers.

A certain number of block copolymers are of practical and academic interest. As mentioned in section 1.1 SBS and SEBS dominate the industrial market of block copolymer based TPEs. In the scientific literature a series of PMMA-*b*-PBd-*b*-PMMA and PSt-*b*-PBd-*b*-PSt (SBS) block copolymers have been synthesized by LA-Pzn.^{112,149,150} Polymers with different compositions and molecular weights were prepared in order to find optimum properties. The best compromise between ultimate tensile strength (σ) and elongation at break (ϵ) was found with samples having about 60:40 PMMA:PBd and $M_{n,\text{PBd}} = 30\text{-}40,000$ ($\sigma \approx 30\text{-}35$ MPa and $\epsilon \approx 1000$ %) and about 60:40 PSt:PBd and $M_{n,\text{PBd}} \approx 60,000$ ($\sigma \approx 30$ MPa and $\epsilon \approx 1000$ %). In addition, P α MeSt-*b*-PIB-*b*-P α MeSt and PSt-*b*-PIB-*b*-PSt with relative good properties ($\sigma \approx 25$ MPa and $\epsilon \approx 4\text{-}500$ %) have been prepared by LC⁺Pzn using sequential addition of monomers.^{151,152} Only one case is known where PMMA-*b*-PIB-*b*-PMMA was synthesized and characterized.¹¹⁶ In this case the properties are not particularly good ($\sigma \approx 15$ MPa and $\epsilon \approx 650$ %) which might be due to less than quantitative blocking efficiency.

One of the objectives in this project is to synthesize and characterize PIB- and PMMA-based TPEs and to compare the properties with existing materials. The characterization of the materials can be performed with small angle X-ray scattering (SAXS), transmission electron microscopy (TEM) dynamic mechanical measurements (DMA), and stress/strain measurements. The first two methods deliver details about the morphology whereas the latter two give information about the physical properties which are a result of the morphology. Considerations regarding compositions and molecular weights made with the mentioned TPEs will serve as starting point for our investigations.

1.3.2.2 Amphiphilic AB block copolymers

The most important feature of amphiphilic AB block copolymers is their ability to form micelles especially in aqueous media.^{153,154} Due to these properties, such materials can be used, e.g. as emulsifier or drug carrier. The size (hydrodynamic radius) and the average number of polymer molecules (aggregation number (Z)) of the micelles can be varied in a predictable way by varying the molecular weight of each segment and the composition¹⁵⁵ (see also section 5.7.2).

In general, AB (or ABA) amphiphilic block copolymers associate to form micelles in a selective solvent, defined as a good solvent for one block but a non-solvent for the other one.¹⁵⁶ It has been shown that the stability of the micelles, i.e. the unimer exchange can also be tuned by altering the parameters characterizing an AB block copolymer.¹⁵⁴ In order to obtain micelles with a unimodal distribution, i.e. avoiding aggregates, it is important to dissolve the polymer in the right solvent at the beginning, and then if necessary, to make an exchange into the wanted solvent either by dialysis or evaporation.¹⁵⁷ However, sometimes aggregates, i.e. a bimodal distribution with two narrowly

distributed peaks cannot be avoided.^{158,159} The smaller particles are normally accepted to represent spherical core-shell micelles, whereas the nature of the larger one is not known for certainty.¹⁵⁸ Three possibilities are listed in this reference:

- 1) A single large spherical or cylindrical micelle.
- 2) An onionlike particle with alternating concentric layers of solvated and undissolved blocks.
- 3) Loose cluster of small regular micelles.

Actually one can distinguish between two kinds of amphiphilic block copolymers: ionic and non-ionic materials. Purely non-ionic amphiphilic block copolymers are mainly based on a PEO segment as the hydrophilic part.¹⁶⁰ In the case of ionic materials, a variety of polyelectrolyte blocks have been used, e.g. poly(acrylic acid)¹⁶¹ or quarternized poly(vinyl pyridine)¹⁵³. However, it has to be noted that these polymers can exist in an equilibrium between the ionic and non-ionic species depending on the pH of the solution. In general, through the characterization of the polymers it has been shown that the surrounding media has a distinct influence on the size, stability, etc. of the micelle. The temperature, the solvent(s), the pH, or the ionic strength of the solution (addition of a salt) are parameters which can be used in order to make a tailored system containing micelles with predetermined properties.^{153,162,163}

The reason why PIB based amphiphilic block copolymers, one of the subject in this project, might be interesting is related to the properties of PIB. It is extremely hydrophobic compared to, for instance polystyrene, and it has a very low T_g (about -55°C). A low T_g can be an advantage, since it is known that if the hydrophobic block which is the core forming segment has a T_g higher than the ambient temperature, the core is in the glassy state which prevents the dynamic exchange of polymers between the micelles.¹⁵³

Information about the properties of these materials for example, in an aqueous solution can be obtained by utilizing static and dynamic light scattering (SLS and DLS), ultracentrifugation, fluorescence correlation spectroscopy (FCS), TEM and SEC.

1.3.2.3 (Amphiphilic) networks

A network is under ideal conditions represented by one single molecule. In the solid state, these materials can have properties varying from hard/brittle to rubbery. In a similar way as with block copolymers the determining factors with regard to mechanical properties are the composition, and in the case of networks the molecular weight between each junction point (M_c) as well. The corresponding material obtained after swelling the network in a solvent, is a gel. Although the fraction of the polymer network normally is relatively small, the gel persists solid-like as well as liquid-like properties^{164,165} which makes it interesting for a variety of biological and chemical systems. The properties or the behavior of a gel is closely related to the environmental conditions in the solution; solvent composition, temperature, ions (salts), pH, light, electrical field etc. and also to

internal conditions (between polymer segments) such as Van der Waals, hydrophobic, and ionic interactions and hydrogen bonding.¹⁶⁶

Flory¹⁶⁷ proposed to subdivide the networks/gels into four different types:

1. Well-ordered lamellar structures, including mesophases.
2. Covalent bonded polymer networks, completely disordered.
3. Networks formed through physical aggregation, predominantly disordered, but with regions of local order (similar to TPE, see above).
4. Particulate, disordered structures.

In this work only networks/gels of type 2 are of interest, and especially those containing both hydrophilic and hydrophobic segments, amphiphilic networks (APNs).

Definition: Amphiphilic networks consist of hydrophilic and hydrophobic chain segments crosslinked by covalent bonds, and are swellable in both hydrophilic and hydrophobic solvents.

The unique properties of APNs are related to the composition of hydrophobic and hydrophilic chain segments. Because of the combination of two different components, the network swells in, e.g. water and n-heptane.^{62,63} Swelling kinetics give to a certain extent information about the degree of crosslinking, since the absorption of a solvent increases with decreasing number of junctions per linear polymer segments. In relation to a hydrogel synthesized by radical polymerization of HEMA and EGDMA, it was shown that the (swelling)/ mechanical properties are directly correlated to the amount of crosslinker, EGDMA.¹⁶⁸ Besides, the degree of swelling changes significantly with the ratio of the hydrophobic and hydrophilic segments.¹⁶⁹

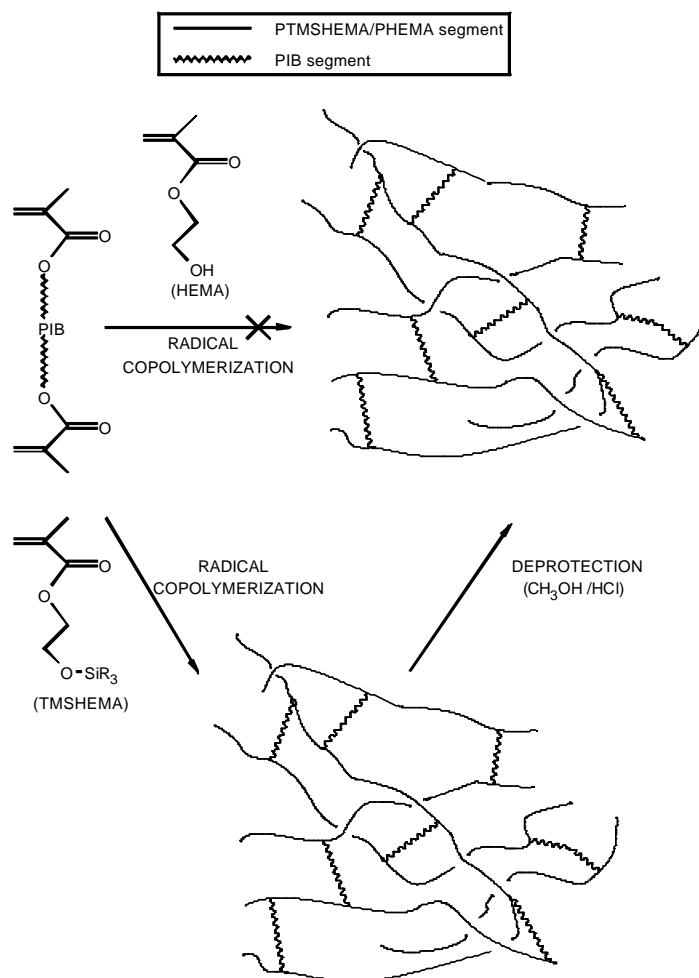
One of the promising applications for these materials are drug release devices due to their ability to perform a gradually (or even constant) drug delivery with known concentration profiles. An important parameter related to this usage is the kinetics of this release process. The rate and type of release can be analyzed by the following expression:

$$M_t/M_g = kt^n,$$

where M_t is the amount released at time t and M_g the total amount loaded, n an exponent characteristic for the mode of delivery and k a system parameter. $n = 0.5$ indicate pure Fickian diffusion, whereas $n > 0.5$ is due to anomalous transport. If $n = 1$ (zero order release) the transport is controlled by polymer relaxation.¹⁶⁹

In general transport through polymeric membranes is described in term of two mechanisms: The pore mechanism and the solution-diffusion mechanism.^{170,171} In the first type, the diffusion rate is controlled primarily by the pore size of the membrane and the molecular volume of the solute. The second mechanism is predominately related to the physical-chemical properties of the solute and the membrane. In order to follow the release UV spectroscopy can be used by monitoring the concentration of the drug in a water reservoir in which a loaded network is placed.

Because of the distinct difference between the segments, DSC traces of such materials show two T_g s indicating microphase separation into, e.g. PDMAA (thermoplastic part) and PIB (rubbery part) domains¹⁶⁹, like corresponding block copolymers, PMMA-*b*-PIB-*b*-PMMA¹¹⁶.



Scheme 1.13: Synthesis of PIB and PHEMA based amphiphilic network by the combination of cationic and conventional radical polymerizations

By the combination of cationic polymerization of IB and radical polymerization of TMSHEMA and telechelic PIBs containing a methacrylic chain end¹⁷² the first generation of PIB-based APNs have been synthesized (Scheme 1.13)⁶³. A similar APN was synthesized by the procedure illustrated in Scheme 1.13 using DMAA as the hydrophilic component. Interesting properties were observed, e.g. swelling profiles and diffusion properties (sustained drug delivery).

The major problem in this procedure (Scheme 1.13) is the statistical distribution of the crosslinking points along the PTMSHEMA or PDMAA backbone leading to an undefined M_c . Therefore, on a microscopic level only the length of the PIB segment is well-defined which makes it difficult to synthesize APNs with predictable properties.

Based on these facts, one of the purposes of this project is to find methods which may lead to a higher degree of control of the microstructure, and thereby to tailored materials which can lead to the more detailed understanding about parameters influencing the properties of an APN and to materials with new potential applications.

2 Motivation

The major motivations, for synthesizing functionalized PIBs, PIB-based block copolymers, and PIB-based amphiphilic networks are directly related to potential (industrial) applications and scientific interests. Applications in biomedical areas are of special interest. However, thermoplastic elastomers with specific properties also show interesting perspectives in material science in general. Regarding functionalized PIBs, the major aims are to find new/simpler synthetic routes for the preparation of common endgroups.

Most of the biomaterials up to now (especially HEMA-based materials) have been prepared by conventional methods like free radical polymerization (and polycondensation), where the structures cannot be controlled. Therefore, the objective is to find methods by which tailored materials can be synthesized, and thereby every parameter characterizing the product can be controlled. When this stage is reached, systematic characterization can be carried out in order to optimize the properties, and to get more knowledge about structure-property relationship at the same time.

By synthesizing block copolymers using different living/controlled polymerization procedures, new materials i.e. substitutes with improved and predictable properties can be obtained. Amphiphilic AB block copolymers are, for example, potential emulsifiers and drug delivery pools. ABA block copolymers can be used e.g., as thermoplastic elastomers, membrane materials, and for design/production of biomedical devices such as implants. Amphiphilic networks in which block copolymers are cured/linked together by a crosslinker represent another level in this regard. Potential applications of these are implants, wound dressings, artificial organs, drug delivery devices, membranes etc.

keeping in mind that each polymerization procedure is limited, e.g. due to the fact that IB can only be polymerized by cationic polymerization and MMA only by anionic or radical polymerization, a certain strategy is needed in order to reach the wanted materials. That means a certain number of questions have to be considered:

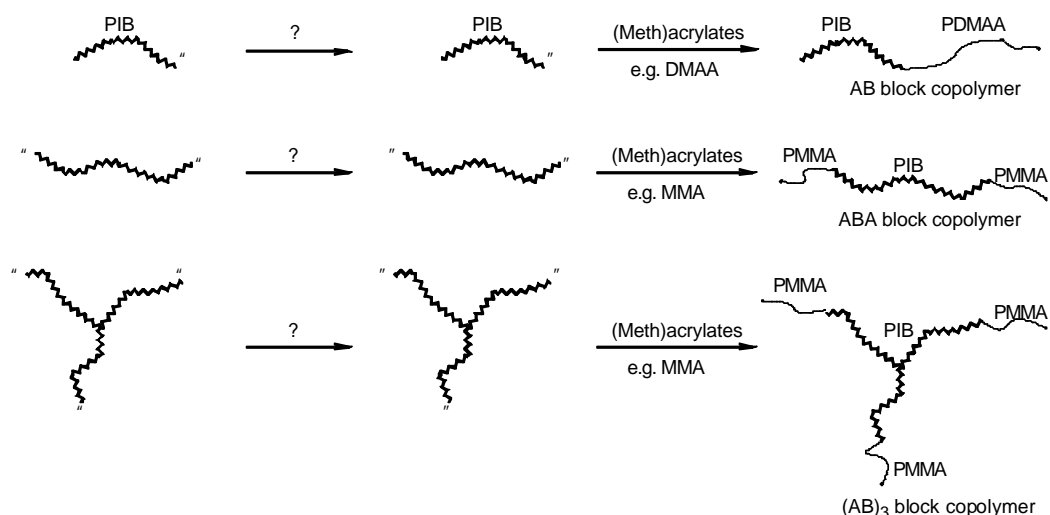
- Which polymer segment is polymerized first and what kind of initiator fragment is used in order to facilitate the cross-over from one method to another?
- Which of the available hydrophilic monomers are of special interest and do some of these involve special complications?
- Which morphologies are desired for different purposes?
 - What are the best compositions and molecular weights of the segments in (water-soluble) AB block copolymers?
 - How are ABA block copolymers obtained, from a difunctional initiator or through coupling of two AB block copolymers, and what compositions and molecular weights of the segments lead to optimum properties?
 - How can tailored amphiphilic network structures be synthesized from block copolymers and what kind of structural defects might be present?

3 Strategy

Based on the results from the literature, which have been introduced in chapter 1, it really seems necessary to start from the beginning concerning considerations about the transformation from living/controlled cationic polymerization (LC^+Pzn) to living/controlled anionic polymerization (LA^-Pzn). The other way around, first LA^-Pzn and then LC^+Pzn is not feasible, since oxygen atoms (e.g. in (meth)acrylates) disturb the polymerization of isobutylene (IB), due to the complexation of the Lewis acid with oxygen atoms.

Therefore, the desired way to solve this problem, is to prepare PIB precursors which contain endgroups suitable for subsequent LA^-Pzn , primarily of, (meth)acrylates. This means, that functional endgroups which can lead to sterically hindered carbanions with a versatile number of counterions are wanted. Two approaches are possible, either addition of DPE to living PIB chains or Friedel-Crafts alkylation of the $-Cl^+$ terminated PIB with diphenylmethane. In both cases the resulting carbanion is similar to $DPH-Li$, a common initiator for LA^-Pzn of (meth)acrylates, and the counterion can be varied due to the fact that metalation can be carried out with different alkali metals. The possibility to vary the counterion is essential, since many monomers can be polymerized optimally with one or two distinct counterions (MMA: Li and Cs; DMAA: Cs; tBMA: Li, K, and Cs; EO: K and Cs).

In order to obtain the desired ABA or $(AB)_3$ block copolymers, two possibilities have to be taken into account. Either the use of a multi-functional initiator in the LC^+Pzn of IB (Scheme 3.1) or a multi-functional quenching agent in the LA^-Pzn . Since, mono-, di-, tri-, and even polyfunctional initiators are accessible in cationic polymerization of IB this way is chosen for the synthesis of these block copolymers (Scheme 3.1).



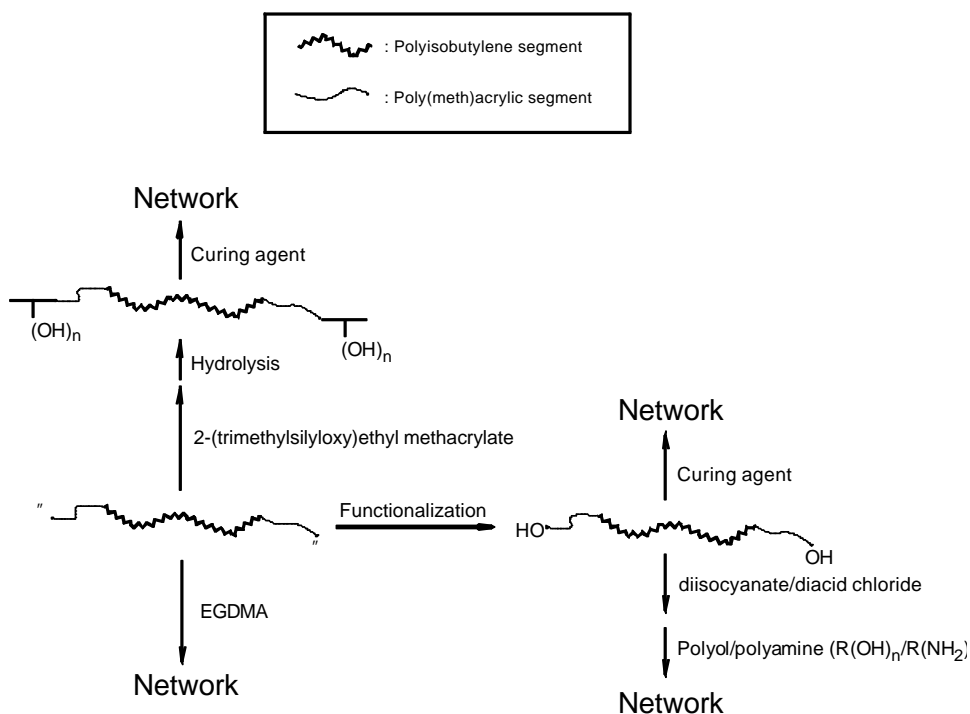
Scheme 3.1: Strategy for the synthesis of PIB-based block copolymers by the combination of cationic and anionic polymerizations.

The choice of molecular weights and compositions of the respective AB, ABA, and $(AB)_3$ block copolymers is based on the values used for similar block copolymers described in the literature. Especially in case of thermoplastic elastomers, optimum properties can mainly be reached

when $M_n = 30-60,000$ and the rubbery:hard segment composition is 60:40-80:20. In order to have AB block copolymers which are soluble in water, the hydrophilic segment needs to have a M_n equal or larger than the hydrophobic chain.

Concerning the synthesis of amphiphilic networks different methods are available (see Scheme 3.2):

- 1) Synthesis of ABC-type block copolymers containing an oligomer segment of HEMA units which can be used as crosslinker together with polyfunctional isocyanates or acid chlorides.
- 2) Synthesis of ABA/(AB)₃ block copolymers which are in situ crosslinked with a dimonomer like ethylene glycol dimethacrylate.
- 3) OH end-functionalized ABA/(AB)₃ block copolymers are crosslinked with polyfunctional isocyanates or acid chlorides.
- 4) OH end-functionalized ABA/(AB)₃ block copolymers are first refunctionalized with a diisocyanate or diacid chloride. These polymers are then crosslinked with polyols (R(OH)_n) or polyamines (R(NH₂)_n).



Scheme 3.2: Strategies for the synthesis of PIB-based amphiphilic networks.

4 Experimental

4.1 Materials

4.1.1 Cationic polymerization

Monomers: Pure isobutylene (IB) was donated by BASF. For purification, it passed through a drying column, "Labclear filter" (Aldrich) containing CaSO_4 and #13 molecular sieves. Isobutyl vinyl ether (Aldrich 99%) was first washed with 10 wt% $\text{NaOH}(\text{aq})$ solution. Then it was washed with distilled water 3 times and separated/dried over KOH pellets. Right before use it was distilled.

Solvents: CH_2Cl_2 was dried over CaH_2 and distilled right before use. *n*-Hexane was first purified by refluxing with sulfuric acid (10 v/v %) for 48 hours in order to remove olefins. The organic layer was washed with distilled water ($\text{pH}\approx 7$) and dried with MgSO_4 and stored over CaH_2 . Right before use it was distilled.

Initiators: TMPCl and CumCl were synthesized from the corresponding olefin compounds 2,4,4-trimethyl-1-pentene (Fluka, 98%) and α -methylstyrene (Merck, 99%) by hydrochlorination with $\text{HCl}(\text{g})$ at 0 °C for 6 h. Right before use, they were distilled under vacuum. $\text{tBuDiCumOH}^{34,173}$, tBuDiCumCl^{34} , and TriCumCl^{174} were prepared as described in the literature, and recrystallised right before use. The IBVE- HCl adduct, used as initiator for IBVE polymerization, was prepared by hydrochlorinating a 1M olefin free hexane solution of IBVE using $\text{HCl}(\text{g})$.

Coinitiators: TiCl_4 (Aldrich, 99.5%), BCl_3 (Aldrich, 1M solution in CH_2Cl_2), and ZnCl_2 (Aldrich, 1M solution in Et_2O) were used as received.

Additives: (DMA) (Aldrich 99+%, <0.005% water), (DtBP) (Aldrich, 97%), and (DPE) (Aldrich, 97%) were used as received.

Gas: In order to purify/dry the nitrogen (99.996% Messer Griesheim), it was passed through a drying column, "Labclear filter" (Aldrich) containing CaSO_4 and #13 molecular sieves.

Quenching agents: HEMA (Röhm GmbH) was purified by fractionated distillation. Ethan-1,2-diol (Aldrich, water-free 99.8%) and butan-1,4-diol (Aldrich 99%) were used as received. PEO 350, PEO 1000, and PEO 5000 (Fluka) were dried over MgSO_4 overnight and filtrated right before use or purified by azeotropic distillation from toluene. Hyperbranched polyols, 5. generation (Aldrich) were either used as received or purified by azeotropic distillation from toluene.

4.1.2 Anionic polymerization

Monomers: **MMA** and **tBMA** (Röhm GmbH) were fractionated by distillation and then stored over CaH_2 in a refrigerator. Both monomers were condensed under reduced pressure into a flask and titrated with AlEt_3 until a yellow color appeared right before use. Finally it was condensed into an ampoule.

TMSHEMA and **TBDMHEMA** were synthesized from HEMA (Röhm GmbH) and the corresponding chlorosilanes, TMS-Cl (Aldrich, 98%) and TBDM-Cl (donated by FMC Corporation Limited (UK)) in the following way:

TMSHEMA: 50 ml (0.41 mole) HEMA and 64 ml (0.46 mole) Et₃N were dissolved in 100 ml dry THF under nitrogen. This solution was cooled to 0°C. Then 47 ml (0.37 mole) TMS-Cl dissolved in 70 ml dry THF was added dropwise during 60 min to the HEMA solution. The reaction mixture was then slowly allowed to warm up to RT. The reaction was continued for additional 20 hours at RT. Then the THF was removed on a rotavap and to the remaining mixture 100 ml H₂O (5 wt% NaOH) was added. Subsequently extraction was performed with Et₂O (4 · 200 ml). The organic layer was finally washed with distilled water until neutral and dried over MgSO₄ overnight. After filtration the ether was removed on a rotavap, and the TMSHEMA was stored over CaH₂, yield: ≈ 100 % (verified, by GC and ¹H NMR), bp. ≈ 40 °C at about ≈ 6 · 10⁻³ mbar.

TBDMHEMA: 36 ml (0.260 mole) HEMA was dissolved in 110 ml dry DMF. To this solution 29.7 g (0.436 mole) imidazole was added and then cooled to 0°C under nitrogen. The reaction was started by dropwise addition of 30.0 g (0.197 mole) TBDM-Cl dissolved in 110 ml dry DMF over 45 min. The reaction mixture was stirred for additional 20 hours under nitrogen at RT. Finally a similar purification procedure was used as for TMSHEMA. Yield: ≈ 95% (verified by GC and ¹H NMR), bp. ≈ 50-55 °C at about ≈ 6 · 10⁻³ mbar.

TMSHEMA and TBDMHEMA were fractionated by distillation right before use. Finally they were purified in a glove-box by passing through a neutral Al₂O₃ column (Al₂O₃, neutral was dried under high vacuum at 250 °C for 48 hours) removing traces of HEMA (2-3%) which is formed during distillation.

DMAA (Aldrich, 99 %) was fractionated and dried by distillation from CaH₂ right before use. Additional purification was attempted on an Al₂O₃ column. However, DMAA was hydrolyzed during this purification step. Therefore, DMAA was only purified by distillation.

EO (Fluka, 99.8 %) was first condensed into a flask containing CaH₂ or BuLi and stirred for 3 hours at -10°C to 0°C. Finally it was condensed into an ampoule.

Solvents: THF was first fractionated by distillation over a 2 m column, then dried over potassium and distilled. On a vacuum-line the THF was first degassed and then dried over K/Na alloy. The THF was condensed into a second flask on the vacuum-line and stored over K/Na alloy. Right before use the THF was condensed into an ampoule. *n*-Hexane (Aldrich) was refluxed over concentrated sulfuric acid for 48 hours in order to remove olefins. The organic layer was washed with distilled water (pH ≈ 7) and dried with MgSO₄ and then first distilled from CaH₂ and finally condensed from K/Na alloy under dry N₂ atmosphere.

(Macro)initiators/(macro)precursors: See below in the respective experimental sections.

Metals/alloys: Cesium (Merck) was used as received. From potassium (Merck, > 98% in paraffin oil) and sodium (Merck, > 99% in paraffin oil) (3:1-5:1) the hydroxide surface was removed and subsequently they were melted in vacuo resulting in an alloy.

Additives: LiCl (Merck, > 99%) was dried for 48 hours at 200 °C under vacuum and stored under nitrogen. TMEDA (Aldrich, 99 %) was fractionated by distillation and dried over CaH₂. MeLi (Aldrich 1.6 M in Et₂O), n-BuLi (Aldrich, 1.6 M in n-hexane), and s-BuLi (Aldrich, 1.4 M in cyclohexane/hexane 92:8) were used as received. LDA (Aldrich, 10 wt % suspension in hexane) was used as received. DPM (Merck, 98%) was purified by distillation under reduced pressure.

Gas: Nitrogen (99.999%, Messer Griesheim) used at the vacuum-line was purified/dried by passing it through an oxisorb filter (Messer Griesheim) containing chromium(II) oxide, and three flasks containing toluene, K/Na alloy, and a small amount of benzophenone.

4.1.3 Network synthesis

Curing agents: MDI(A) (Aldrich, 98%), MDI(B) (BASF, 98%), HMDI (Aldrich, 98%), BTCTCl (Aldrich, 98%) AADCl (Aldrich, 98%) were used as received.

EGDMA (Aldrich, 98%) was first purified by fractionated distillation and then stored over CaH₂. Right before use it was condensed under reduced pressure into an ampoule. In a glove-box it was passed through an Al₂O₃ column in order to remove the last traces of impurities

Catalysts: DABCO (Aldrich, 98%), pyridine (Fluka, H₂O < 0.005%, 99.8%) were used as received.

4.2 Cationic polymerization

4.2.1 Synthesis of TMP-DPOMe and TMP-DPV

CH₂Cl₂ (100ml), n-hexane (220 ml), TMPCl (3.36 · 10⁻² mole), and DMA (3.36 · 10⁻² mole) were added to a three necked flask (reactor) equipped with a nitrogen fitting, a septum, and a magnetic stirrer. In a separate flask a stock solution of TiCl₄ was prepared: TiCl₄ (0.134 mole), DtBP (4.2 · 10⁻⁴ mole, final concentration: 10⁻³ M), and CH₂Cl₂ (50 ml). Both solutions were cooled to -78 °C and subsequently mixed. After 10 min premixing a prechilled solution of DPE (3.69 · 10⁻² mole, 10% excess) in 20 ml CH₂Cl₂ and 30 ml n-hexane was transferred by a transfer needle to the reactor. The reaction was quenched after 90 min with precooled methanol and right after (2 min) 220 ml NH₃ (aq, 5N) and 450 ml CH₃OH was added.

In order to obtain DPTMH, the living solution is quenched only with methanol. Sometimes further reaction with HCl (in CHCl₃) is needed for quantitative elimination of methanol.

Purification : In order to obtain the wanted material TMP-DPOMe and TMP-DPV 100% pure (free of e.g. DMA or DPE) recrystallisation is necessary. n-Hexane was used for recrystallisation of TMP-DPOMe and ethanol for recrystallisation of TMP-DPV.

4.2.2 Cationic polymerization of isobutylene

All polymerization experiments are performed by a simple laboratory process.^{35,175} In the following examples a monofunctional initiator has been used. Similar experiments have been carried out with di- and trifunctional initiators. In order to obtain polymers with other M_n's only small changes in molar ratios and concentrations of the components are utilized.

One-step procedure using TiCl_4 as Lewis acid:

Procedure 1:

To a mixture of 230 ml n-hexane and 155 ml CH_2Cl_2 in a three necked flask (reactor) equipped with a nitrogen fitting, a septum, and a magnetic stirrer (in experiments where more than 10 g polymer was prepared a mechanical stirrer was used), 0.47 ml ($5.0 \cdot 10^{-3}$ mole) DMA was added. This mixture was cooled to -78°C . In a separate flask 744 mg ($5.0 \cdot 10^{-3}$ mole) TMPCl was diluted with 10 ml n-hexane and 6 ml CH_2Cl_2 and cooled to -78°C . Pure TiCl_4 5.5 ml ($5 \cdot 10^{-2}$ mole) was added to the reactor containing the DMA solution. After 3 min premixing the prechilled TMPCl solution was transferred to the reactor. 2 min later, 7 ml IB (0.09 mole) was added by syringe. The polymerization was quenched with prechilled methanol 20 min after the addition of IB.

Procedure 2:

To a mixture of 80 ml n-hexane and 80 ml CH_2Cl_2 in a three necked flask (reactor) equipped with a nitrogen fitting, a septum, and a mechanical stirrer, 450 mg ($3 \cdot 10^{-3}$ mole) TMPCl and 0.28 ml ($3 \cdot 10^{-3}$ mole) DMA were added. This solution was cooled to -78°C . 10 ml (0.129 mole) IB was then added by syringe. After 5 min premixing a stock solution of 40 ml CH_2Cl_2 , 100 ml n-hexane, 6,6 ml (0.06 mole) TiCl_4 , and 0.1 ml DtBP was added by a transfer needle to the reactor. 10 min later a second amount of IB, 11 ml (0.141 mole) was added. The polymerization was quenched with prechilled methanol 20 min after the second addition of IB.

One-step procedure using BCl_3 as Lewis acid:

100 ml CH_2Cl_2 , 0.19 ml ($2 \cdot 10^{-3}$ mole) DMA, and 296 mg ($2 \cdot 10^{-3}$ mole) TMPCl are transferred to a three necked flask (reactor) equipped with a nitrogen fitting, a septum and a magnetic stirrer. This solution is cooled to -78°C . In a second flask 70 ml (1 M BCl_3 in CH_2Cl_2) is cooled to -78°C . The BCl_3 solution is added using a transfer needle to the reactor. After 5 min premixing 3 ml (0.039 mole) IB was added by syringe. 15 min after the addition of IB, the polymerization was quenched with prechilled methanol.

Two-step procedure using BCl_3 and TiCl_4 as Lewis acids:

(1st step): 160 mg ($1.04 \cdot 10^{-3}$ mole) CumCl, 40 ml CH_2Cl_2 , and 91 mg ($1.04 \cdot 10^{-3}$ mole) DMA were poured into a three necked flask equipped with a nitrogen fitting, a septum, and a magnetic stirrer (in the experiments where more than 10 g polymer was prepared a mechanical stirrer was used). This mixture was cooled to -78°C . 20 ml of a prechilled 1M solution of BCl_3 in CH_2Cl_2 (0.02 mole) was transferred by a needle to the reactor. After 5 min premixing, 2 ml condensed IB was added by syringe.

(2nd step): After 60 min reaction time, a stock solution of n-hexane (90 ml), containing 1.1 ml ($1.04 \cdot 10^{-2}$ mole) TiCl_4 and 30 μl ($1.5 \cdot 10^{-4}$ mole) DtBP was charged by a transfer needle to the reactor. Subsequently additional 2.2 ml IB was added. 30 min later a third amount of IB (≈ 2.2 ml) was added. Finally the polymerization was quenched with methanol after a total polymerization time of 120 min.

Purification of polyisobutylene:

The solvents, CH_2Cl_2 , n-hexane, and CH_3OH were removed in vacuo. Because of the relatively labile tertiary chloro chain ends, the mixture cannot be heated up to more than about 30°C (elimination can take place). The brown polymer mixture containing PIB, inorganic boron and titanium compounds was dissolved in n-hexane. This solution was washed with concentrated HCl (32%) and water until $\text{pH} = 6-7$, and subsequently dried over MgSO_4 overnight. A small amount of the dry polymer solution was taken out for GPC analysis. The rest was added slowly to acetone or CH_3OH under stirring. n-Hexane and a part of the acetone/methanol were evaporated in the hood. This precipitation step was repeated one or two times. Finally the polymer was placed in a vacuum oven at ambient temperature until constant weight was reached.

4.2.3 Synthesis of DPE-capped PIB

Synthesis of diphenylmethoxy-ended PIB: When a combined $\text{BCl}_3/\text{TiCl}_4$ coinitiator system was used the following procedure was carried out for IB polymerization. To a three-necked flask (reactor) equipped with a septum, a mechanical stirrer, and a nitrogen inlet, 18 ml CH_2Cl_2 , 0.08 ml N,N-dimethylacetamide (DMA), and 128 mg TMPCl were added and then cooled to -78°C . 2 ml IB was charged to the reactor by a syringe. After 5 min stirring, 18 ml BCl_3 (1M in CH_2Cl_2) was transferred to the reactor by a transfer needle. After 10 min, 0.5 ml TiCl_4 in 54 ml n-hexane (olefin-free) containing 0.03 ml 2,6-di-*tert*-butylpyridine (DtBP) was added. Subsequently, additional 4 ml IB was charged to the polymer solution. 10 min later a solution containing 0.76 ml DPE (5 times excess relative to the living chain ends), 3 ml n-hexane, and 2 ml CH_2Cl_2 was added. The color of the solution changed from slightly yellow to orange. DPE was allowed to react with the living chain ends for 25 min. Finally, the reaction was quenched by addition of 30 ml prechilled methanol. 2 min later a mixture of 40 ml NH_3 (aq) and 160 ml methanol was added in order to obtain $\text{pH} > 8$, thus avoiding elimination of methanol.

When only TiCl_4 was used as a coinitiator, to a three-necked flask equipped with a septum, a mechanical stirrer, and a nitrogen inlet, 80 ml CH_2Cl_2 , 80 ml n-hexane (olefin-free), 0.28 ml DMA, and 450 mg TMPCl were added and then cooled to -78°C . 10 ml IB was charged to the reactor by a syringe. After 5 min stirring a stock solution of TiCl_4 (40 ml CH_2Cl_2 , 100 ml n-hexane, 6.6 ml TiCl_4 , and 0.1 ml DtBP) was transferred to the reactor by a transfer needle. After 10 min a second addition of 11 ml IB followed. 10 min later a solution of DPE (2.65 ml DPE, 6 ml n-hexane, and 4 ml CH_2Cl_2) was added to the polymerization system (the color of the solution changed from slightly yellow to dark red). DPE was allowed to react with the living chain ends for 20 mins. Finally the reaction was quenched by addition of 30 ml prechilled methanol. 2 min later a mixture of 100 ml NH_3 (aq) and 400 ml methanol was added.

Synthesis of diphenylvinyl-ended PIB: Nearly the same procedure as for the synthesis of diphenylmethoxy-ended PIB was used, only pure methanol was used for quenching. The crude polymer solution (acidic) was allowed to stand for a least 4 hours in order to provide elimination of

methanol at the chain end. Sometimes subsequent treatment with catalytic amount of HCl in CHCl_3 at RT was necessary in order to obtain quantitative elimination of methanol.

Similar experiments were performed with the 5-*tert*-butyl-1,3-dicumylchloride (tBuDiCumCl) and 1,3,5-tricumylchloride (TriCumCl) initiators in order to obtain di- and trifunctional polyisobutylenes.

Purification of polyisobutylene:

After quenching the polymerizations, the crude mixture was filtered in order to remove the titanium complexes. During filtration additional *n*-hexane was added. Then the *n*-hexane phase was isolated and washed once with $\text{NH}_3(\text{aq})$ and subsequently with water until neutral. The organic layer was separated and dried over MgSO_4 for about 2 hours. Subsequently, the solution was filtered and the solvent was removed on a rotavap. Then the polymer was redissolved in a small amount of *n*-hexane and precipitated two or three times into acetone in order to remove excess DPE.

4.2.4 Quenching of living DPE-capped PIB with different alcohols

As described in 4.2.3 regarding the synthesis of diphenylmethoxy-ended PIB, living DPE-capped PIBs were quenched in a comparable way with different alcohols; HEMA, butan-1,4-diol, ethan-1,2-diol, PEOs containing 1 or 2 OH groups, and hyperbranched polyols containing 16 or 128 OH groups instead of methanol.

4.2.5 Synthesis of OH-functionalized PIB using the isopropenyl-ended PIB

Dehydrochlorination of -Cl^t terminated PIB:

Method 1: 1.0 g PIB ($M_n = 5,300$) and 1.0 g tBuOK were dissolved in 45 ml THF at RT. This solution was either a) refluxing (65 °C) for 20 h, b) reacting at 40 °C for 27-122 h or c) at RT for 24-72 h.

Method 2: 1.0 g tBuOK was dissolved in 20 ml THF and heated to 65 °C. To the refluxing tBuOK solution, 1.0 g PIB ($M_n = 5,300$) in 25 ml THF was added slowly during 20 min. The reaction was stopped after 20 h.

In both cases 10 ml *n*-hexane was added when the polymer solution was cooled to RT. Subsequently, 10 ml distilled water was added and stirred for 10 min. Finally the hexane solution was washed with distilled water until neutral and dried over MgSO_4 .

Hydroboration/oxidation of isopropenyl-ended PIB:

5 ml 9-BBN (0.5M in THF) was diluted with 15 ml THF. To this solution 1.0 g isopropenyl-ended PIB dissolved in 20 ml THF was slowly added (30 min). The mixture was stirred for 5 h under nitrogen. Then 4 ml 3N KOH in methanol and 1 ml 30 wt% $\text{H}_2\text{O}_2(\text{aq})$ was transferred to the reactor. During the addition of KOH/ H_2O_2 the temperature was kept below 45 °C. The reaction was continued for 4 h at RT. At the end 10 ml *n*-hexane was added and stirred for 5 min. Subsequently, the solution was washed with $\text{K}_2\text{CO}_3(\text{aq})$ until neutral and then the organic layer was separated and dried over MgSO_4 overnight.

4.2.6 Synthesis of OH functionalized PIB using ethylene oxide

100 mg PIB, $M_n = 1,100$ ($n_{\text{endgroups}} = 9.1 \cdot 10^{-5}$ mole) was dissolved in 20 ml THF. Metalation with K/Na alloy was performed as described in section 4.4. After filtration, the macroinitiator solution was cooled to 0 °C. To this solution about 0.5 g EO was added. Within less than 10 min the solution became colorless and subsequently it was quenched with $\text{CH}_3\text{COOH}/\text{CH}_3\text{OH}$. The solvents were removed by a rotavap, and the crude product was directly analyzed.

A similar experiment was also carried out with the metallated model compound, leading to 5,5,7,7-tetramethyl-3,3-diphenyloctan-1-ol.

4.2.7 Polymerization of vinyl ethers and attempted functionalization

150 ml CH_2Cl_2 , 8.0 ml ($6.16 \cdot 10^{-2}$ mole) IBVE, and 20 ml IBVE-HCl (0.1 M in n-hexane, $2 \cdot 10^{-3}$ mole) are transferred to a three necked flask (reactor) equipped with a nitrogen fitting, a septum, and a magnetic stirrer. This solution is cooled to -15 °C. In a second flask 20 ml ZnCl_2 ($2 \cdot 10^{-3}$ M in 19.96 ml $\text{CH}_2\text{Cl}_2/0.04$ ml Et_2O) is cooled to -15 °C. In order to get information about the kinetics, samples are withdrawn by syringe and quenched with methanol. After 180 min the polymerization was stopped by quenching with methanol.

In a second experiment using the same amounts as above, 1.35 ml DPE ($7.5 \cdot 10^{-3}$ mole) was added before the final quenching with methanol, in order to get DPE-capped PIBVE.

4.3 Lithiation/metalation experiments with TMP-DPV, DPM, and with Cl^t -capped PIB

4.3.1 Lithiation of TMP-DPV and DPM

A detailed description of the experimental conditions used for lithiation of TMP-DPV and DPM is found in Table 5.3 and 5.4.

4.3.2 Metalation of Cl^t -capped PIB

Metalation of Cl^t -capped PIB was carried out under different conditions. The temperature and the solvent were varied.

Purification of PIB: 1.0 g PIB ($M_n = 3,700-6,500$) was dissolved in THF and dried over CaH_2 for more than 24 hours. The solution was filtered in a glovebox. THF was then removed under high vacuum (48 hours at RT).

The PIB sample was redissolved in 50 ml freshly distilled THF or n-hexane. Metalation was performed with 2 g K/Na alloy at -78°C or 20°C. The reaction was quenched after a certain time with methanol.

4.4 Metalation of TMP-DPV, TMP-DPOMe, and the corresponding PIB precursors

Metalation was either carried out with K/Na alloy at RT in THF or THF:n-hexane (70:30) or with Cs metal at 35°C in THF or with a Na mirror at RT in THF. The concentration of TMP-DPOMe,

TMP-DPV, and PIB chain ends were in range $1.5\text{-}5 \cdot 10^{-3}$ M. The UV-VIS spectrum was recorded in a quartz cuvette (10 mm, equipped with a 9.8 mm spacer) attached to a glass reactor in which the metalation took place (see below). The absorbance was followed at $\lambda_{\text{max}} = 480$ nm. At the time when constant absorbance was reached subsequent polymerization could be performed (see section 4.5 below).

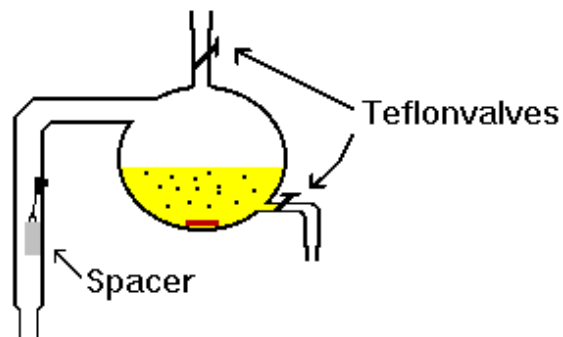


Figure 4.1: UV cell connected to the reactor used for following the degree of metalation.

4.5 Anionic polymerization

4.5.1 Synthesis of PIB-*b*-PtBMA and PIB-*b*-PMAA block copolymers

1.0 g DPOMe-capped PIB ($M_n = 5,800$) was dissolved in THF and dried over CaH_2 for more than 24 hours. The solution was filtered in a glovebox either using an Al_2O_3 column or a millipore filter. THF was then removed under high vacuum (48 hours at RT). The PIB was redissolved in 60 ml freshly distilled THF. Metalation was performed with 2 g K/Na alloy at RT. After constant absorbance was observed at $\lambda_{\text{max}} = 480$ nm, the suspension was filtered into a flamed reactor in a glovebox. On a vacuum line the solution was cooled to -78 °C. tBMA was added in bulk to the initiator solution during 10-20 sec, and after 90 min the polymerization was quenched with methanol.

Hydrolysis of PIB-*b*-PtBMA leading to polyisobutylene-*b*-poly(methacrylic acid) (PIB-*b*-PMAA) was carried out in refluxing dioxane (≈ 10 wt-% polymer solution) containing 5 times excess water relative to tBMA units in the form of a HCl solution (32 wt-% HCl) for 24 hours. In order to remove colored impurities and unreacted PIB nearly all of the dioxane was removed by rotavap, then the polymer was stirred with diethyl ether (PIB with $M_n < 10,000$ is soluble in Et_2O) for more than 24 hours. Finally, the ether suspension was centrifuged. The precipitated polymer was separated by decantation and dried in a vacuum oven at room temperature.

In order to obtain a homogeneous water solution of some of the PIB-*b*-PMAA block copolymers (for the characterization experiments involving, e.g. DLS, SLS, etc.) two different solvent exchange procedures were utilized:

Samples 1 and 2 (see Table 5.24): 5 g block copolymer was dissolved in 50 ml CH_3OH . To this solution 50 ml water was added. Subsequently neutralization with $\approx 150\text{-}200$ ml (0.2 M NaOH) was performed (about equimolar NaOH relatively to the acid groups, until $\text{pH} \approx 12.5$). Then the methanol was nearly removed (100 ppm) by evaporation (70 °C and 250 mbar) leading to a 3 wt-%

polymer solution. Traces of undissolved material was removed by filtration. This solution was used directly or diluted for the characterization.

Samples 3 and 4 (see Table 5.24): 5 g block copolymer was swollen in 5 ml CH₃OH and then dissolved in 500 ml THF. To this solution 500 ml water was added followed by neutralization with \approx 150-200 ml (0.2 M NaOH) was performed (about equimolar NaOH relatively to the acid groups, until pH \approx 12.5). Subsequently some of the solvents were removed by evaporation (70 °C and 250 mbar) leading to a 3 wt-% polymer solution. Traces of undissolved material was removed by filtration. This solution was used directly or diluted for the characterization.

Samples 5-8 (see Table 5.25): The samples are directly soluble in alkaline water (pH > 10).

Sample 9 (see Table 5.25): The sample is directly soluble in neutral water.

4.5.2 Synthesis of PMMA-*b*-PIB-*b*-PMMA and PIB-*b*-(PMMA)₃ block copolymers

After reaching constant absorption in the UV-visible spectrum of telechelic DPOMe- or DPV-ended PIB metallated with K/Na alloy, the reaction mixture was filtered, and LiCl (10 times excess) was added and stirred for 20 min. The polymerization of MMA was carried out at -78 °C and quenched with methanol after 90 min. Then the solvents were removed by rotavap. The polymer was subsequently dissolved in about 20 ml THF and precipitated into 300 ml CH₃OH in order to remove inorganic salts. The polymer was separated by filtration and dried in a vacuum oven at 40 °C.

4.5.3 Synthesis of homopolymers of N,N-dimethylacrylamide

- I) 55 mg DPOMe ($1.7 \cdot 10^{-4}$ mole) was dissolved in 70 ml THF and metallated as described in section 4.4 with Cs metal. After filtration the initiator solution was cooled to -78 °C. 1.2 g DMAA was added during 10 sec to the reactor. The polymerization was quenched after 40 min with methanol.
- II) In an identical experiment (as I)) a second amount of DMAA (3.2 g) was added to the living PDMAA chain end after 40 min. The polymerization was quenched with methanol after a total reaction time of 80 min.
- III) In an identical experiment (as I)) 3.8 g MMA was added to the living PDMAA chain end after 40 min. The polymerization was quenched with methanol 60 min after the addition of MMA.

PIB-based block copolymers can be synthesized in a similar way (as I)) using mono-, di-, and trifunctional PIB precursors.

4.5.4 Synthesis of homo- and block copolymers of ethylene oxide

50 mg ($1.7 \cdot 10^{-4}$ mole) TMP-DPV was dissolved in 50 ml THF. Metalation with K/Na alloy or Cs metal was performed as explained in section 4.4. The initiator solution was cooled to 0 °C. Then 0.5 g EO diluted in 5 ml THF was added. During 60 min the solution was allowed to warm slowly to RT. For additional 2 hours, it was kept at this temperature before it was heated to 50 °C.

After 24 hours at 50 °C the polymer solution was quenched with CH₃COOH/CH₃OH. The solvents were removed by a rotavap, the crude product was directly analyzed.

Similar experiments were carried out with TMP-DPOMe, mono-, di-, and trifunctional PIB precursors leading to the desired block copolymers. The materials are precipitated and freeze-dried after analysis in order to obtain pure and dry polymers for subsequent curing reactions.

4.5.5 Hydrolysis experiments with tBMA, TBDMHEMA, TMSHEMA, and DMAA

About 0.2 ml monomer (tBMA, TBDMHEMA, TMSHEMA, and DMAA) was diluted with 10 ml THF and 1 ml distilled water. To this solution 0.09 ml CH₃COOH or 0.08 ml HCOOH or 0.16 ml HCl (37 wt%) was added. Samples were withdrawn during the hydrolysis and directly analyzed with GC.

4.5.6 Synthesis of ABC type block copolymers of IB, tBMA/DMAA/TBDMHEMA, and TMSHEMA

Synthesis of PtBMA ($P_n = 35$) with a short block of HEMA ($P_n = 3-10$) chain segments: 170 mg LiCl and 43 mg methyl α -lithio isobutyrate (MiBLi) were dissolved in 70 ml THF and cooled within 10 min to -20 °C. tBMA (2.0 g) diluted in 5 ml THF was added during 2 sec. After 10 min reaction time at -20 °C, the solution was cooled to -78°C (during 5 min). Subsequently, the calculated amount of TMSHEMA (240-800 mg) diluted in 5 ml THF was added to the living PtBMA solution during 2 sec. The TMSHEMA was allowed to react for 25 min. Finally the polymerization was quenched with methanol. The obtained material was precipitated into a 1:3 v/v H₂O:CH₃OH mixture.

Selective hydrolysis of the TMSHEMA segment was performed with formic acid in the following way: 2 g polymer was dissolved in 20 ml THF and 2 ml water. To this solution 2 times molar excess of HCOOH was added and allowed to react for 18 hours at RT. Then half of the solvent was removed on a rotavap. The concentrated polymer solution was precipitated into a 1:3 v/v H₂O:CH₃OH mixture. Finally the polymers were freeze-dried from benzene.

Similar experiments were carried out with mono-, di-, and trifunctional PIB precursor in order to obtain the desired ABC type block copolymers.

4.6 Synthesis of amphiphilic networks

4.6.1 Method 1

The curing reactions were performed in an apparatus containing teflon molds as illustrated in the following sketch:

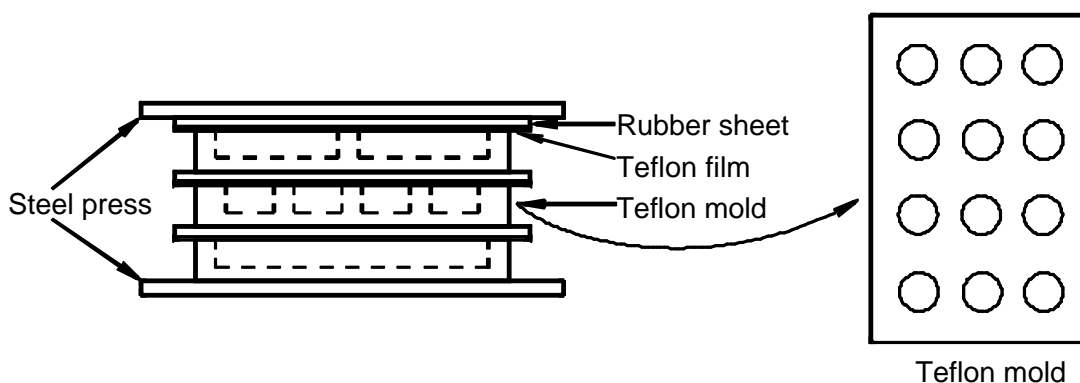


Figure 4.2: Teflon apparatus used for curing reactions with isocyanates or acid chlorides and HEMA containing polymers.

4.6.1.1 Synthesis of star polymers of PtBMA by curing with diisocyanates

Synthesis of star-shaped PtBMA was performed in the following way by curing PtBMA-*b*-PHEMA with MDI/HMDI: Solvent: toluene or THF (3 ml), PtBMA-*b*-PHEMA ($DP_{n, \text{HEMA}} = 3-10$, $m_{\text{polymer}} = 200$ mg), and catalyst: DABCO or dibutyltin didodecanoate (5 mole % regarding free OH groups) were mixed together in a teflon mold or a glass flask under nitrogen in a glove-box and subsequently placed in a oven. Reaction time: Toluene: 48-150 h, at 80 °C and 16 hours where the solution was slowly cooled to RT; THF: 44 h at 60 °C, and 16 h where the solution was slowly cooled to RT.

4.6.1.2 Synthesis of star polymers of PtBMA by curing with di- and triacid chlorides

Synthesis of star-shaped PtBMA was performed in the following way by curing PtBMA-*b*-PHEMA with MDI/HMDI: Solvent: toluene or THF (3 ml), PtBMA-*b*-PHEMA ($DP_{n, \text{HEMA}} = 3-10$, $m_{\text{polymer}} = 100-200$ mg), and pyridine (5 times excess regarding free OH groups) were mixed together in a teflon mold or a glass flask under nitrogen in a glove-box and subsequently placed in a oven. Reaction time: THF: 44-144 h at 20-40 °C.

4.6.2 Method 2

4.6.2.1 Synthesis of amphiphilic networks of PMAA-*b*-PIB-*b*-PMAA block copolymers crosslinked with EGDMA

0.95 g PIB ($M_n = 5700$, $n_{\text{endgroups}} = 3.33 \cdot 10^{-4}$ mole) was dissolved in 70 ml THF ($[C^-] = 4.8 \cdot 10^{-3}$ M). Metalation was performed in the usual way (see section 4.4). After constant absorbance was reached, filtration was carried out and subsequently 10 times excess LiCl ($3.33 \cdot 10^{-3}$ mole, 140 mg) was added. The macroinitiator solution was cooled to -20 °C. Then, 1.57 g tBMA was added during ≈ 10 sec. After 10 min reaction time the solution was cooled further to -78 °C during 10 min. EGDMA ($1.66 \cdot 10^{-3}$ mole, 330 mg, $n_{\text{EGDMA}} = 5 \cdot n_{\text{endgroups}}$) diluted in 5 ml THF was added. After 16 hours the reaction was quenched with methanol. The obtained network was hydrolyzed in the following way in order to get the PMAA segments: the crude product, about 2.5 g was mixed with 25 ml dioxane and 1.35 ml 37 wt % HCl(aq) ($n_{\text{tBMA}} = 5 \cdot n_{\text{water}}$) and this solution was refluxed for 24 hours. The solvents were removed on a rotavap and subsequently mixed with distilled water and

neutralized with KOH (pH = 7-9). Finally the material was dried in a vacuum oven until constant weight was reached.

4.7 Characterization methods

4.7.1 Size exclusion chromatography (SEC)

In SEC, the polymers are separated through the diffusion into the pores of the column material. Polymers with a low M_n pass a higher number of pores on their way through the column and therefore, they are eluated later than high molecular weight polymers. Thermodynamically it correlates to the entropy (ΔS).

The molecular weights and molecular weight distributions (MWD) were determined by SEC calibrated with PIB, PMMA, and PtBMA standards. For the block copolymers a weighted average of the homopolymer calibration curves were used.

Data related to used SEC apparatus: Eluent: THF (flowrate: 1.0 ml/min); temperature: RT; detectors: 2 x JASCO-UVIDEC 100 III with variable wavelength, Bischoff RI detector 8110; columns: PSS SDV-gel 5 μ , 60 cm, 1x linear (10^2 - 10^5 Å), 1x 100 Å. Software: Win-GPC4.0 from PSS.

SEC measurements of PDMAA samples are discussed in chapter 5.

4.7.2 High Performance Liquid Chromatography (HPLC) under critical conditions

In HPLC the separation of polymers is achieved by adsorption on the pore material which corresponds to the thermodynamic quantity, enthalpy (ΔH). The critical point of adsorption is related to a chromatographic situation (through the choice of solvents and temperature), where the entropic and enthalpic interaction of the polymers and the column material compensate for each other. The free energy of the polymer does not change when entering the pores of the stationary phase ($\Delta G = 0$, $T\Delta S = \Delta H$).¹⁷⁶ Based on this relation, the distribution coefficient $K_d = 1$ ($\Delta G = -RT \ln K_d$, where K_d is equal to the ratio of the analyte concentration in the stationary phase and in the mobile phase), meaning all polymers with chemically equal structure elute in one peak irrespective of the molar mass.

Therefore, this analysis method can be used to separate homopolymers with different endgroups and homopolymers from block copolymers. In case of block copolymers the conditions are adjusted in a way where one of the segments is "invisible" at the critical point and the second in SEC mode and thereby, blocking efficiencies can be calculated.

Data related to the used HPLC apparatus: Temperature: 35 °C; Solvents: depend on the analyzed polymers; Pump: Thermo Separation products (TSP) P4000, flow-rate: 0.5 ml/min; UV-detector (TSP UV3000) with variable wave-lengths; Evaporating light scattering detector (Polymer Laboratories): analysis temperature: 40-60 °C and gas flow-rate: 3-4 l/min; columns: depend on the analyzed polymers. Software: Win-GPC4 from PSS.

The conditions for critical HPLC analysis of PtBMA are: Column combination: Modified-YMC, S-5 μ m, 25 cm x 4 mm, RP18, 120 Å and 300 Å and solvent mixture: THF:CH₃CN 53:47.

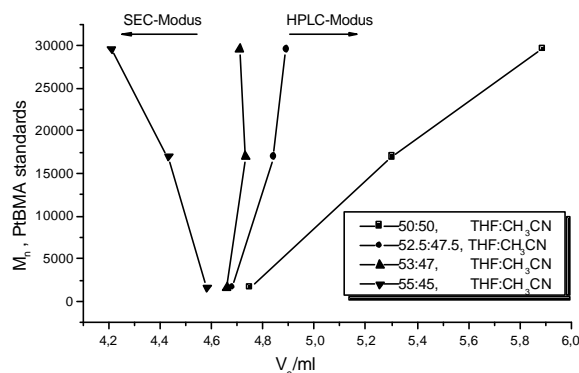


Figure 4.3: The influence of different solvent mixtures of THF and CH₃CN on the molecular weight versus elution volume for three PtBMA standards (M_n: 1640, 17,000, and 29,600) is shown.

In Figure 4.3, the results related to different ratios of THF and CH₃CN are illustrated. It is easy to see that even small changes in the solvent composition shifts the chromatographic mode from SEC to HPLC and vice versa.

In a similar way it was attempted to find the critical conditions for PIB. In chapter 5 details are given for these experiments.

4.7.3 NMR spectroscopy

¹H NMR spectra, e.g. for endgroup analysis and block copolymer composition, were recorded, on a Bruker AC-200 spectrometer, primarily in CDCl₃, and some in d⁸-THF and D₂O.

4.7.4 UV spectroscopy

In order to detect the degree of metalation of TMP-DPOMe, TMP-DPV, and different PIB precursors, UV-spectra were recorded on a Shimadzu (UV 240) Graphcord connected with a Shimadzu Graphic printer (PR-1) (see also section 4.4).

4.7.5 Light scattering (dynamic and static)

The aggregation number Z and the micellar diameter $2 R_h$ were determined by static and dynamic light scattering. The apparatus was a wide angle light scattering equipment from ALV GmbH, Langen Germany, a Nd:YAG laser (Coherent, 400 mW, 532 nm), scattering angle 30° and 90°, correlator AVL 3000.

The block copolymer concentration usually was 1 g/l. Solvent: Water (NaOH(aq)) at pH = 10. Filtration: 0.45 μ m in all cases. The refractive index increments were 0.176 ml/g.

4.7.6 Fluorescence correlation spectroscopy

Aqueous solutions with different concentrations of a PIB-*b*-PMAA block copolymer are treated with a fluorescence labeled C₁₆-fatty acid. If only unimers, i.e. no micelles, are present the fatty acid will stick to the surface of the flask. Therefore, subsequently when the measurements are

carried out, no fluorescence absorbance can be detected in the solution. When micelles are formed this fatty acid associates with the hydrophobic micelle core leading to a certain fluorescence absorbance in the aqueous solution. The critical micelle concentration (CMC) is by definition the concentration at which the formation of micelles starts. In this case it is defined as the point where the fluorescence absorbance starts to change significantly.

The micelle size (R_h) is calculated from the following equations (see also section 5.7.2):

$$G(t) - 1 = (r^2/N) \cdot (1/(r^2 + 4Dt))$$

D: The diffusion coefficient of the specie, r: diameter of the observed volume V, $N = c \cdot V \cdot N_a$: The number of species in volume V, G(t): Intensity-autocorrelation function of the fluorescence light.

$$R_h = kT/(6\pi\eta D)$$

4.7.7 Transmission electron microscopy

Amphiphilic AB block copolymers in aqueous solution:

I) Uranyl acetate contrasting and solvent evaporation

The aqueous block copolymer solutions were mixed with a 2 wt-% uranyl acetate solution. The uranyl acetate reacts with the acid group and leads to contrasting of the PMAA-phase. A drop of this solution was placed on a filmed ELMI-net and dried. Subsequently it was washed with distilled water. The pictures obtained by TEM show the micelle border which is here the PMAA-phase.

II) Cryo-Replica:

The cryo-replica method involves a freeze-fracturing technique where a drop of the aqueous solution is first shock-frozen in liquid ethan (-183 °C, cooling rate: 10^4 K/sec). Secondly an inner surface of the drop is obtained by fracturing and partial sublimation of the ice at -120 °C in a vacuum chamber, followed by deposition of Pt/C vapor (about 5 nm) onto the sample at a precise angle. Subsequently, additional 20 nm carbon was deposited onto the sample as reinforcement. The drop was then thawed and the polymer was removed from the replica using chloro sulfuric acid. Finally the replica was pictured in a TEM. The contrasting was achieved from the fluctuation of the Pt/C-layer thickness due to the shadow effects gained by the oblique deposition. Thereby, a quasi-3D-picture of the micelles in their original size is obtained.

Thermoplastic elastomers, films:

Polymer films were prepared by casting a 10 wt-% toluene solution of the block copolymers into a teflon mold (THF solutions led to macrophase separated films). After 1 day evaporation in a hood, the film was placed in a vacuum oven for 1 day at RT, for further 2 days at 50 °C, and finally 3 h at 140 °C (annealing). The prepared films were then sectioned (40 nm) at -140 to -130 °C and

placed on a gold grid. Finally the contrasting was performed with RuO₄ vapor for 60 sec right before it was pictured in a TEM (120 kV, LAB6 cathode)

4.7.8 Analytical ultracentrifugation

The ultracentrifugation measurements were performed in sedimentation mode. Schlieren-optics was utilized for the detection.

4.7.9 Dynamic-mechanical analysis, stress-strain measurements, and small angle X-ray scattering measurements

For the dynamic-mechanical, stress-strain, and SAXS analyses of TPEs, polymer films were prepared in the following ways: **(A)** casting a 10 wt-% toluene solution of the block copolymers into a teflon mold (THF solutions led to macrophase separated films). After 1 day evaporation in a hood, the film was placed in a vacuum oven for 1 day at RT, for further 2 days at 50 °C, and finally 3 h at 140 °C (annealing). **(B)** Press mold films were made under high pressure at 130 °C for 30 min. Some of these samples were subsequently annealed at 150 °C for 2 h.

Dynamic-mechanical analysis were carried out with a RSAII-Rheometrics (1 K/min).

Stress-strain were analysis was made with a Hütting-Baldwin Messtechnik apparatus either with a rate of 1 mm/min (ABA block copolymers) or 10 mm/min ((AB)₃ block copolymers).

Small angle X-ray scattering (SAXS) experiments have been performed using a setup consisting of a rotating anode X-ray generator (Rigaku) with a pinhole beam colimation and of a two dimensional position sensitive detector (Siemens) with 512 · 512 pixels. The Cu K_α radiation was used ($\lambda = 0.154$ nm). The beam diameter was about 0.5 mm and the sample to detector distance was 1.2 m. The recorded intensity distribution $I(\theta, \mu)$ have been integrated over azimuthal angle (μ) and are here presented in arbitrary units as $I(s)$, where s is the scattering vector. The measurements were performed at room temperature with samples of about 1 mm thickness.

The following three equations are important for SAXS measurements, i.e. for the calculation of, the long period (domain distance) and estimation of the morphology.

$$n \cdot \lambda = 2 \cdot d_{\text{SAXS}} \cdot \sin\theta, \text{ Bragg's law.}$$

$$s = 4\pi/\lambda \cdot \sin\theta, \text{ the scattering vector.}$$

$$d_{\text{SAXS}} = (2 \cdot \pi \cdot n)/s, \text{ the relation between the long period and the scattering vector.}$$

Depending on the geometry/morphology the real distance between two domains can be calculated from d_{SAXS} (the long period) (see chapter 5).

4.7.10 Differential scanning calorimetry measurements

DSC was performed with a Mettler apparatus using a heating rate of 20 K/min (the curves correspond to the 2nd heating). Extrapolation of heating rate was not performed.

5 Results and discussion

In this chapter the synthesis and characterization of tailored polymers will be described in detail. To some extent, strategies (including potential problems) and preliminary results regarding preparation of well-defined amphiphilic networks will be discussed. As a starting point, relevant literature dealing with the synthesis of PIB-based block copolymers was analyzed and partially used in this work. However, after preliminary investigations, primarily involving modification of existing combinations of cationic and anionic polymerizations, a new procedure leading to tailored PIB-based block copolymers nearly free of homopolymers was developed. The resulting polymers were characterized with various analytical techniques (SEC, NMR, SAXS, DSC, etc.) in order to verify the usefulness and advantage of this method and to investigate the properties of the new macromolecular systems.

5.1 Cationic polymerization of isobutylene

Synthesis of PIBs with different molecular weights and different endgroups - depending on the subsequent applications - were aimed in this project. In order to obtain the desired products, careful selection of the initiating system is necessary. In Table 5.1 potential combinations of initiators and cointiators are listed together with the corresponding M_n for which narrow MWD PIBs can be prepared. For our purposes more than one of these systems have to be utilized since PIBs with $M_n = 1,000-50,000$ are needed, e.g. for water-soluble amphiphilic diblock copolymers ($M_{n,PIB} < 10,000$) and thermoplastic elastomers ($M_{n,PIB} = 20-50,000$).

Table 5.1: Potential initiating systems for the cationic polymerization of IB. The M_n -values shown represent the range in which narrow MWD ($M_w/M_n < 1.2$) can be reached.

Initiating system	M_n , g/mole
I. CumOH/TiCl ₄	no polymerization
II. CumCl or CumOMe/TiCl ₄	<2000 and >10000
III. CumOH/BCl ₃	<3000
IV. CumOH/BCl ₃ /TiCl ₄	>3000
V. CumCl or TMPCl/BCl ₃ /TiCl ₄	>3000

Nearly all of the systems mentioned in Table 5.1 have been tested as summarized in Table 5.2. PIBs with $M_w/M_n < 1.15$ (unimodal distribution, see Figure 5.1) and near to $M_{n,th}$ have been synthesized, with the exception of sample 10. One of the critical events in the two-step method (see section 1.2.1.3 and 4.2.2) (Table 5.2, sample 12-16) is the amount of IB in the first step, where only CH₂Cl₂ is present as solvent. At $M_n \approx 3,000-3,500$ g/mole precipitation takes place. Therefore, the M_n was normally chosen to be in the range $M_n = 1,500-2,500$ (Table 5.2, sample 9 and 11) in the first step, since precipitation leads to a broader or even multimodal MWD as illustrated in Table 5.2, sample 10 and Figure 5.1b. As solvent either CH₂Cl₂ or a mixture of CH₂Cl₂/n-hexane 40:60 were used. Here it is important to note that the polymerization of IB is significantly faster in CH₂Cl₂ than in CH₃Cl. Under similar conditions the yield was less than 40 % in CH₃Cl³², whereas about 70 %

conversion was detected in CH_2Cl_2 at the same polymerization time. Due to the danger of indane formation^{15,16} after the first monomer addition with DiCumOH, this compound was not used for preparative purposes. Instead, the sterically protected tBuCumCl or tBuCumOH were used.

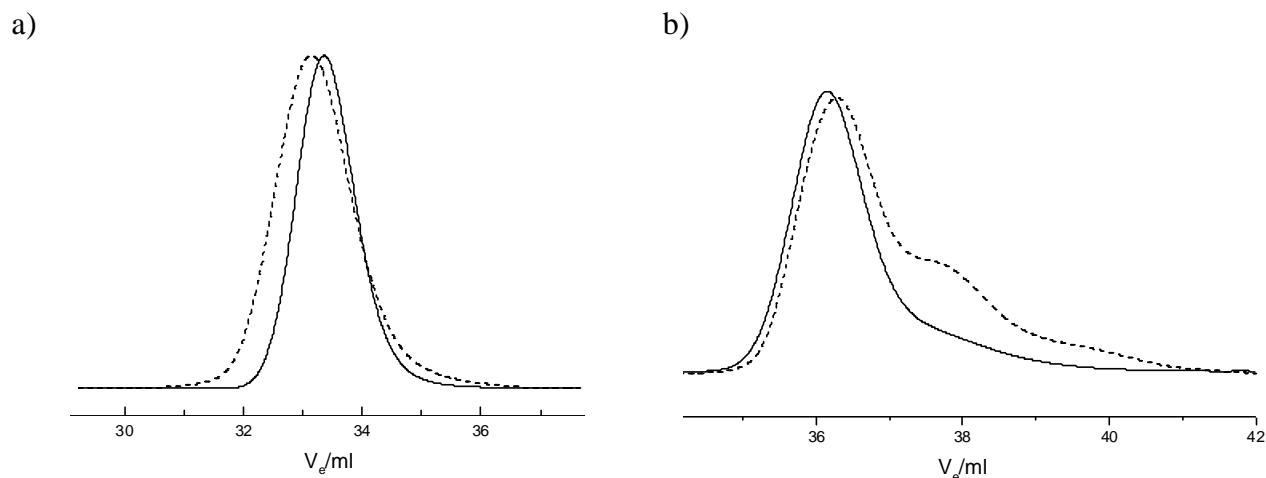


Figure 5.1: SEC traces of the polyisobutylenes (PIBs) obtained by using, a) TiCl_4 (---) (sample 2) and $\text{BCl}_3/\text{TiCl}_4$ (—) (sample 16), b) BCl_3 (---) (sample 10) and $\text{BCl}_3/\text{TiCl}_4$ (—) (sample 14) as coinitiators.

Table 5.2: Initiators ($[\text{I}]_0 = 0.75\text{-}1.25 \cdot 10^{-2} \text{ M}$) and coinitiators ($[\text{coinitiator}] = 8\text{-}20 \cdot [\text{I}]_0$) used for the synthesis of PIBs and the corresponding theoretical and SEC molecular weights and molecular weight distributions of the resulting products. Monomer: $[\text{IB}]_0 \approx 1 \text{ M}$ regulated by incremental IB addition. Solvent: n-hexane: CH_2Cl_2 (60:40) in all cases except in sample 9-11 where only CH_2Cl_2 is used. DMA was used as electron donor in all experiments ($[\text{DMA}] = [\text{C}^+]$), and DtBP as proton trap ($[\text{DtBP}] = 10^{-3} \text{ M}$) in case of sample 6-8, 10-11, and 12-16.

Sample no.	Initiator	Coinitiator	$10^3 \cdot M_{n,\text{theo}}$	$10^3 \cdot M_n$	M_w/M_n
1	TMPCl	TiCl_4	1	1.1	1.08
2	TMPCl	TiCl_4	5	5.8	1.18
3	TMPCl	TiCl_4	10	10.4	1.12
4	TMPCl	TiCl_4	20	20.5	1.07
5	TMPCl	TiCl_4	80	> 70.0	1.25
6	tBuDiCumCl	TiCl_4	20	17.5	1.07
7	TriCumCl	TiCl_4	7.5	9.3	1.15
8	TriCumCl	TiCl_4	45	45.5	1.07
9	TMPCl	BCl_3	1	1.3	1.07
10	tBuDiCumOH	BCl_3	5	4.6	1.37
11	DiCumOH	BCl_3	2.5	2.9	1.12
12	TMPCl	$\text{BCl}_3/\text{TiCl}_4$	5	5.2	1.09
13	CumCl	$\text{BCl}_3/\text{TiCl}_4$	4	4.0	1.09
14	tBuCumOH	$\text{BCl}_3/\text{TiCl}_4$	5	4.8	1.14
15	tBuCumCl	$\text{BCl}_3/\text{TiCl}_4$	5	5.3	1.09
16	TriCumOH	$\text{BCl}_3/\text{TiCl}_4$	5	5.2	1.08

Important observation can be made from the results summarized in Table 5.2. In the experiments with TiCl_4 only it can be clearly seen that MWD gets narrower with increasing M_n from 5,000 up to 50-60,000. Above 70,000 the MWD increases again (sample 5) due to the very high viscosity of the polymer solution. In order to make higher molecular weight PIB (limited to $M_n = 100\text{-}130,000$) a lower initiator concentration ($[\text{I}]_0$) is necessary. However, with the experimental procedure applied in our studies involving normal syringe technique without high-vacuum apparatus polymerization, $[\text{I}]_0 \ll 10^{-2} \text{ M}$ cannot be used due to the presence of impurities causing either transfer or incidental initiation of polymer chains.

The lack of transfer in the applied system ($[\text{I}]_0 = 1\text{-}2 \cdot 10^{-2} \text{ M}$, see Experimental) has been verified by ^1H NMR analysis. Vinylic protons in the range 4-5 ppm are absent, see Figure 5.2a. Any kind of transfer will lead to vinyl-terminated PIB as illustrated in Scheme 1.2. Subsequent dehydrochlorination demonstrates the presence of the desired *tert*-chlorine endgroups, yielding the expected olefin chain ends as exhibited in Figure 5.2b. For this work it is essential that transfer is absent, otherwise synthesis of well-defined end-functionalized PIB and PIB-based block copolymers would not be possible.

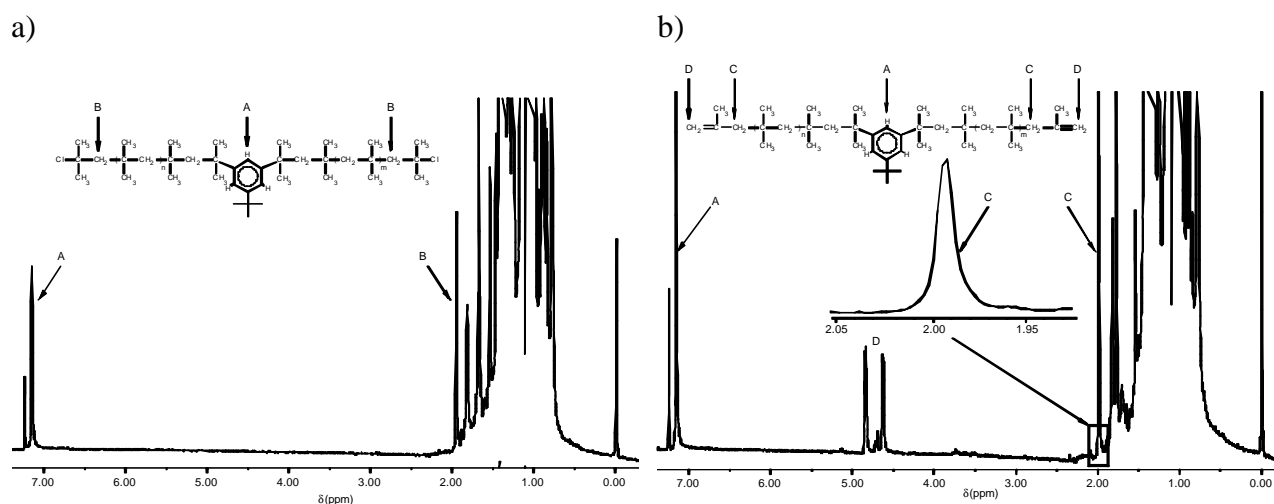


Figure 5.2: ^1H NMR spectra of a) PIB sample 15 and b) the resulting product after dehydrochlorination with $t\text{BuOK}$.

At relatively low M_n ($< 2,000$) it is possible to get as good results with TiCl_4 as with BCl_3 (Table 5.2, sample 1 and 9). In these two experiments the IB was added relatively slowly to the initiator solution. This means, that not only the Lewis acid is important but also the way IB is added (slow, fast, incremental, or continuous), i.e. effective mixing seems to be a problem in these polymerization systems. In one experiment, similar to sample 2 (same M_n , about 6,000), only the addition of IB was changed. Instead of fast addition of the total amount of IB (sample 2), IB was added slowly in three portions. The PDI changed from 1.18 to 1.13. Therefore, further work might be needed in order to get detailed information about experimental parameters (e.g., the order/rate by which the reagents are added) which have an influence on the MWD.

Incidental initiation is especially important when polyfunctional initiators (Figure 5.3) are used due to the fact that the impurities are primarily monofunctional initiators, e.g., a proton (and to some extent difunctional ones, e.g. phosgene in CH_2Cl_2). If they are present, not only broader MWD

can be observed but also mixtures of different block copolymers in the case where PIB is used for subsequent synthesis of ABA/(AB)₃ block copolymers. By the use of a proton trap (DtBP) in case of polyfunctional initiators and of freshly distilled CH₂Cl₂, incidental initiation could not be detected as verified by the fact that changes of the MWD regardless of the functionality of the initiator are not observed (Table 5.2, samples 12,13,15, and 16 and results related to the synthesis of PMMA-*b*-PIB-*b*-PMMA, see also section 5.6).

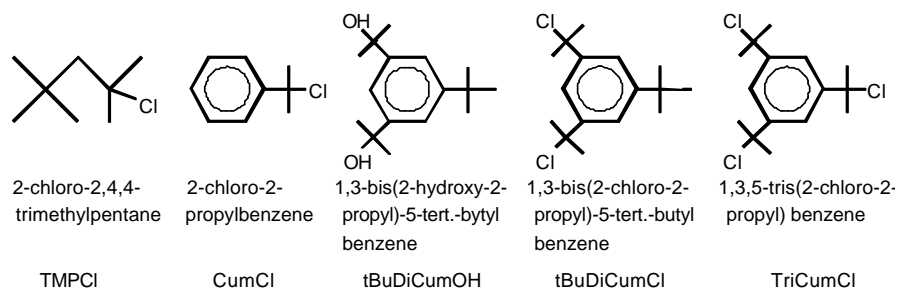


Figure 5.3: The chemical structures of the initiators used in cationic polymerization of IB.

Concerning the initiators TMPCl and CumCl (see Figure 5.3), 1-2% vinyl compounds were normally detected, since distillation carried out at elevated temperature (30-50 °C) is the only purification method, whereas the other initiators can be recrystallized several times in order to obtain > 99.5 % purity. If the vinyl compounds are present they can act as a monomer causing a lower initiating efficiency. In order to make sure that the initiators were pure, ¹H NMR analysis was carried out just before use. The advantage of using cumyl alcohols instead of cumyl chlorides in the two-step process is due to the fact that the chlorine compound is synthesized from the corresponding alcohol by hydrochlorination, i.e. an extra synthetic step can be saved. Secondly, the stability of the cumyl alcohols is significantly higher than that of cumyl chlorides. However, it was reported that cumyl alcohols initiate LC⁺Pzn of IB only in conjunction with BCl₃ by rapidly converting *in situ* the alcohol into the corresponding effective chlorinated initiator.^{36,177} In Table 5.2 the results with tBuDiCumCl and tBuDiCumOH verify that the two types of initiators lead to the same high quality polymer, i.e. narrow MWD and nearly theoretical M_n which means ≈ 100% initiating efficiency.

In the discussion above on the influence of the Lewis acids in the polymerization of IB only the M_w/M_n values are evaluated. However, one has to be aware also on effects on the functionality of the chain end. For instance, end-quenching of living cationic chain ends with 1,1-diphenylethylene leads to quite different results depending on the Lewis acids present in the system.³⁰ This effect is mainly due to the value of the ionization equilibrium constants (Scheme 1.1) which depends on the strength of the Lewis acid. Dramatic effects of the nature of the Lewis acid was also observed, i.e. different degree of capping, in the course of quenching with allyltrimethylsilane.^{28,178,179}

5.2 End-functionalized PIBs

As discussed in the introduction (section 1.3.1), Cl⁺-terminated PIB which is obtained by direct quenching with methanol can be converted into many different chain ends by subsequent organic reactions. A second, easier and more elegant way to introduce the desired endgroup is reached by quenching (one-step reaction), using a nucleophilic compound which can react with the

tertiary living cation. Different functional PIBs were synthesized primarily in order to investigate potential strategies for combining cationic and anionic polymerizations.

5.2.1 Vinyl, hydroxy, and tolyl functionalized polyisobutylenes

Several functional groups can be obtained by converting the primarily formed *tert*-chlorine chain end of PIB. The objective of this section is to summarize and evaluate the potential problems arising with endgroups considered for subsequent anionic polymerizations.

Vinyl-terminated PIBs can be obtained by using a sterically hindered base, like tBuOK for dehydrochlorination.¹²⁷ Since the wanted external vinyl group is the thermodynamically less favored (Saytzeff's law) two different procedure were investigated. By comparing the results related to sample 1 and 2 in Table 5.3, it is obvious that the way tBuOK and PIB are mixed together is without importance:

Sample 1: To a boiling THF solution of tBuOK, PIB dissolved in THF is added slowly.

Sample 2: PIB in THF and solid tBuOK are mixed at RT and subsequently heated to the desired temperature.

Table 5.3: Dehydrochlorination of PIB-Cl^t with tBuOK in THF at different temperatures. $M_n = 5200$, $M_w/M_n = 1.09$. The degree of functionalization was determined by ¹H NMR.

Sample no.	Reaction temperature (°C)	Reaction time (h)	Total conversion (%)	External double bond (%)
1	65	22	100	97
2	65	22	100	97
3	20	45	15	100
4	20	72	21	100
5	40	53	20	100
6	40	122	43	95
7	65	20	≈ 95	98
8a	65	16	≈ 95	95

^aSample 8: $M_n = 1800$, $M_w/M_n = 1.07$

Therefore, samples 3-8 were all performed in the same way as with sample 2. However, from the results in Table 5.3 it is clear that elevated temperature is needed, else quantitative dehydrochlorination cannot be reached. However, at 65 °C (samples 1-2 and 6-8) a small amount of internal double bonds are formed (2-5 %), see Figure 5.4. If such a PIB is directly used for the generation of an anion (see section 1.2.4) two anions with most likely different reactivity will subsequently be present. Both of these anions cannot be utilized for the LA-Pzn of (meth)acrylates due to the high nucleophilicity (see section 1.2.2.3). In addition, hydroboration with 9-BBN cannot be carried out with an internal double bond.

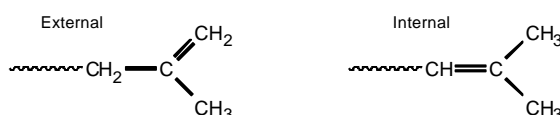
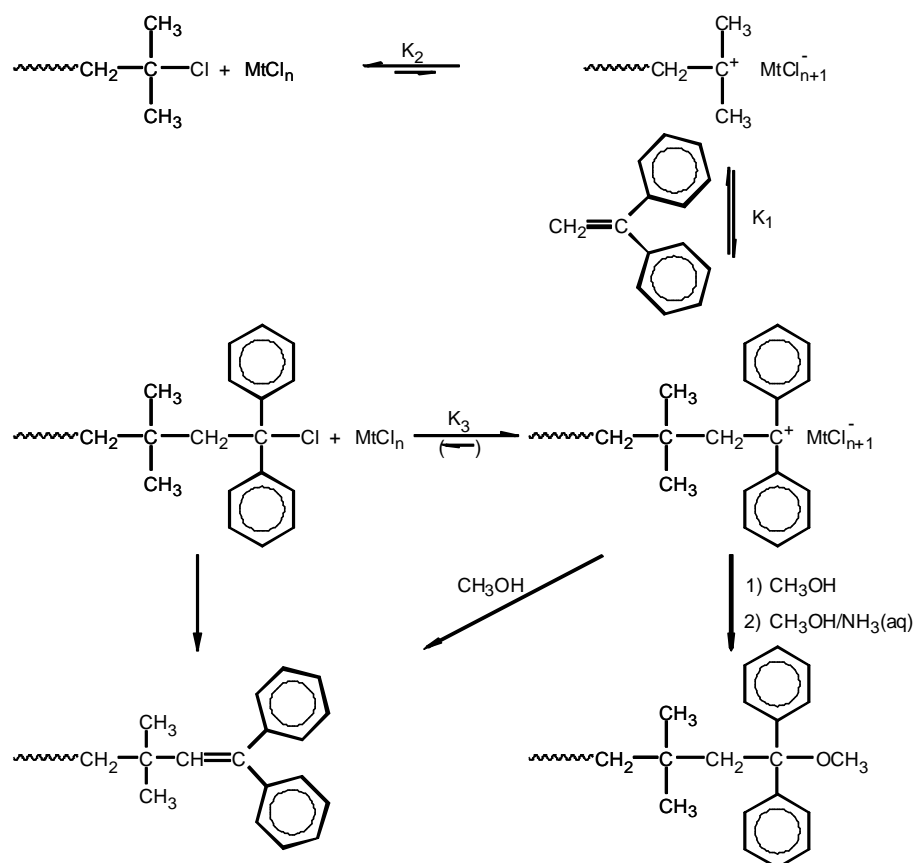


Figure 5.4: The two vinyl groups obtained by dehydrochlorination with tBuOK.

The vinyl-terminated PIB was also obtained by quenching with allyltrimethylsilane (Scheme 1.12).^{28,29} In this case only one vinyl compound is present. However, the reaction seems to be influenced significantly by the Lewis acid(s), solvent mixture and temperature of the polymerization system due to the shift of the equilibrium between inactive and active species in one or the other direction (Scheme 1.1). B. Iván *et al.* have reached 99% functionalization with TiCl_4 in $\text{CH}_2\text{Cl}_2/n$ -hexane and $\text{BCl}_3/\text{TiCl}_4$ in $\text{CH}_3\text{Cl}/n$ -hexane at $-70\text{ }^\circ\text{C}$ ^{28,29} whereas experiments with $\text{BCl}_3/\text{TiCl}_4$ in $\text{CH}_2\text{Cl}_2/n$ -hexane at $-78\text{ }^\circ\text{C}$ lead to max. 50% functionality.¹⁸⁰ In our experiment, $\text{BCl}_3/\text{TiCl}_4$ in $\text{CH}_2\text{Cl}_2/n$ -hexane was also used but the quenching reaction was performed with the following temperature profile: 1 hour at $-78\text{ }^\circ\text{C}$ and then slow heating to $0\text{ }^\circ\text{C}$ over a period of 5 hours. The degree of functionality was here $>96\%$. That means, the quenching reaction has to be carried out under carefully selected condition.

5.2.2 Functionalization of living polyisobutylene with 1,1-diphenylethylene

In situ functionalization of living PIB with DPE, a non-homopolymerizable monomer (Scheme 5.1) was carried out in order to obtain PIBs which might be used as potential macroinitiators for anionic polymerization of different monomers, e.g. (meth)acrylates.



Scheme 5.1: Functionalization of living PIB chain ends with DPE.

Detailed kinetic and thermodynamic investigations of the DPE addition to living PIB have been treated elsewhere by Faust *et al.*^{30,123,181,182} The most important equations used to determine the equilibrium constant of the reaction between DPE and living PIB chain ends are³⁰ (see also Scheme 5.1):

$$K_1 = [\text{PIBDPE}^+\text{Ti}_2\text{Cl}_9^-]/([\text{PIB}^+\text{Ti}_2\text{Cl}_9^-][\text{DPE}]), K_2 = [\text{PIB}^+\text{Ti}_2\text{Cl}_9^-]/([\text{PIBCl}][\text{TiCl}_4]^2)$$

$$K_e = K_1K_2, K_e = [\text{PIBDPE}^+\text{Ti}_2\text{Cl}_9^-]/([\text{PIBCl}][\text{TiCl}_4]^2[\text{DPE}])$$

$$K_3 = ([\text{PIBDPE}^+\text{Ti}_2\text{Cl}_9^-][\text{TiCl}_4]^2)/[\text{PIBDPE}^+\text{Ti}_2\text{Cl}_9^-]$$

Two procedures were investigated for the synthesis of living PIB and subsequent end-capping with DPE: A two-step system with sequential polarity change and addition of two different cointiators, BCl_3 and TiCl_4 , and a one-step polymerization in which only TiCl_4 was used as cointiator, see section 5.1.

The amount of DPE (normally 2-5 times excess) relative to the tertiary cation, and thereby the time needed for the capping reaction seems to be relatively important factors. In a model study, 0.9-1:1 [cation]:[DPE] was used (reaction time 180 min). Partial alkylation on the phenyl rings took place verified by the presence of two symmetrical peaks in the area 7.5-8.0 ppm, see Figure 5.5 (1). Therefore, partial para-substitution of the aromatic rings may lead to side-products under these conditions. Excess of DPE (1.1-5) and short reaction time ($t = 25$ min) leads to the absence of alkylation indicated by the absence of peaks in the range 7.5-8.0 ppm appear, see Figure 5.5 (2). At $t > 2$ h, the tertiary cation generated from TMPCl and TiCl_4 leads to a modified Friedel-Crafts reaction. Normally, AlCl_3 is used for the alkylation of phenyl rings as discussed in section 1.3.1. In this case para-substitution was also observed. Specifically related to TMPCl , one has to be aware of the kinetic difference between TMPCl and a living PIB chain end in regard to the addition of DPE. It has been shown that TMPCl reacts 10 times slower than the corresponding PIB.¹⁸³

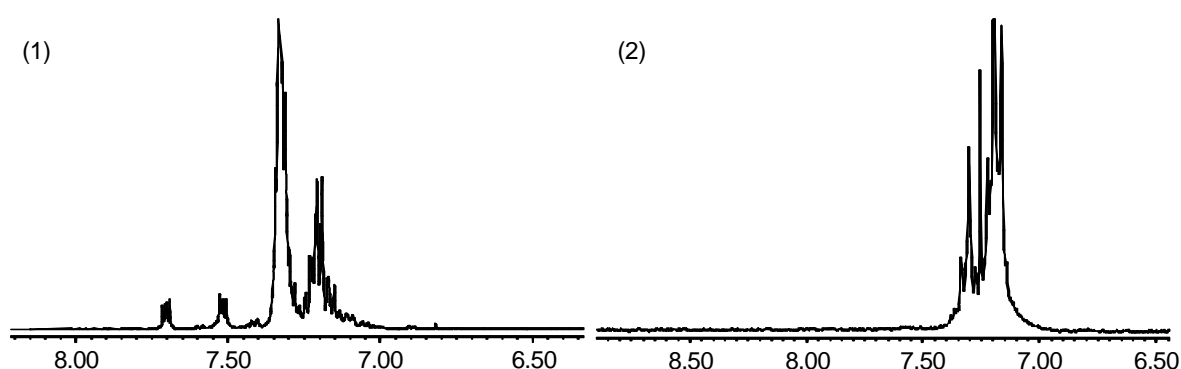


Figure 5.5: ^1H NMR spectra (200 MHz, in CDCl_3) of the product obtained by quenching a cation with stoichiometric amount of DPE, 180 min reaction time (1) and with excess DPE (2-5 times), 25 min reaction time (2).

The major processes occurring in the course of end-capping of living PIB with DPE are shown in Scheme 5.1 (a similar scheme can be drawn with TMPCl instead of PIB-Cl). Quenching the DPE-capped living polymers with methanol-ammonia leads to quantitative formation ($> 98\%$,

verified by ^1H NMR) of 1,1-diphenyl-1-methoxy (DPOMe) endgroups when only TiCl_4 is used. The integration ratio between the ^1H NMR peaks of the methoxy group and the CH_2 -group ($-\text{CH}_2\text{C}(\text{Ph})_2\text{OCH}_3$) is exactly 3.0:2.0. Therefore, the existence of the corresponding chloro endgroup ($-\text{CH}_2\text{-C}(\text{Ph})_2\text{Cl}$) which by coincidence might have had peaks overlapping those of the DPOMe endgroup can be excluded. In addition, this result confirms that the equilibrium between inactive and active DPE-capped PIBs is shifted quantitatively toward the active ionized species in contrast to the uncapped PIB which has a very low degree of ionization (see section 1.2.1). 2,2-Diphenylvinyl (DPV) chain ends were obtained quantitatively when only methanol was used as quenching agent and the quenched polymer solution was left for more than four hours before further purification. The formation of DPV termini is due to the acidic nature of the solution leading to elimination of methanol from the DPOMe-termini formed initially. In some cases dissolution of the polymer in CHCl_3 containing traces of HCl provided quantitative elimination. When only BCl_3 was used as coinitiator less than quantitative capping ($< 10\%$ at $-80\text{ }^\circ\text{C}$) was found in $\text{CH}_3\text{Cl}/n$ -hexane (40:60 v/v) solvent mixture since the DPE addition is an equilibrium reaction.³⁰ However, in the two-step procedure $>96\%$ capping efficiency was reached for an equimolar ratio of the two Lewis acids in $\text{CH}_2\text{Cl}_2/n$ -hexane (40:60 v/v) mixture.

The DPE-capped PIB (DPOMe/DPV) was synthesized not only by *in situ* addition of DPE to a living PIB solution. In some experiments, purified Cl^{t} -terminated PIBs (polymerized with BCl_3) were reinitiated with TiCl_4 using the same conditions as for normal polymerization experiments (solvents, electron donor (ED), temperature, etc) and then DPE was added. In these cases similar capping efficiencies were reached ($> 98\%$). The rate of the capping reaction depends to a certain extent on the M_n of the PIB ($M_n < 5,000$: $\approx 100\%$ capping after 20 min, $M_n \approx 10,000$: $\approx 90\%$ capping after 20 min, and $M_n \approx 20,000$: $\approx 80\%$ after 20 min).

The reaction temperature is important for obtaining quantitative DPE-capping.³⁰ In an experiment carried out in the usual way at $-78\text{ }^\circ\text{C}$ ($\text{CH}_2\text{Cl}_2/n$ -hexane and TiCl_4/DMA) the polymerization system was allowed to warm up slowly, and samples were withdrawn at different temperatures. The yield of DPE-capped product is shown as a function of temperature in Figure 5.6. While quantitative end-capping is observed at $-78\text{ }^\circ\text{C}$, the capping yield rapidly decreases with increasing temperature indicating that the addition of DPE is exothermic. ^1H NMR spectra show 90% DPE capping ($-\text{CH}=\text{C}(\text{Ph})_2$, 6.12 ppm and $-\text{OCH}_3$, 3.00 ppm) and 10% *tert*-chlorine ($-\text{CH}_2\text{-C}(\text{CH}_3)_2\text{Cl}$, 1.96 ppm) endgroups at $-60\text{ }^\circ\text{C}$, and no DPE-capping at $-40\text{ }^\circ\text{C}$. These results are in good agreement with those obtained by Faust et al.³⁰

In order to further investigate this phenomenon, DPOMe-ended PIB was prepared, purified, and then dissolved in $\text{CH}_2\text{Cl}_2/n$ -hexane solvent mixture (40/60 v/v), cooled to $-78\text{ }^\circ\text{C}$, and polymerization conditions were created by adding DMA and TiCl_4 . This system was also allowed to warm up, and samples were withdrawn at different temperatures. Results identical to the experiment shown in Figure 5.6 were observed, indicating that retroaddition of DPE takes place from the DPOMe-ended PIB in the presence of coinitiator.

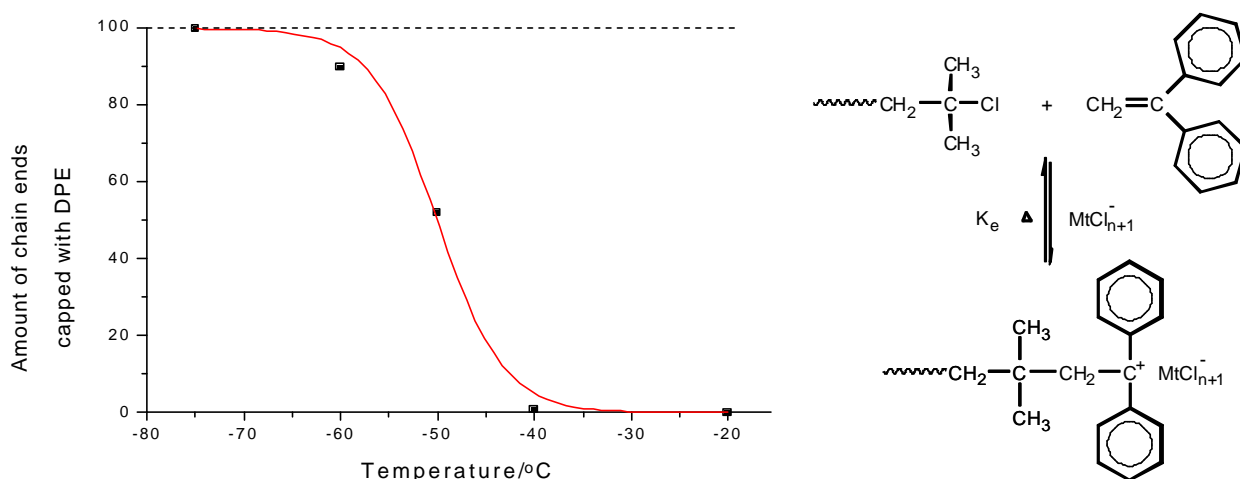
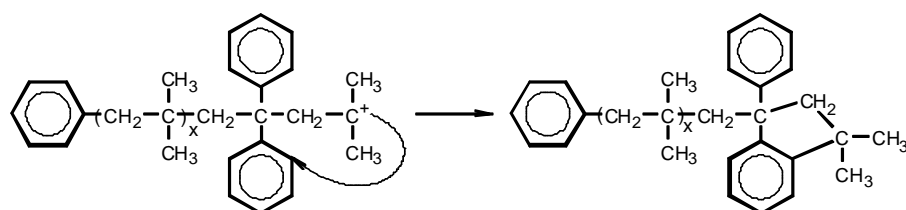


Figure 5.6: Effect of temperature on the equilibrium addition of DPE to living PIB chain ends (solvent, 60:40 *n*-hexane/CH₂Cl₂, TiCl₄, $n_{\text{initiator}} = n_{\text{DMA}} = 0.2 \cdot n_{\text{DPE}}$).

In conclusion, the polymerization temperature should be kept below -75 °C in order to reach quantitative end-capping under the conditions used in this project (*n*-hexane:CH₂Cl₂ (60:40), [I]₀ ≈ 10⁻² M, [DMA] ≈ 10⁻² M, [TiCl₄] ≈ 10⁻¹ M, and [DPE]₀ ≈ 5 · 10⁻² M).

At this stage it has been proved that DPE adds to a living PIB chain end quantitatively under the above-mentioned conditions. Since a DPE-capped PIB can be used as macroinitiator for the cationic polymerization of vinyl ethers, e.g. isobutyl vinyl ether (IBVE) leading to PIB-*b*-PIBVE¹⁸⁴, it is important to know whether IB can be added in a similar way to PIB-DPE[⊕]. If yes, it is decisive that DPE is added after 100% conversion of IB, else a polymer with undefined chain ends might be formed. The following three polymers are possible: a) one containing several DPE units at the chain end, b) one which does not have a functional DPE endgroup, and c) one having an inactive DPE endgroup due to indane formation (Scheme 5.2). In order to investigate this potential problem, several experiments were performed. In three experiments IB, DPE and CumCl (initiator) were mixed together and initiated with three different coinitiator/solvent systems.



Scheme 5.2: Indane formation leading to an inactive DPE-capped PIB ($x \geq 1$).

The SEC traces corresponding to the three experiments where DPE, IB, and CumCl are initiated with different Lewis acid solutions (Figure 5.7) indicate that only small amount of oligomeric material is formed (the peak at $V_e = 45$ ml corresponds to DPE). It is not possible to interpret the ¹H NMR spectra because of the complexity/number of peaks.

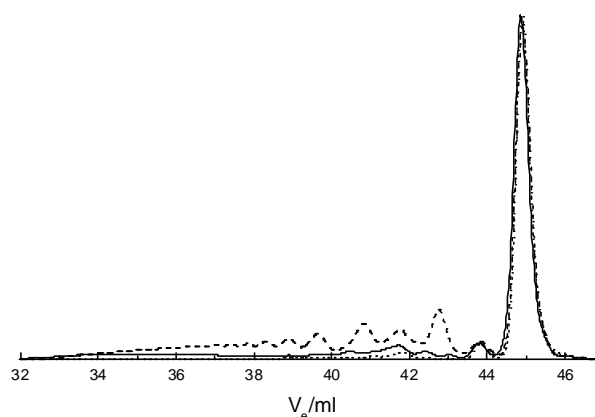


Figure 5.7: SEC traces (RI-signals) of the products obtained by initiating a mixture of DPE, IB, and CumCl with TiCl_4 in CH_2Cl_2 (—), BCl_3 in CH_2Cl_2 (····), and TiCl_4 in $n\text{-hex}/\text{CH}_2\text{Cl}_2$ (---).

In a fourth experiment IB was added to a PIB-DPE^{\oplus} precursor in the presence of excess DPE ($n_{\text{DPE}} = 5 \cdot n_{\text{ini}}$) and allowed to react for 30 min. In order to avoid potential initiation by protons, DtBP was used as proton trap. The SEC result indicates that IB does not add quantitatively (maybe partially) to the diphenyl cation. The M_n of the product corresponds roughly to the one of the PIB-DPE^+ precursor ($M_{n,\text{SEC}} \approx 1,900$ and unimodal MWD) and not to the one expected if the total amount of IB was polymerized (then $M_n \approx 6,000$). Detailed information about the product (endgroups) was obtained by ^1H NMR analysis, Figure 5.8. Between 2.0 and 3.2 ppm several new peaks appeared in the spectrum of the product obtained after IB addition, compared to the one of the PIB-DPE^+ precursor (no peaks in the range 2.0-3.2 ppm). The area of the two peaks at 2.39 and 2.41 ppm is about 1/3 compared to the singlet at 6.12 ppm ($-\underline{\text{CH}}=\text{C}(\text{Ph})_2$). This most likely means, that different unspecified endgroups, e.g. the indane endgroup (Scheme 5.2) and/or one containing several DPE units are present (5-15 %). Therefore, well-defined functionalized PIBs can only be prepared if DPE is added after quantitative conversion of IB. However, under our reaction conditions this is reached after ≈ 5 min.⁵¹

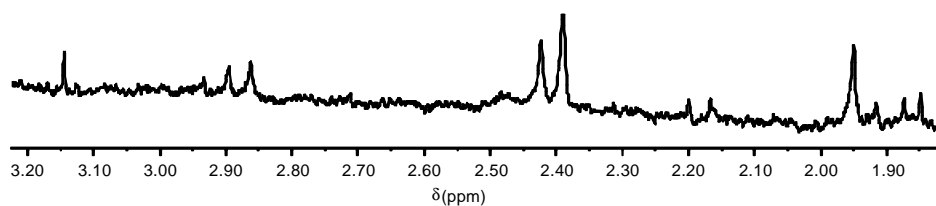


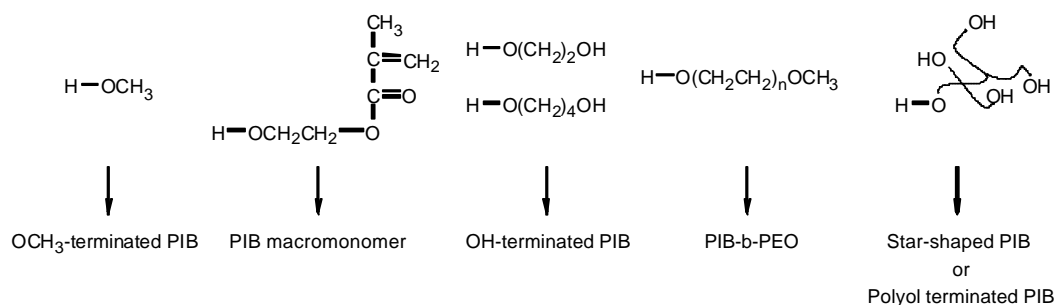
Figure 5.8: ^1H NMR spectrum (200 MHz in CDCl_3) of the DPE-capped PIB after IB addition.

As described above, quantitatively DPE-capped PIBs (< 98 %) can be synthesized under specified conditions and the relative proportion of the DPOMe- and the DPV-capped PIB can be controlled just by careful selection of the quenching conditions. Different PIBs, mono-, di-, and trifunctional with > 98 % functionality and $M_n = 1\text{-}50,000$ ($M_w/M_n < 1.15$) have been prepared for different purposes (see later). In addition, the quenching of the 1,1-diphenylcation leads to a methoxy- and not to a Cl^{t} -endgroup due to the presence of a highly stabilized cation (see Scheme 5.1). Therefore, quenching with any kind of alcohols which might contain a second functionality would in principle lead to a similar ether compound in quantitative yield.

5.2.3 Quenching of the living PIB-DPE^Å with different alcohols

Based on the results gained from the capping with DPE, especially the possibility to obtain a methoxy endgroup by quenching with methanol in quantitative yield (Scheme 5.1), a new synthetic route toward *in situ* end-functionalization of polyisobutylene has been investigated. It was found that the C-O bond of the 1-methoxy-1,1-phenyl endgroup is stable under nearly all conditions, i.e. in media containing moisture and acetic acid at elevated temperature (up at least 40 °C). However, if it comes in contact with traces of HCl, cleavage takes place within less than 2 hours at room temperature. The possibility to cleave the C-O bond under mild (specific) conditions might be an advantage for some applications (see later).

The purpose of this study is to vary the functionality attached to the 1,1-diphenyl chain end by the use of the following alcohols: 2-Hydroxyethylmethacrylate (HEMA), ethyleneglycol, butan-1,4-diol, oligo(ethylene oxide) methylether ($P_n = 7$), and different hyperbranched polyols (up to 128 OH groups per molecule), see Scheme 5.3.



Scheme 5.3: Alcohols which can be used for quenching living DPE-capped PIB.

Quenching with HEMA provides *in situ* formation of a PIB-macromonomer which otherwise has to be synthesized in a 4-step reaction-sequence.¹⁷² The fact that the C-O bond scission proceeds smoothly might here have interesting perspectives, at least from a scientific point of view. For instance, comb-shaped copolymers or networks (obtained by using a difunctional macro-monomer) can be cleaved into fragments and analyzed by SEC. Precise information about the M_n of the backbone in a comb-shaped copolymer can be obtained which would else be impossible or after a certain morphology has been established by microphase separation the polymer is cleaved and one component is extracted (e.g. PIB with *n*-hexane) which might be used for synthesis of membranes.

In order to obtain OH-terminated PIBs, diols like ethylene glycol or 1,4-butanediol were used. A potential side-reaction might be partial coupling. However, it can easily be avoided by using a large excess of the diol. A step further is the use of a polyol such as a hyperbranched polyol containing 16-128 OH-groups per molecule. In this case, two structures are possible, one where exactly one PIB chain is linked to the polyol and one where several PIB chains are attached to the polyol core leading to a star-shaped polymer. Polyols like different type of saccharides might be utilized as well.

Finally, polymers containing exactly one OH endgroup, e.g. PEOs, are here used for *in situ* synthesis of amphiphilic AB block copolymers. The crucial point is stoichiometric addition of the

OH-capped polymer. However, if mono-initiated PIB and mono OH-terminated PEO are used, selective extraction can subsequently be performed in order to separate the PIB-*b*-PEO block copolymer from PEO and potential unreacted PIB.

Table 5.4: Results related to the functionalization of a living DPE-capped PIB with different alcohols, $M_{n,PIB} = 2500-7000$, $M_w/M_n = 1.15-1.25$. The degree of functionalization was determined by 1H NMR. The side-product is DPV-capped PIB.

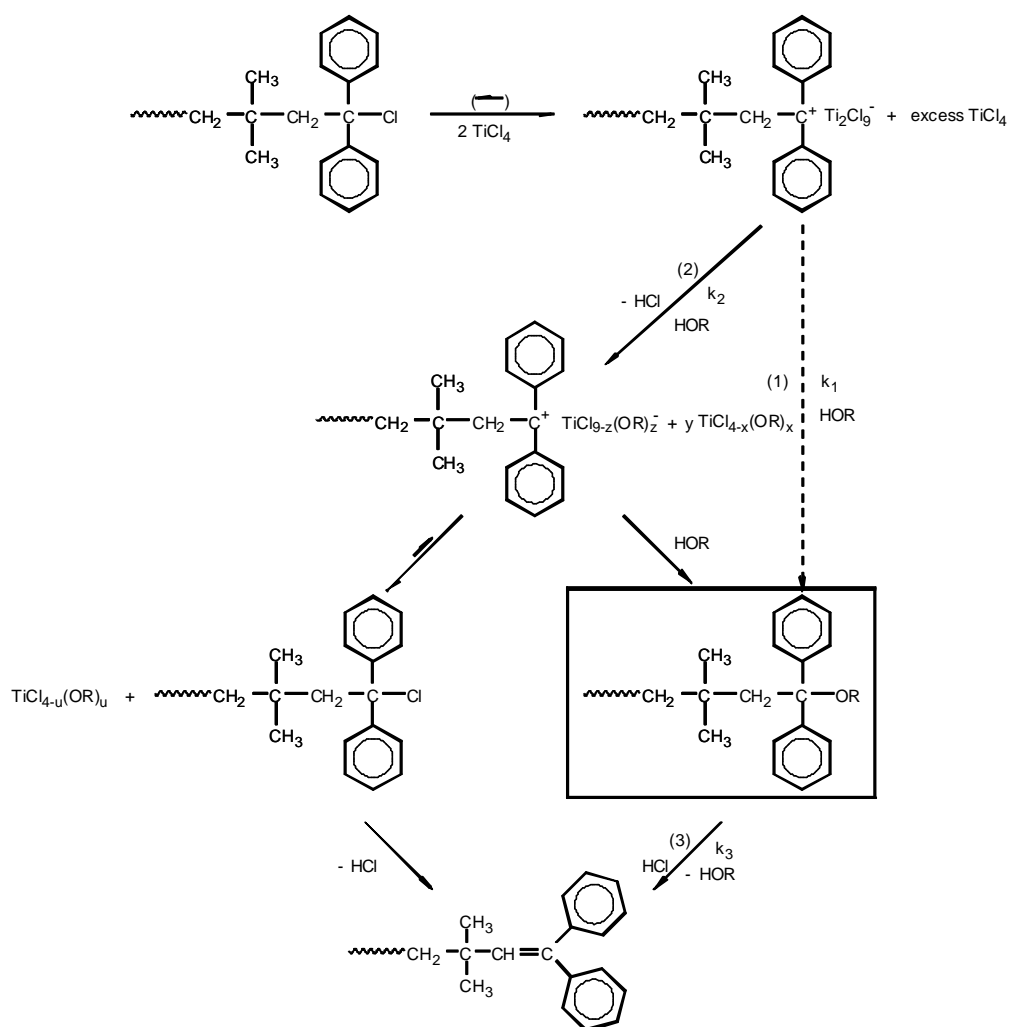
No.	Quenching agent	Functional chain ends (mole %)	Remarks
1	CH ₃ OH	> 98	2-5 min after the addition of CH ₃ OH (colorless polymer solution) NH ₃ (aq)/CH ₃ OH was added.
2	HEMA	65	1-2 min after the addition of HEMA (colorless polymer solution) Et ₃ N in CH ₂ Cl ₂ was added.
3	HEMA	60	During the addition of HEMA, additional TiCl ₄ was added with a second syringe. Finally Et ₃ N was added.
4	HEMA	50	The HEMA solution contained Et ₃ N.
5	HEMA	40	Before HEMA was added Ti(OiPr) ₄ ($n_{Ti(OiPr)_4} = 0.6n_{TiCl_4}$) was transferred to the solution.
6	HO(CH ₂) ₂ OH	0	The solution was allowed to warm up to -20 °C during quenching.
7	HO(CH ₂) ₂ OH	< 10	The ethylene glycol solution contained NH ₃ (g)
8	HO(CH ₂) ₄ OH	50	Butanediol was allowed to react for 30 min then Et ₃ N was added to the polymer solution although it was still red.
9	PEO	20	NH ₃ (aq)/CH ₃ OH was added at the time when the polymer solution was colorless.
10	PEO	20	Et ₃ N in CH ₂ Cl ₂ was added at the time when the polymer solution was colorless.
11	PEO	10	The PEO solution contained Et ₃ N.
12	Hyperbr.-polyol	0	PIB endgroups:OH, 1:6.
13	Hyperbr.-polyol	0	PIB endgroups:OH, 1:128.

From the results in Table 5.4 it is clear that quantitative functionalization is only reached with methanol with the system used (TiCl₄, *n*-hexane/CH₂Cl₂, 60:40). The major problem is that three different reactions are competing: (1), (2), and (3) (Scheme 5.4). Substitution i.e. formation of the desired ether compound (in the frame, Scheme 5.4) occurs if (1) is much faster than (2). In the opposite case the ionization equilibrium is shifted to the dormant side since Ti(OR)₄ is a weaker Lewis acid than TiCl₄. In addition, the formed HCl causes elimination of HOR (3) with a certain rate. Based on these considerations, the wanted compound is only formed in high yield if:

$$k_1 \gg k_2 \text{ and } k_3.$$

In the experiments involving HEMA max. 65 % conversion is attained (see Figure 5.9a, 1H NMR of sample 4, 50% conversion, determined by comparing the integration of the three vinyl proton 5-7 ppm). The reason might be related to the fact that quenching with HEMA is not spontaneous (the disappearance of red color) like with methanol. In contrast to methanol, HEMA contains two oxygen atoms with lone-pair electrons and a double bond with π -electrons. During quenching these functional groups might form a stronger complex (polydentate ligand) with titanium and thereby influence the competition between reaction (1) and (2) (i.e. the ratio $k_1:k_2$) to a different extent compared to similar

experiments with CH₃OH. In order to influence these reactions, additional TiCl₄ was added simultaneously together with HEMA. However, only a small change in product composition was observed. A second problem is elimination of HEMA caused by the presence of HCl (Scheme 5.4, reaction (3)). This reaction might also proceed faster than with CH₃OH. Therefore, in a third experiment the HEMA solution contained Et₃N in order to capture the HCl directly. However, Et₃N does also form a complex with titanium, leading to further deactivation of the Lewis acid. As a consequence, lower degree of functionalization is detected. This means, that the major problem seems to be related to deactivation of the Lewis acid, and thereby to the equilibrium between the ionized and inactive chain ends. Based on the expectation that Ti(OCH₃)₄ is much stronger than Ti(HEMA)_x (x ≤ 4) a fourth experiment was performed in which Ti(OiPr)₄ was added right before HEMA. Expecting that HEMA will only react with TiCl₄ and not with Ti(OiPr)₄, a different product mixture must be formed. Indeed, a certain change is observed but in the undesired direction since the influence of Ti(OiPr)₄ concerning the shift toward the dormant specie is more pronounced than expected ([Ti(OiPr)₄] = 0.6 · [TiCl₄]).



Scheme 5.4: A potential mechanism which summarizes the reactions proceeding during quenching with alcohols.

The crucial point concerning ethylene glycol is its melting point ($T_m = -12$ °C) leading to crystallization in the solution < -20 °C. In the first experiment, the solution was allowed to warm up to -20 °C before methanol was added (below -20 °C the solution was still colored). However, as shown before (Figure 5.6) retroaddition of DPE takes place at elevated temperature. In this case the

product contained > 98% Cl^t-terminated PIB chain ends. In a second experiment, the ethylene glycol solution contained NH₃. The ethylene glycol did not crystallize/precipitate in this quenching solution because of NH₃, but right after addition to the polymer solution it precipitated. The color of the solution disappeared within less than 1 min at -78 °C (in contrast to the first experiment). The obtained product contained < 10% of the desired OH group. Instead, > 90% of the chains were capped with a NH₂ group due to quenching with NH₃, verified by ¹H NMR (-CH₂C(Ph)₂NH₂, 2.54 ppm (triplet)). This result is in agreement with the result obtained by Faust *et al.*¹³¹ The reaction between the 1,1-diphenylcation and ammonia seems to be an easy and quantitative way to introduce an NH₂ endgroup. With 1,4-butanediol the melting point is even higher (T_m = 16 °C). However, in order to see whether it adds to the chain the reaction was quenched with Et₃N after 30 min although it was still colored (50% conversion, Figure 5.9b). Even addition of water does not lead to spontaneous quenching. After 60 min the solution was still red. A mixture of 1-alkoxy-1,1-diphenyl, DPV, and Cl^t endgroups were observed due to retroaddition at elevated temperature.

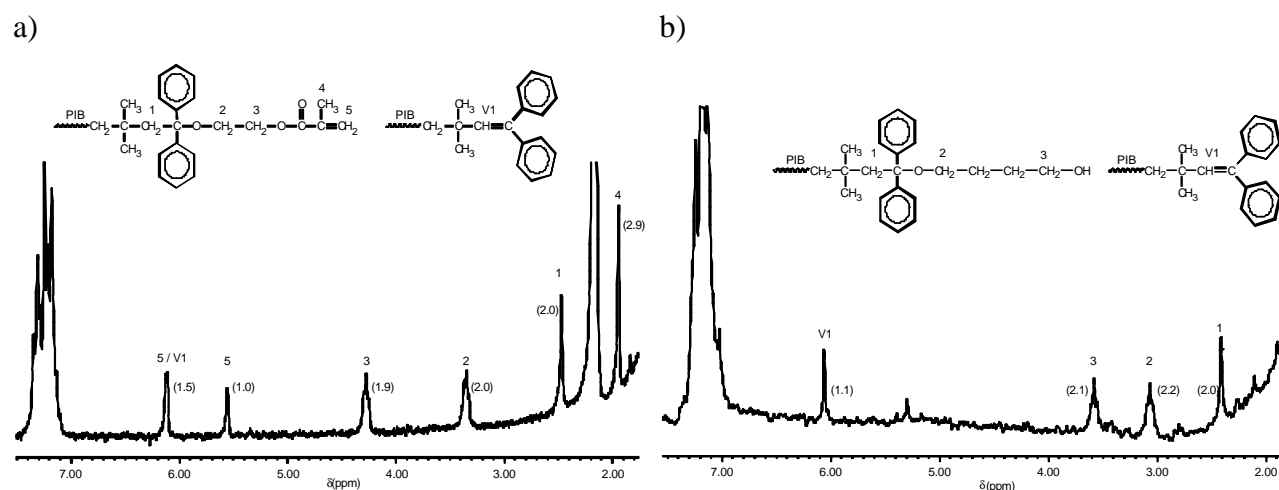


Figure 5.9: ¹H NMR spectrum (200 MHz, in CDCl₃) of a) a partially HEMA-functionalized PIB and b) a partially OH-functionalized PIB.

In the experiments with PEO (soluble at -78 °C) even lower capping efficiencies were reached most likely due to the number of oxygen atoms which complex titanium. In addition, two chain ends have to react with each other which slows the reaction down.

Quenching with the hyperbranched polyol did not work at all due to solubility problems. The polyol was only soluble in DMA (electron donor) or DMA/DMF. Two experiments were carried out with different ratios of OH groups to living chain end. In both cases a DMA/DMF solution of the polyol was used. Since DMA and DMF do also complex titanium, 0 % conversion of the polyol is simply due to a shift of the equilibrium in Scheme 5.4. The advantage of this quenching reaction (if it works) is that quantitative conversion is not required in order to get interesting products. Homo-PIB can be separated by extraction. Therefore, the major problem which has to be solved, is to find a solvent in which the polyol is soluble and which does not interact with the Lewis acid.

In conclusion, the problems related to this type of quenching are due to competition between three different reactions: Quenching of the 1,1-diphenyl cation (1), deactivation of the Lewis acid (2), and elimination of the alcohol due to the presence of HCl (3). Therefore, thorough/systematic

investigations concerning the influence of Lewis acids, solvent(s), and R-groups of the alcohols on the rates of reaction (1), (2), and (3) (Scheme 5.4) are required. Optimum conditions are reached when $k_1 \gg k_2$ and k_3 . It might even be necessary to reinitiate a methoxy-terminated PIB in a second step under selected conditions and then quench the 1,1-diphenylcation with the desired alcohol.

5.3 Cationic polymerization of vinyl ethers and attempted functionalization with DPE

Based on the results and the experiences gained by the DPE-capping of PIB, the aim is in this section to investigate whether functionalization of vinyl ethers is possible with DPE. Vinyl ethers do also show interesting properties, such as low T_g , hydrophobic or hydrophilic character, depending on the alkyl group. Only isobutyl vinyl ether (IBVE) was investigated. In the literature, it has been demonstrated that block copolymers of PIBVE-*b*-PSt can be synthesized by sequential monomer addition (styrene to an active PIBVE) using SnCl_4 as coinitiator.¹⁸⁵ Taking the similarities between styrene and DPE into account (the stabilization of the cation by the phenyl ring(s)) it might be possible to add DPE to the active PIBVE. A somewhat different initiating system involving ZnCl_2 is used here, since the blocking efficiency is less than quantitative with SnCl_4 .

Several important differences compared to the IB system have to be taken into consideration:

- The Lewis acid is ZnCl_2 (much weaker than TiCl_4), and it is used in a substantial lower ratio relative to the initiator (1:370) compared to the IB system (10-20:1).
- The poly(vinyl ether) acts as a nucleophile and deactivates the Lewis acid.
- The polymerization temperature is normally $-15\text{ }^\circ\text{C}$ instead of $-78\text{ }^\circ\text{C}$.

First the normal kinetics of IBVE polymerization had to be analyzed, since after 100 % monomer conversion the endgroups tend to eliminate HCl irreversibly leading to a chain end unable to react with DPE. After 180 min full conversion was reached with the applied system. Thus the ideal progress of such a capping reaction is that DPE is added right after full conversion of IBVE and then the reaction has to proceed within a short period of time. In one experiment DPE was added to the active PIBVE after 180 min, at the time when the polymer solution went slightly yellow (> 96 % conv. of IBVE) at $-15\text{ }^\circ\text{C}$. After 120 min the DPE-capping reaction was quenched with methanol.

The SEC traces, Figure 5.10, indicate no changes in M_n as expected, but a remarkable change of the RI/UV ratio. However, the ^1H NMR spectra of the products before and after addition of DPE are nearly identical and do not contain signals in the aromatic region, indicating that the PIBVE is not capped with DPE. Therefore, the UV signal at 260 nm is due to elimination of HCl which is possibly followed by further elimination starting from the chain end leading to a conjugated chain segment, since the monomer itself does not absorb at 260 nm.

One problem might be that the capping reaction is performed at a relatively high temperature, $-15\text{ }^\circ\text{C}$, at which no capping was observed in case of PIB (see Figure 5.7). Therefore, one experiment was performed in the following way: After full conversion of IBVE at $-15\text{ }^\circ\text{C}$ the solution was cooled to $-78\text{ }^\circ\text{C}$. Then DPE was added and allowed to react for 60 min. The ^1H NMR spectrum proves that DPE addition does not take place. The crucial point seems to be the equilibrium between active and

inactive species (Scheme 1.1) which again is related to the Lewis acid and potential additives. Further work is needed in order to find a possible system where DPE-capping of poly(vinyl ethers) can be carried out.

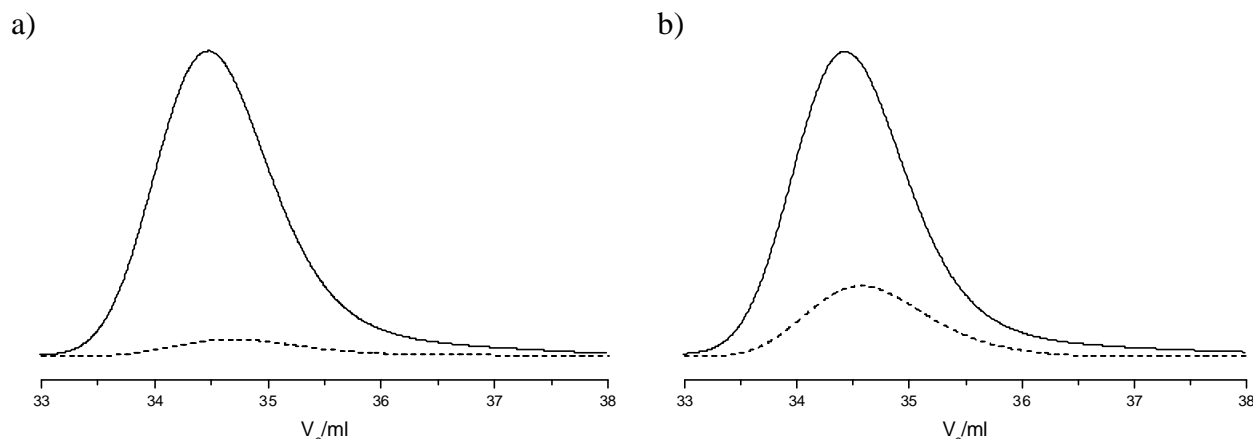


Figure 5.10: SEC trace of a poly(isobutyl vinyl ether) (PIBVE) a) before and b) after addition of DPE, (—) RI-signal and (---) UV signal (260 nm).

5.4 Cross-over from cationic to anionic polymerization

One of the major objectives of this project is to find a suitable way to combine cationic and anionic polymerizations in order to overcome the limited number of monomers which can be used in each procedure and thus, to obtain new materials. In chapter 1 the efforts reported so far in this field have been introduced. However, none of these methods gave high quality materials because of insufficient blocking efficiencies and involved multi-step procedures.

5.4.1 Screening experiments with different potential initiators for anionic polymerization

Different approaches were investigated taking into account general aspects concerning anionic initiators and former attempts (chapter 1).

A standard initiator for LA-Pzn of (meth)acrylates is synthesized by adding BuLi to DPE leading to 1,1-diphenylhexyllithium (see Scheme 1.7). In section 5.2.2 it has been demonstrated that DPV-capped PIBs can be synthesized in quantitative yield. This structure is similar to DPE, only a proton is exchanged with a PIB chain (alkyl group). The model compound 3,3,5,5-tetramethyl-1,1-diphenylhex-1-ene (TMP-DPV, obtained by adding DPE to TMPCl in the presence of TiCl_4 (see Scheme 5.1) was used for studying the lithiation reaction. Table 5.5 summarizes results of these experiments. It is seen that relatively low BuLi (or MeLi):TMP-DPV ratios led to low lithiation conversion. Even nearly two orders of magnitude excess n-BuLi resulted only in $\approx 70\%$ lithiation. The most reasonable explanation for these unexpected low lithiation yields (compared to the addition of BuLi to DPE) is steric hindrance by the two methyl groups next to the carbon atom reacting with the alkyl group of the alkyllithium compounds. Therefore, three experiments were also carried out with MeLi. However, MeLi reacts only with the phenyl ring.

The major consequence of incomplete lithiation is the presence of homopolymer of PIB together with the desired block copolymer. Besides, unreacted BuLi can separately initiate anionic

polymerization of methacrylates or it can make a nucleophilic substitution on the ester group generating an alkoxide. The easiest way to remove excess BuLi is to heat the THF solution to room temperature, since BuLi reacts with THF at elevated temperature, forming ethylene and ethenolate.

Table 5.5: Lithiation of TMP-DPV with alkyllithium compounds under different conditions

[TMP-DPV] · 10 ² (M) solvent	Temp. (°C)	Time (hours)	R(Li)/TMP-DPV ratio	Yield (%)	Remarks
1.55 THF	-78 20	4 20	2:1 (<i>n</i> -BuLi)	18	Quenched at -78 °C.
1.03 THF	-78 20	3 2	60:1 (<i>n</i> -BuLi)	72	Quenched at -78 °C.
0.70 THF	20	3	40:1 (<i>n</i> -BuLi)	65-70	The amount of BuLi was added stepwise during 3 hours. Quenched at -78 °C
0.90 THF	-78 20	1.5 3	10:1 (<i>s</i> -BuLi)	44	Quenched at -78 °C.
0.85 THF	0 20	6 1	4:1 (MeLi)	22	The lithiation proceeds only at the phenyl rings. Performed in the presence of TMEDA, ($n_{\text{TMEDA}} = n_{\text{TMP-DPV}}$)
0.85 <i>n</i> -hexane	40-50	7.5	4:1 (<i>n</i> -BuLi)	≈0	After 4 h no reaction occurred (the solution was colorless). TMEDA ($n_{\text{TMEDA}} = n_{\text{BuLi}}$) was added. After 5 min an orange color appeared. The reaction was continued for additional 3.5 h. Quenched at RT.
0.85 <i>n</i> -hexane	40-50	2	4:1 (MeLi)	0	Quenched at RT.
0.85 benzene	40-50	6	4:1 (<i>n</i> -BuLi)	0.5-1	The reaction was performed in the presence of TMEDA ($n_{\text{TMEDA}} = n_{\text{BuLi}}$). Quenched at RT.
0.85 ethylbenzene	40-50	28	4:1 (<i>s</i> -BuLi)	58	Quenched at RT.

The steric problems observed with TMP-DPV might be avoided if diphenylmethane (DPM) is used. It is known that toluene can be attached to the Cl^t-terminated PIB chain end by a Friedel-Crafts alkylation.¹¹⁸ Therefore, it is assumed that a similar reaction can be carried out with DPM.

Preliminary experiments were performed to check carbanion formation from DPM by metalation. As shown in Table 5.7, a variety of metalation agent led to relatively low yields, and only extremely long reaction times provided ≈ 80 % conversions (≈ 90 %, was reached with KNH₂)¹⁸⁶. Based on these results, PIBs containing a DPM endgroup were not synthesized.

Table 5.6: Metalation of DPM under different conditions.

[DPM] · 10 ² (M) solvent	Temp. (°C)	Time (hours)	R(K)Li/DPM ratio	Yield (%)	Remarks
3.9 THF	-78	3	5.8 (<i>s</i> -BuLi)	48	Quenched with CH ₃ OD at -78 °C.

4.5 THF	-78	7	1.2 (<i>s</i> -BuLi)	73	Quenched with CH ₃ OD at -78 °C.
4.5 THF	-78	12	1.2 (<i>s</i> -BuLi)	84	Quenched with CH ₃ OD at -78 °C.
4.5 ethylbenzene	50	8.5	1.2 (<i>s</i> -BuLi)	5-10	Quenched with CH ₃ OD at RT.
4.5 THF	0	14	1.2 (MeLi)	51	Quenched with CH ₃ OD at RT.
2.5 THF	20	5	1.1 (LDA)	44	Quenched with CH ₃ OD at RT.
2.5 THF	20	18	1.3 (LDA)	71	Quenched with CH ₃ OD at RT.
2.5 THF	20	30	1.3 (LDA)	81	Quenched with CH ₃ OD at RT.
2.5 THF	20	12	1.3 (NaphK)	50	Quenched with CH ₃ I at RT.

A few experiments were also carried out with triphenylmethane (TPM), but similar low metalation yields were achieved (< 80 %). If one continued experiments with DPM and TPM one possibility might be metalation with K/Na alloy or Cs metal.

The Cl^t-terminated PIB might also be metallated (Scheme 5.5), forming a tertiary carbanion. Subsequent alteration of nucleophilicity, e.g. by addition of DPE is needed for polymerization of (meth)acrylates (see chapter 1). As shown in Figure 5.11a, a 100 % cleavage of the C-Cl bond was obtained within less than 60 min verified by ¹H NMR. The peak at 1.96 ppm corresponding to the CH₂ group (-CH₂C(CH₃)₂Cl) is absent after metalation. In addition, a slow reduction of M_n was observed during metalation in THF at room temperature (M_n = 3700 (t = 0 min), M_n = 3600 (t = 60 min), and M_n = 3400 (t = 2880 min)). This can be attributed to a depolymerization process of the PIB anion. Unfortunately, the ceiling temperature (T_c) of PIB is not exactly known (has been reported to be in the range, T_c = 50-175 °C)^{187,188}. Wurtz coupling was not detected. The absence of Wurtz coupling is either due to the low concentration of chain ends (10⁻² M) or to the fact that the formed PIB anion abstracts a proton right away from THF at RT (it is known that tBuLi reacts with THF at room temperature forming ethene and potassium ethenolate). The reaction between THF and the metallated PIB was investigated by adding para-methylstyrene (pMeSt) to the THF solution after 60 min of metalation and removal of K/Na alloy by filtration. The resulting SEC traces are shown in Figure 5.11b (M_n ≈ 80,000 and M_w/M_n ≈ 1.2 of the high molecular weight peak). The M_n corresponds to an initiating efficiency of 10-20 % relative to the number of PIB-Cl^t chain ends (the conversion of pMeSt is about 100 %). Taking into account the RI response factors of PpMeSt and PIB (RI_{PpMeSt}/RI_{PIB} = 1.73) the blocking efficiency can also be calculated from the area under each peak (Figure 5.11b). It was ≈ 0-10 % indicating nearly quantitative reaction with THF. The formed PpMeSt is either initiated by the PIB anions or traces of K/Na alloy. Initiation by the potassium ethenolate from the reaction with THF is very improbable. Potential initiation by traces of K/Na alloy can be excluded since PpMeSt was not formed in the sample where metalation was stopped after 15

min, only in the samples after 30 and 60 min of metalation (same equipment/ procedure was used). Therefore, the species initiating the polymerization of pMeSt are a small fraction ($\approx 10\%$) of metallated PIB. The reason why depolymerization proceeds even after 60 min might be related to subsequent and continuous abstraction of the tertiary proton at the chain end by K.

In order to obtain the desired carbanion other conditions, such as lower temperature or another solvent, are needed. Since the melting point of the K/Na alloy is at 0-5 °C, a K-mirror has to be used for metalation at low temperature. One experiment was carried out in THF at -20 °C. After 30 min the solution was filtered and then pMeSt was added to the PIB solution. The blocking efficiency was also $\approx 0-10\%$. Therefore, in THF the temperature has to be much lower but then the rate of metalation will be very slow. Instead, another solvent might be the solution.

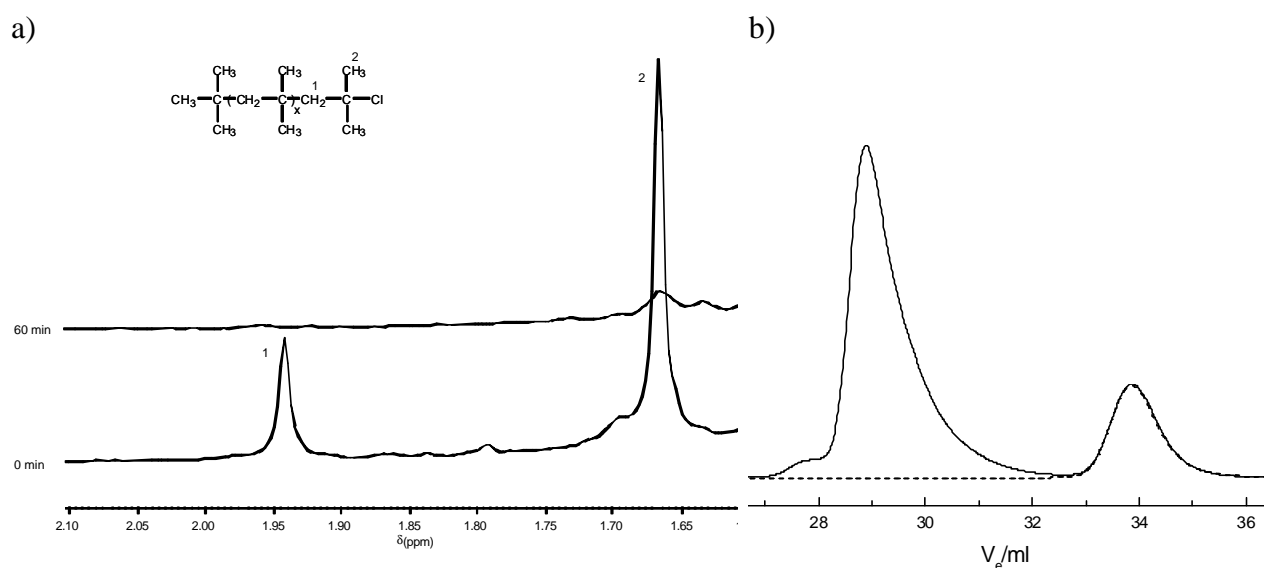
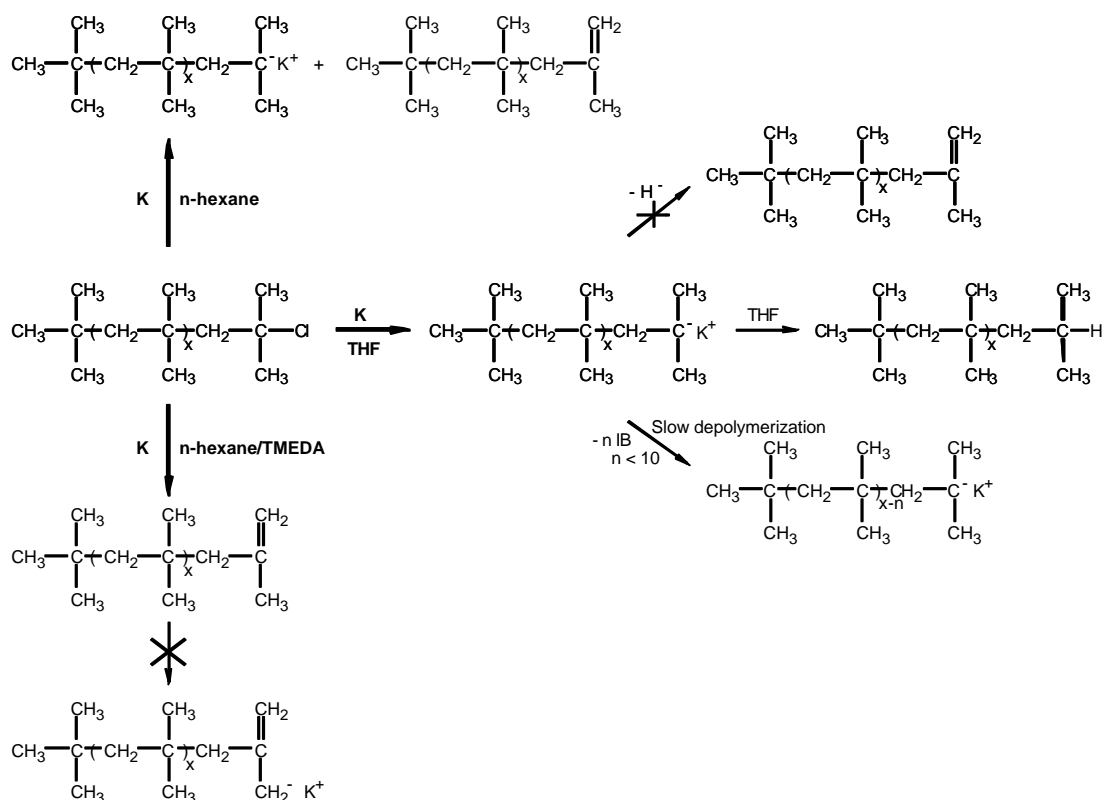


Figure 5.11: a) ¹H NMR spectra (200 MHz in CDCl₃) of a Cl^t terminated PIB (0 min) and the corresponding product obtained by metalation with K/Na alloy in THF at room temperature (60 min) quenched with methanol. b) SEC traces of the PIB-Cl^t precursor (---) and the product obtain after addition of pMeSt (—).

In *n*-hexane at RT the metalation was rather slow. After 60 min 75 % Cl^t-terminated PIB was still present. However, after 240 min a mixture of 30 % Cl^t, 15 % vinyl (Scheme 5.5), and 55 % H endgroups was obtained, proved with ¹H NMR. The problem in this case is partial dehydrochlorination proceeding simultaneously during metalation. The resulting vinyl group might also subsequently be metallated since the allylic protons are relatively acidic (from the literature it is known that BuLi can abstract allylic protons)¹²⁰ and then two different carbanions are present. However, if DPE is added similar carbanions would be formed. Attempts toward metalation of the isopropenyl chain end (and 2,4,4-trimethylpent-1-ene) with K/Na alloy did not work proved by subsequent addition of DPE (¹H NMR analysis indicate 0 % metalation since signals in the aromatic area due to potential addition of DPE could not be detected). In a second experiment with *n*-hexane, TMEDA ($n_{\text{TMEDA}} = 1.2 \cdot n_{\text{endgroups}}$) was added in order to increase the rate of metalation. The reaction is faster (< 5 % Cl^t-terminated PIB, after 240 min), but the competing elimination of HCl is now much faster, > 95 % isopropenyl capped PIB. In contrast to the experiments with tBuOK this procedure leads to a product completely free of internal double bond (see section 5.2.1). The question is now what influence TMEDA has on this reaction. TMEDA is a base and might be the

substance causing the elimination of HCl. However, from the result presented in Table 5.3 where tBuOK was used (tBuOK is a stronger base than TMEDA), only 15 % elimination was reached after 45 h at RT. A control experiment with TMEDA and without K/Na alloy proved the absence of elimination, as expected. Therefore, the effect of TMEDA, i.e. the mechanism for the elimination of HCl is not straightforward and at the present time not clear. Optimization of the conditions, i.e. the ratio of TMEDA to Cl^t chain ends and/or the reaction temperature is in progress at the present time in order to use this method primarily for dehydrochlorination and not for metalation of PIB-Cl^t. Compared to the previous method involving tBuOK this one has several advantages: 100 % external vinyl groups are obtained (see Figure 5.4), the reaction is faster, and subsequent purification of the end-product is easier.



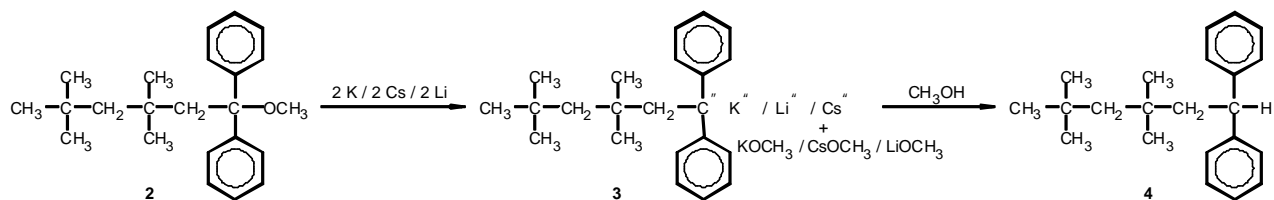
Scheme 5.5: Possible reaction during metalation of Cl^t-terminated PIB.

In conclusion, different synthetic routes have been investigated toward the generation of a carbanion at the PIB chain end. None of these approaches led to acceptable results (less than quantitative conversion was reached) and further work is needed in order to find potential usability of these possibilities. However, under specified conditions a new improved method for dehydrochlorination of PIB-Cl^t has been found involving TMEDA and K/Na alloy in *n*-hexane.

5.4.2 Metalation of 1-methoxy-3,3,5,5-tetramethyl-1,1-diphenylhexane (TMP-DPOMe) and 3,3,5,5-tetramethyl-1,1-di-phenylhex-1-ene (TMP-DPV)

Since quantitative lithiation of TMP-DPV with a variety of lithiating agents, e.g. alkyllithiums, could not be achieved, our attention turned towards direct metalation reactions leading to the desired diphenyl-stabilized carbanions. It was reported by Ziegler and coworkers^{75,76} that certain ethers, such as 1-methoxy-1,1-diphenylethane and 2-methoxy-2-propylbenzene (CumOMe), can be cleaved by

potassium. However, the yields of such ether cleavage reactions were either not determined or were found less than quantitative with the examined compounds and by the applied methods. Recently, even an improved metalation of CumOMe with K/Na alloy led only to 85 % conversion⁷⁷, most likely because this reaction is not free from side reactions such as coupling and dianion formation.



Scheme 5.6: Metalation of TMP-DPOMe with different alkali metals.

As outlined in Scheme 5.6, K/Na alloy, Cs metal, or Li dispersion were selected for carrying out ether cleavage of **2** in our studies. The reaction mixture becomes dark red, which is characteristic of the diphenyl-substituted carbanion **3** right after the addition of a THF solution of **2** to a K/Na suspension in THF. The extent of the metalation reaction was followed by UV-visible and ¹H NMR spectroscopies. The UV-visible spectrum of the THF solution of the formed carbanion **3** has an absorption maximum at $\lambda = 480$ nm. As Figure 5.12a shows, the relative absorbance at this wavelength reaches a constant value after about 30 min with K/Na and 45 min in the presence of Cs. Metalation with lithium (30% w/w lithium-dispersion in mineral oil, containing < 0.05% Na) is about 100 times slower than with K/Na or Cs. In the latter case the consistency of the Li-dispersion might have some influence on the rate of metalation. $\lambda_{\text{max}} = 502$ nm for the lithium compound is somewhat higher than for the K or Cs one (both about 480 nm), and it is in good agreement with $\lambda_{\text{max}} = 496$ nm observed for 1,1-diphenylhexyllithium.¹⁸⁹ From the UV absorbance an absorption coefficient of $\epsilon \approx 2 \cdot 10^4 \text{ mole}^{-1} \cdot \text{l} \cdot \text{cm}^{-1}$ is calculated. This value is in good agreement with literature data on comparable compounds.¹⁹⁰ The resulting carbanionic species exhibit high stability in THF at room temperature as indicated by the fact that the value of the absorption does not change even after storing the solutions under inert atmosphere for more than ten days.

a)

b)

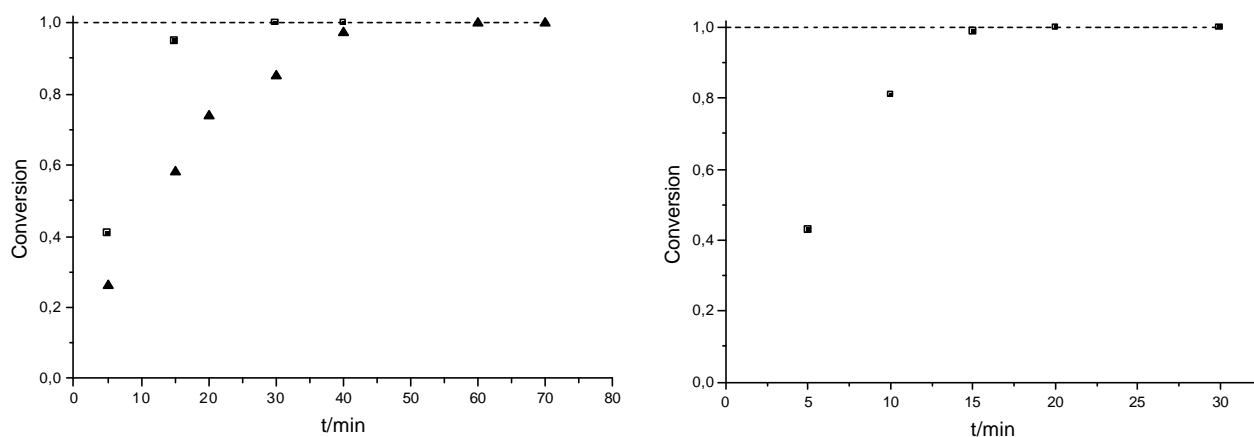


Figure 5.12: Conversion as determined by UV absorption (at $\lambda_{\max} = 480$ nm) during metallation of a) 1-methoxy-3,3,5,5-tetramethyl-1,1-diphenylhexane and b) 3,3,5,5-tetramethyl-1,1-diphenylhex-1-ene with K/Na alloy (■) and Cs metal (▲).

Quenching the carbanionic system with methanol leads to the hydrogenated product 3,3,5,5-tetramethyl-1,1-diphenylhexane (**4**) (Scheme 5.6). This reaction was used to determine the yield of the metallation reaction.

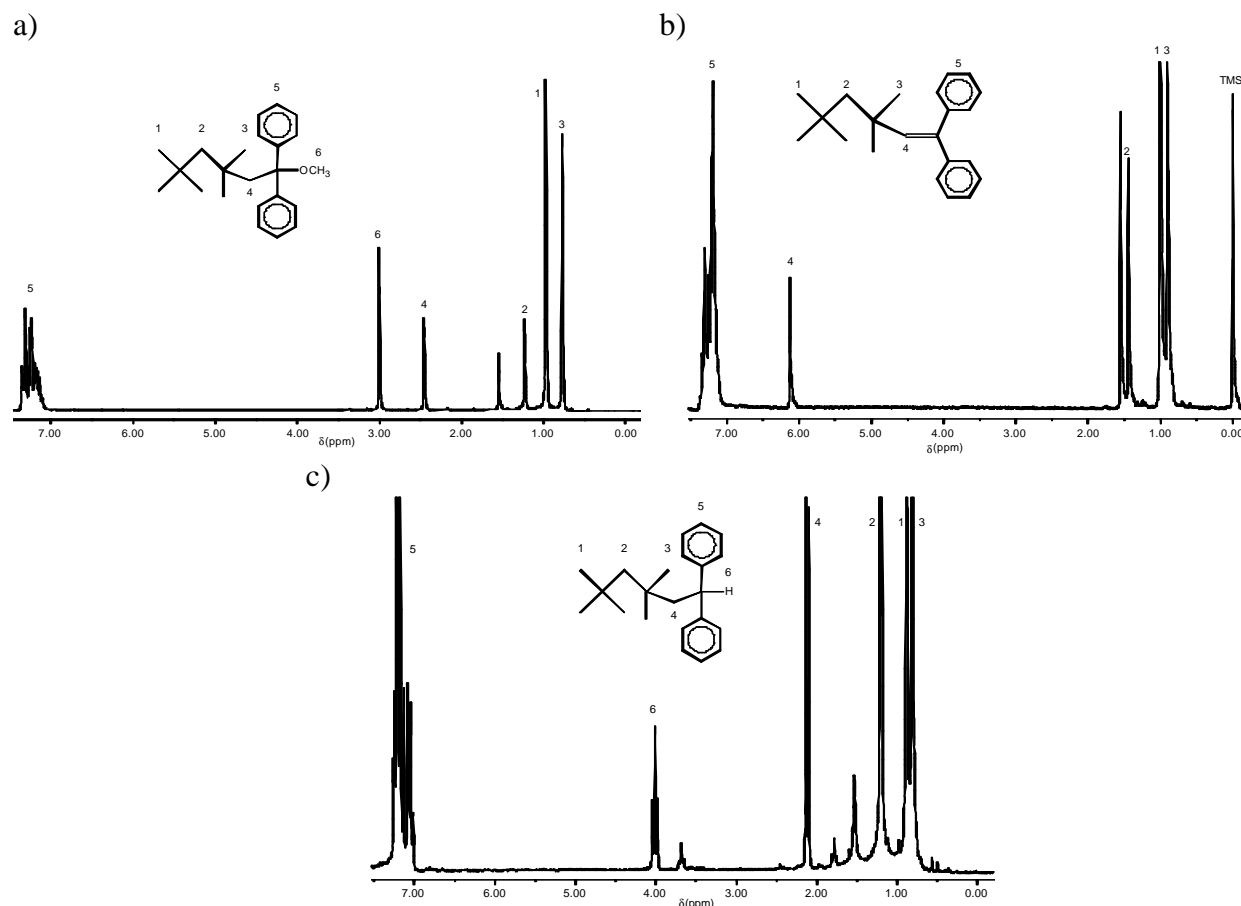
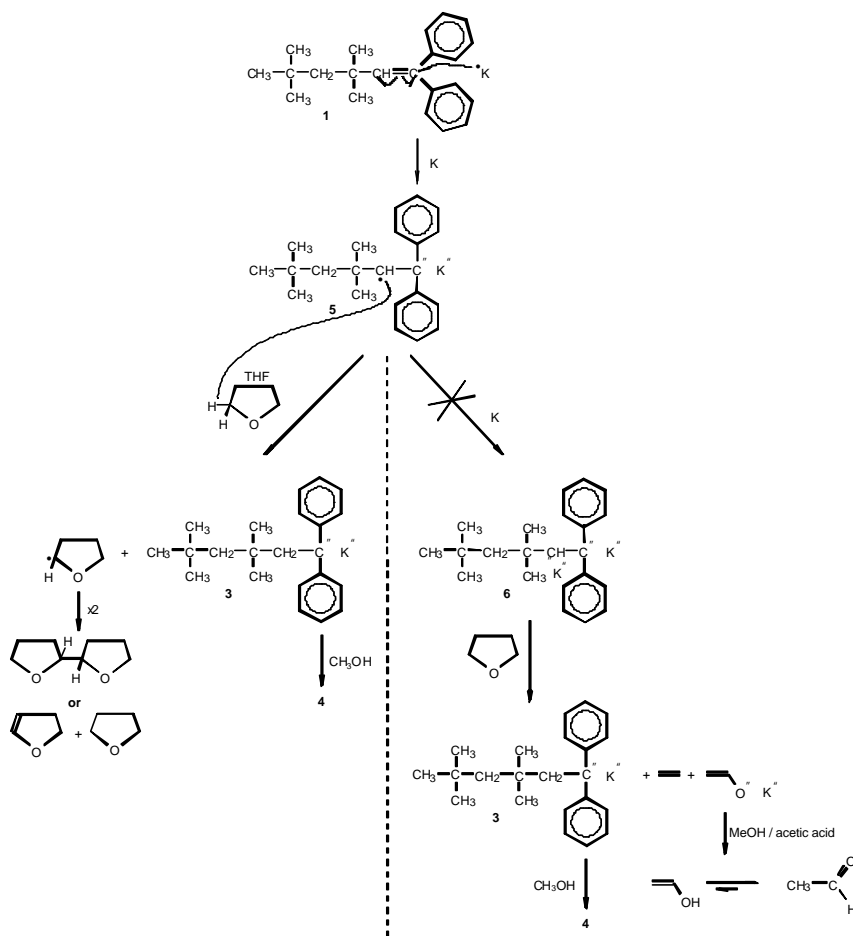


Figure 5.13: ¹H NMR spectra (200 MHz in CDCl₃) of a) TMP-DPOMe, b) TMP-DPV, and c) the metallated product after quenching with methanol (TMP-DPH).

As shown in Figure 5.13a/c, the characteristic signal for the methyl protons of the methoxy group completely disappears after reacting **2** with K/Na for 30 min, and a triplet at 4.0 ppm appears after quenching with methanol. Integrals are in agreement with the given structures. These data indicate that the metallation reaction quantitatively leads to carbanion **3**. This finding also proves that

the constant relative absorption value of the UV-visible spectra after a certain reaction time corresponds to quantitative metalation.

Metalation of DPE with K/Na alloy at room temperature is known to lead to the formation of a radical anion which subsequently couples, resulting in a 1,1,4,4-tetraphenyl butyl dianion which is a difunctional initiator.⁷⁴ Metalation of **1** with K/Na alloy was also attempted. As shown in Figure 5.12b, this reaction also leads to quantitative metalation. It exhibits the relative absorbance of the formed carbanion indicating quantitative reaction within 15 min. Figure 5.13b shows the ¹H NMR spectra of the starting compound, **1**. The ¹H NMR spectrum of the product formed by quenching the carbanionic system with methanol is identical to the one from TMP-DPOMe (Figure 5.13c). Complete disappearance of the vinyl proton signal at 6.12 ppm is an evidence for quantitative metalation. Surprisingly, no coupling could be detected by ¹H NMR. The integration ratio of the signals at 2.15 ppm and 4.0 ppm is 2:1 as expected. In case of coupling the signal at 2.15 ppm would change from a doublet to a triplet, and the integration ratio relative to the one at 4.0 ppm would be 1:1. The UV-visible spectrum of the resulting product is identical with that of the carbanion formed by reacting **2** with K/Na or Cs. Both carbanions have an absorption maximum at $\lambda = 480$ nm. Further evidence verifying this postulate is given later together with the polymerization results. Metalation of **2** was also performed with Na-mirror but it is sluggish. After 4 days only 76 % conversion was detected most likely due to the relatively low surface area.



Scheme 5.7: Potential mechanism for the metalation of 3,3,5,5-tetramethyl-1,1-diphenylhexene involving the formation of an intermediate radical anion.

It is assumed that the metalation reaction of **1** with K/Na alloy in THF occurs by formation of a radical anion **5** in the first step as shown in Scheme 3. Most probably **5** quickly abstracts a hydrogen atom from the solvent THF leading to the stable carbanion **3**. THF radicals easily disappear by recombination or disproportionation. An alternative possibility is the reaction between the radical anion **5** with a second K atom leading to an unstable dianion **6**. This yields **3** by abstracting a proton from THF and the cyclic anion will decompose to ethylene and vinyl alcoholate (acetaldehyde enolate). In order to test whether acetaldehyde is present or not, metalation with K/Na alloy was performed in THF- d_8 . After quenching with methanol and acetic acid the crude product was analyzed immediately by ^1H NMR. Not even traces of aldehyde protons in the range 9-10 ppm could be detected. GC measurements also indicate the absence of acetaldehyde. Based on these results we assume that the metalation proceeds by the mechanism mentioned first. Later in section (5.5.1), further evidence for this postulation can be found.

These new quantitative metalation reactions have great synthetic significance. The product formed quantitatively between a cationic species and DPE can be a mixture of DPV- and DPOMe-containing compounds depending on reaction conditions (section 5.2.2). Since the metalation of both groups leads to the same carbanion quantitatively, converting such cationically obtained products to diphenyl-stabilized carbanionic species is not sensitive at all to the composition of the mixture containing **1** and **2**. The product, TMP-DPH formed by quenching **1** and **2** (see Figure 5.13c) can also be metallated with K/Na alloy (the TMP-DPH used in this metalation experiment was donated by Faust *et al.*). However, the rate of metalation is orders of magnitude slower compared to the one of TMP-DPOMe, Figure 5.14. Therefore, it is important to avoid any kind of quenching during or after metalation, else quantitative initiating efficiency can not be reached in subsequent anionic polymerization. One problem might be that the K/Na alloy reacts simultaneously with **1/2** and impurities, and then **3** with the rest of impurities leading to the formation of TMP-DPH. Using CH_3OD as a quenching agent, it was proved that only traces of **1/2** were quenched by protons. Therefore, it can be concluded that during the induction period which is normally observed (after addition of K/Na alloy to the THF solution the red color first appeared after 5-20 sec up to several min) an effective purification of the system takes place before metalation of **1/2** proceeds.

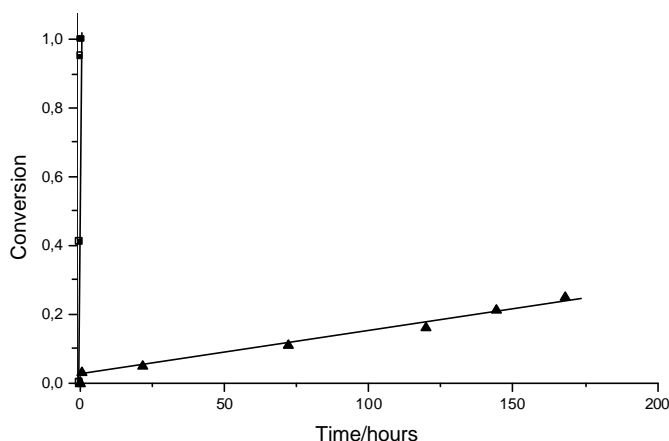


Figure 5.14: Degree of metalation of TMP-DPOMe (■) and TMP-DPH (▲) in THF with K/Na alloy followed by UV-spectroscopy at $\lambda_{\text{max}} = 480$ nm.

The formation of **3** was also proved by using this stable carbanion for the initiation of living anionic polymerization of methyl methacrylate (MMA). After replacing K^{\oplus} with Li^{\oplus} by adding excess LiCl (10 times), the initiating ability of the resulting anions were tested by charging MMA. The results of these polymerization experiments are shown in Table 5.7. As these data indicate, metalation of either **1** or **2** followed by replacement of K^{\oplus} with Li^{\oplus} results in new anionic initiators with quantitative initiating efficiencies leading to PMMA with desired M_n and narrow molecular weight distribution. These findings directly prove that the metalation of **1** and **2** with K/Na alloy or Cs metal is quantitative and leads to stable carbanions capable to initiate living anionic polymerizations. On the basis of these results coupling of **5** to form a dianion can be excluded too, since this should result in doubling of the molecular weight and to an apparent initiating efficiency, $f = 0.5$.

Table 5.7: Precursor, initial concentrations of initiator, $[I]_0$, and monomer, yield, number average molecular weight, M_n , polydispersity index, M_w/M_n , and initiating efficiency, f , in polymerization of methyl methacrylate (MMA) by lithiated **1** and **2**.

Precursor	$[I]_0 \cdot 10^3$ M	[MMA] M	yield %	$M_n \cdot 10^{-3}$ (SEC)	M_w/M_n (SEC)	f
1	2.29	0.35	100	16.2	1.04	1.04
2	6.16	0.32	100	5.5	1.09	1.00
2	4.00	0.26	100	6.6	1.07	0.97

Transmetalation from K to Li is needed for the polymerization of primary methacrylates like MMA and HEMA derivatives in order to control the polymerization in THF at $-78\text{ }^{\circ}\text{C}$. With lithium $PDI < 1.1$ (Table 5.7) whereas with potassium $PDI > 5.0$. A shift of λ_{max} from 480 nm to 502 nm (see Figure 5.15) and a color change from dark red to pink/red are observed during transmetalation indicating that the Li salt has been formed.

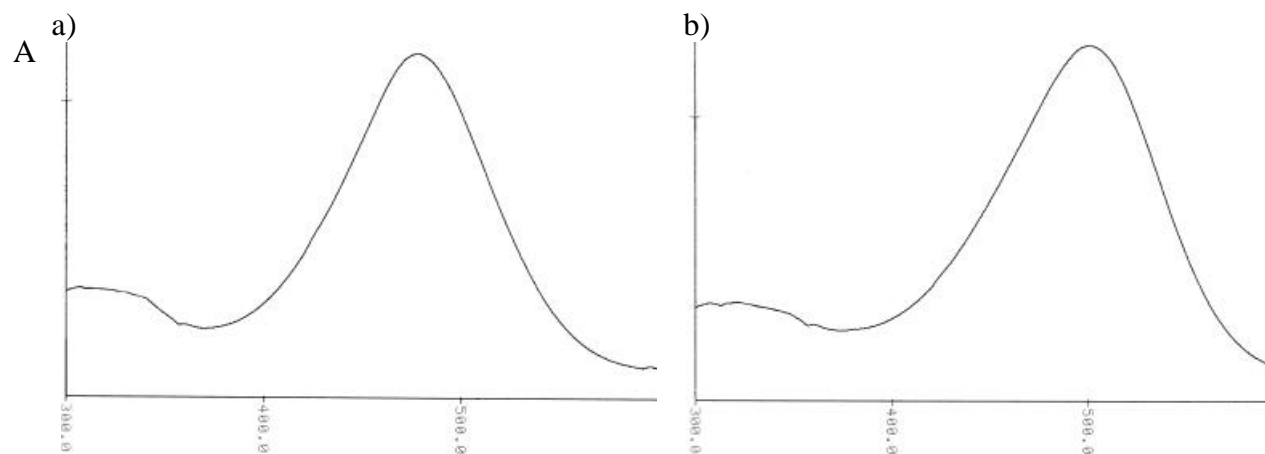


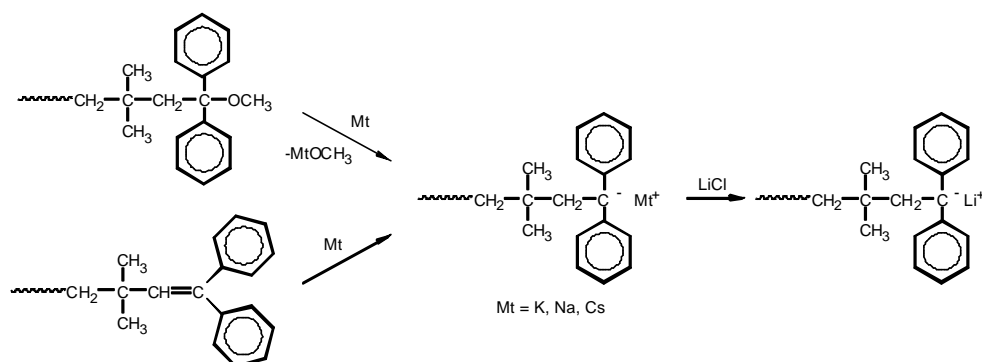
Figure 5.15: UV-spectra of the metallated TMP-DPOME before a) ($\lambda_{\text{max}} = 478\text{ nm}$, $\epsilon \approx 1.96 \cdot 10^4\text{ cm}^{-1} \cdot \text{M}^{-1}$) and after b) ($\lambda_{\text{max}} = 502\text{ nm}$, $\epsilon \approx 2.12 \cdot 10^4\text{ cm}^{-1} \cdot \text{M}^{-1}$) addition of 10 times excess of LiCl.

On the basis of these results, not only a large variety of new low molecular weight materials but new types of polymeric architectures can be synthesized with macroinitiators obtained by metalation of compounds or polymers containing DPV and/or DPOMe endgroups. Details concerning

the synthesis and characterization of AB and ABA block copolymers will be reported later in this chapter.

5.4.3 Metalation of DPE-ended PIB precursors

As discussed above, metalation of model compounds of the corresponding PIB chain ends, i.e. 1-methoxy-1,1-diphenyl-3,3,5,5-tetramethylhexane and 1,1-diphenyl-3,3,5,5-tetramethylhex-1-ene, is straightforward and quantitative with K/Na alloy and Cs metal (Na mirror and Li suspension has to be further investigated for optimization). The resulting carbanions led to living anionic polymerization of methacrylic monomers with $\approx 100\%$ initiating efficiency (Table 5.7). In order to prepare the desired block copolymers, it is of interest whether the quantitative metalation results obtained with the model compounds can be converted to the PIB macroprecursors within a broad range of molecular weights ($M_n = 1\text{-}50,000$).



Scheme 5.8: Metalation of DPOME/DPV-capped PIB leading to a PIB macroinitiator with different counterions.

Scheme 5.1 and 5.8 outline the chemical transformations in the course of endcapping of living PIB chains with DPE and the subsequent formation of the carbanionic macroinitiator upon metalation, respectively. Figure 5.16 summarizes the time-conversion plots obtained by UV-visible spectroscopy for PIB samples with the degree of polymerization in the range of $2 \leq P_n \leq 570$; later PIBs with $P_n \approx 800$ were metallated fast and quantitatively, too.

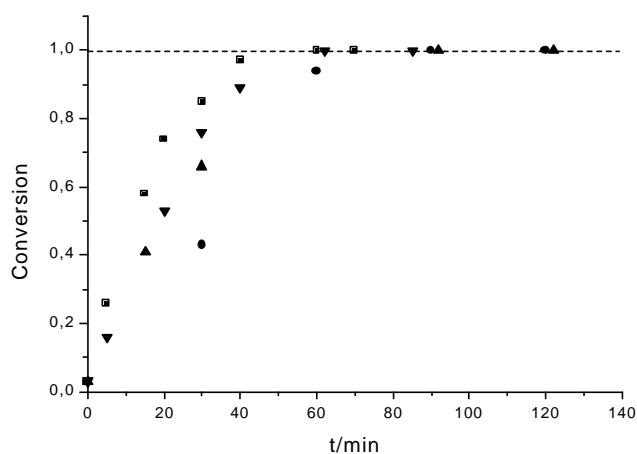


Figure 5.16: Time-conversion plots for metalation of DPE-capped PIBs with K/Na alloy as followed by UV-VIS absorbance at $\lambda_{\max} = 480$ nm ($\epsilon \approx 2 \cdot 10^4$), $M_n = 150$ (■), $M_n = 5000$ (●), $M_n = 17,500$ (▲), $M_n = 32,000$ (▼).

As shown in this figure, the molecular weight has no significant effect on the rate of metalation. Quantitative metalation of DPE-capped PIBs can be achieved within 60 minutes (constant absorbance). The metalation products were further analyzed by ^1H NMR. In all cases 100 % metalation was observed.

As stated above coupling could also be expected when metallating DPV-ended PIB. However, as shown in Figure 5.17, the SEC eluograms of PIB with DPV endgroups before and after 60-420 min metalation are identical, indicating the absence of coupling upon metalation. This confirms results obtained with the corresponding model compounds by ^1H NMR analysis (Figure 5.13) and by the quantitative initiating efficiency for MMA polymerization (Table 5.7). The stability of the PIB-DPE $^-$ K $^+$ ion pair was also tested. It was found that the intensity of the UV-visible absorption at 480 nm did not change either even after 10 days, indicating the same high stability of these macroinitiators as for the model compounds in THF at room temperature.

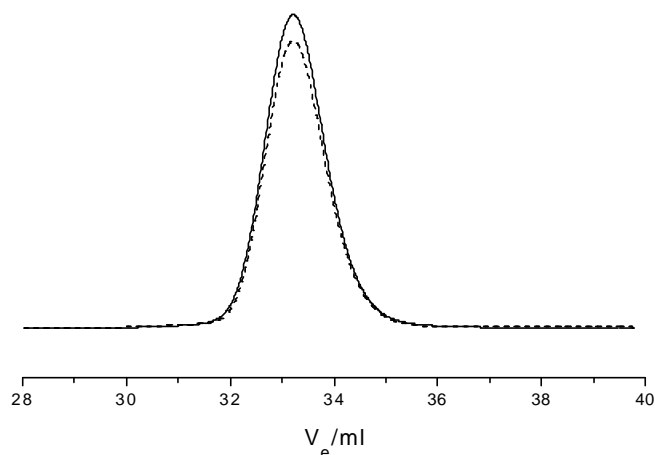


Figure 5.17: SEC traces (RI signal) of a DPV-ended PIB precursor before (---) and after (—) metalation

The effect of non-quantitative end-capping on the metalation process was also investigated. A difunctional PIB sample having 85% DPV and 15% *tert*-chlorine chain ends was metallated with K/Na alloy as described in the Experimental Section. After 60 min the reaction was quenched with methanol, and the resulting material was analyzed by SEC. As shown in Figure 5.18a, coupling occurs between the carbanion and the *tert*-chlorine containing endgroups. This reaction is exhibited in Figure 5.18b. Since the precursor PIB is difunctional, multiple coupling occurs resulting in a multimodal MWD with peak maxima corresponding to multiples of the molecular weight of the precursor. There are two important consequences of these findings: On one hand, the endcapping reaction with DPE should be quantitative during LC $^+$ Pzn of IB. On the other hand, the absence of coupling during metalation of the DPE-capped PIB is an indirect proof for quantitative endcapping. Since even relatively low amounts of coupling can be detected by SEC, this can be utilized for testing the yield of DPE capping for high molecular weight PIBs ($M_n > 10000$) when ^1H NMR or UV-VIS spectroscopies cannot be used for reliable endgroup analysis.

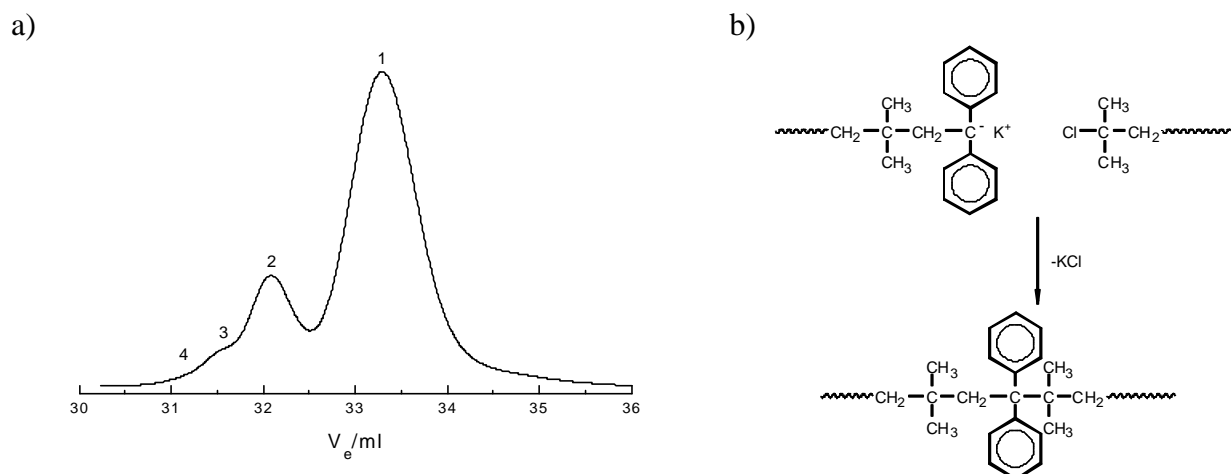


Figure 5.18: a) SEC trace (RI signal) of a difunctional PIB sample (peak 1; $M_p = 6000$) containing 85% DPV and 15% $-Cl^t$ endgroups after 60 min metalation with K/Na alloy in THF at room temperature (peak 2; $M_p = 12000$, peak 3; $M_p = 18000$, peak 4; $M_p = 24000$), b) the corresponding coupling reaction.

The coupling reaction illustrated in Figure 5.18b is based on the fact that Wurtz coupling is not observed when metalation is carried out under the same conditions (in THF at RT) with a PIB only having $-Cl^t$ endgroups (see section 5.4.1). This means, that after the fast metalation of the DPE-capped PIB (less than 30 min) a nucleophilic substitution of the tertiary chlorine takes place. This coupling reaction is actually unexpected because the product is sterically unfavored, two tertiary carbon atoms are linked together. Since the PIB used in this metalation experiment is initiated with a difunctional initiator a blend of four PIBs is obtained as illustrated in Figure 5.18a.

As presented in this and previous sections, quantitative formation of carbanions can be achieved by metalation of DPV- and DPOMe-capped PIBs. In the course of these studies, the next crucial point was the verification of high (quantitative) blocking efficiency of the PIB macroanion by LA-Pzn. Different experiments were carried out at the beginning with a PIB precursor ($M_n = 5,800$) (Table 5.8). The M_n of the block copolymer was intentionally chosen so that two well-separated peaks in the SEC traces will be present in case of less than quantitative blocking efficiency.

Table 5.8: Conditions and results of the anionic polymerization of tBMA with a PIB macroinitiator: the counterion, the molar concentration of the DPOMe endgroups, the molar concentration of tBMA, the theoretical M_n of the tBMA segment, if $f=1$, yield concerning conversion of tBMA, f the blocking efficiency calculated from the SEC UV-results, and f_c the blocking efficiency taking into account that only $\approx 70\%$ of the chain ends were metallated.

Sample no.	Counterion	$[I] \cdot 10^3$ M	$[tBMA]$ M	Reaction time (min) ^b	$M_{n,theo.}$ tBMA	Yield %	f	f_c
AB11	K^+	3.5	0.5	10	20000	>98	0.75	1.0
AB12	^a Li^+	3.5	0.5	90	20000	≈ 100	0.72	1.0
AB13	K^+	2.8	0.1	15	6000	>95	0.50	0.7
AB14	K^+	3.0	0.6	15	20000	>95	0.70	1.0
AB16	K^+	2.9	0.5	90	26000	>95	>0.95	-

^a10 times excess of LiCl was used. ^bThe polymerizations were carried out at $-78^\circ C$.

The first four experiments were performed without using UV detection of the progress of metalation. In all cases about 70 % blocking efficiency was obtained. However, subsequent ^1H NMR analysis of the product proved that only 70-75 % of the endgroups were metallated (25 % OCH_3 was present). Taking the ^1H NMR results into account the blocking efficiency, f_c of the metallated polymer chains is nearly quantitative. As demonstrated in Figure 5.16, PIBs carefully purified can be quantitatively metallated within 1 hour. In the fifth experiment UV spectroscopy was utilized in order to follow the progress of metalation (less than 60 min were needed). This PIB was purified extra thoroughly, evacuated 48 hours on a vacuum-line. In Figure 5.19 a SEC eluogram of this AB block copolymer (AB16), polyisobutylene-*b*-poly(*tert*-butyl methacrylate) (PIB-*b*-PtBMA) is shown (crude product before precipitation). By integration of the respective UV signals at 260 nm corresponding to the precursor and the block copolymer, a blocking efficiency of > 95 % could be determined.

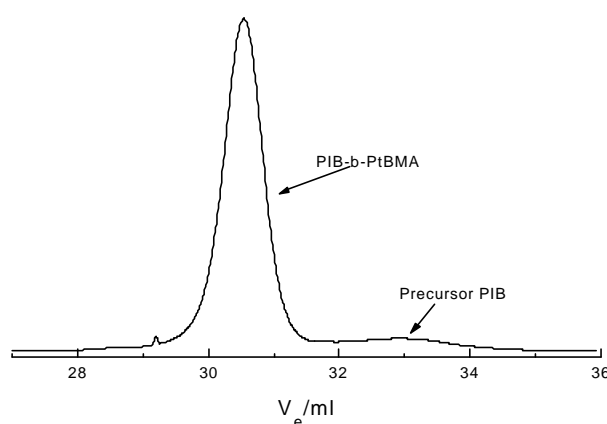


Figure 5.19: SEC trace (UV signal at 260 nm) of PIB-*b*-PtBMA (sample AB16) ($M_n \approx 32,000$, $M_w/M_n \approx 1.05$) obtained from a PIB precursor with $M_n = 5,800$.

The rate of metalation of PIB samples seems to be rather sensitive to potential impurities. The induction period (before the red color appears, normally 1-20 min) is directly caused by proton impurities which are removed in advance of the desired metalation. However, it is still unclear what kind of compounds are able to inhibit the metalation process. In some cases the rate of metalation of the same PIB sample (but differently purified) varied with a factor of 2-20. In the subsequent work all the PIBs were at least evacuated for 48 hours on a vacuum-line in order to remove traces of low molecular weight materials (e.g., solvents).

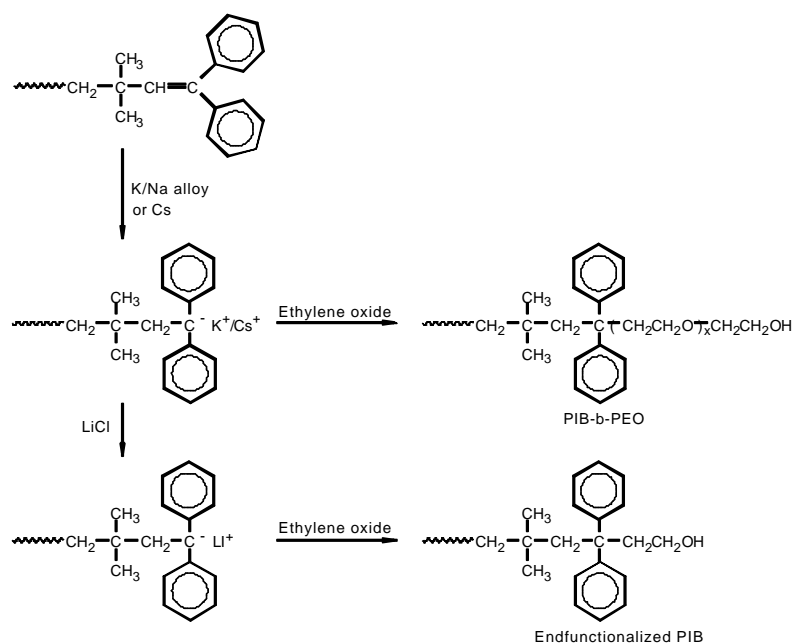
In order to test the stability of the synthesized PIB-*b*-PtBMA (AB16) block copolymer, a THF solution of sample AB16 was exposed to UV light ($\lambda = 254$ nm) for 24 hours and pure AB16 was heated to 140 °C in a vacuum oven for 6 hours. From the SEC traces no changes in molecular weight could be detected.

5.5 Anionic polymerization experiments

Based on the results from previous sections, designed synthesis of tailored PIB-based block copolymers can now be carried out for various applications, such as thermoplastic elastomers, amphiphilic diblock copolymers, and functionalized block copolymers.

5.5.1 Experiments with ethylene oxide

In the experiments with EO the aim is to synthesize two different types of materials. First of all preparation of PIB-*b*-PEO amphiphilic block copolymers are of interest. The AB block copolymers might have interesting properties regarding micelle formation and linear ABA and star-shaped (AB)₃ block copolymers are desired for subsequent synthesis of amphiphilic networks. The second objective of using EO in carbanion chemistry is the synthesis of OH-functionalized PIB which can be utilized for a versatile number of applications (e.g., urethane linkage and synthesis of macro-monomers). The synthetic routes for these approaches are summarized in Scheme 5.9. The second route takes into account that EO does not homopolymerize with Li as counterion (see section 1.2.2).



Scheme 5.9: Polymerization or functionalization of PIB with EO.

Three experiments were carried out with the model compound, TMP-DPV using Li, K, and Cs as counterions (reaction temperature 50 °C, and reaction time 24 h). As discussed in section 1.2.2, initiation with Li⁺ leads only to mono addition of EO, which indeed occur as verified by ¹H NMR (yield: > 95 %). In the experiments with K⁺ and Cs⁺, PEOs with unimodal distributions were prepared and in both cases similar products were obtained, $M_n \approx 6000$ (PIB-calibration), and $M_w/M_n < 1.1$. Using ¹H NMR and the SEC trace (UV signal at 260 nm) an initiating efficiency of > 95 % could be calculated for the potassium experiment. A central question is now whether the methoxy precursor, i.e. DPOMe (and the corresponding PIB compound) which is present in the crude product can be used as initiator, since the side-product of the ether cleavage CH₃O⁻ Cs⁺/K⁺ initiate the polymerization of EO, too. The metalation of the precursor TMP-DPOMe was carried out in a separate flask, and in order to remove residual metal, filtration of the initiator solution was performed. Due to low solubility of CH₃OCs, [CH₃OCs] = 3.5 · 10⁻⁵ M in THF at RT¹⁹¹, it also nearly quantitatively removed. Therefore, since the concentration of CH₃OCs is about 2 orders lower than the initiator concentration used (2.5-5 · 10⁻³ M), the influence of the methoxide salts can be ignored when Cs is present as counterion. However, the solubility of CH₃OK in THF at RT was determined as, [CH₃OK] ≈ 6 · 10⁻⁴ M. CH₃OK was prepared *in situ* by reacting K/Na alloy with

CH₃OH in THF. The filtered THF solution was then analyzed by GC). In this case the amount of undesired initiation is too high. If DPOMe-capped PIB was metallated with K/Na alloy and used for the preparation of PIB-*b*-PEO, about 10 % of the EO would be present as homopolymer which is unacceptable. Based on these findings two possibilities exist with regard to the synthesis of PIB-*b*-PEO. Either Cs metal is utilized and both endgroups (DPOMe/DPV) can be present or K/Na alloy and only the DPV-terminated PIB (carefully prepared under selected conditions) can be applied.

From the ¹H NMR analysis of the above-mentioned TMP-DPV-K⁺ alloy polymerization experiment a further important detail can be also clarified concerning the metalation mechanism postulated for TMP-DPV/DPV-capped PIB in Scheme 5.7. If it proceeds through a dicarbanion leading to the formation CH₂=CHOK, a second initiator suitable for polymerization of EO would be present. Since the solubility of CH₂=CHOK is expected to be higher than that of CH₃OK in THF, more than 10 % of the PEO chains would contain a vinyl endgroup. However, even traces of the vinyl proton at ≈ 6.4 ppm (CH₂=CHOR) could not be detected. Therefore, the ¹H NMR result of this experiment is an additional verification for the proposed mechanism in Scheme 5.7.

In order to test the application of the lithium compound for synthesis of OH-functionalized PIB, EO was added to a low molecular weight (M_n = 1,100) PIB-DPE·Li⁺ macroinitiator. The red color of the THF solution disappeared right after addition of EO which indicates quantitative quenching with EO (or potential impurities). The product was characterized by ¹H NMR (see Figure 5.20a).

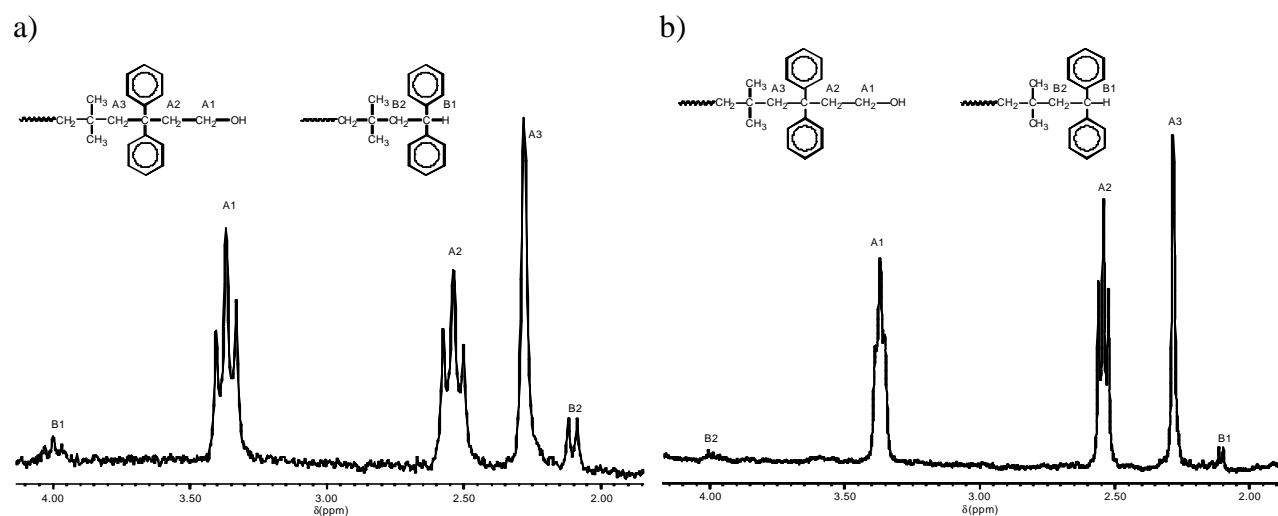


Figure 5.20: ¹H NMR spectra (200 MHz, in CDCl₃) of a) the products obtained after reacting EO with metallated DPE-capped PIB having Li⁺ as counterion

As shown in Figure 5.20a the product contains a certain amount of proton-terminated PIB, ≈ 13 % calculated from the areas under peak A1/A2 and B2. However, the product is free of Cl⁻-terminated PIB (100 % DPE-capping) and the 2,2-diphenylvinyl-capped PIB precursor (100 % metalation). Therefore, the problem regarding less than quantitative OH endgroups seems to be related to impurities in EO. Based on these results another experiments were carried out with EO which was more carefully dried and degassed several times over BuLi and CaH₂. The resulting material consists of OH terminated PIB with a degree of functionality > 97%, as confirmed by ¹H NMR (see Figure 5.20b).

Compared to other synthetic routes for preparation of PIB with OH endgroups (see section 1.3.1) this method has several advantages. EO reacts fast and nearly quantitative ($> 97\%$) to the PIB-DPE \cdot Li $^+$ chain end. This is in fact an one pot functionalization procedure, since DPE is added *in situ* to the living PIB chain. In the other procedure used for the preparation of OH-ended PIB (see section 1.3.1 and 5.2.1) a hydroboration/oxidation reaction is necessary, as illustrated in Scheme 1.10. Compared to the simple addition of EO (without further purification), is much more time consuming, including the subsequent purification of the resulting PIB-OH.

The next important topic is the synthesis of PIB-*b*-PEO (PEO-*b*-PIB-*b*-PEO) amphiphilic block copolymers. At the beginning, one experiment was carried out with a monofunctional DPOMe-capped PIB ($M_n \approx 5,600$) and K/Na. As discussed above CH₃OK will lead to homopolymerization of EO. As expected, in Figure 5.21a a bimodal MWD is observed. However, due to the UV signal in the low molecular weight peak, PIB (less than 100 % blocking efficiency caused by impurities in EO) as well as PEO homopolymer are present. Since the RI/UV ratios of the high and low molecular weight peak are nearly identical (the UV signal stems from the two phenyl groups), the compositions of PIB/PEO have to be similar in the two peaks. By subsequent extraction with *n*-hexane PIB was removed. The corresponding SEC trace proves the disappearance of the PIB homopolymer precursor (Figure 5.21b) and the presence of a certain amount of remaining PEO.

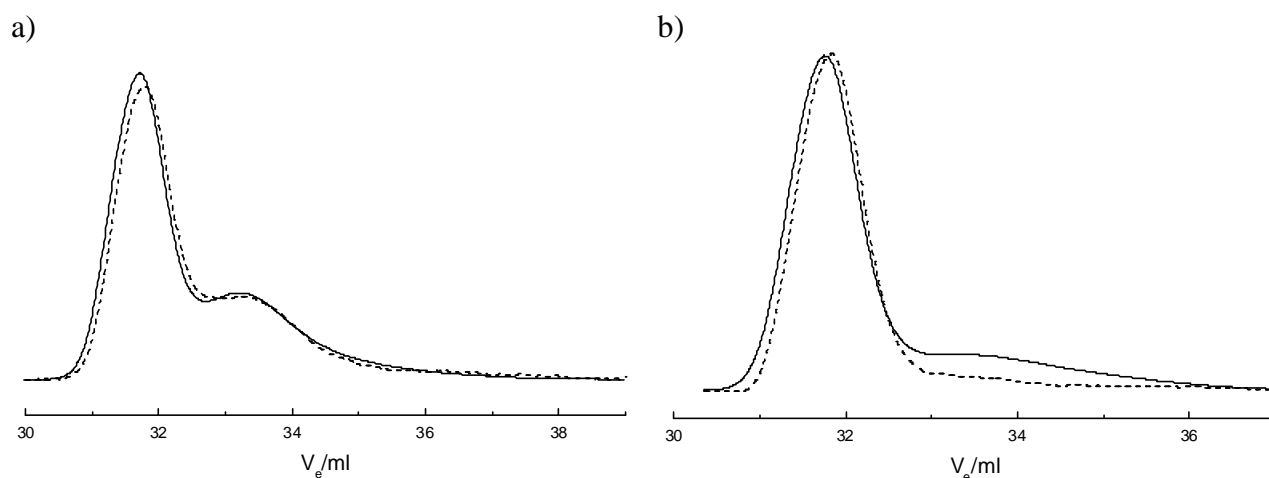


Figure 5.21: SEC traces of a polymer blend of PIB-*b*-PEO, PIB, and PEO before a) and after b) extraction with *n*-hexane. (—) RI signal and (---) UV signal at 260 nm (precursor: DPOMe-capped PIB, counterion: K $^+$).

With the same DPOMe-capped PIB precursor two experiments were performed with Cs as counterion. In the first one the precursor was metallated for 48 hours at 35 °C. Surprisingly, the MWD of the polymer obtained after EO polymerization is bimodal and the low molecular weight peak does not correspond to the PIB precursor although it has an UV-signal, Figure 5.22a. Selective extraction of PEO was attempted by water and acetone in order to analyze the PEO fraction by ^1H NMR, but due to the micelle formation of the block copolymer it was impossible to separate the two polymer fractions.

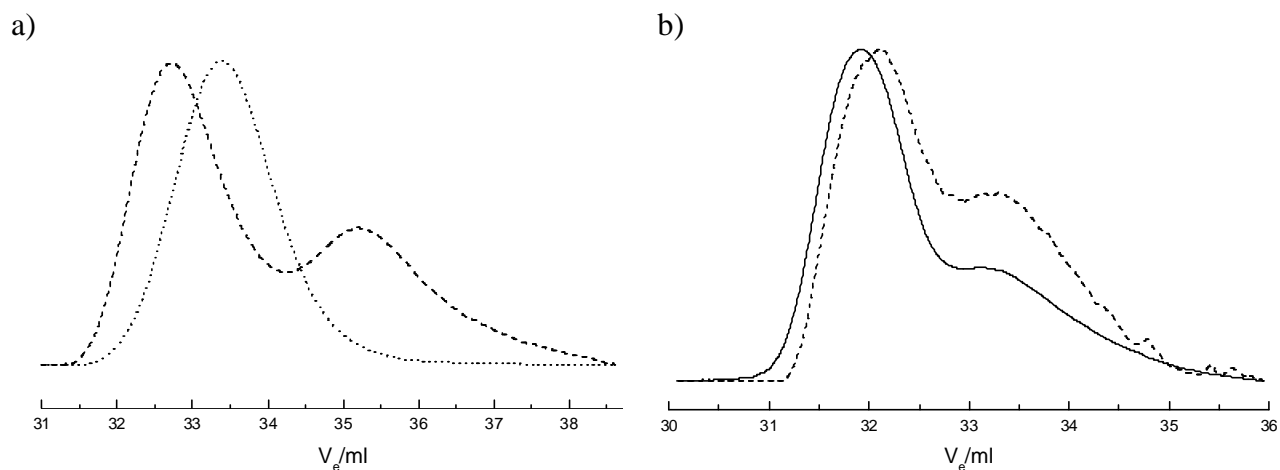


Figure 5.22: SEC traces of a PIB-*b*-PEO: a) a DPOMe-capped PIB precursor metallated for 48 h with Cs (···) and the resulting product (---), UV signals at 260 nm. b) RI-signal (—) and UV signal (---) of the product obtained from a DPOMe-capped PIB precursor metallated for 6 h with Cs.

In the second experiment the precursor was only metallated for 6 h with Cs (UV measurements indicate quantitative metalation). In this case the MWD is again bimodal, but in this case the low molecular weight peak corresponds to PIB quenched with impurities in EO. The RI/UV ratio of the peak at 33.2 ml (Figure 5.22b) is significantly different from the one in Figure 5.21a (the ratio is nearly identical to that of the PIB precursor) indicating that the product in Figure 5.22b is more or less free of PEO. The explanation for the strange result observed in Figure 5.22a might be due to partial decapping of DPE at elevated temperature (35 °C) when metalation proceeds over a long period of time (48 h). The last experiment involving synthesis of a PIB-*b*-PEO block copolymer was performed with a DPV-capped PIB ($M_n = 1,100$). From the UV signal at 260 nm (SEC trace) a blocking efficiency $> 93\%$ could be estimated (Figure 5.23). The block copolymer is unimodal ($M_w/M_n \approx 1.15$) and the theoretical M_n of the PEO block is $\approx 23,000$. The last PIB-*b*-PEO was compared with similar PIB-*b*-PMAA (see section 5.7).

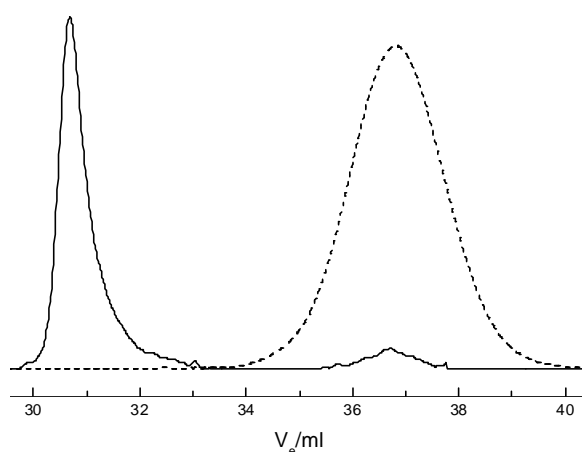


Figure 5.23: SEC trace (UV signals at 260 nm) of a PIB-*b*-PEO ($M_{n,theo} \approx 24,000$) (—) and the DPV-capped PIB precursor ($M_n = 1,100$) (---) (counterion: K^+)

Further investigations with EO is needed in order to reach high quality block copolymers (from both PIB precursors) without homopolymers of PIB and PEO. As discussed in this section the major problem seems to be related to the purification of EO.

5.5.2 Polymerization of N,N-dimethylacrylamide

In order to analyze the LA-Pzn of DMAA three different samples of poly(N,N-dimethylacrylamide) (PDMAA) were prepared. PDMAA is an important highly hydrophilic, water soluble polymer for the synthesis of amphiphilic block copolymers and amphiphilic networks (APNs). Based on the results by Hogen-Esch *et al.*⁶⁴, DMAA can only be polymerized in a living manner with Cs⁺ as counterion since polymerization with, e.g. Li⁺ leads an insoluble PDMAA (the tacticity i.e. the solubility is influenced by the counterion). The model compound, TMP-DPOMe metallated with Cs was used as initiator. In the first experiment DMAA was added in one portion just to see whether a narrow unimodal MWD can be obtained (DMAA1). The second experiment was performed with sequential addition of DMAA (DMAA2). The aim was to test the livingness/stability of the chain end by adding the second amount of DMAA 40 min after the first portion. Normally, the major problem with acrylates is irreversible termination caused by "back-biting" (see chapter 1). Finally, in the third experiment the objective was to analyze the possibility to make ABC-type PIB-*b*-PDMAA-based block copolymers with different methacrylates (primarily 2-hydroxyethyl methacrylate (HEMA) derivatives) (DMAA3). In respect to subsequent synthesis of APNs (section 5.9) the ability to add methacrylates to PDMAA is very important. The most promising strategies for the synthesis of APNs involve addition of either HEMA derivatives or ethylene glycol dimethacrylate (EGDMA) to different living chains. In this preliminary study MMA was added to PDMAA ($n_{\text{MMA}}:n_{\text{DMAA}}$ about 1:4).

From synthetic point of view it is important to note that the monomer DMAA is rather unstable under certain conditions. For instance, attempted purification over an Al₂O₃ column caused hydrolysis of DMAA.

The prepared polymers were investigated by SEC. However, considerable complications, i.e. suitable/reproducible conditions for SEC measurements were not easy to find. The samples were analyzed under different conditions at four different institutes. In Table 5.9 the results obtained in CHCl₃, THF containing 1 % Et₃N, and THF are summarized.

Table 5.9: SEC results related to PDMAA samples measured under different conditions.

Sample	CHCl ₃		THF (1 % Et ₃ N)		THF	
	M _n	M _w /M _n	M _n	M _w /M _n	M _n	M _w /M _n
DMAA1	6,100	1.66	8,100	1.15	-	-
DMAA2	8,400	1.74	10,700	1.10	-	-
DMAA3	24,000	1.87	-	-	16,000	2.1

It is clear that the results obtained in CHCl₃ and THF (1 % Et₃N) deviate, although PDMAA standards for calibration were used in both cases. The MWD appears much broader in CHCl₃ (but unimodal) than in THF (1 % Et₃N) indicating some adsorption of PMAA to the column material when CHCl₃ is used as eluent. The most important information obtained from these four measurements is that the MWD is unimodal, proving the livingness/stability of the polymer chains. The SEC traces of

DMAA3 in CHCl_3 reveal a bimodal distribution due to less than quantitative blocking efficiency (80-90 %, calculated from the UV signal at 260 nm). The measurements in pure THF damaged the column irreversibly, the homopolymers sticking on the column. Only the block copolymer, DMAA3 passed through the column. A bimodal MWD is observed, but due to the damage of the column it cannot be used as a real evidence since also PMMA standards became bimodal. In a fourth attempt the samples were measured with a mixture of 49.5 % THF, 49.5 % CH_3OH , and 1 % Et_3N . Here the samples are all bimodal or even trimodal and relatively broad. The multimodality seems to be an artifact since the same additional/small peak appeared in all measurements. Furthermore M_p of DMAA1 is higher than M_p of DMAA2. Therefore, under these conditions the measurements are carried out in HPLC mode and not as expected in SEC mode.

Based on these results, several conclusions can be drawn. PDMAA with unimodal MWD can be synthesized indicating straightforward LA-Pzn of DMAA by using the diphenylalkyl cesium initiator (DMAA1). Incremental monomer addition leads to PDMAA with unimodal MWD verifying the absence of termination (DMAA2). Synthesis of PDMAA-*b*-PMMA block copolymers was attempted, but only with a blocking efficiency in the range 80-90 % (DMAA3). Further experiments are needed in order to optimize the cross-over step from acrylamide to methacrylates. The major interest in such polymers is related to the synthesis of tailored PIB-*b*-PDMAA-*b*-PHEMA block copolymers (see section 5.9).

Due to the complication of characterizing PDMAA samples by SEC, further experiments involving the synthesis of PIB-*b*-PDMAA and other block copolymers were not carried out at this point. In addition, micelle formation might be a second problem when the block copolymers are analyzed.

5.5.3 Synthesis of tailored poly(methacrylates)

A variety of polymethacrylates are of significant interest in many applications. In the course of this study synthesis and characterization ABA and AB block copolymers were attempted. For the synthesis of PIB-based thermoplastic elastomers methyl methacrylate (MMA) was applied. In section 5.4.2 it was demonstrated that MMA can be polymerized in a controlled/living manner with the diphenylalkyl lithium initiator and LiCl, but not with potassium as counterion. *Tert*-butyl methacrylate (tBMA) and protected-HEMA derivatives are desired for the synthesis of PIB-based amphiphilic AB block copolymers. By hydrolysis, PtBMA is converted into poly(methacrylic acid) (PMAA) and protected-HEMA into HEMA.

5.5.3.1 Block copolymers/homopolymers containing a 2-hydroxyethyl methacrylate oligomer segment

The objective in this section is to find a synthetic route for the preparation of polymers containing a terminal segment with several OH groups suitable for subsequent crosslinking/curing reactions (see section 5.9). One possibility is the preparation of block copolymers containing a short (oligomer) segment of PHEMA. PHEMA chain segments can be prepared by LA-Pzn through the use of silyl-protected monomers like 2-[(*tert*-butyldimethylsilyl)oxy]ethyl methacrylate (TBDMHEMA)

and 2-[(trimethylsilyl)oxy]ethyl methacrylate (TMSHEMA) (alternatively the corresponding acetal-protected HEMA)¹⁰. Subsequent (selective) hydrolysis leads to the desired PHEMA containing polymer. Since these polymers have to be obtained by sequential monomer addition, it is important to know some details about the respective monomers. On the basis of these thoughts the preparation of PtBMA-*b*-PHEMA was investigated. Three potential problems have to be clarified. First, when is the tBMA consumed quantitatively? Less than 100 % conversion would lead to a tapered block copolymer (an interface of a statistical copolymer of TMSHEMA and tBMA) which will complicate the following network formation (see section 5.9). Secondly, is the living polymer chain stable for a certain time, e.g. can "back-biting" be excluded? Finally, does this cross-over step from tBMA to TBDMHEMA/TMSHEMA proceed quantitatively?

a) Preliminary studies

As shown in Figure 5.24, polymerization of tBMA under different conditions was carried out in order to find the right time for the addition of TMSHEMA/TBDMHEMA. In all cases polymers with narrow MWD and theoretical M_n were prepared. Since MMA (a primary ester), and therefore most likely also TBDMHEMA/TMSHEMA (primary esters) cannot be polymerized in a controlled way with K as counterion (see also below Figure 5.25), Li was also used for tBMA, avoiding transmetalation during the polymerization. In order to get a fast and controlled polymerization of tBMA with the lithium initiator, this block segment is prepared at -20 °C. Subsequently, the solution is cooled to -78 °C and then TMSHEMA/TBDMHEMA is added.

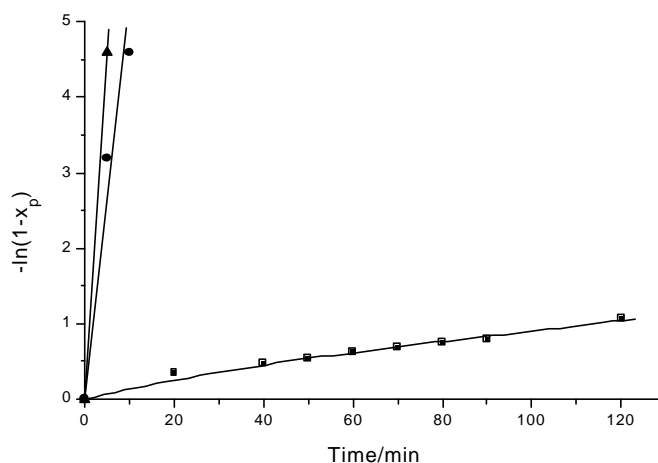


Figure 5.24: First order time/conversion plot for the LA-Pzn of tBMA in THF, $[C^-] \approx 5 \cdot 10^{-3}$ M, temperature/counterion: K⁺ at -78 °C (▲), Li⁺/LiCl (10 times excess) at -20 °C (●), and Li⁺/LiCl (10 times excess) at -78 °C (■), PDI < 1.1 in all cases.

In a preliminary experiment MMA is added to a living PtBMA-Li. The M_n 's are chosen so that the precursor and the AB block copolymer are well-separated in the corresponding SEC eluogram, Figure 5.25. This experiment proves that under the conditions used (lithium as counterion, 10 times excess of LiCl, and THF at -20/-78 °C) MMA can be added to a living PtBMA chain end with a blocking efficiency near to 100 % (indicating absence of termination e.g., "back-biting"). Based on this result, experiments with TMSHEMA/TBDMHEMA were carried out, under the assumption that MMA and TMSHEMA/TBDMHEMA react with comparable rate and in the same way to the living PtBMA.

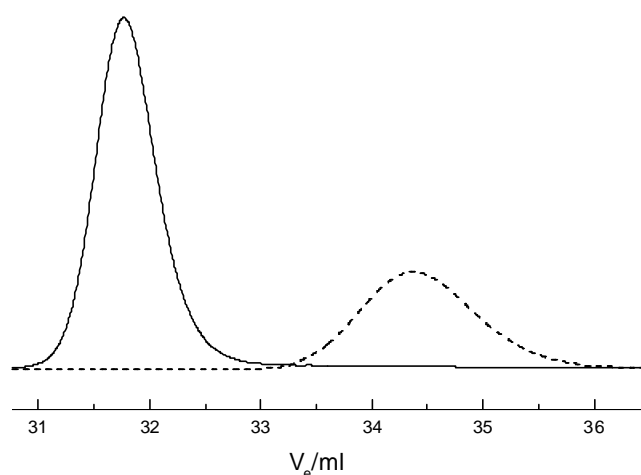


Figure 5.25: SEC traces (RI signals) of the PtBMA precursor (---) and the corresponding PtBMA-*b*-PMMA (—) obtained by sequential monomer addition in THF with Li⁺/LiCl (10 times excess) at -20 °C (polymerization of tBMA) and -78 °C (polymerization of MMA).

First, kinetics of the LA-Pzn of TBDMHEMA was investigated. Figure 5.26 shows that with Cs⁺ and K⁺ as counterion the reaction is too fast to be controlled. As expected, well-defined polymers with narrow MWD can be synthesized only with the lithium initiator. From these results the wanted block copolymers are now attainable.

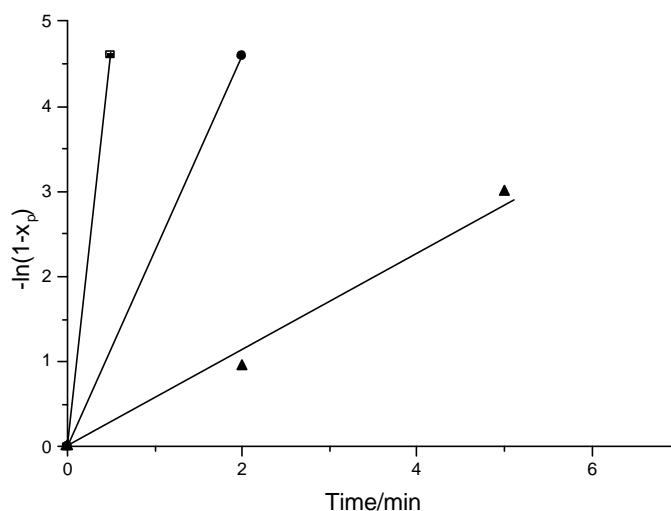


Figure 5.26: First order time/conversion plot for the anionic polymerization of TBDMHEMA in THF at -78°C, [C] $\approx 5 \cdot 10^{-3}$ M, counterions: Cs⁺, $M_w/M_n = 1.25$ (■), K⁺, $M_w/M_n = 1.7$ (●), and Li⁺/LiCl (10 times excess) $M_w/M_n < 1.10$ (▲)

However, before the polymers are prepared it is crucial to have conditions where the silyl protected HEMA is selectively hydrolyzed leading to a polymer where reactive sites are only present at the chain end.

b) Hydrolysis studies

Hydrolysis experiments with TMSHEMA, TBDMHEMA, tBMA and DMAA under identical conditions (Table 5.10) indicate that selective hydrolysis of TMSHEMA can be carried out in less than 20 min with HCOOH, verified by GC measurements. The difference in stability between TBDMHEMA and tBMA under acidic conditions is too small. From the literature¹⁹² it is known that TMSHEMA is about 4 orders of magnitude less stable toward hydrolysis than TBDMHEMA.

Therefore, for this specific application it is important to chose TMSHEMA and not TBDMHEMA. Concerning the hydrolysis of DMAA it has been shown that PDMAA was quantitatively hydrolyzed to PMAA with HCl in dioxane/water at 120 °C within less than 2 hours¹⁹³.

Table 5.10: Reaction time needed for quantitative hydrolysis of tBMA, TBDMHEMA, TMSHEMA, and DMAA using different acids (HCl, $pK_s = 0$, HCOOH, $pK_s = 3.75$, CH₃COOH, $pK_s = 4.75$) at room temperature in THF /H₂O (10:1), [monomer] $\approx 1-1.6 \cdot 10^{-1}$ M and [acid] $\approx 1.5 \cdot 10^{-1}$ M. The conversion was determined by GC

Monomer	Reaction time/min		
	HCl	CH ₃ COOH	HCOOH
tBMA	< 180	> 1080	> 1080
TBDMHEMA	80	-	-
TMSHEMA	5	190 (70% conv.)	15
DMAA	> 1200 (< 5% conv.)	-	-

However, these hydrolysis experiments (Table 5.10) might be primarily considered only as a tendency, since the deprotection of the corresponding polymers proceeds slower¹³⁰. The decisive prove for selective hydrolysis of PTMSHEMA will be that no insoluble material (network) is formed during the synthesis of homo-PtBMA stars due to potential free acid groups (see later in section 5.9). The degree of hydrolysis of the oligo-TMSHEMA was estimate by using ¹H NMR (in CDCl₃). In all cases, quantitative hydrolysis could be detected within experimental error (10-20 %). Due to potential micelle formation in CDCl₃ with HEMA in the core the calculations can only be made by comparing the integration of the peaks at 3.9 ppm (-CH₂CH₂-OSiR₃) and 4.1 ppm (-CH₂CH₂-OH) and not by using signal from the PtBMA segment.

c) Copolymerizations

Table 5.11: Synthesis of PtBMA-*b*-oligo-HEMA copolymers. Initiator: methyl α -lithio isobutyrate (MiBLi), [MiBLi] $\approx 5.7 \cdot 10^{-3}$ M, [MiBLi]/[LiCl] = 10, [tBMA]_o/[I]_o ≈ 35 , solvent: THF, T = -20 °C for polymerization of tBMA and -78 °C for polymerization of TMSHEMA.

Sample no.	[HEMA] _o /[I] _o	¹ M _{n,block,app}	M _w /M _n	ΔM_n^2	Cross-over efficiency ³
M1TBMA1	3	5300	1.07	300	73 %
M1TBMA2	5	6300	1.08	800	90 %
M1TBMA3	10	6500	1.12	2000	97-99 %
M1TBMA4	5	7000	1.12	-	85 %
M1TBMA7	10	8500	1.12	2200	97-99 %

¹M_n of the PtBMA-*b*-oligo-TMSHEMA determined by SEC, using PIB calibration.

² ΔM_n is the difference observed before (PtBMA-*b*-oligo-TMSHEMA) and after (PtBMA-*b*-oligo-HEMA) hydrolysis.

³Determined by HPLC under critical conditions using a reverse-phase column, and THF:CH₃CN 53:47.

Based on the kinetics of polymerization of tBMA and TBDMHEMA (Figure 5.24/5.26) the cross-over experiments with MMA (Figure 5.25) and the hydrolysis results, the synthesis of the

desired block copolymers, PtBMA-*b*-PHEMA should be possible. In Table 5.11 the difference in molecular weights before and after hydrolysis, ΔM_n s are listed. The ΔM_n together with the qualitative evaluation of the ^1H NMR spectra indicate that three polymers with different composition have been synthesized and that hydrolysis proceeded nearly quantitatively. The $[\text{HEMA}]_0/[\text{I}]_0$ ratio is the theoretical one based on the amount of initiator and HEMA added to the system. If the initiating efficiency is lower than expected it will be somewhat higher. The difference between the M_n of M1TBMA3 and M1TBMA7 might indicate that the real ratio is a little bit higher in sample M1TBMA7, 11-14 (see also section 5.9, different curing reactions proceeded) since the same amounts were used. The next crucial question is the efficiency of cross-over, i.e. functionality of the polymers. From the result with MMA, Figure 5.25 it is expected to be quantitative, but in these experiments only a few monomer units of TMSHEMA are attached to PtBMA which might lead to complications depending on the monomer reactivity ratios or better the respective rate constants (for MMA(1)/tBMA(2) copolymerization $k_{11} \approx 20 \text{ l} \cdot \text{mole}^{-1} \cdot \text{s}^{-1}$ and $k_{21} \approx 5 \text{ l} \cdot \text{mole}^{-1} \cdot \text{s}^{-1}$)⁸⁵. Since $k_{11}/k_{21} \approx 4$, the $[\text{HEMA}]_0/[\text{I}]_0$ ratio has to be at least in the range 3-4 in order to obtain quantitative capping.

Normal SEC cannot be utilized for quantitative measurement due to the fact that the two peaks of the PtBMA precursor and the functionalized PtBMA (with a few HEMA units) are not well-separated. Instead, HPLC under critical conditions (HPLCCC) is used to characterize the PtBMA samples (see also section 4.7.2). The separation is achieved on the basis of the difference of endgroup structure, either a proton due to impurities in TMSHEMA or an oligomer segment of HEMA. In Figure 5.27 the traces obtained by critical HPLC of the samples are illustrated. These clearly indicate that sample M1TBMA3 is nearly free of pure PtBMA, whereas M1TBMA2-3 contain a certain amount of non-functionalized PtBMA verified by the presence of a peak at 4.75 ml (PtBMA standards elute at 4.75 ml irrespective of the molecular weight). Besides, the HPLC traces of the HEMA-capped PtBMAs are multi-modal indicating that a separation depending on the number of HEMA units takes place. The peak at 4.5 ml is expected to correspond to the mono-capped and the somewhat broader peak at the left side correlates to a distribution of HEMA units. Less than quantitative end-capping in case of 3-5 HEMA units (M1TBMA1-2,4) is most likely related to a slow initiation of TMSHEMA with PtBMA-Li as initiator. Only when the number of HEMA units is increased to 10, near to quantitative functionalization is reached. In addition, due to the increase of HEMA units the relative amount of mono-capped PtBMA chains decreases significantly.

The samples M1TBMA1-3 and M1TBMA7 are used in further curing reactions with isocyanates and acid chlorides for the synthesis of PtBMA star-shaped polymers (section 5.9). A potential problem regarding this curing reaction might be undesired network formation if the chain length of the PHEMA segment gets too long (section 5.9).

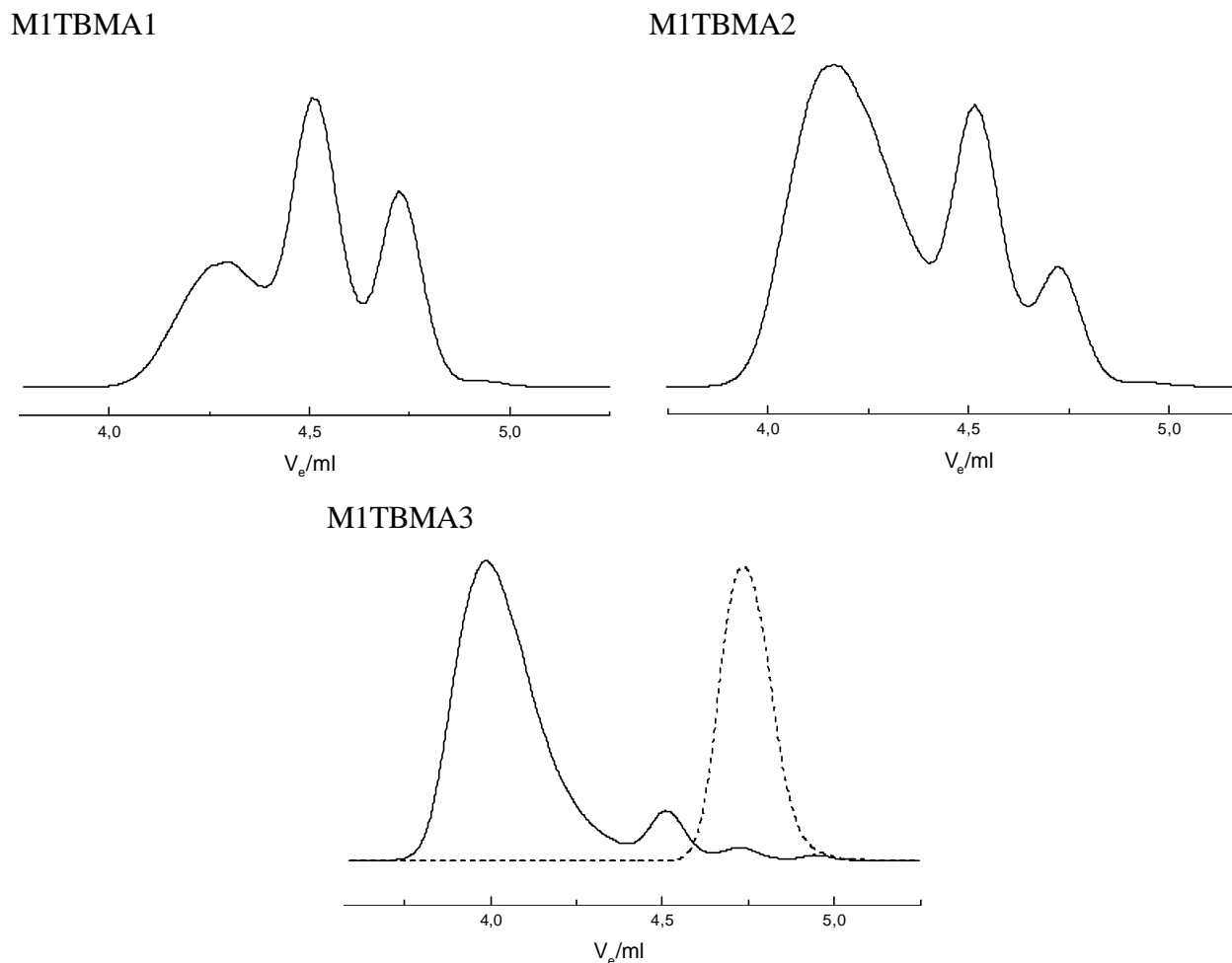


Figure 5.27: HPLC traces under critical conditions (of PtBMA) of MITBMA1-3 (—) and a PtBMA standard containing a proton at the chain end (---). Column: reverse-phase and eluate: THF:CH₃CN 53:47.

In conclusion, a method has been found for the synthesis of well-defined PtBMA polymers containing a short oligo-HEMA block segment. Due to the relative rate constants of TMSHEMA addition to PtBMA- and PTMSHEMA chain ends quantitative capping can only be reached when $P_{n,HEMA} > 5$. The kinetic results, including the cross-over from tBMA to a primary methacrylate can also be used in the experiments involving addition of ethylene glycol dimethacrylate (EGDMA) to PtBMA chains (see section 5.9).

5.5.4 Synthesis of OH-terminated polymers

OH-terminated polymers can be used for a number of versatile reactions, as already discussed in Chapter 1. Therefore, tailored polymers with OH endgroups are of interest in this project (see section 5.9). Two possibilities exist for the introduction of such a functionality, either through selected quenching or by the use of an initiator bearing a protected OH group. Since, the initiators here, are primarily prepared from PIB macroprecursors the latter method is excluded. Addition of aldehydes to anionic chain ends should lead to secondary alcohols (or primary ones with formaldehyde) Scheme 5.10.

5.5.4.1 End-functionalization with benzaldehyde and p-nitrobenzaldehyde

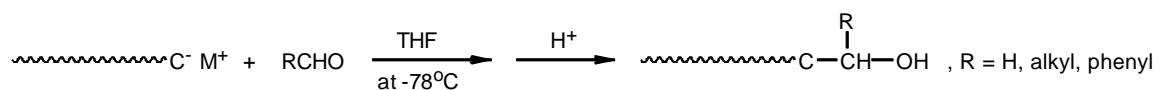
Quenching experiments performed with living PtBA and benzaldehyde (THF/Li/LiCl-system), led to > 85 % functionality.⁷ Similar attempts were performed with tBMA in this project. In one case THF and K⁺ as counterion were used and in another one THF, Li⁺, and LiCl. In both experiments the functionality was only ≈ 50 %, verified by ¹H NMR. This means, that due to the change in endgroup structure from acrylate to methacrylate a much lower capping efficiency is reached. In order to increase the ability of the aldehyde group to undergo a nucleophilic attack, p-nitrobenzaldehyde was also investigated. The nitro group is electron-withdrawing leading to a decrease of the electron density at the carbonyl carbon. An improvement was observed; typically ≈ 65 % OH functionality independent of the counterion (PtBMA⁻Li⁺ or PtBMA⁻K⁺) was reached.

It seems impossible to obtain quantitative capping with benzaldehyde and derivatives in case of living PtBMA. Besides, the resulting alcohol is secondary. Therefore, in the following section possibilities related to formaldehyde are examined.

5.5.4.2 End-functionalization with formaldehyde

Formaldehyde is a gas at RT and is only available as an aqueous solution or as para-/metaformaldehyde. As illustrated in Scheme 5.10 the latter two compounds can be converted into monomeric formaldehyde thermally or under acidic conditions (hydrolysis of an acetal).

Preliminary experiments were performed with ethyl α-lithio isobutyrate (model of the living PMMA⁻Li⁺ chain end) in THF and with 10 times excess LiCl. ¹H NMR of the resulting product indicates a high conversion, based on the integration ratio of the -CH₂OH (3.35 ppm, doublet) (the singlet at 3.30 belongs to traces of CH₃OH) and the -OCH₂CH₃ (4.00 ppm, quartet), see Figure 5.28. Furthermore, the tertiary proton of ethyl isobutyrate (4), expected at 2.55 ppm (multiplet), is only present in small amount (if at all) under the peak at 2.5 ppm. GC measurements show a small contents of ethyl isobutyrate and a second peak. Based on the ¹H NMR spectrum in Figure 5.28 this latter peak most likely corresponds to the desired alcohol.



Scheme 5.10: Quenching of living anionic polymer chain ends with aldehydes.

Subsequent experiments with PMMA⁻Li⁺ and PtBMA⁻K⁺ did not give the expected results. Only a small amount of functionality (< 5 %) if any at all could be proved by ¹H NMR and HPLC under critical conditions. Therefore, the results presented in Figure 5.28 have to be taken with caution. Either, the reactivity of ethyl α-lithio isobutyrate is much higher than PMMA⁻Li⁺ or the doublet (1) in Figure 5.28 is not the expected CH₂ group although several facts (see above) speak for the alcohol compound.

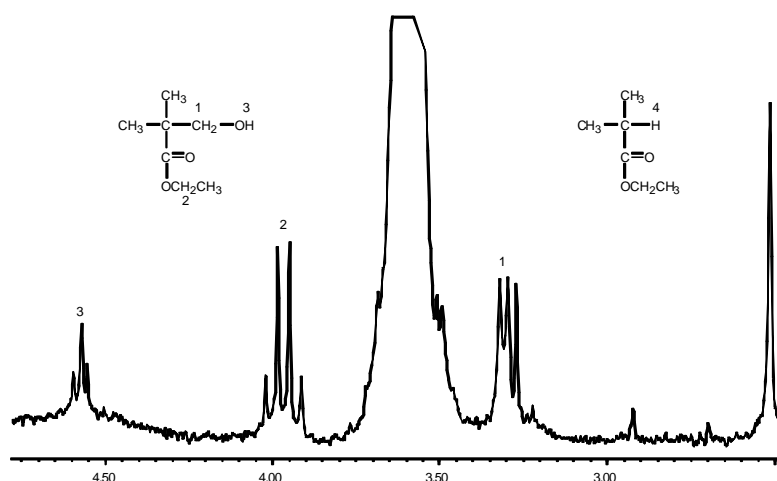


Figure 5.28: ^1H NMR spectrum (200 MHz, CDCl_3) of the reaction between HCHO and ethyl α -lithio isobutyrate.

Since the experiments with the aldehydes are not promising, a third method was attempted involving quenching with silyl-protected 2-iodoethanol. It is known that allyl iodide reacts nearly quantitatively with living PMMA (subsequent hydroboration/oxidation gives the primary OH group)¹³⁸. The product obtained here after quenching with silyl-protected 2-iodoethanol was analyzed with ^1H NMR and HPLC under critical conditions. Both analysis methods indicate 0 % functionality. The reason for this unexpected result is either due to lower reactivity of this iodo compound or to the polymerization system, i.e. to the structure of the living chain end (ion-pair). In this case THF/ Li^+/LiCl was used instead of the reported toluene/ $\text{Li}^+/\text{AIR}_3/\text{TMEDA}$ -system¹³⁸ in the allyl iodide quenching reaction.

In conclusion, substantial investigations have to be carried out in order to find an appropriate way to prepare poly(methacrylates) with OH endgroups. The quenching reactions all involve nucleophilic attack of the ion-pair endgroup on the quenching agent. Therefore, it is important to analyze the effects of the ion-pair structure, i.e. counterion and solvent effects.

5.6 Linear ABA and star-shaped $(\text{AB})_3$ block copolymers (thermoplastic elastomers)

The aim in this section is to synthesize different PIB/PMMA block copolymers processing TPE properties. For this purpose, di- and trifunctional PIB precursors with $M_n > 15,000$ were prepared. By varying the topology, the block lengths, and the composition of the two segments (usually a rubbery mid-segment of 50-80 wt-%) the intention is to study the influence of these parameters on the resulting morphologies (and distance between each domain) and material properties.

5.6.1 Synthesis and SEC measurements

At the start of this series of blocking experiments the effect of the PIB endgroup structure with regard to block efficiency was investigated. As previously discussed (sections 5.4.2 and 5.4.3) metalation of DPV- and DPOMe-capped PIBs lead to the same diphenylalkyl carbanion (Scheme 5.8). To one reactor a DPOMe-capped PIB was added, and to another one a 50:50 mixture of DPOMe- and DPV-capped PIB. After metalation with K/Na alloy tBMA was charged to both

reactors. In both cases, nearly identical blocking efficiencies were obtained which proves that the metalation and the subsequent polymerization are not influenced by the ratio of the two chain ends. The independence of the metalation and anionic polymerization on the ratio of the DPV and DPOMe endgroups is an important finding. This means, that it is not necessary at all to care about the chain end composition of the DPE-capped PIB in the course of its preparation by LC^+Pzn .

In an orienting experiment, the molecular weight of the difunctional PIB macroinitiator was relatively small compared to the outer PMMA segments in order to obtain sufficient separation by SEC between the PIB precursor and the expected triblock which then allows direct determination of the blocking efficiency (using the UV 260 nm signal). As shown in Figure 5.29, the resulting block copolymer has a unimodal and narrow MWD. The SEC eluograms in this figure also indicate high blocking efficiency which is in agreement with previous results gained with a monofunctional PIB precursor (Figure 5.19). Indeed, extraction by *n*-hexane removed only ≈ 4 wt-% PIB and AB block copolymer after 1 month. These results clearly verify nearly quantitative blocking efficiency and the formation of the desired PMMA-*b*-PIB-*b*-PMMA block copolymer.

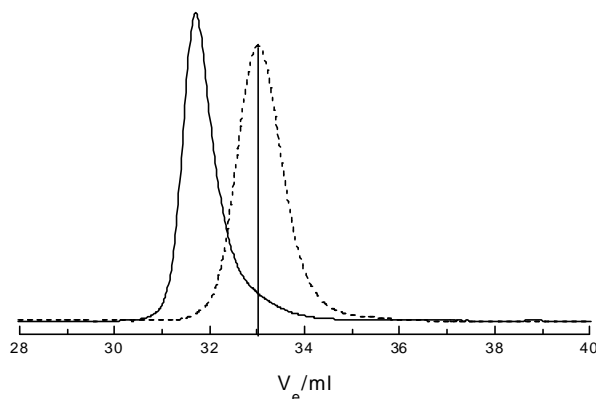


Figure 5.29: SEC traces (RI signal) of a difunctional PIB precursor ($M_n = 6300$, $M_w/M_n = 1.12$) (---) and the corresponding triblock copolymer ABA1 (—) after anionic polymerization of MMA ($M_n = 18,000$, $M_w/M_n = 1.13$)

In nearly all experiments involving di- and trifunctional PIBs with $M_n > 15,000$ a temporary precipitation was observed right after the addition of MMA. The precipitate dissolves after about 10-15 min. The precipitation is most likely due to the aggregation of the lithiated chain ends surrounded by the non-polar PIB leading to the formation of a coordinative network which is redissolved after a certain length of the PMMA segments is reached, see Figure 5.30.

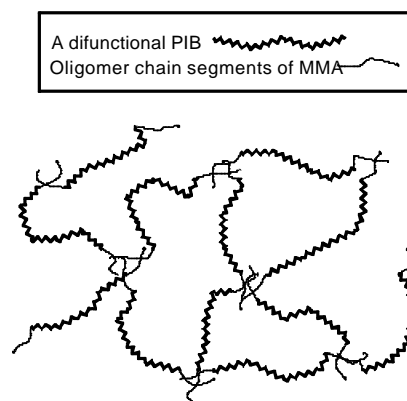


Figure 5.30: A proposed structure of a temporary/non-covalent bonded i.e. coordinative network of PMMA-*b*-PIB-*b*-PMMA block copolymers.

An alternative interpretation would be the formation of micelles with PIB in the core and a surface of charges chain ends. However, this kind of aggregation is less probable since the micelles would most likely not precipitate. At the present time the former explanation is expected, although the presence of LiCl generally reduces the aggregation of carbanions.

The first series of PMMA-*b*-PIB-*b*-PMMA was synthesized with a difunctional PIB macroinitiator, $M_n \approx 17,500$ in pure THF at -78°C . The theoretical M_n and the one determined by SEC using a weighted calibration correlated rather good (see Table 5.12). This means, that a relatively precise M_n of the block copolymer can be estimated from SEC when the respective homopolymer calibration curves exist and the composition is known.

Table 5.12: SEC results of PMMA-*b*-PIB-*b*-PMMA block copolymers with a difunctional PIB precursor, $M_n \approx 17,500$, $M_w/M_n \approx 1.06$.

Sample no.	PMMA (%)	$M_{n,theo}$ (PMMA) outer segment ^a	$M_{n,theo}$ (block) total	$M_{n,SEC}$ (block) total	M_w/M_n
TPE32	21	2,200	21,900	21,100	1.09
TPE31	27	3,200	23,900	23,600	1.09
TPE33	41	5,800	29,100	27,000	1.11

^aPer block.

The SEC eluograms in Figure 5.31 show uniform shifts to higher molecular weights after block formation. Since the eluograms of the PIB precursor with $M_n \approx 17,500$ and the ABA block copolymer having outer PMMA segments with $M_n = 2-6,000$ overlap, it is difficult to use SEC for the verification of quantitative blocking efficiency in this range of block copolymer composition (see below). However, the resulting triblocks are unimodal with a narrow MWD and expected M_n which is a good indication for controlled synthesis of the desired triblock copolymer. Subsequent characterization (e.g., stress-strain and small angle X-ray scattering (SAXS)) of these might also give some qualitative information about the blocking efficiency.

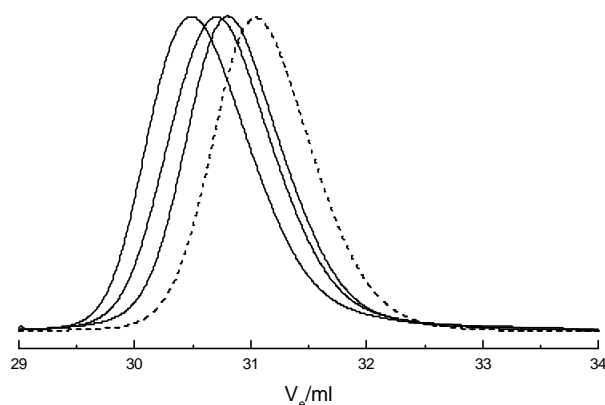


Figure 5.31: SEC traces of a series of linear PMMA-*b*-PIB-*b*-PMMA block copolymers (—) and the corresponding precursors (---) $M_n = 17,500$.

A second PIB precursor with $M_n \approx 32,000$ ($M_w/M_n \approx 1.08$) was used for the synthesis of another series of triblock copolymers. However, solubility problems arose during the polymerization of MMA since the precursor precipitated in pure THF below -55 °C. At -53 to -50 °C two polymerizations of MMA with the high molecular weight PIB macroinitiator resulted in polymers with multimodal MWDs due to uncontrolled polymerization of MMA (Figure 5.32a). In order to increase the solubility of PIB at -78 °C, anionic polymerizations of MMA were subsequently performed in a 70:30 THF/*n*-hexane mixture. This process yielded PMMA-*b*-PIB-*b*-PMMA with unimodal MWD and low polydispersity ($M_w/M_n = 1.10$ - 1.15) indicating high blocking efficiency (Figure 5.32b). The composition of the block copolymers illustrated in Figure 5.32b varied from 22-36 wt-% PMMA.

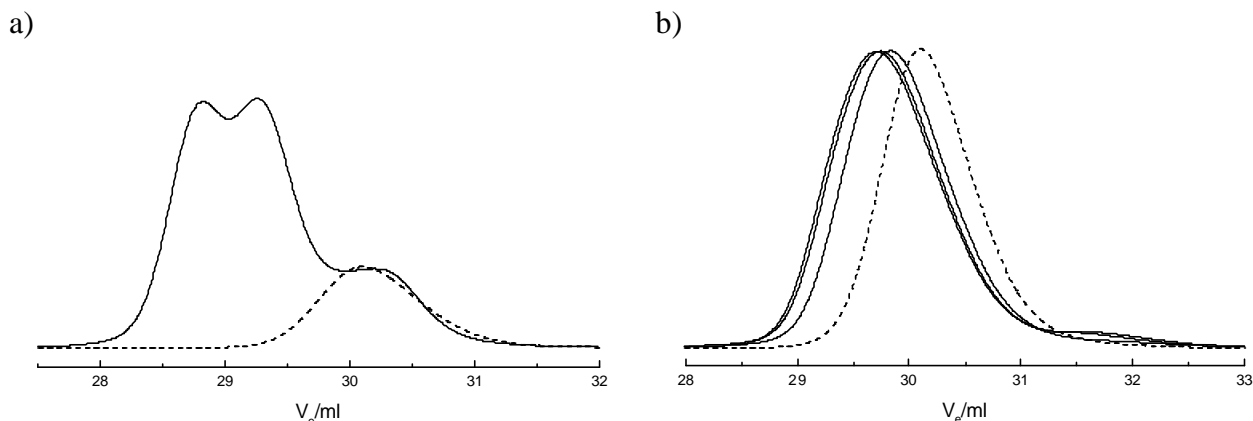


Figure 5.32: SEC traces of a) a linear PMMA-*b*-PIB-*b*-PMMA block copolymer (—) where MMA is polymerized in pure THF at -50 °C and b) a series of linear PMMA-*b*-PIB-*b*-PMMA block copolymers (—) where MMA is polymerized in 70:30 THF/*n*-hexane at -78 °C (and the corresponding precursor (---) $M_n = 32,000$).

It has to be noted, that the presence of 30 v/v-% *n*-hexane slows down the rate of metalation by a factor of ≈ 2 as illustrated in Figure 5.33. This result reveals a certain influence of the solvent polarity on the rate of metalation. The potential kinetic changes regarding MMA polymerization was not investigated further in this project.

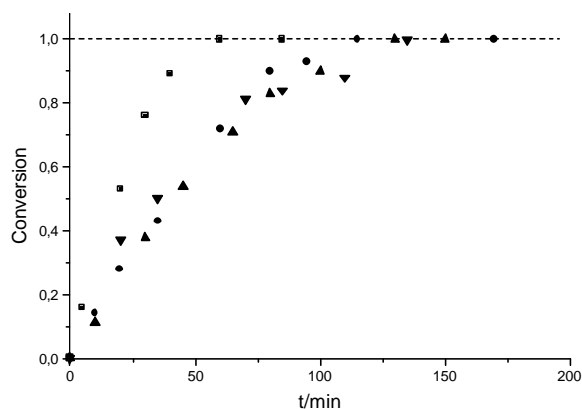


Figure 5.33: Degree of metalation of in THF (■) and in THF:n-hexane (70:30) (●), (▲), and (▼) with K/Na alloy followed by UV-spectroscopy at $\lambda_{\text{max}} = 480 \text{ nm}$ ($[\text{P}^*] = 1.5 \cdot 10^{-3} \text{ M}$ in all experiments).

Polyisobutylene-*b*-poly(methyl methacrylate) (PIB-*b*-PMMA)₃ star-shaped block copolymers were also synthesized by using a trifunctional initiator (TriCumCl) for LC⁺Pzn of IB. The 3-arm star PIB precursors had $M_n = 30\text{-}45,500$. This value is apparent only since calibration was performed with linear PIB standards. A solvent mixture of THF and *n*-hexane (70:30) was also used, in order to avoid solubility problems with these PIB samples at low temperature (-78 °C). As shown in Table 5.13/5.14 and Figure 5.34 two series of block copolymers with 10-46 and 22-42 wt-% MMA were prepared with low polydispersity ($M_w/M_n < 1.10$).

Table 5.13: SEC results related to (PIB-*b*-PMMA)₃ block copolymers with a triarmed star PIB precursor, $M_n = 30,000$, $M_w/M_n = 1.07$

Sample no.	% PMMA	$M_{n,\text{theo}}$ (PMMA) arm	$M_{n,\text{theo}}$ (block) total	$M_{n,\text{SEC}}$ (block) total	M_w/M_n
TRI30_0	46	8,500	55,500	60,000	1.09
TRI30_1	37	5,900	47,700	51,000	1.07
TRI30_2	27	3,700	41,100	44,000	1.08
TRI30_3	20	2,500	37,500	40,000	1.08
TRI30_4	10	1,100	33,300	37,000	1.07

The theoretical M_n 's and those estimated from SEC using weighted calibration of linear standards correlate good. In one series the theoretical M_n 's are somewhat lower than measured by SEC (Table 5.13), and *vice versa* in the second series (Table 5.14). The small differences are within the expected experimental error of 10 %.

Table 5.14: SEC results related to (PIB-*b*-PMMA)₃ block copolymers with a triarmed PIB precursor, $M_n = 45,500$, $M_w/M_n = 1.07$

Sample no.	% PMMA	$M_{n,\text{theo}}$ (PMMA) arm	$M_{n,\text{theo}}$ (block) total	$M_{n,\text{SEC}}$ (block) total	M_w/M_n
TRI45_2	42	10,900	78,000	78,000	1.09
TRI45_3	30	6,400	65,000	63,000	1.08
TRI45_4	22	4,200	58,000	56,000	1.09

a)

b)

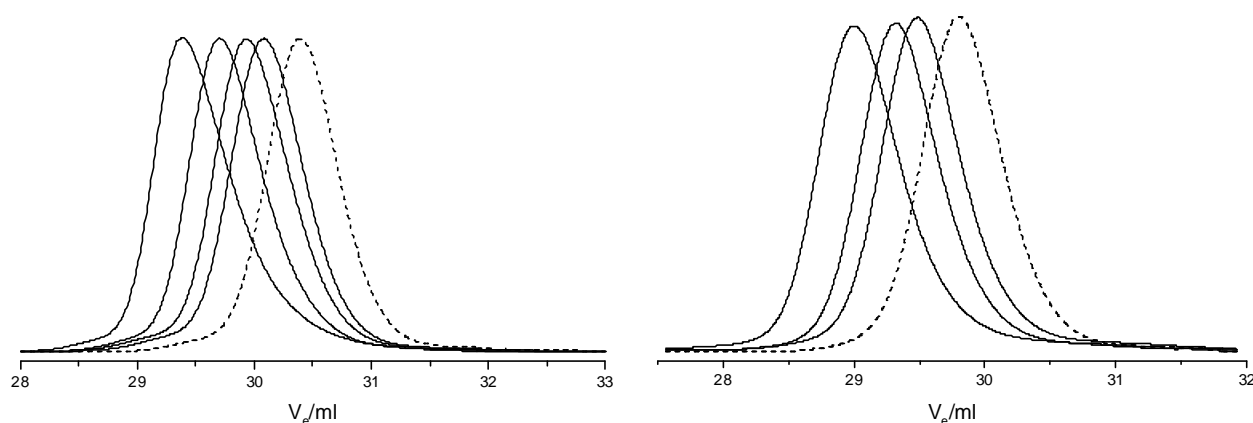


Figure 5.34: SEC traces of two series of star-shaped $(\text{PIB-}b\text{-PMMA})_3$ block copolymers (—) and the corresponding precursors (---) a) PIB, $M_n = 30,000$ and b) PIB, $M_n = 45,500$.

In all of the SEC eluograms of TPEs the peaks of the PIB precursors are not well-separated from the corresponding ones of the $\text{ABA}/(\text{AB})_3$ block copolymers. Therefore, SEC cannot be used as direct evidence for quantitative blocking efficiency in case of TPEs. However, based on preliminary results, e.g. Figure 5.29, it can be anticipated that the blocking efficiencies are $> 95\%$. Due to the high M_n 's, quantitative ^1H NMR analysis (endgroup analysis, detection of $-\text{CH}_2-\text{C}(\text{Ph})_2-\text{OCH}_3/ -\text{CH}=\text{C}(\text{Ph})_2$, due to less than quantitative metalation or $-\text{CH}_2-\text{C}(\text{Ph})_2-\text{H}$ due to quenching during metalation/polymerization) of the resulting block copolymer is also not possible.

A third method which is frequently used for analysis of block copolymers and endgroup structures ($M_n = 1\text{-}100,000$) is HPLC under critical conditions. Above (see section 5.5.3.1, e.g. Figure 5.27) this method was successfully used for analyzing PtBMA samples. However, in the literature critical conditions for PIB have not been found yet, it is only reported for oligomers of butadiene.¹⁹⁴ A large number of analyses were carried out with different solvent mixtures (THF: CH_3CN , THF:acetone, hexane:acetone, hexane: CH_2Cl_2 , hexane:THF:acetone, THF:DMF), different compositions, and with reversed-phase as well as normal-phase columns. None of these measurements lead to applicable results since they were all in SEC mode. The major problem seems to be related to the fact that before HPLC mode is reached PIB precipitates in the solvents used. In contrast to poly(meth)acrylates, PIB does not contain functional groups which can interact with the column material. Therefore, it might be impossible to find critical conditions for PIB. During the attempts of finding the critical point for PIB, Much *et al.*¹⁹⁵ found the critical conditions for polyisoprene (PI) with $M_n < 100,000$ using a solvent mixture of *tert*-butylmethylether:isopropanol on a reversed-phase column. Similar conditions were subsequently applied for PIB, but likewise to the other attempts, before HPLC mode is reached the PIBs precipitate. This means, that the small difference between the two types of polymer is enough to accomplish critical conditions for PI but not for PIB. Based on these findings, the PIB-based block copolymers $(\text{ABA}/(\text{AB})_3)$ can not be separated from potential A and B homopolymers or AB impurities in a traditional way by HPLC at the critical point of PIB. The last possibility to obtain a higher resolution than in normal SEC of a mixture of PIB, PIB-*b*-PMMA, and PMMA-*b*-PIB-*b*-PMMA (see Figure 5.35a) is to use a solvent mixture (THF:*n*-hexane) where the PMMA segment is measured slightly in HPLC mode (PIB in SEC mode). The critical point on a silicagel column for PMMA is about 81:19 THF:*n*-hexane. In theory, adsorption of

TPE32	21	-55	94	1.7	150	0.4	150
TPE31	27	-55	106	4.1	230	1.3	120
TPE33	41	-56	110	8.1	310	4.4	90

^aToluene-cast films. ^bPress-mold films.

The first analysis method was differential scanning calorimetry (DSC) in order to clarify whether at all the PMMA-*b*-PIB-*b*-PMMA/(PIB-*b*-PMMA)₃ block copolymers are phase-separated. A representative DSC curve is shown in Figure 5.36. As indicated in this figure and in Table 5.15, the block copolymers have two glass transitions indicating a microphase separation of the two segments. The T_g 's are near to the expected ones for the pure homopolymers. The fact that microphase separation occurs is essential for the formation of different morphologies which is the determining parameter regarding stress-strain properties. In case of a homogeneous polymer matrix, different morphologies will not be present and the resulting materials will most likely have properties which do not change remarkably with changes in composition etc.

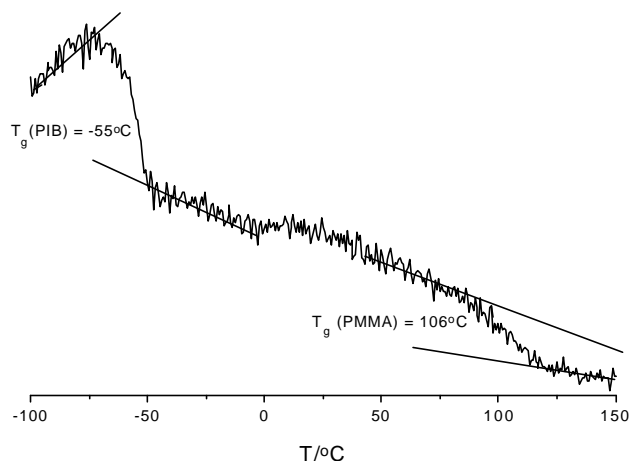


Figure 5.36: DSC curve of PMMA-*b*-PIB-*b*-PMMA (TPE31) (see Table 5.15) (2nd heating, 20 K/min)

5.6.2.2 Morphology studies

Two methods are available, either SAXS or TEM for morphology investigations of the TPEs. Until the present time, morphology studies of PIB/PMMA block copolymers have not been reported at all in the literature yet. Therefore, subsequent comparison in respect to existing materials will be made with PIB/PSt(P α MeSt)^{151,152} and PBd/PMMA¹¹² TPEs.

Table 5.16: Characteristic reflections of different crystal lattices observed in SAXS diffraction curves.

Morphology	Allowed reflections (s_1/s_n)				
Spherical (bcc)	1	2 ^{0.5}	3 ^{0.5}	4 ^{0.5}	5 ^{0.5}
Cylindrical	1	3 ^{0.5}	4 ^{0.5}	7 ^{0.5}	9 ^{0.5}
Lamellar	1	2	3	4	5

The morphology is estimated from the relative ratio of the length of the scattering vectors $s_1:s_n$ obtained from the SAXS measurements (see Table 5.16 and section 4.7.9)¹⁹⁶.

Table 5.17: SAXS results obtained with toluene-cast films (TPE31-3S) and press-mold films of linear PMMA-*b*-PIB-*b*-PMMA block copolymers (s_1 , s_2 , s_3 , and s_n scattering maxima).

Sample no.	PMMA (wt-%)	s_1	d_{SAXS} (L) (nm)	s_2	s_3	Morphology
TPE32S	21	0.057	17.5 (20.1)	0.098 ($\approx 3^{0.5}s_1$)	0.15 ($\approx 7^{0.5}s_1$)	cylindrical
TPE31S	27	0.0495	20.2	-	0.15 ($\approx 3s_1$)	lamellar
TPE33S	41	0.051	19.6	-	0.15 ($\approx 3s_1$)	lamellar
TPE32	21	0.055	18.2 (20.9)	0.0953 ($\approx 3^{0.5}s_1$)	0.145 ($\approx 7^{0.5}s_1$)	cylindrical
TPE31	27	0.0418	23.9	0.081 ($\approx 2s_1$)	0.123 ($\approx 3s_1$)	lamellar
TPE33	41	0.0363	27.5	-	-	(lamellar)
TPE44	36	0.0226	44.2	-	-	(lamellar)
TPE45	30	0.0220	45.5	-	-	(lamellar)
TPE46	20	0.0246	40.7 (46.8)	-	-	(cylindrical)

In Tables 5.17 and 5.18 the results of the SAXS measurements are summarized. The interpretation of the SAXS traces is in some cases difficult due to, e.g. the presence of only one peak maximum, partially overlapping of peaks (shoulders), or that expected peaks are missing. In the series TPE44-6 and TRI452-4 (high molecular weight materials) only one peak maximum can be observed indicating either defect in the structures or a certain fluctuation of the domain distance. As a result, it is impossible to detect any long range order due to destructive interference. Therefore, the morphologies presented in the brackets are partially based on the stress-strain results (see below) and the expected ones taking the composition into account. When more than one peak or shoulder are present, different morphologies can be estimated by calculating the relative ratios between maxima s_1, s_2 , and s_n (see Table 5.16). In Tables 5.17 and 5.18 these relative numbers are presented in brackets. When a cylindrical and spherical morphology is detected, the true distance (L) between two domains is somewhat different depending on geometric package of the domains in the PIB matrix. Below all the cylindrical morphologies are expected to be packed in a hexagonal lattice.

$$\text{Hexagonal lattice of cylinders: } L = d_{\text{SAXS}} / \sin(60^\circ) = 2 / (3^{0.5}) \cdot d_{\text{SAXS}} \approx 1.15 \cdot d_{\text{SAXS}}$$

Two SAXS traces illustrating different morphologies are shown in Figure 5.37. In addition to the problem that frequently only one peak can be observed, curvatures with well-separated peaks are not formed with this polymer system. Instead, shoulders are detected which makes the evaluation more difficult.

a)

b)

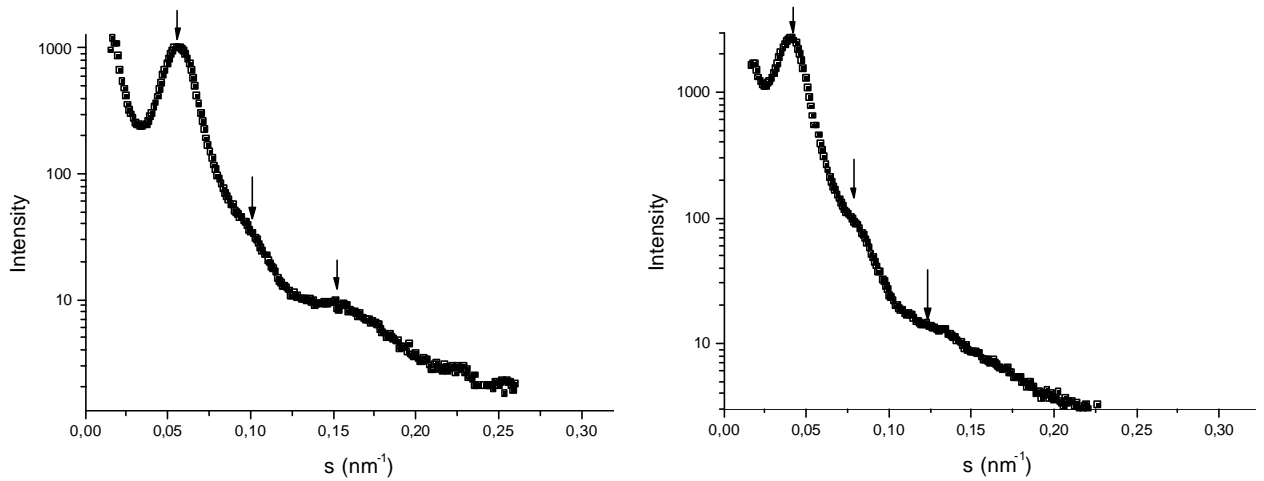


Figure 5.37: SAXS diffraction curves of a) TPE32S with a cylindrical morphology and b) of TPE31 with a lamellar morphology.

The domain distances of the star-shaped polymers (Table 5.18) are similar to the linear series in Table 5.17 (e.g., TRI30_1 and TPE33) when the composition and block lengths are comparable, as expected. However, the morphology changes in some cases although the composition and block length of each arm are nearly the same, e.g. TRI30_2 (cylindrical) and TPE31 (lamellar). Since the real morphology (and package of domains) of sample TRI30_4 cannot be evaluated, the true distance between the domains cannot be calculated, too. The relative ratio of s_1 and s_2 is exactly between those expected for cylindrical and spherical morphologies. However, due to the low PMMA content a spherical morphology is assumed.

Table 5.18: SAXS results obtained with press-mold films of star-shaped (PIB-*b*-PMMA)₃ block copolymers.

Sample no.	PMMA (wt-%)	s_1	d_{SAXS} (L) (nm)	s_2	$s_{3(4-5)}$	Morphology
TRI30_0	46	0.0322	31.1	-	-	(lamellar)
TRI30_1	37	0.0340	29.4	-	-	(lamellar)
TRI30_2	27	0.0445	22.5 (25.9)	0.0760 ($\approx 3^{0.5}s_1$)	0.1236 ($\approx 7.7^{0.5}s_1$)	cylindrical
TRI30_3	20	0.0545	18.4 (21.2)	0.0930 ($\approx 3^{0.5}s_1$)	0.1609 ($\approx 9^{0.5}s_1$)	cylindrical
TRI30_4	10	0.0736	13.6	0.0736 ($\approx 2.5^{0.5}s_1$)	-	spherical or (cylindrical)
TRI45_2	42	0.0275	36.4	-	-	(lamellar)
TRI45_3	30	0.0238	42.0	-	-	(lamellar)
TRI45_4	22	0.0340	29.4 (33.8)	-	-	(cylindrical)

Figure 5.38: TEM picture of sample TPE33 stained with RuO₄ (1 mm is equal to 4.5 nm).

TEM analysis was attempted with the PIB/PMMA-system. The major experimental problem is the contrasting of these block copolymers. In the literature RuO₄ is used for the PIB/PSt-systems (the PSt domains are stained)¹⁵². In case of the PBd/PMMA-system, OsO₄ reacts with the double bonds of PBd leading to a contrasting of the PBd domains. Since the PIB/PMMA-system does not contain any double bonds RuO₄ was utilized. However, a real lamellar morphology could not be detected with the TPE33 sample (Figure 5.38). By comparing the SAXS measurement of this sample with corresponding TEM pictures, a difference near to a factor of 5-10 regarding the domain size is observed (SAXS: \approx 20 nm and TEM: \approx 2-5 nm). Therefore, the small periodic differences in the TEM picture (Figure 5.38) are most likely an artifact and not potential lamellae. Further optimizing of the contrasting is needed in order to get reliable information about the morphology of the PIB/PMMA-system.

5.6.2.3 Mechanical properties

Dynamic-mechanical analysis also verifies the presence of the transitions in the vicinity of -60 °C and 110 °C as displayed in Figure 5.39. The dynamic-mechanical measurements were performed with solvent-cast films (from toluene) of the three triblock copolymers having the same PIB precursor but different PMMA chain length (see Table 5.15).

The dynamic-mechanical analysis of the other two samples (Table 5.15) are similar to the one of TPE31. However, due to the low PMMA content in sample TPE32, it broke before the flow region, i.e. the second $\tan\delta$ maximum was not reached indicating poor mechanical properties. In addition, the storage modulus (E') and the loss modulus (E'') are about one order of magnitude smaller than those of TPE31/TPE33.

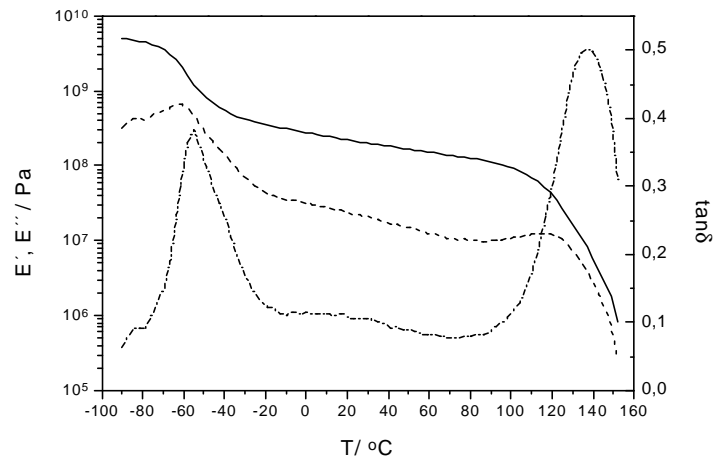


Figure 5.39: Dynamic mechanical analysis of TPE31 obtained from a toluene cast film, see Table 5.15; E' (—), E'' (---), $\tan\delta$ (-·-·)

Samples from the same toluene cast films were then analyzed in respect to stress-strain properties (see Figure 5.40 and Table 5.15). Compared to the results gained by Kennedy *et al.* (12 MPa and 550 %) ¹¹⁶ these are rather unsatisfactory. One problem might be the molecular weight of the PIB-midblock ($\approx 50,000$ for Kennedy's samples and here 17,500, see later). Another difference is the preparation of the films, here toluene was used instead of THF. One attempt was performed for casting the film from THF. However, before and after annealing macroscopic domains, i.e. a heterogeneous film was obtained. A second problem concerning the films is the annealing (see later Figure 5.42).

The shape of the curves in Figure 5.40a gives additional information about the morphology, too. TPE31/TPE33 have a yield point, i.e. a high slope at the beginning is a potential indication for a lamellar structure. The explanation is that both the hard and the rubbery phases stretch at the beginning (plastic deformation of the PMMA phase) in contrast to spheres and cylinders where primarily the rubbery phase is strained leading to a continuous increase of the tensile strength, see TPE32 Figure 5.40a. In some cases when the cylinders are oriented mainly in one direction, a small yield point might be observed.

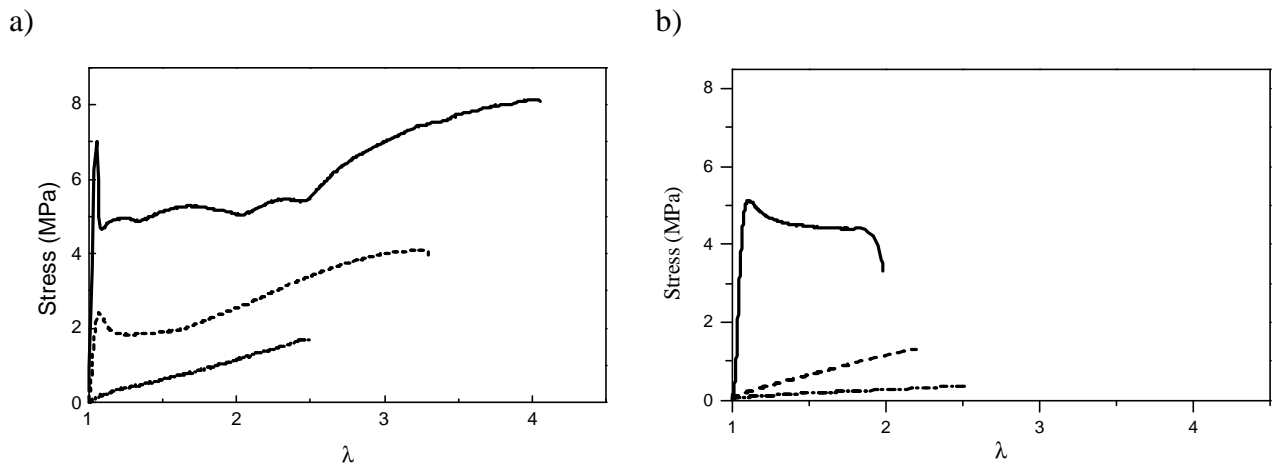


Figure 5.40: Stress-strain results obtained from a) toluene-cast films and b) from press-mold films of TPE31 (---), TPE32 (-·-·), and TPE33(—).

As described above the preparation of the film has a significant influence on the results. By comparing the results of toluene cast films and press mold films (Figure 5.40a and 5.40b) the decisive difference is obvious. First of all, much lower tensile strengths and elongations are observed with the latter type of films. Secondly, even two different morphologies might be obtained in case of the TPE31 sample since the yield point present in Figure 5.40a is absent in Figure 5.40b. Solvent-casting most likely leads to a lamellar structure and press-molding to cylindrical/spherical or possibly to a mixture of different structures. However, the SAXS measurements (see Table 5.17) indicate the presence of only lamellar morphologies. Therefore, the discrepancy of the stress-strain analyses might simply be related to defects in the press mold film caused by insufficient annealing. With these PIB/PMMA block copolymers, obtaining films which are in equilibrium, i.e. films with a homogeneous morphology, seems to be a problem in the investigated cases.

Table 5.19: Composition, tensile strength, and elongation at break of PMMA-*b*-PIB-*b*-PMMA block copolymers obtained from a) toluene-cast films and b) from a press-mold film (precursor: difunctional PIB with $M_n = 32,000$)

Sample	PMMA (%)	Ultimate tensile strength (MPa) ^{a)}	Elongation at break (%) ^{a)}	Ultimate tensile strength (MPa) ^{b)}	Elongation at break (%) ^{b)}
TPE44	36	6.3	430	2.2	13
TPE45	30	6.8	460	2.3	45
TPE46	22	-	-	0.5	80

Since one of the reasons for the difference between our results and those achieved by Kennedy *et al.*¹¹⁶ (Table 5.15) might be related to the molecular weight of the PIB midblock, a second series of TPEs with a difunctional PIB precursor having $M_n = 32,000$ were prepared. However, even lower tensile strength and elongations were obtained with these materials. Again, the crucial problem seems to be the preparation of the films (Table 5.19). Due to the higher molecular weights of these polymers it is more difficult to reach the morphology corresponding to the equilibrium state (relaxation time $\propto M_n$). Based on the results presented in Table 5.19, it is to be expected that the films analyzed in this case are far from the equilibrium state. As with the first series (Table 5.15) further analyses with these polymer samples are needed in order to investigate the effects of different preparation procedures including annealing as well.

Table 5.20: Composition, tensile strength, and elongation at break of star-shaped (PIB-*b*-PMMA)₃ block copolymers obtained from a press-mold film (precursor: trifunctional PIB with $M_n = 30,000$)

Sample no.	PMMA (%)	Ultimate tensile strength (MPa)	Elongation at break (%)
TRI30_0	46	23.4	180
TRI30_1	37	21.5	450
TRI30_2	27	13.6	670
TRI30_3	20	7.6	690
TRI30_4	10	0.7	290 ^a

^aThe low elongation might be due to the fact that the sample slipped out during the measurement.

In order to analyze the effects of the topology on the mechanical properties, two series of star-shaped (tri-armed) block copolymers were synthesized (see Table 5.20 and 5.21). The major advantage of this topology compared to the linear one is that less than 100 % blocking efficiency would lead to a mixture of ABA and $(AB)_3$ type block copolymers both able to form the proposed morphologies introduced in Figure 1.6. For the ABA system the presence of AB might decrease the properties remarkable. As illustrated in Figure 1.6 if the three arms are placed in three different PMMA domains, improved tensile strength might be observed.

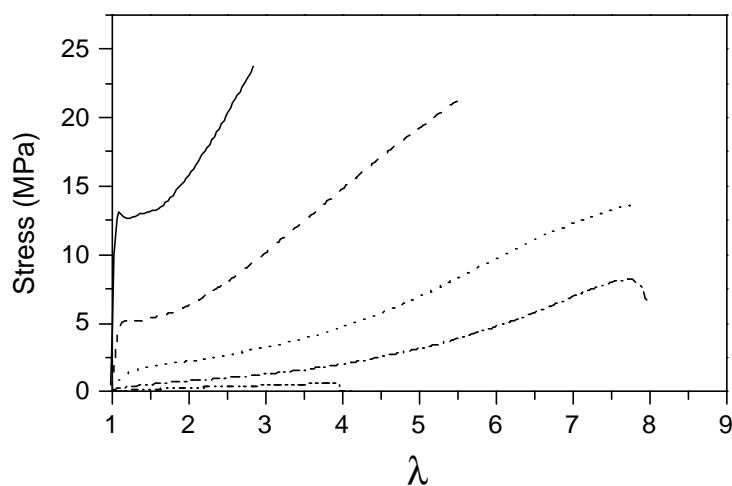


Figure 5.41: Stress-strain results obtained from press-mold films of TRI30_0 (—), TRI30_1 (---), TRI30_2 (···), TRI30_3 (-·-·-), and TRI30_4 (- - - -).

Indeed, outstanding properties are obtained with the star-shaped $(\text{PIB-}b\text{-PMMA})_3$ block copolymers (Table 5.20 and Figure 5.41). The tensile strengths exceed 20 MPa. Interestingly, only an increase of $\approx 10\%$ PIB contents (TRI30_0 and TRI30_1) enhances the elongation by a factor of 3. Based on the properties summarized in Table 5.20 different materials can be prepared just by regulating the composition of the $(\text{PIB-}b\text{-PMMA})_3$ block copolymers.

Table 5.21: Composition, tensile strength, and elongation at break of star-shaped $(\text{PIB-}b\text{-PMMA})_3$ block copolymers obtained from a press-mold film (precursor: trifunctional PIB with $M_n = 45,500$)

Sample no.	PMMA (%)	Ultimate tensile strength (MPa)	Elongation at break (%)
TRI45_2	42	16.3	200
TRI45_3	30	10.3	290
TRI45_3 ^a	30	11.3	520
TRI45_4	22	8.9	430

^aThis polymer film was annealed for additional 120 min at 150 °C.

The second series of star-shaped TPEs are based on a PIB precursor with $M_n \approx 45,500$. Better properties than those presented in Table 5.20 were expected. The problem of poorer properties shown in Table 5.20 is again related to the discussed complications regarding film preparation. In one case, sample TRI45_3, further annealing was carried out. A significant change in

max. elongation was detected after annealing (similar changes were also observed by Kennedy *et al.*)¹¹⁶. Even longer annealing time, e.g. several days, might increase the properties further.

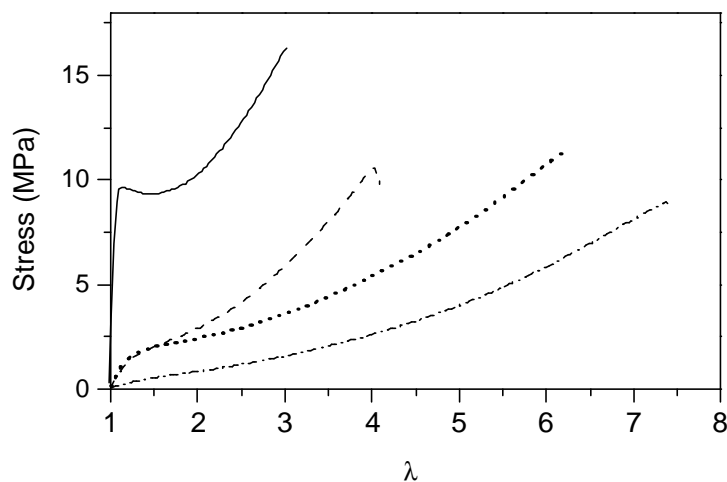


Figure 5.42: Stress-strain results obtained from press mold films of TRI45_2 (—), TRI45_3 (---), TRI45_3 (· · ·) (annealed for additional 120 min at 150 °C), TRI45_4 (- · -).

In the literature, stress-strain results of linear and star-shaped PIB/PSt-based block copolymers have been compared.²³ The tensile strengths are comparable and the elongation is $\approx 200\%$ higher for the linear one. The question is, why the results for the linear polymers, especially those presented in Table 5.19, are much worse compared to the star-shaped macromolecules. The compositions, the molecular weights of each arm (considering the initiator fragment as the core), and the film preparations are comparable. The only difference is the topology. Are the improvements observed in Figure 5.41 and Figure 5.42 exclusively due to the topology causing, e.g. to a higher mobility of the polymer molecules leading to faster formation of the morphology at equilibrium state? A second possibility (also connected to the different topologies) might be the presence of a small amount of AB block copolymers (in case of ABA systems) as a consequence of less than quantitative blocking efficiency. At the present time it is difficult/impossible to draw any decisive conclusions in relation to this problem.

Most of the PIB-based TPEs described in the literature are linear PSt-*b*-PIB-*b*-PSt (or P α MeSt and PpMeSt) TPEs.^{151,152,197} The optimum properties (stress-strain/elongation) of the star-shaped PIBs in this work are comparable with those of the star-shaped styrene TPEs.²³ The major difference between the two types of TPEs is related to the dissimilarity of the two block segments. In case of PIB/PMMA block copolymers it is higher ($\Delta\delta_{\text{PIB,PMMA}} > \Delta\delta_{\text{PIB,PSt}}$). The effects are, for instance, a smaller interface (correlated to the χ_{AB} parameter) and morphology differences when the PIB content and M_n are the same compared to those with PSt (Table 5.22).

Table 5.22: Comparison of morphologies obtained with different polymer systems and different compositions.

Morphology	PIB/PMMA-system PMMA content (%)	PIB/P α MeSt-system P α MeSt content (%) ¹⁵¹	PBd/PMMA-system PMMA content (%) ¹¹²
Spheres	≤ 10 (TRI30_4)	≈ 20	≤ 13
cylinders	≈ 20 (TPE32)	≈ 30	20-35

lamellae ≥ 27 (TPE31/TPE33) ≈ 40 ≥ 53

The maximum tensile strength published for PIB-based TPEs is ≈ 24 -25 MPa (Table 5.23) whereas for PBd-based TPEs up to 35 MPa have been reached (might be due to partial crosslinking of the PBd phase during annealing).

Table 5.23: Comparison of the mechanical properties obtained with different polymer systems.

	Vulcanized rubber ¹⁹⁸	PIB/PMMA-system	PIB/PSt-system ²⁴	PIB/P α MeSt-system ¹⁵¹	PBd/PMMA-system ¹¹²
Max. tensile strength (MPa)/(corresponding elongation (%))	25	23.4/(180)	25.3/(750)	24.5/(370)	34/(900)
Max. elongation (%)/(Max. tensile strength (MPa))	750-950	690/(7.6)	1350/(1.8)	830/(11.5)	1300/(15)

The limit of PIB-based TPEs is related to the fact that the failure is most probably in the elastomeric phase¹⁵¹, in contrast to PSt-*b*-PBd-*b*-PSt TPEs where the tensile failure mechanism is a ductile failure in the styrene phase². This postulate is in good agreement with the reported tensile strength of vulcanized butyl rubber (25 MPa)¹⁹⁸. The reason for the discrepancy between PIB- and PBd-based TPEs regarding mechanical properties might be due to the different cross-sections of the respective polymer chains i.e. the density of the covalent bonds at the backbone able to process the strain (the density is higher for PBd than for PIB). An indirect evidence for this postulate is the fact that the tensile strength of PBd-based TPEs depends significantly on the amount of 1,2-addition. A decrease of tensile strength from 34 MPa to 26 MPa was detected with two PMMA-*b*-PBd-*b*-PMMA samples having nearly the same M_n and composition, but in one case 43 % and in the other 68 % 1,2-addition.¹¹²

In conclusion, a new type of thermoplastic elastomers containing PIB and PMMA segments has been synthesized and characterized. Primarily due to problems regarding film preparation, the characterization is difficult and might not always present the truth. A significant improvement was observed when the topology was changed from linear to star-shaped block copolymers. With the latter type of materials nearly maximum tensile strength was achieved using vulcanized butyl rubber as reference.

5.7 Amphiphilic AB block copolymers

In contrast to thermoplastic elastomers discussed previously, the most interesting properties characterizing amphiphilic block copolymers are those of solutions. One of the crucial properties of amphiphilic block copolymers is their ability to form micelles. The dimensions of such species e.g., micelle size ($D_m = 2R_h$ and R_g), aggregation number (Z), and critical micelle concentration (CMC) deliver quantitative information about the amphiphilic block copolymer in a specified solvent system (which can be used for subsequent comparison). Here, only aqueous solutions are investigated.

A number of methods are available for the characterization of AB block copolymer systems in solution, e.g. static and dynamic light scattering (SLS and DLS), fluorescence correlation spectroscopy (FCS), analytical ultracentrifugation (AUC), and transmission electron microscopy TEM (Cryo-replica/contrasting).

The objective was to synthesize amphiphilic AB block copolymers, and to make detailed analyses of primarily PIB-*b*-PMAA block copolymers in aqueous media, first of all, in order to observe potential effects of molecular weight and composition on the above-mentioned parameters. Secondly, the results gained from each method will be critically compared due to potential artifacts occurring during these analyses. Finally, since this is a new polymer system, comparison with existing system will also be carried out.

5.7.1 Synthesis of PIB-*b*-PMAA and PIB-*b*-PEO block copolymers and preparation of aqueous polymer solutions

Polyisobutylene-*b*-poly(*tert*-butyl methacrylate) (PIB-*b*-PtBMA) and polyisobutylene-*b*-poly(ethylene oxide) (PIB-*b*-PEO) block copolymers were synthesized by using various PIB-DPE⁻K⁺ macroanions as initiators for the polymerization of tBMA and EO.

Preliminary experiments were carried out for investigating the blocking efficiency (see section 5.4.3). The block lengths were chosen in a way that the peaks of the PIB precursor and the PIB-*b*-PtBMA block copolymer in the SEC eluogram are separated from each other. Figure 5.19 shows the SEC eluogram (UV signal at 260 nm) for such a block copolymer. It can be seen that only a small peak appears for the unreacted PIB. Since only the aromatic rings absorb at this wavelength, integration of the UV signal peaks are used for estimation of the blocking efficiency. In this case it is higher than 95 % and the resulting block copolymer has narrow MWD with $M_w/M_n = 1.06$.

Polyisobutylene-*b*-poly(methacrylic acid) (PIB-*b*-PMAA) was prepared by hydrolysis of the *tert*-butyl ester group under acidic conditions, using HCl(aq) in dioxane at 100 °C for 24 h (see section 4.5.1). After hydrolysis a new amphiphilic diblock copolymer is formed.

Concerning the first four polymer samples (Table 5.24) it was not possible to dissolve them directly in alkaline water. Therefore, two different solvent exchange procedures (see section 4.5.1) were utilized in order to obtain a homogeneous aqueous solution needed for subsequent characterization.

Table 5.24: SEC results for PIB-*b*-PMAA block copolymers: P_n and M_n of the PIB segment, P_n and M_n of the PMAA segment is estimated from the PtBMA precursor, and M_w/M_n .

Sample no.	P_n (PIB)	M_n (PIB)	P_n (PMAA)	M_n (PMAA)	M_w/M_n
1	70	3,900	52	4,500	1.06
2	70	3,900	70	6,000	1.07
3	134	7,500	145	9,600	1.04
4	134	7,500	228	19,600	1.03

In contrast to the first four samples (see Table 5.24) the following block copolymers (see Table 5.25, sample 5-8) are directly soluble in alkaline water (pH > 10) at RT. Sample 9, the PIB-*b*-PEO block copolymer is soluble in neutral water. However, in order to get it dissolved, the water polymer mixture was shortly heated to about 50 °C. After cooling to RT a clear solution remained.

Table 5.25: SEC results for PIB-*b*-PMAA and PIB-*b*-PEO block copolymers: P_n and M_n of the PIB segment (M_n determined by ^1H NMR is identical), P_n and M_n of the PMAA segment estimated from the PtBMA precursor, M_n of the PEO segment is calculated from the conversion of EO ($\approx 100\%$), and M_w/M_n .

Sample no.	P_n (PIB)	M_n (PIB)	P_n (PMAA)	M_n (PMAA)	M_w/M_n
5	20	1,100	102	8,800	1.16
6	20	1,100	242	20,800	1.20
7	20	1,100	281	24,200	1.10
8	20	1,100	427	36,700	1.20
	P_n (PIB)	M_n (PIB)	P_n (PEO)	M_n (PEO)	
9	20	1,100	523	23,000	1.16

5.7.2 Characterization of PIB-*b*-PMAA block copolymers

The results discussed in this section are primarily related to samples 1-4. Concerning the other 5 samples only preliminary investigations have been carried out at this point. However, due to the pronounced difference in composition and molecular weight, different results are expected. At least the latter samples are easily dissolved in aqueous media.

In Table 5.26 the data from DLS and SLS experiments are summarized. The first important observation (see Figure 5.44 and 5.45) is that depending on the scattering angle (either 30° or 90°) different results are achieved for some of the samples, especially samples 3 and 4. At 30° a bimodal distribution with two well-separated peaks is detected and at 90° either a narrow or a broad but unimodal distribution is observed. Since the size distributions of sample 1 (Figure 5.44) and sample 2 at the two scattering angles are nearly identical and narrow, the analytical procedure seems to be working at least. Therefore, the bimodal distribution (see Figure 5.45) at 30° might be due to the existence of two species, micelles and aggregates since the D_m difference is about a factor of 4.

Table 5.26: Micelle size (R_h and R_g) M_w of the micelles, aggregation number (Z), and package density of sample 1-4 determined with DLS and SLS ($Z = M_{w,micelle}/M_{w,block\ copolymer}$).

Sample no.	DLS		SLS			
	$D_m = 2R_h$ (nm)		$2R_g$ (nm)	$M_w \cdot 10^{-6}$ (g/mole)	Aggregation number (Z)	Packing density (%)
	30°	90°				
1	25	25	< 20	1.58	188	24
2	30	30	< 20	1.90	192	24
3	54	70	46	2.66	133	6
4	58	100	118	3.90	144	6

From the SLS measurements the aggregation number (Z) is determined. It is seen that Z is more or less independent of the M_n of the PMAA segment but decreases significantly with increasing M_n of the PIB segment. The M_w and the R_h values increase with increasing $M_{n,\text{total}}$. That means, although Z decreases, the actual size of the micelle increases. In order to find the connection between aggregation number/micelle size and the lengths of each block segment (N_A and N_B) different theories have been proposed in the literature.¹⁵⁵ In these equations the nature of the monomer units are not taken into account. The following relation (5.7.1) between Z and N_A/N_B fits to many different polymer systems with strongly segregated blocks (the A monomer is solvophobic and the B monomer solvophilic).¹⁵⁵

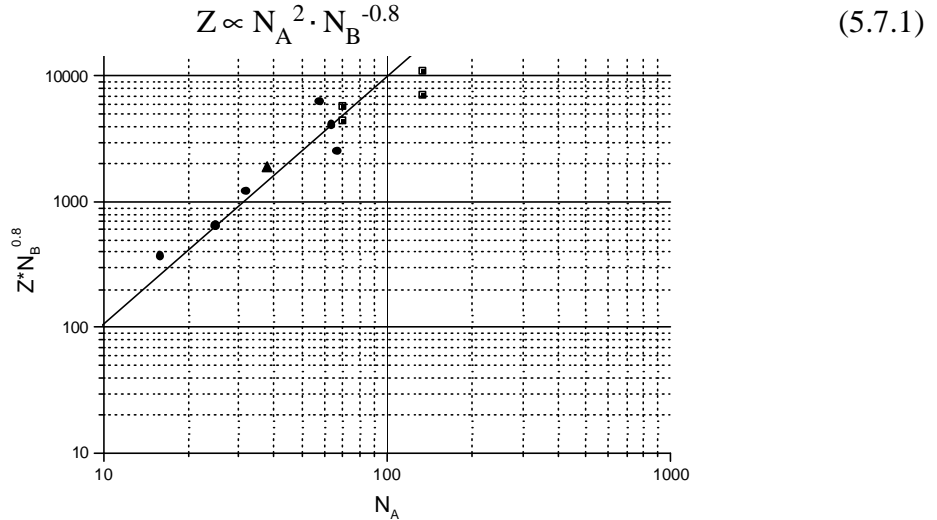


Figure 5.43: The reduced aggregation number ($Z \cdot N_B^{0.8}$) as function of N_A for different block copolymers; (■) **PIB-*b*-PMAA**, (●) **PMMA-*b*-PMAA**, and (▲) **PMMA-*b*-PMA**. The line is calculated from $Z = Z_o \cdot N_A^2 \cdot N_B^{-0.8}$, using $Z_o \approx 0.9$.

As illustrated in Figure 5.43, plotting the reduced aggregation number ($Z \cdot N_B^{0.8}$) as function of N_A , equation (5.7.1) can be used for different type of polymers including the investigated PIB-*b*-PMAA block copolymer system, since the points nearly fit the straight line ($Z = Z_o \cdot N_A^2 \cdot N_B^{-0.8}$).

Another important information from the DLS/SLS measurements is that small species i.e. single polymer chains (unimers) are not detectable indicating that in case of sample 1-4 the micelles are thermodynamically much more stable in aqueous solution compared to the unimers (see Table 5.28 regarding CMC).

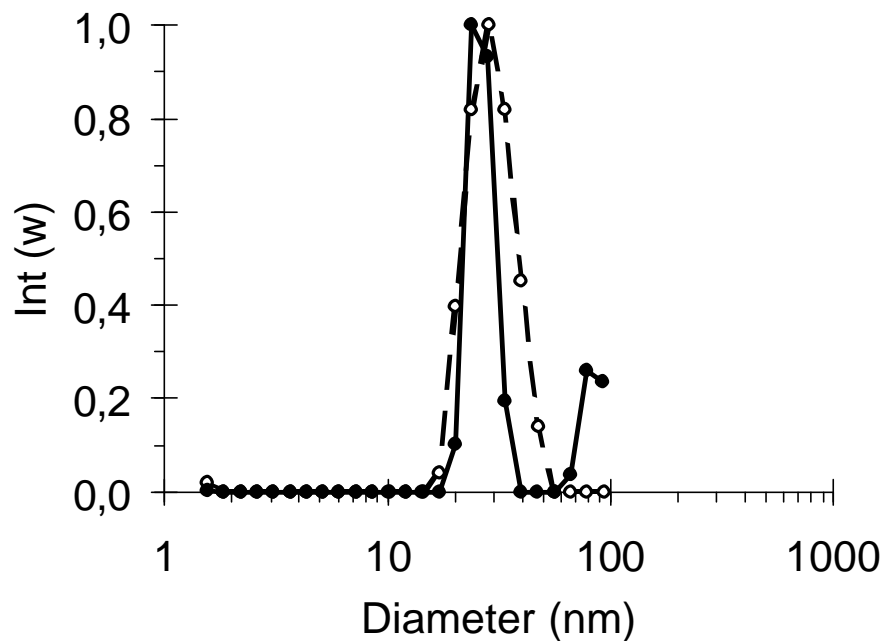


Figure 5.44: Evaluation of the micellar diameter $2R_h$ from DLS data of sample 1 in NaOH(aq) (pH \approx 12.5) at 25 °C (○: 30° and ●: 90°).

The relatively broad distribution of the peak at 90° in case of sample 4 (Figure 5.45) compared to the one of sample 1 (Figure 5.44) might be due to the presence of less defined micelles in sample 4 (a similar result was gained with sample 3). Therefore, the M_n of the PIB block in sample 3 and 4 might have exceeded a critical value.

Figure 5.45: Evaluation of the micellar diameter $2R_h$ from DLS data of sample 4 in NaOH(aq) (pH \approx 12.5) at 25 °C.

The DLS results indicate the presence of two species, micelles and aggregates based on the large difference between the D_m values. However, in the AUC measurements (Table 5.27 and Figure 5.46) a bimodal distribution is also observed, but the distance between the peak maxima is only a few nanometers. This result might be related to different types of micelles (e.g. spheres or discs/cylinders) without any aggregates. At this point it is difficult to make any conclusions regarding

the shape of the micelles. The bold number in Table 5.27 representing the size of main fraction and are used for the estimation of the micelle diameter.

Table 5.27: Micelles size, D_m of sample 1-4 determined with AUC.

Sample no.	Sed.-coef. \propto $\Delta\rho \cdot D_m^2$ (Sved)	The main D_m (packing density 50 %) (nm)
1	22/ 26	25
2	22/ 28	26
3	4.1/ 20/25	17
4	5.4/ 15	14

The micelle diameters, D_m are only comparable with the DLS (Table 5.26) in case sample 1 and 2 assuming a packing density of 50 % for the PMAA block (i.e. it is assumed that the polyelectrolyte expand to 200 % in water compared to the bulk state) (see TEM results later). Concerning sample 3 and 4 a significant difference is observed. The question is whether the anticipation regarding packing density is right. In addition, it is strange that the D_m of sample 3 is higher than for sample 4. Based on these results it can only be concluded that further AUC investigation, e.g. determination of the right packing density is needed.

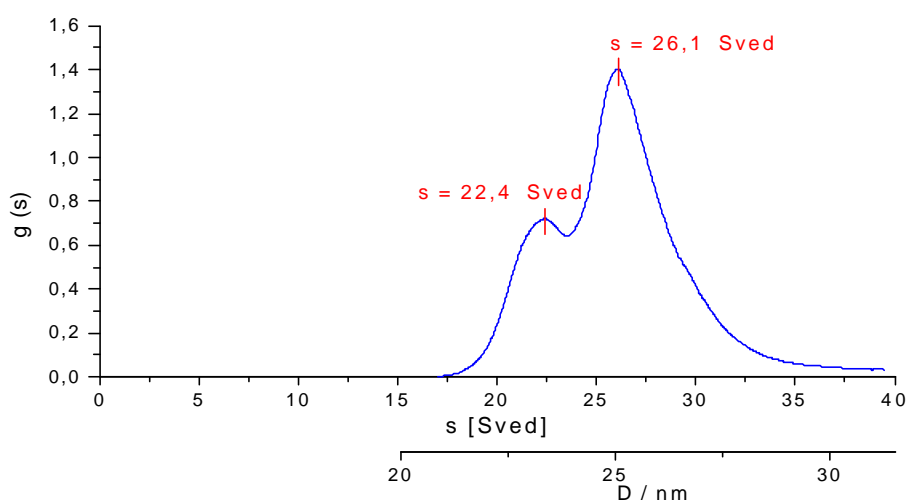


Figure 5.46: AUC trace of sample 1, where the D_m is estimated using a packing density of 50 %.

Due to an extremely low CMC in the samples, SLS could not be used for the detection of CMCs. Instead FCS (higher sensitivity) was applied for this purpose. The addition of a salt (Na_2SO_4 , 1 M) did not have any influence on the CMC. In all cases it is in the range $< 0.03\text{-}0.10$ mg/l which is about 2 order lower than for similar PMMA-*b*-PMAA block copolymers (see later).

The size of the micelles ($D_m = 2R_h$) is estimated in the following way: The diffusion of the fluorescence label is calculated from equation (5.7.2) and then by using the Stokes-Einstein equation (5.7.3) the hydrodynamic radius is calculated (assuming a spherical geometry):

$$G(t) - 1 = (r^2/N) \cdot (1/(r^2 + 4Dt)) \quad (\text{see also section 4.7.6}) \quad (5.7.2)$$

$$R_h = kT/(6\pi\eta D) \quad (5.7.3)$$

Similar to the AUC results, the D_m values obtained from FCS are also only in agreement with the DLS measurements in case of sample 1 and 2. The problem concerning the FCS method might be some kind of artifact related to the interaction between the fluorescence label (a C_{16} fatty acid) and the micelles which is more pronounced when M_n of the PIB exceed a certain value. Therefore, at this point it is impossible to say anything about the real size of the micelles in case of sample 3 and 4.

Table 5.28: Critical micelle concentration without and with Na_2SO_4 and micelle size, D_m of sample 1-4 as determined by FCS.

Sample no	CMC (mg/l)		$D_m = 2R_h$ (nm)
	without salt	with Na_2SO_4	
1	< 0.03	< 0.05	26
2	< 0.03	< 0.05	26
3	< 0.05	< 0.10	30
4	< 0.08	< 0.10	38

The last analytical method used for studying sample 1-4 is TEM (see Table 5.29). Two different procedures were utilized, cryo-replica and contrasting with uranyl acetate. As summarized in Table 5.29 a significant difference between the methods is detected which is primarily due to the preparation of the samples. In case of cryo-replica partially swollen micelles are pictured (see Figure 5.47). Besides, the shadow effect in cryo-replica might pretend bigger micelles than actually present. A third problem is that the micelles might undergo changes during the cooling leading to species different from those in the equilibrium state at RT in water.

From the ratio between the R_h (cryo-replica) ($R_{h,CR}$) and R_h (UO_2^+ contrasted) ($R_{h,UC}$) the packing density (PD) can be estimated (5.7.4):

$$PD = (R_{h,UC}/R_{h,CR})^3 \quad (5.7.4)$$

These packing density results (Table 5.29) clearly show that the assumed 50 % used for the AUC calculation is most likely much too high. Therefore, the AUC results are encumbered with a large error making it impossible to compare them with the other results.

Table 5.29: The micelle size, D_m of sample 1-4 determined with cryo-replica and UO_2^+ contrasted TEM estimated packing densities for samples 2 and 4.

Sample no	TEM		Packing density (%)
	Cryo-Replica	UO_2^+ contrasted	
1	-	20-30 nm, spheres	-
2	40-60 nm (80), spheres	10 nm, spheres and flocks	0.5-1.6

3	-	10 nm, spheres and flocks	-
4	50-70 nm (90), spheres	20 nm, spheres and flocks	2.4-6.7

Figure 5.47: TEM (Cryo-replica) of sample 4 (see also Table 5.29).

The cryo-replica picture indicates the presence of micelles (white frame) and aggregates (dark spots) (see Figure 5.47). The size of the micelles does not correlate with those determined with the other methods. In addition, the difference between D_m of sample 2 and 4 is too small only about 10 nm which is an indirect evidence for the appearance of different artifacts during the preparation of the samples. Besides, in the DLS analysis aggregates were not observed in sample 2.

a)

b)

Figure 5.48: TEM (UO_2^+ contrasted) of a) sample 1 and b) sample 4 (see also Table 5.29).

The D_m obtained from contrasting TEM is generally too small, however, in most cases uniform (sample 1, Figure 5.48a). In addition, the difference between the D_m 's is too small, and the one of sample 1 is even larger than the one of sample 3 (Table 5.29). The problem in this procedure is that the water is removed during preparation which most likely leads to a shrinkage of the micelles. In most of the pictures flocks (aggregates) are also present (Figure 5.48b). In order to obtain pictures where the micelles are not influenced by the preparation procedure, further work is needed.

From the results gained above with sample 1-4 using DLS, SLS, AUC, FCS, and TEM the following conclusions can be drawn. The PIB-*b*-PMAA block copolymer tend to form uniform (spherical, TEM pictures) micelles and to some extent aggregates of these. None of the methods indicate the presence of unimers i.e. an equilibrium between unimers and micelles which is in agreement with extremely low CMCs (< 0.03-0.10 mg/l). The aggregation number of the micelles is primarily influenced by the chain length of the PIB segment and not that much by that of the PMAA block. Due to the discrepancy between the results, the size of the micelles stated in Table 5.26-29 can only be interpreted as relative values where the magnitude for instance, can be used in subsequent comparison with the PMMA-*b*-PMAA system.

Preliminary DLS measurements with sample 7 indicate the presence of unimers ($R_h \approx 2$ nm) and micelles ($R_h \approx 88$ nm, $M_w \approx 1.1 \cdot 10^6$ g/mole, and $Z \approx 44$) i.e. an equilibrium between the two species. This means, due to the ratio $P_{n,PIB}:P_{n,PMAA}$ which in case is about 1:14 instead of 1:1-2 in sample 1-4 the tendency to form micelles is lower. Therefore a significant change in CMC is expected.

Different polymer systems have been characterized in the literature (see section 1.3.2.2). However, most of the research include non-aqueous systems (e.g. toluene) which makes a direct comparison difficult. One system involving PMMA-*b*-PMAA block copolymers (having comparable M_n 's and compositions) have been analyzed under the same conditions, i.e. in aqueous media and with the same apparatus. Due to the extremely high hydrophobicity and lower T_g of PIB compared to PMMA significant differences are observed. The CMCs of the PMMA-*b*-PMAA block copolymers are about 2-3 orders higher (3-100 mg/l) than for the PIB-*b*-PMAA system. From the SLS the aggregation number Z was estimated. A typical value of Z is in the range of 20-70 for the PMMA-*b*-PMAA system, whereas $Z = 130-190$ in case of the PIB-*b*-PMAA block copolymers (see Table 5.28). The DLS analyses show a bimodal distribution with all samples (and with both scattering angles) which at least proves that other systems also tend to form aggregates of several micelles and even to a higher extend.

5.8 Synthesis and characterization of star polymers and amphiphilic networks

Preliminary investigations towards the synthesis of amphiphilic networks (APNs) were performed. In the following, three strategies for the synthesis of APNs derived from PIB-based block copolymers introduced in chapter 3 will be partially discussed particularly with respect to synthetic problems.

Due to the fact that well-defined linking units (linear ABA and star-shaped $(AB)_3$ block copolymers) are used for the network formation, the distance between the junction points is well-defined (see below) and can be varied, e.g. $M_n = 3,000-50,000$. Besides, the composition ratio of the hydrophilic and hydrophobic segments can be adjusted in order to optimize swelling and mechanical properties. Another parameter characterizing a network is the number of chains emanating from one junction point. In method 1 and 2, only an average number of chains can be reached, e.g. $n = 3-10$, whereas in method 3 the number of chains is equal to the functionality of the curing agent.

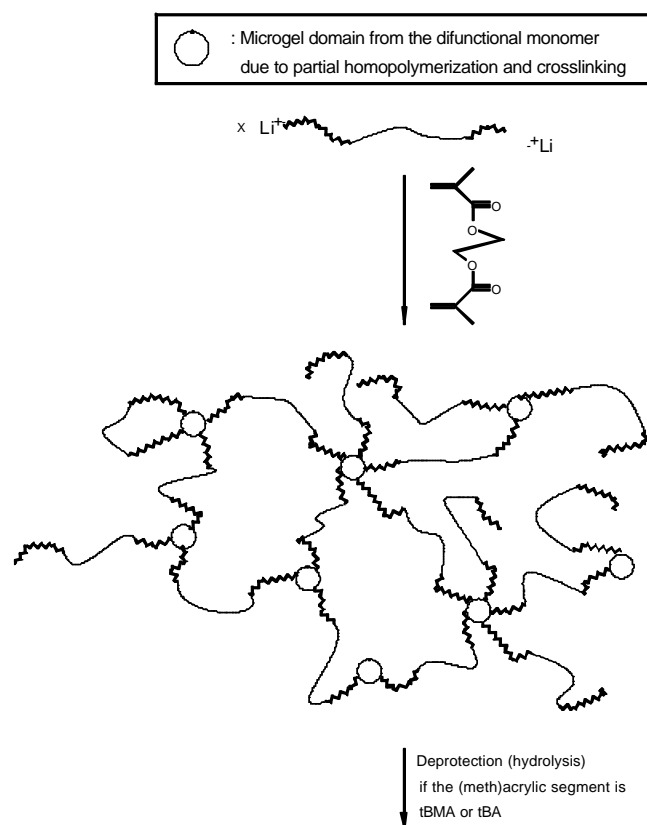
The advantage of using block copolymers and not the corresponding homopolymer (e.g. OH-terminated PIB and partially hydrolyzed PTBDMHEMA which are crosslinked with isocyanates) is first of all the control of the distance between the crosslinking points. A second advantage is related to a practical problem arising when different type of polymers (polymer segments) are present in a solution, namely, phase separation. In the case of homopolymers large domains are expected to be formed during the curing process, leading to a heterogeneous material with, e.g. poor mechanical properties. However, by using the block copolymers as unit in the network the domain size can be minimized.

As discussed in previous sections the block copolymers i.e. the precursors intended to be used for the APNs are tailored materials, e.g. M_n and the composition can be varied in a controlled way within a broad range and the MWD of these is narrow ($PDI < 1.15$). However, during the crosslinking process involving the reaction between the block copolymer and the curing agent uncontrolled reactions/structures might appear which may affect the properties of the end-product and perhaps lead to less-defined materials:

- Loop formation might take place, leading to, e.g. cyclic structures and a higher number of non-crosslinked chain ends.
- Less than quantitative curing might be observed, leading to dangling chain ends in the network.
- The degree of entanglements might (in addition to the molecular weight) also depend on the reaction conditions (temperature, concentration, solvent, etc.), leading to materials with different swelling/mechanical properties.
- The topologies might (in addition to the composition ratio of the two block segments) also depend on the reaction conditions during the curing process (temperature, concentration, solvent, etc.), leading to materials with different swelling/mechanical properties.

5.8.1 Method 1: Living block copolymers crosslinked with ethylene glycol dimethacrylate

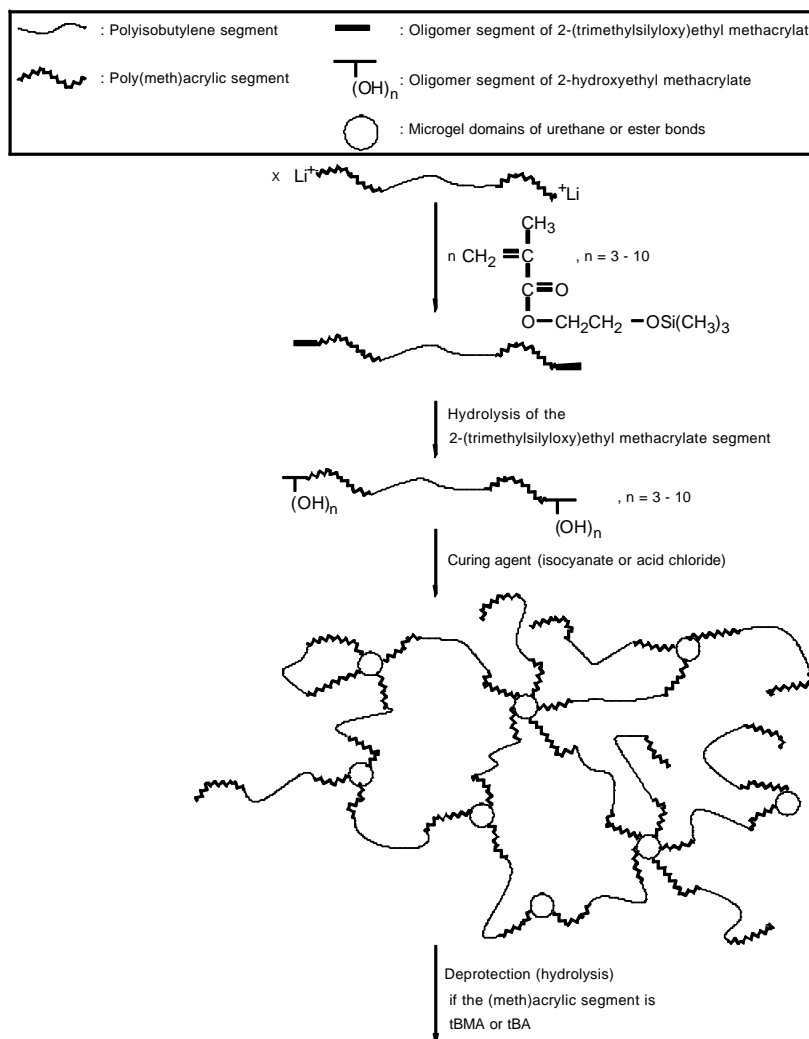
Different APNs were synthesized by this method using a di- and trifunctional PIB precursor i.e. linear ABA and star-shaped $(AB)_3$ block copolymers of tBMA or TBDMHEMA ($[P^*]:[EGDMA] = 5$) (Scheme 5.11). The major problem related to this method is that the network formation proceeds in a dilute THF solution leading to materials with reduced mechanical properties. In all experiments a gel is formed after a certain reaction time with EGDMA. However, a significant change was observed when a trifunctional PIB was utilized instead of the corresponding difunctional PIB under identical conditions. Whereas after 5 h reaction time with EGDMA the viscosity of the solution with the difunctional precursor was low enough allowing effective stirring (first after about 10 h a highly viscose gel is formed), with the trifunctional one a gel was detected within less than 45 min.



Scheme 5.11: Method 1: Synthesis of APNs using linear ABA (or star-shaped $(AB)_3$) PIB-based block copolymers and EGDMA as crosslinker.

In these preliminary experiments it has been shown that networks can be prepared by adding EGDMA to a living block copolymer solution containing 2 or 3 chain ends. Subsequent, addition of THF to the dried (non-hydrolyzed) network led to swelling (20-25 fold mass increase) of the material indicating a high crosslinking efficiency (extraction of potential free block copolymer was not carried out at this point). However, if this method has to be used for the synthesis of tailored APNs, further investigations have to be performed with highly concentrated polymer solutions, where > 95 % of the THF is evaporated before EGDMA is added. The above-mentioned method might also be applied for the preparation of star-shaped amphiphilic block copolymers using AB precursors. In the literature this method has been described with respect to the synthesis of star-shaped homopolymers.¹⁴³

5.8.2 Method 2: Block copolymers crosslinked with polyfunctional curing agents



Scheme 5.12: Method 2: Synthesis of APNs using ABCBA-type block copolymers containing an oligomer segment of HEMA and polyfunctional isocyanates or acid chlorides.

Method 2 involves the application of ABCBA-type block copolymers with outer oligo-HEMA segments (containing primary alcohol groups) (Scheme 5.12). For the curing reaction two classes of compounds are of special interest, either polyfunctional isocyanates or acid chlorides (see Figure 5.49). Concerning the reaction with isocyanates it is important to notice that a primary alcohol reacts much faster than a secondary as discussed in chapter 1. (NH_2 -groups react about two orders of magnitude faster than any alcohols with isocyanates, but appropriate methods for introduction of amino endgroups are not available at the present time).

Potential complications related to this kind of curing process are:

- The solvent(s) can have some influence on the rate and degree of curing, since the precursor might form micelles (with the HEMA segment in the core) in a nonpolar solvent like toluene. Thus the use of a polar solvent might be necessary.
- The ratio HEMA units to isocyanate/acid chloride groups is essential in order to optimize the degree of curing, e.g. due to sterically hindrance.

- Depending on the reaction condition (temperature, concentration, solvent, etc.) the polyfunctional curing agent might to a certain extent react with neighboring OH groups leading to a decrease of crosslinking.
- If the HEMA segment is too long uncontrolled network formation might take place in this segment leading to a APN with HEMA microgel (and/or macro-domains of HEMA).

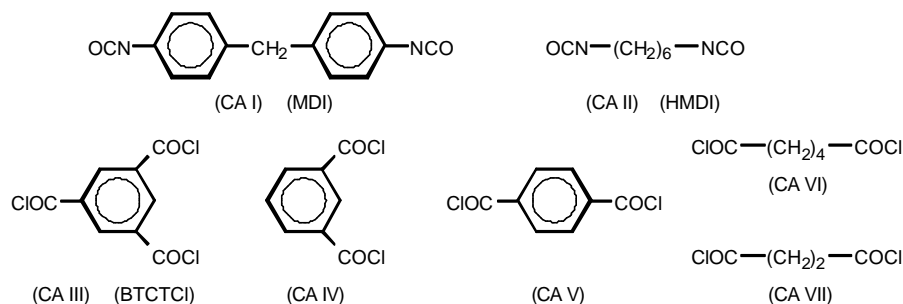


Figure 5.49: Curing agents, isocyanates and acid chlorides used for synthesis of APNs by method 2.

In order to evaluate these complications and find the optimum conditions for the curing reaction preliminary studies involving synthesis of star-shaped PtBMA homopolymers were carried out. The objective is here to follow the conversion of the PtBMA-*b*-oligo-HEMA precursor and the formation of the resulting star-shaped polymer by SEC analysis. PtBMAs with 3-10 monomer units of HEMA were prepared, Table 5.11. As discussed in section 5.5.3.1 conditions have been found under which selective hydrolysis of TMSHEMA can be made, leading to the wanted PtBMA-*b*-oligo-HEMA precursor. Besides, details of the kinetics related to the polymerizations of tBMA and TBDMHEMA including sequential monomer addition experiments are investigated in section 5.5.3.1, too.

The ΔM_n (Table 5.11) before and after hydrolysis, together with the qualitative evaluation of the ^1H NMR both indicate that polymers with different contents of TMSHEMA have been synthesized. Using HPLC under critical conditions the cross-over efficiency from tBMA to TMSHEMA were calculated. In the samples having theoretically 10 HEMA units, $\approx 99\%$ of the PtBMA chains were functionalized whereas samples with 3-5 HEMA units contain about 10-27 % homo-PtBMA with a proton endgroup (Table 5.11). Although M1TBMA1 and M1TBMA2 contain a certain amount of homo-PtBMA they were also utilized for synthesis of star-shaped polymers in order to observed possible effects of the number of HEMA units on the curing process.

With three different precursors containing 3-10 HEMA units, a series of experiments was carried out under the same conditions (temperature, solvent, catalyst, and reaction time) in order to investigate only the influence of the number of HEMA units per polymer chain and the ratio of HEMA to isocyanate groups (diphenylmethane-4,4'-diisocyanate (MDI)) on the degree of curing (Table 5.30). The first tendency observed in Table 5.30 is that when the ratio $[\text{HEMA}]/[\text{MDI}]$ increases the amount of residual arms i.e. unreacted polymer chains decreases (as determined by integrating the SEC peaks (RI signal) of the precursor and the star polymer). That means that due to the rate difference between the reaction of MDI with PtBMA-*b*-oligo-HEMA and polymer containing MDI units with PtBMA-*b*-oligo-HEMA, the number of HEMA units must be present in a certain excess

relative to the isocyanate groups. A second problem might be sterical hindrance meaning that only a fraction of the HEMA units can participate in the crosslinking process.

Table 5.30: Synthesis of star-shaped PtBMA using different ratios of HEMA:I and HEMA:MDI, Solvent: toluene, reaction temperature: 80°C, reaction time: 44 hours (16 hours slowly cooling to RT), catalyst: DABCO (5 mole % relative to OH). $M_{n,PtBMA} = 5-7,000$.

Sample no.	[HEMA]/[I]	[HEMA]/[MDI]	[HEMA]/[NCO]	Amount of residual arms, wt-%
M1STB1-1	3	1.5	0.75	70 (43) ^a
M1STB1-2	3	2	1	75 (48) ^a
M1STB1-3	3	3	1.5	40 (13) ^a
M1STB2-1	5	1.5	0.75	60 (50) ^a
M1STB2-2	5	2	1	55 (45) ^a
M1STB2-3	5	3	1.5	40 (30) ^a
M1STB3-1	10	1.5	0.75	93
M1STB3-2	10	2	1	80
M1STB3-3	10	3	1.5	60

^aThe conversion in the brackets is related to the fraction of HEMA-functionalized PtBMA chains (see Table 5.11).

The second tendency noticed in Table 5.30 is that with an increased number of HEMA units per polymer chain the amount of residual arms increases. (In this case it is important to use the numbers in brackets, taking into account that less than quantitative functionalization was detected in some of the PtBMA samples (see Table 5.11)). The most plausible explanation for this observation is that the precursors tend to form micelles with increasing amount of HEMA. The HEMA segment is in the core since toluene is a nonpolar solvent which either slows down the curing reaction and/or even reduces the maximum conversion due to sterical hindrance.

Table 5.31: Synthesis of star-shaped PtBMA using different ratios of HEMA:I and HEMA:MDI, Solvent: THF, reaction temperature: 60 °C, reaction time: 44 hours (16 hours slowly cooling to RT), catalyst: DABCO (5 mole % relative to OH). $M_{n,PtBMA} = 5-7,000$.

Sample no.	[HEMA]/[I]	[HEMA]/[MDI]	[HEMA]/[NCO]	Amount of residual arms, wt-%
M1STB1-4 ^b	3	3	1.5	45 (18) ^a
M1STB1-5	3	3	1.5	50 (23) ^a
M1STB2-4	5	3	1.5	36 (26) ^a
M1STB3-4	10	3	1.5	25

^aThe conversion in the brackets is related to the fraction of HEMA-functionalized PtBMA chains (see Table 5.11).

^bDABCO (10 mole-% relative to OH).

In order to see whether micelle formation is a problem i.e. the solvent has any influence on the reaction, the solvent was changed. Instead of toluene, THF was utilized which is significantly more polar. The results (Table 5.31) now clearly indicate that the number of HEMA units does not have any distinct influence on the degree of crosslinking when the solvent is polar.

The question is now whether the type of isocyanate has an effect on the reaction. The above-mentioned experiments involved only MDI. Two similar experiments were carried where the only difference is the isocyanate, samples M1STB2-8 and M1STB2-9 (Table 5.32). The influence of the type of isocyanate, either aromatic (MDI) or aliphatic (1,6-hexamethylene diisocyanate (HMDI)) can be ignored since the conversions are identical.

Table 5.32: Synthesis of star-shaped PtBMA using different ratios of HEMA:I and HEMA:MDI or HEMA:HMDI, Solvent: toluene, reaction temperature: 80°C, reaction time: see below, catalyst: Dibutyltin didodecanoate $[\text{CH}_3(\text{CH}_2)_{10}\text{CO}_2]_2\text{Sn}[(\text{CH}_2)_3\text{CH}_3]_2$ (5 mole % relative to OH). $M_{n,\text{PtBMA}} = 5-7,000$.

Sample no.	[HEMA]/[I]	[HEMA]/[HMDI]	[HEMA]/[MDI]	Amount of residual arms, wt-%
M1STB2-7 ^{a)}	5	-	3	35 (25) ^{d)}
M1STB2-8 ^{b)}	5	-	3	29 (19) ^{d)}
M1STB2-9 ^{a)}	5	3	-	32 (22) ^{d)}
M1STB7-3 ^{a)}	(10) ^{c)}	-	3	(< 5) microgel
M1STB7-4 ^{a)}	(10) ^{c)}	-	5	(< 5) microgel

Reaction time ^a44 hours or ^b134 hours (16 hours slowly cooling to RT)

^cThe real number might be 11-14 due to low initiating efficiency.

^dThe conversion in the brackets is related to the fraction of HEMA-functionalized PtBMA chains (see Table 5.11).

The reason, why $\approx 25\%$ residual arms are still present (M1STB2-7/2-9) after 60 h might be due to the fact that the reaction time is too short. In an experiment identical to M1STB2-7 the reaction time was extended to 150 h (sample M1STB2-8). However, the conversions and the products are nearly identical, verified by SEC (Figure 5.50). Therefore, less than quantitative conversion seems to be related to potential impurities in the polymer, since 75-80 % conversion was reached in all three experiments (M1STB2-7-M1STB2-9) independent of the reaction time and the curing agent.

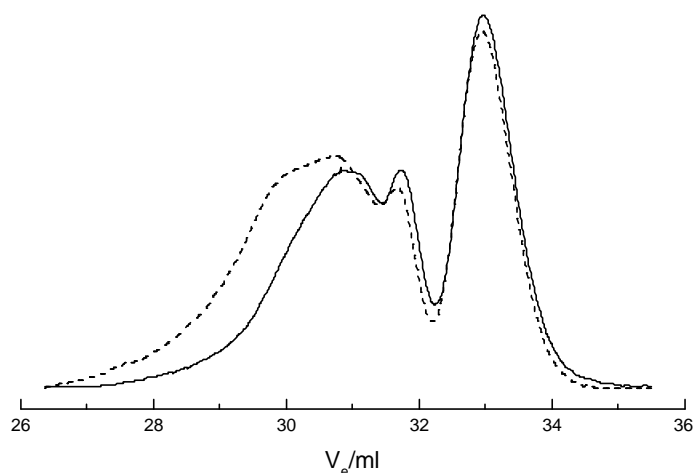


Figure 5.50: SEC trace (RI signal) of a attempted star polymer synthesis using precursor: MITBMA2, curing agent: MDI, and catalyst: dibutyltin didodecanoate, a) sample: M1STB2-7, reaction time 60 h; b) M1STB2-8, reaction time 150 h.

Concerning samples M1STB7-3/7-4 a SEC trace similar to the one illustrated in Figure 5.51 was obtained indicating microgel formation (the high molecular weight fraction has a $M_n > 10^6$). The explanation is that due to a potential low initiating efficiency (70-90 %) in this experiment

(M1TBMA7) the number of HEMA units has exceeded a critical value (11-14) where the length of the HEMA segment i.e. the lack of sterical hindrance lead to partial microgel formation within the HEMA segment.

Table 5.33: Synthesis of star-shaped PtBMA using different ratios of HEMA:I and HEMA:1,3,5-Benzenetricarbonyl trichloride (BTCTCI). Solvent: THF, catalyst: Pyridine (5 times excess relative to OH). $M_{n,PtBMA} = 5-7,000$.

Sample no.	[HEMA]/[I]	[HEMA]/[BTCTCI]	[HEMA]/[COCl]	Amount of residual arms, wt-%
M1STBT1-1 ^{a)}	3	6	2	50 (23) ^d
M1STBT2-1 ^{a)}	5	4.5	1.5	25 (15) ^d
M1STBT3-1 ^{a)}	10	4.5	1.5	25
M1STBT3-2 ^{a)}	10	6	2	50
M1STBT7-1 ^{b)}	(10) ^c	4.5	1.5	(< 5) microgel
M1STBT7-2 ^{b)}	(10) ^c	4.5	1.5	(< 5) microgel
M1STBT7-3 ^{a)}	(10) ^c	4.5	1.5	(< 5) microgel

^aReaction temperature: 25 °C, reaction time: 144 hours

^bReaction temperature: 40 C, reaction time: 44 hours.

^cThe real number might be 11-14 due to low initiating efficiency.

^dThe conversion in the brackets is related to the fraction of HEMA-functionalized PtBMA chains (see Table 5.11).

In previous experiments only isocyanates were utilized. A second possibility is acid chlorides. In order to investigation potential influence of the curing agent, a trifunctional acid chloride 1,3,5-benzenetricarbonyl trichloride (BTCTCI) was used for the last series of experiments (Table 5.33). The result of the first four sample in Table 5.33 are comparable with those in Table 5.31 performed under similar conditions with MDI. Since 20-25 % rest arm is present in all experiments (Tables 5.31 and 5.33) it can once more be concluded that traces of impurities (e.g. moisture) most likely reduce the degree of crosslinking. The difference between M1STBT3-1/3-2 verify the high sensitivity of this system regarding the ratio HEMA units to COCl/(NCO) units. A second important detail observed in Table 5.33 (comparing M1STBT3-1 with M1SBT7-1) is the decisive influence of the number of HEMA units per polymer chain. If a certain value is exceeded the fraction of microgel compared to the wanted star polymer is conspicuously high (Figure 5.51).

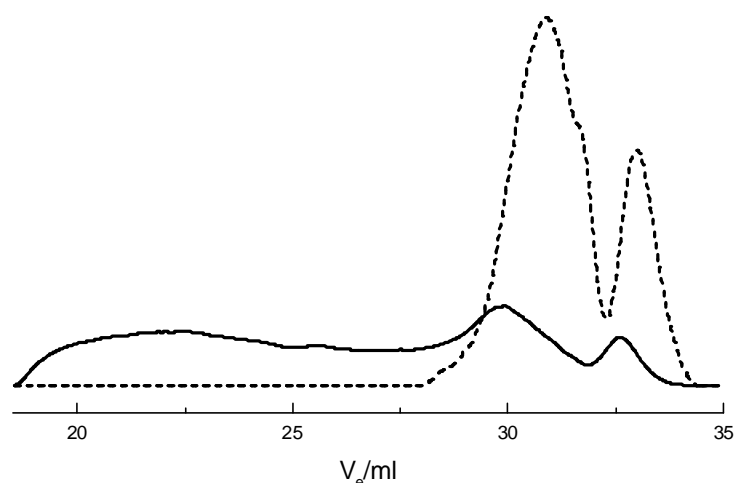


Figure 5.51: SEC traces (RI signals) of M1STBT7-2 (—), indicating partial microgel formation and M1STBT3-1 (---) where microgel formation is absent (see Table 5.33).

In Figure 5.52a the SEC traces of the MITBMA2 precursor (with 5 HEMA units) and one of the curing products are illustrated. The most important detail is the RI/UV ratio of the precursor before and after curing. A significant increase of the UV signal at $\lambda = 260$ nm (Figure 5.52b, $V_e \approx 33$ ml) is observed after curing. The reason is either that a fraction of the acid chloride groups has been deactivated due to impurities leading only to addition of BTCTCl without further crosslinking or that a fraction of the BTCTCl reacts with neighboring HEMA units in one polymer chain which reduces the crosslinking efficiency.

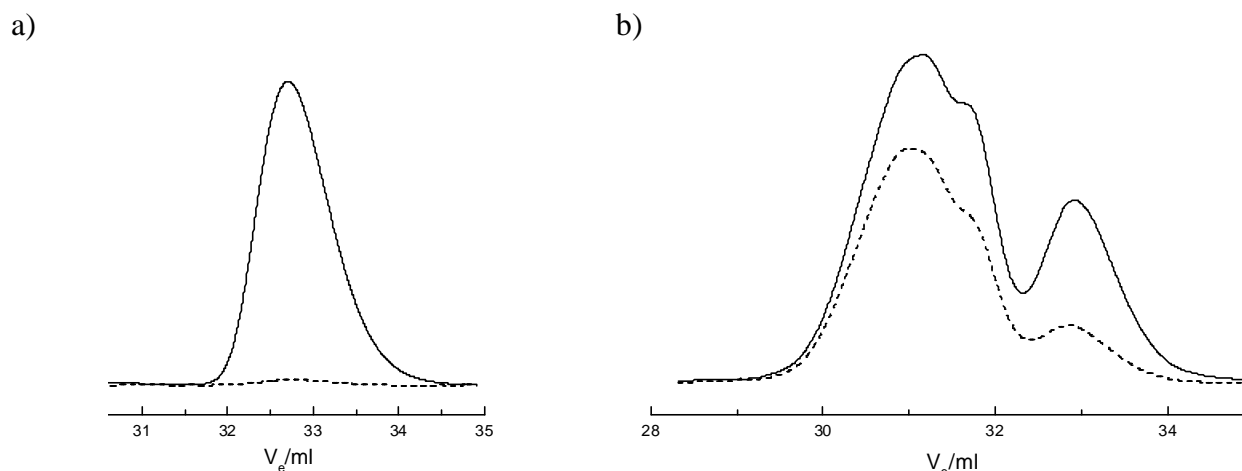
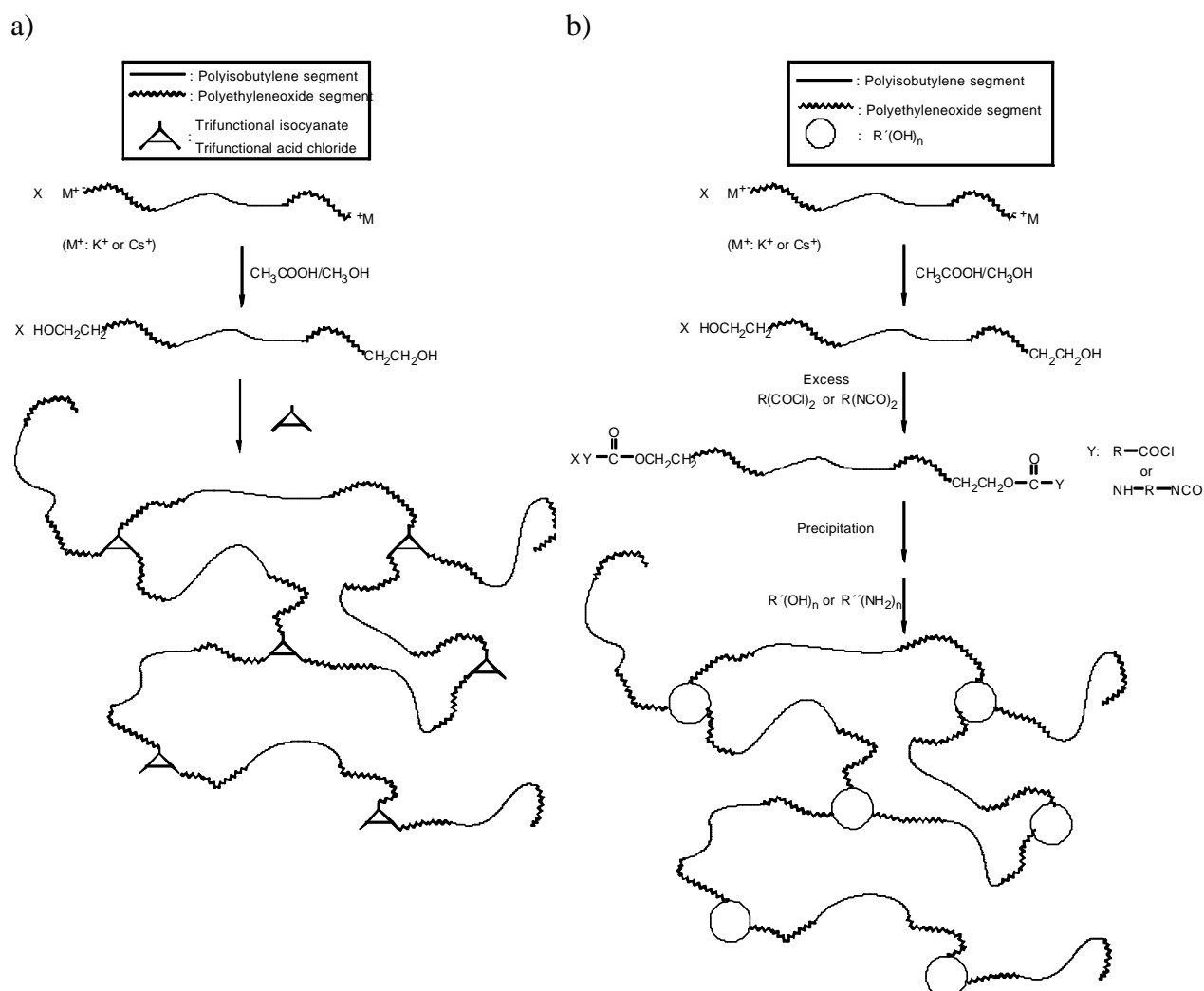


Figure 5.52: SEC traces, RI signals (—) and UV signals (260 nm) (---) of a) MITBMA2 and b) the product obtained after reaction with 1,3,5-benzenetricarbonyl trichloride (M1STBT2-1).

In conclusion, the curing reaction between PtBMA-*b*-oligo-HEMA precursors and polyfunctional isocyanates and acid chlorides is highly sensitive toward the ratios $[\text{HEMA}]:[\text{I}]$ and $[\text{HEMA}]:[\text{NCO/COCl}]$. Only if $[\text{HEMA}]:[\text{I}] > 5$, quantitative functionalization of PtBMA is reached. However, if $[\text{HEMA}]:[\text{I}] > 11-14$ substantial amount of uncontrolled microgel formation takes place. Therefore, subsequent work has to be carried out with precursors, where $5 < [\text{HEMA}]:[\text{I}] < 11-14$. Regarding the ratio $[\text{HEMA}]:[\text{NCO/COCl}]$, the best results have been gained when it is $\gg 1.5$. Since, none of the experiments led to quantitative conversion of the precursor (independent of the conditions and curing agent max. conversion is about 75-80 %) further work will also have to include investigations regarding the purity of the precursors.

5.8.3 Method 3: End-functionalized PIB/PEO-based block copolymer crosslinked with polyfunctional curing agents

At the present time a procedure for the synthesis of quantitative OH-terminated (meth)acrylates is not available (see section 5.5.4). Only polymerization of EO leads to well-defined OH-terminated polymers. The aim of this chapter is to introduce a third method for the synthesis of APNs (see Scheme 5.13) involving end-functionalized PIB/PEO-based block copolymers. Compared to the first two methods, the number of arms emanating from one junction point is in this case equal to the number of functional sites on the curing agent expecting quantitative conversion. The (poly)alcohol(s), $R'(OH)_n$ or (poly)amino compounds, $R''(NH_2)_n$ which are of interest (Scheme 5.13b) might contain biological active segments which at the same time lead to THF-soluble compounds. At this point experimental work was not performed.



Scheme 5.13: Method 3: Synthesis of APNs using a) OH-terminated linear PEO-*b*-PIB-*b*-PEO (or star-shaped (PIB-*b*-PEO)₃) block copolymers and polyfunctional isocyanates or acid chlorides and b) NCO/COCl-terminated linear PEO-*b*-PIB-*b*-PEO (or star-shaped (PIB-*b*-PEO)₃) block copolymers and polyfunctional alcohols or amines.

6 Appendix

6.1 Titration of BuLi

n-Butyllithium (n-BuLi) (Aldrich) ≈ 1.6 M in n-hexane was used as received. Since the purchased solution of n-BuLi contains other components than just n-BuLi, it is titrated using the procedure described below.

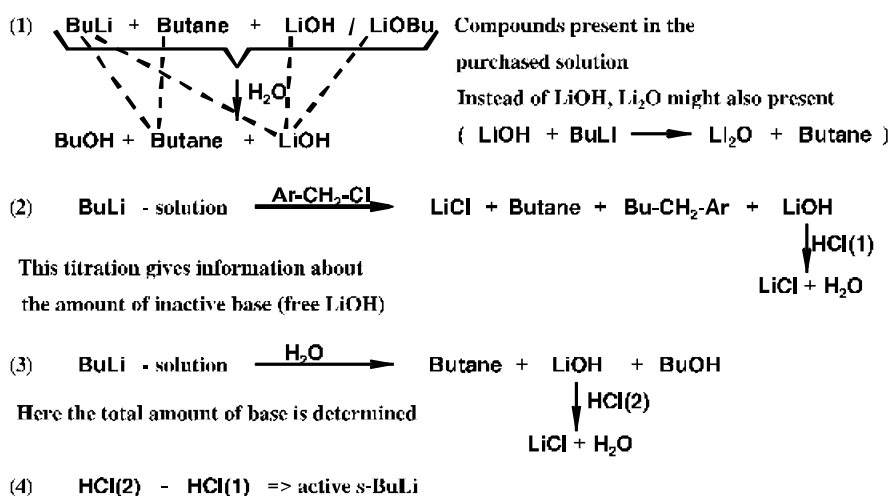
The concentration is: $c_{\text{n-BuLi}} = 1.58 \pm 0.02$ M

s-Butyllithium (s-BuLi) (Aldrich) ≈ 1.4 M in n-hexane/cyclohexane (8/92) was titrated for exact molarity (in a glove-box), using a standard HCl(aq) solution. The concentration of HCl(aq) was determined by the use of NaOH(aq) and potassium hydrogen phthalate (standard acid, $\text{KOOCC}_6\text{H}_4\text{COOH}$).

Since BuLi easily decomposes in the presence of moisture, resulting in the formation of LiOH, titration is required to have reliable information about the actual concentration of active BuLi. A method described by Price was used with a slight modification.¹⁹⁹ A 5 ml sample of the s-BuLi solution was added using a syringe into a beaker. This was followed by slowly charging 1 ml benzyl chloride (distilled from CaH_2) by a syringe into the solution (selective removal of BuLi by benzylation), and the mixture was allowed to react for 1 h. Then the it was diluted with 5 ml freshly distilled THF and was poured into distilled water which was subsequently titrated with the above mentioned HCl(aq) using phenolphthalein (3 drops) as indicator. The concentration obtained by this procedure was subtracted from the result obtained by titrating 5 ml s-BuLi solution quenched directly by distilled water. The difference represents the concentration of active s-BuLi.

The concentration is: $c_{\text{s-BuLi}} = 1.27 \pm 0.02$ M

The following equations illustrate the principle chemistry of this titration procedure.



Scheme A1: Details concerning titration of a butyl lithium solution.

References

- 1) M. Yokoyama, T. Okano, Y. Sakurai, H. Ekimoto, C. Shibazaki, K. Kataoka, *Cancer Res.* **51**, 3229 (1991)
- 2) N. R. Legge, G. Holden, H. E. Schroeder, "Thermoplastic Elastomers", Hanser Publishers: Munich 1987
- 3) B. Keszler, J. P. Kennedy, *J. Macromol. Sci., Chem.* **A21**, 319 (1984)
- 4) J. P. Kennedy, *J. Macromol. Sci., Pure Appl. Chem* **A31**, 1771 (1994)
- 5) B. D. Ratner, *Polym. Prepr. (Am. Chem. Soc., Div. Polym. Chem.)* **34(2)**, 50 (1993)
- 6) Y. Ikada, *Adv. Polym. Sci.* **57**, 103 (1984)
- 7) S. K. Varshney, P. Bayard, C. Jacobs, R. Jérôme, R. Fayt, P. Teyssié, *Macromolecules* **25**, 5578 (1992)
- 8) A. Hirao, H. Kato, K. Yamaguchi, S. Nakahama, *Macromolecules* **19**, 1294 (1986)
- 9) M. Iijima, Y. Nagasaki, M. Kato, K. Kataoka, *Polymer* **38(5)** (1997)
- 10) H. Mori, O. Wakisaka, A. Hirao, S. Nakahama, *Macromol. Chem. Phys.* **195**, 3213 (1994)
- 11) K. Yamaguchi, A. Hirao, K. Suzuki, K. Takenaka, S. Nakahama, N. Yamazaki, *J. Polym. Sci. Polym. Lett. Ed.* **21**, 395 (1983)
- 12) B. Iván, *Makromol. Chem., Macromol. Symp.* **67**, 311 (1993)
- 13) J. P. Kennedy, B. Iván, "Designed Polymers by Carbocationic Macromolecular Engineering: Theory and Practice", Hanser Publishers: Munich, 1992
- 14) P. Sigwalt, *Makromol. Chem., Macromol. Symp.* **47**, 179 (1991)
- 15) V. S. C. Chang, B. Iván, J. P. Kennedy, *Polym. Bull.* **3**, 339 (1980)
- 16) R. Faust, A. Nagy, J. P. Kennedy, *J. Macromol. Sci., Chem.* **A24(6)**, 595 (1987)
- 17) K. Matyjaszewski, C. H. Lin, *Makromol. Chem., Macromol. Symp.* **47**, 221 (1991)
- 18) M. Zsuga, J. P. Kennedy, T. Kelen, *Makromol. Chem., Macromol. Symp.* **32**, 145 (1990)
- 19) B. Iván, M. Zsuga, F. Gruber, J. P. Kennedy, *Polym. Prepr. (Am. Chem. Soc., Div. Polym. Chem.)* **29(2)**, 33 (1988)
- 20) B. Iván, J. P. Kennedy, *Macromolecules* **28**, 2880 (1990)
- 21) M. Szwarc, *Makromol. Chem., Macromol. Symp.* **67**, 83 (1993)
- 22) I. Majoros, J. P. Kennedy, T. Kelen, T. M. Marsalko, *Polym. Bull.* **31**, 255 (1993)
- 23) G. Kaszas, J. E. Puskas, J. P. Kennedy, W. G. Hager, *J. Polym. Sci., Part A: Polym. Chem.* **29**, 427 (1991)
- 24) M. Gyor, Z. Fodor, H. C. Wang, R. Faust, *J. Macromol. Sci., Chem. Pure Appl. Chem.* **A31(12)**, 2055 (1994)
- 25) S. Hadjikyriacou, R. Faust, *Macromolecules* **29**, 5261 (1996)
- 26) S. Jacob, I. Majoros, J. P. Kennedy, *Macromolecules* **29**, 8631 (1996)
- 27) K. Matyjaszewski, "Cationic Polymerizations: Mechanisms, Synthesis, and Applications", Marcel Dekker Inc.: New York / Basel / Hong Kong 1996
- 28) B. Iván, J. P. Kennedy, *Polym. Mater. Sci. Eng.* **58**, 869 (1988)
- 29) B. Iván, J. P. Kennedy, *J. Polym. Sci. Part A: Polym. Chem.* **28**, 89 (1990)
- 30) Y. C. Bae, Z. Fodor, R. Faust, *Polym. Prepr. (Am. Chem. Soc., Div. Polym. Chem.)* **37(1)**, 801 (1996)
- 31) L. V. Nielsen, R. R. Nielsen, B. Gao, J. Kops, B. Iván, *Polymer* **38**, 2529 (1997)
- 32) C. C. Chen, G. Kaszas, J. E. Puskas, J. P. Kennedy, *Polym. Bull.* **22**, 463 (1989)
- 33) R. Faust, B. Iván, J. P. Kennedy, *J. Macromol. Sci., Chem.* **A27**, 1571 (1990)
- 34) R. F. Storey, Y. Lee, *J. Macromol. Sci., Pure Appl. Chem* **A29**, 1017 (1992)
- 35) J. Feldthusen, B. Iván, A. H. E. Müller, J. Kops, *Macromol. Rapid Commun.* **18**, 417 (1997)
- 36) C. C. Chen, J. Si, J. P. Kennedy, *J. Macromol. Sci., Pure Appl. Chem* **A29**, 669 (1992)
- 37) L. Balogh, R. Faust, L. Wang, *Macromolecules* **27**, 3453 (1994)
- 38) L. Balogh, Z. Fodor, T. Kelen, R. Faust, *Macromolecules* **27**, 4648 (1994)
- 39) L. Wang, S. T. McKenna, R. Faust, *Macromolecules* **28**, 4681 (1995)
- 40) O. Nuyken, H. Kroener, H. Aechtner, *Makromol. Chem., Macromol. Symp.* **32**, 181 (1990)
- 41) M. Sawamoto, T. Higashimura, *Makromol. Chem., Macromol. Symp.* **32**, 131 (1990)
- 42) K. Matyjaszewski, P. Sigwalt, *Polym. Int.* **35**, 1 (1994)
- 43) M. K. Mishra, C. C. Chen, J. P. Kennedy, *Polym. Bull.* **22**, 455 (1989)

- 44) R. Faust, B. Iván, J. P. Kennedy, *J. Macromol. Sci., Chem.* **A28**, 1 (1991)
- 45) G. Kaszas, J. E. Puskas, J. P. Kennedy, C. C. Chen, *J. Macromol. Sci., Chem.* **A26(8)**, 1099 (1989)
- 46) R. Faust, B. Iván, J. P. Kennedy, *Polym. Prepr. (Am. Chem. Soc., Div. Polym. Chem.)* **31(1)**, 466 (1990)
- 47) M. Gyor, H. C. Wang, R. Faust, *J. Macromol. Sci., Chem. Pure Appl. Chem.* **A29(8)**, 639 (1992)
- 48) M. Gyor, Z. Fodor, H. C. Wang, R. Faust, *Polym. Prepr. (Am. Chem. Soc., Div. Polym. Chem.)* **34(2)**, 562 (1993)
- 49) A. Dembinski, Y. Yagci, W. Schnabel, *Polym. Commun.* **34**, 3738 (1993)
- 50) R. Faust, J. P. Kennedy, *J. Polym. Sci. Part A: Polym. Chem.* **25**, 1847 (1987)
- 51) D. Held, Iván, B., A. H. E. Müller, F. de Jong, T. Graafland, *ACS Symp. Ser.* **665**, 63 (1997)
- 52) T. Kelen, M. Zsuga, L. Balogh, I. Majoros, G. Deak, *Makromol. Chem., Macromol. Symp.* **67**, 325 (1993)
- 53) T. Pernecker, J. P. Kennedy, *Polym. Bull.* **26**, 305 (1991)
- 54) G. V. Schulz, *Adv. in Chem. Sci.* **128**, 1 (1973)
- 55) R. Fayt, R. Forte, R. Jacobs, R. Jérôme, T. Ouhadi, P. Teyssié, S. K. Varshney, *Macromolecules* **20**, 1442 (1987)
- 56) K. Hatada, T. Kitayama, K. Ute, *Progr. Polym. Sci.* **13**, 189 (1988)
- 57) A. H. E. Müller, "Carbanionic Polymerization: Kinetics and Thermodynamics", in: *Comprehensive Polymer Science*, G. Allen and J. C. Bevington, Eds., Pergamon: Oxford (1988)
- 58) H. L. Hsieh, R. P. Quirk, "Anionic Polymerization: Principles and Practical Applications", Marcel Dekker, Inc.: New York / Basel / Hong Kong 1996
- 59) S. K. Varshney, C. Jacobs, J.-P. Hautekeer, P. Bayard, R. Jérôme, R. Fayt, P. Teyssié, *Macromolecules* **24**, 4997 (1991)
- 60) J. P. Kennedy, *Trends Polym. Sci* **1(12)**, 381 (1993)
- 61) Y. Mori, H. Nagaoka, H. Takiuchi, T. Kikuchi, N. Noguchi, H. Tanzawa, Y. Noishiki, *Transactions of the American Society of Artificial Internal Organs* **28**, 459 (1982)
- 62) B. Iván, J. P. Kennedy, P. W. Mackey, *Polym. Prepr. (Am. Chem. Soc., Div. Polym. Chem.)* **31(2)**, 215 (1990)
- 63) B. Iván, J. P. Kennedy, P. W. Mackey, *Polym. Prepr. (Am. Chem. Soc., Div. Polym. Chem.)* **31(2)**, 217 (1990)
- 64) X. Xie, T. E. Hogen-Esch, *Macromolecules* **29**, 1746 (1996)
- 65) J. M. Yu, P. Dubois, R. Jérôme, *Macromolecules* **29**, 8362 (1996)
- 66) F. J. Gerner, H. Höcker, A. H. E. Müller, G. V. Schulz, *Eur. Polym. J.* **20**, 349 (1984)
- 67) V. Warzelhan, G. Löhr, H. Höcker, G. V. Schulz, *Makromol. Chem.* **179**, 2211 (1978)
- 68) S. Boileau, "Anionic ring-opening polymerization: epoxides and episulfides", in: *Comprehensive Polymer Science*, G. Allen and J. C. Bevington, Eds., Pergamon: Oxford (1988)
- 69) H. Reuter, I. L. Berlinova, S. Höring, J. Ulbricht, *Eur. Polym. J.* **27(7)**, 673 (1991)
- 70) I. Cabasso, A. Zilkha, *J. Macromol. Sci., Chem.* **A8**, 1313 (1974)
- 71) C. J. Chang, R. F. Kiesel, T. E. Hogen-Esch, *J. Am. Chem. Soc.* **95**, 8446 (1973)
- 72) K. S. Kazanskii, A. A. Solovyanov, S. G. Entelis, *Eur. Polym. J.* **7**, 1421 (1971)
- 73) T. Holm, *Acta Chem. Scand.* **B32**, 162 (1978)
- 74) H. C. Wang, G. Levin, M. Szwarc, *J. Am. Chem. Soc.* **100**, 6137 (1978)
- 75) K. Ziegler, B. Schnele, *Liebigs Ann. Chem.* **437**, 227 (1924)
- 76) K. Ziegler, H. Dislich, *Chem. Ber.* **90**, 1107 (1957)
- 77) Z. Hruska, G. Hurtez, S. Walter, G. Reiss, *Polymer* **33**, 2447 (1992)
- 78) S. Antoun, J. S. Wang, R. Jérôme, P. Teyssie, *Polymer* **37**, 5755 (1996)
- 79) A. Davidjan, N. I. Nikolaev, V. Zgonnik, B. Belenkii, V. Nesterow, B. Erussalimsky, *Makromol. Chem.* **177**, 2469 (1976)
- 80) Elf-Atochem S.A. invs. A. Maurer, A. H. E. Müller, P. Teyssié, FR FR (1997)
- 81) J. S. Wang, R. Jérôme, R. Warin, H. Zhang, P. Teyssié, *Macromolecules* **27**, 3376 (1994)
- 82) R. N. Young, R. P. Quirk, L. J. Fetters, *Adv. Polym. Sci.* **56**, 1 (1984)
- 83) S. K. Varshney, Z. Gao, X. F. Zhong, A. Eisenberg, *Macromolecules* **27**, 1076 (1994)
- 84) D. Kunkel, A. H. E. Müller, L. Lochmann, M. Janata, *Makromol. Chem., Macromol. Symp.* **60**, 315 (1992)
- 85) D. Kunkel, Dissertation, Mainz 1992

- 86) J.-S. Wang, R. Jérôme, R. Warin, P. Teyssié, *Macromolecules* **26**, 5984 (1993)
- 87) O. W. Webster, W. R. Hertler, D. Y. Sogah, W. B. Farnham, T. V. RajanBabu, *J. Am. Chem. Soc.* **105**, 5706 (1983)
- 88) E. P. O. Pat. EP 68887 (1983), E. I. du Pont de Nemours & Co.invs. O. W. Webster, W. B. Farnham, D. Y. Sogah, *Chem. Abstr.* 098:144031g
- 89) D. Y. Sogah, W. B. Farnham, "Group transfer polymerization. Mechanistic studies", in: *Organosilicon and Bioorganosilicon Chemistry*, H. Sakurai, Ed., Wiley: New York 1986
- 90) I. B. Dicker, *Polym. Prepr. (Am. Chem. Soc., Div. Polym. Chem.)* **29(2)**, 114 (1988)
- 91) O. W. Webster, *Makromol. Chem., Macromol. Symp.* **53**, 307 (1992)
- 92) W. G. Ruth, M. W. Brittain, J. Si, J. P. Kennedy, *Polym. Prepr. (Am. Chem. Soc., Div. Polym. Chem.)* **34**, 479 (1993)
- 93) H. Yasuda, H. Yamamoto, K. Yokota, S. Miyake, A. Nakamura, *J. Am. Chem. Soc.* **114**, 4908 (1992)
- 94) H. Yasuda, H. Yamamoto, M. Yamashita, K. Yokota, A. Nakamura, S. Miyake, Y. Kai, N. Kanehisa, *Macromolecules* **26**, 7134 (1993)
- 95) S. Inoue, *Prepr., IUPAC Intl. Symp. on Macromol., Kyoto* (1988)
- 96) H. Yasuda, H. Yamamoto, Y. Takemoto, M. Yamashita, K. Yokota, S. Miyake, A. Nakamura, *Makromol. Chem., Macromol. Symp.* **67**, 187 (1993)
- 97) H. Yasuda, E. Ihara, M. Morimoto, *Polym. Prepr. (Am. Chem. Soc., Div. Polym. Chem.)* **35**, 532 (1994)
- 98) T. Aida, S. Inoue, *Makromol. Chem., Macromol. Symp.* **73**, 27 (1993)
- 99) S. Inoue, T. Aida, H. Sugimoto, C. Kawamura, M. Kuroki, *Makromol. Chem., Macromol. Symp.* **88**, 117 (1994)
- 100) J. Wang, K. Matyjaszewski, *Macromolecules* **28**, 7901 (1995)
- 101) K. Matyjaszewski, J. Qiu, *Acta Polym.* **48**, 169 (1997)
- 102) K. Matyjaszewski, S. Coca, S. G. Gaynor, M. Wei, B. E. Woodworth, *Macromolecules* **30**, 7348 (1997)
- 103) J. Xia, K. Matyjaszewski, *Macromolecules* **30**, 7697 (1997)
- 104) M. K. Georges, R. P. N. Veregin, P. M. Kazmaier, G. K. Hamer, *Macromolecules* **26**, 2987 (1993)
- 105) M. K. Georges, R. P. N. Veregin, P. M. Kazmaier, G. K. Hamer, *Trends Polym. Sci* **2**, 66 (1994)
- 106) C. J. Hawker, *Trends Polym. Sci.* **4**, 183 (1996)
- 107) S. G. Gaynor, K. Matyjaszewski, *Macromolecules* **30**, 4241 (1997)
- 108) C. J. Hawker, D. Mecerreyes, E. Elce, J. Dao, J. L. Hedrick, I. Barakat, P. Dubois, R. Jerome, W. Volkson, *Macromol. Chem. Phys.* **198**, 155 (1997)
- 109) K. Matyjaszewski, T. Shigemoto, J. M. J. Frechet, M. Leduc, *Macromolecules* **29**, 4167 (1996)
- 110) C. Forder, C. S. Patrickios, S. P. Armes, N. C. Billingham, *Macromolecules* **29**, 8160 (1996)
- 111) S. Hadjikyriacou, R. Faust, *Polym. Prepr. (Am. Chem. Soc., Div. Polym. Chem.)* **36(2)**, 174 (1995)
- 112) J. M. Yu, P. Dubois, P. Teyssié, R. Jérôme, *Macromolecules* **29**, 6090 (1996)
- 113) X. F. Zhong, S. K. Varshney, A. Eisenberg, *Macromolecules* **25**, 7160 (1992)
- 114) T. Kitayama, T. Nishiura, K. Hatada, *Polym. Bull.* **26**, 513 (1991)
- 115) T. Nishiura, T. Kitayama, K. Hatada, *Polym. Bull.* **27**, 615 (1992)
- 116) J. P. Kennedy, J. L. Price, K. Koshimura, *Macromolecules* **24**, 6567 (1991)
- 117) A. Takács, R. Faust, *Macromolecules* **28**, 7266 (1995)
- 118) J. P. Kennedy, M. Hiza, *J. Polym. Sci. Polym. Chem. Ed.* **21**, 3573 (1983)
- 119) M. Gyor, K. Kitayama, N. Fujimoto, T. Nishiura, K. Hatada, *Polym. Bull.* **32**, 155 (1994)
- 120) S. Nemes, J. P. Kennedy, *J. Macromol. Sci., Chem.* **A28**, 311 (1991)
- 121) R. Nomura, M. Narita, T. Endo, *Macromolecules* **27**, 4853 (1994)
- 122) M. J. M. Abadie, F. Schue, T. Souel, D. B. Hartley, D. H. Richards, *Polymer* **23**, 445 (1982)
- 123) S. Hadjikyriacou, Z. Fodor, R. Faust, *J. Macromol. Sci., Chem. Pure Appl. Chem.* **A32(6)**, 1137 (1995)
- 124) J. Feldthusen, B. Iván, A. H. E. Müller, J. Kops, *Macromol. Reports* **A32**, 639 (1995)
- 125) J. Feldthusen, B. Iván, A. H. E. Müller, J. Kops, *Macromol. Symp.* **107**, 189 (1996)
- 126) M. K. Mishra, "Macromolecular Design: Concept and Practice", Polymer Frontiers International, Inc.: New York 1994
- 127) J. P. Kennedy, V. S. C. Chang, R. A. Smith, B. Iván, *Polym. Bull.* **1**, 575 (1979)

- 128) B. Iván, J. P. Kennedy, V. S. C. Chang, *J. Polym. Sci. Polym. Chem. Ed.* **18**, 3177 (1980)
- 129) J. P. Kennedy, M. Hiza, *Polym. Bull.* **10**, 146 (1983)
- 130) J. Feldthusen, Diploma, Mainz/Lyngby 1994
- 131) S. Hadjikyriacou, R. Faust, *PMSE Prepr. (Am. Chem. Soc., PMSE Div.)* **76**, 300 (1997)
- 132) Y. C. Bae, Z. Fodor, R. Faust, *Macromolecules* **30**, 198 (1997)
- 133) A. Yamagishi, M. Szwarc, L. Tung, G. Y.-S. Lo, *Macromolecules* **11**, 607 (1978)
- 134) R. P. Quirk, *Makromol. Chem., Macromol. Symp.* **63**, 259 (1992)
- 135) J. J. Ma, R. P. Quirk, *J. Polym. Sci. Part A: Polym. Chem.* **26**, 2031 (1988)
- 136) A. Hirao, I. Hattori, T. Sasagawa, K. Yamaguchi, S. Nakahama, N. Yamazaki, *Makromol. Chem., Rapid Commun.* **3**, 59 (1982)
- 137) N. R. Legge, *Rubber Chem. Technol.* **60**, G83 (1987)
- 138) K. Hatada, T. Nishiura, T. Kitayama, M. Tsubota, *Polymer Bull.* **36**, 399 (1996)
- 139) K. Antolin, J.-P. Lamps, P. Rempp, Y. Gnanou, *Polymer* **31**, 967 (1990)
- 140) J. S. Wang, R. Jérôme, P. Teyssié, *J. Polym. Sci., Polym. Chem. Ed.* **30**, 2251 (1992)
- 141) B. H. Zimm, R. W. Kilb, *J. Polym. Sci.* **37**, 19 (1959)
- 142) E. Malmström, A. Hult, *J. Macromol. Sci., Rev. Macromol. Chem. Phys.* **C37**, 555 (1997)
- 143) V. Efstratiadis, G. Tselikas, N. Hadjichristidis, J. Li, Y. Wan, J. W. Mays, *Polym. Int.* **33**, 171 (1994)
- 144) R. F. Storey, K. A. Shoemake, B. J. Crisholm, *J. Polym. Sci., Part A: Polym. Chem.* **34**, 2003 (1996)
- 145) H. Eschwey, W. Burchard, *Polymer* **16**, 180 (1975)
- 146) C. Tsitsilianis, P. Lutz, S. Graff, J. P. Lamps, P. Rempp, *Macromolecules* **24**, 5897 (1991)
- 147) G. Odian, "*Principles of Polymerization*", 3rd, Wiley-Interscience, New York 1991
- 148) F. S. Bates, G. H. Frederickson, *Ann. Rev. Phys. Chem.* **41**, 525 (1990)
- 149) J. M. Yu, Y. S. Yu, P. Dubois, R. Jérôme, *Polymer* **38**, 2143 (1997)
- 150) Y. S. Yu, P. Dubois, P. Teyssié, R. Jérôme, *Macromolecules* **30**, 7356 (1997)
- 151) D. Li, R. Faust, *Macromolecules* **28**, 4893 (1995)
- 152) R. F. Storey, B. J. Crisholm, M. A. Masse, *Polymer* **37**, 2925 (1996)
- 153) K. Prochazka, T. J. Martin, P. Munk, S. E. Webber, *Macromolecules* **29**, 6518 (1996)
- 154) S. Creutz, J. Stam, F. C. Schryver, R. Jérôme, *Macromolecules* **31**, 681 (1998)
- 155) S. Förster, M. Zisenis, E. Wenz, M. Antonietti, *J. Chem. Phys.* **104**, 9956 (1996)
- 156) Z. Tuzar, P. Kratochvil, *Adv. Colloid Interface Sci.* **6**, 201 (1976)
- 157) F. L. Baines, S. P. Armes, N. C. Billingham, Z. Tuzar, *Macromolecules* **29**, 8151 (1996)
- 158) R. Xu, M. A. Winnik, F. R. Hallet, G. Riess, M. D. Croucher, *Macromolecules* **24**, 87 (1991)
- 159) T. N. Khan, R. H. Mobbs, C. Price, J. R. Quintana, R. B. Stubbersfield, *Eur. Polym. J.* **23(3)**, 191 (1987)
- 160) J. R. Dorgan, M. Stamm, C. Toprakcioglu, R. Jérôme, L. J. Fetters, *Macromolecules* **26**, 1825 (1993)
- 161) L. Zhang, H. Shen, A. Eisenberg, *Macromolecules* **30**, 1001 (1997)
- 162) J. Selb, Y. Gallot, *Makromol. Chem.* **182**, 2523 (1981)
- 163) Z. Tuzar, P. Kratochvil, K. Prochazka, P. Munk, *Collect. Czech. Chem. Commun.* **58**, 2362 (1993)
- 164) O. Kramer, "*Biological and Synthetic Polymer Networks*", Elsevier: London 1988
- 165) A. H. Clark, S. B. Ross-Murphy, *Adv. Polym. Sci.* **83**, 60 (1983)
- 166) M. Shibayama, T. Tanaka, *Adv. Polym. Sci.* **109**, 1 (1993)
- 167) P. J. Flory, *Disc. Farad. Soc.* **57**, 1 (1974)
- 168) A. B. Clayton, T. V. Chirila, X. Lou, *Polym. Int.* **44**, 201 (1997)
- 169) B. Iván, J. P. Kennedy, P. W. Mackey, in "Polymeric Drugs and Drug Delivery Systems", Eds., R. L. Dunn and R. M. Otterbrite, ACS Symp. Ser. **469**, 203, Am Chem. Soc., Washington, D. C. (1991)
- 170) B. B. Bonvin, M. M. Bertorello, *Polym. Bull.* **32**, 69 (1994)
- 171) M. Mulder, "*Basic Principles of Membrane Technology*", Kluwer Academic Publishers: Dordrecht / Boston / London 1992
- 172) J. P. Kennedy, M. Hiza, *J. Polym. Sci., Polym. Chem. Ed.* **21**, 1033 (1983)
- 173) B. Wang, M. K. Mishra, J. P. Kennedy, *Polym. Bull.* **17**, 205 (1987)

- 174) M. K. Mishra, B. Wang, J. P. Kennedy, *Polym. Bull.* **17**, 307 (1987)
- 175) H. Everland, J. Kops, A. Nielsen, B. Iván, *Polym. Bull.* **31**, 159 (1993)
- 176) H. Pasch, B. Trathnigg, "*HPLC of Polymers*", Springer-Verlag: Berlin / Heidelberg 1998
- 177) D. Jamois, M. Teyssié, E. Marechal, *J. Polym. Sci. Part A: Polym. Chem.* **31**, 1923 (1993)
- 178) L. Wilczek, J. P. Kennedy, *J. Polym. Sci. Polym. Chem. Ed.* **25**, 3255 (1987)
- 179) L. Wilczek, J. P. Kennedy, *Polym. Bull.* **17**, 37 (1987)
- 180) L. V. Nielsen, Diploma, Lyngby 1995
- 181) Y. C. Bae, Z. Fodor, R. Faust, *ASC Symp. Ser. in press* 1997
- 182) B. Charleux, M. Moreau, J. P. Vairon, S. Hadjikyriacou, R. Faust, "*Model kinetic study of titanium tetrachloride ionization of polyisobutylene capped with diphenylethylene. Application to the synthesis of block copolymers*", International Symposium on Ionic Polymerization, Paris (1997)
- 183) R. Faust, *Private communication* (1997)
- 184) S. Hadjikyriacou, R. Faust, *Macromolecules* **28**, 7893 (1995)
- 185) T. Ohmura, M. Sawamoto, T. Higashimura, *Macromolecules* **27**, 3714 (1994)
- 186) R. S. Yost, C. R. Hauser, *Am. Soc.* **69**, 2325 (1947)
- 187) J. Brandrup, E. H. Immergut, "*Polymer Handbook*", Wiley: New York 1989
- 188) H. Sawada, "*Thermodynamics of Polymerization*", Dekker: New York 1976
- 189) R. Waack, M. A. Doran, *J. Phys. Chem.* **67**, 148 (1963)
- 190) Y. Okamoto, T. Takeda, K. Hatada, *Chem. Lett.*, 757 (1984)
- 191) A. H. E. Müller, Dissertation, Mainz 1976
- 192) S. E. Thomas, "*Organic Synthesis. The Roles of Boron and Silicon*", Oxford Science Publications: Oxford 1991
- 193) C. B. Chapman, *J. Polym. Sci.* **45**, 237 (1960)
- 194) D. Hunkeler, M. Janco, D. Berek, *ACS Symp. Ser.* **635**, 250 (1995)
- 195) H. Much, *Private communication* (1998)
- 196) D. W. Schwark, Dissertation, Amherst 1992
- 197) Z. Fodor, R. Faust, *J. Macromol. Sci., Pure Appl. Chem* **A32**, 575 (1995)
- 198) J. Brandrup, E. H. Immergut, "*Polymer Handbook*" 1966
- 199) J. L. Price, Dissertation, Akron 1993

Acknowledgments

I wish to thank....

....Prof. Dr. A. H. E. Müller for the chance to perform my Ph.D. at the University of Mainz and for his valuable supervision during my Ph.D. project in every respect.

....Prof. Dr. B. Iván for initiating this project and for his valuable supervision during my Ph.D. project in every respect.

....Prof. Dr. R. Faust for helpful and interesting discussions during my Ph.D. project and the supply of different tailored materials.

....Dr. H. Schuch, Dr. T. Frechen, Dr. D. Urban, Dr. K. Mattauer, Dr. Gerst, Dr. Rossmannith at the BASF AG for a good corporation regarding characterization and discussion of the results related to amphiphilic block copolymers in aqueous media.

....Dr. T. Pakula for his help regarding SAXS and stress-strain measurements of thermoplastic elastomers and for the discussion of the results.

....Prof. Dr. T.E. Hogen-Esch, Dr. W. Batsberg, and Dr. T. Ishizone for SEC measurements of N,N-dimethylacryl amide samples.

....Dr. S. Förster for DLS and SANS measurements of amphiphilic block copolymers in aqueous media.

....Dr. Andrea Müller for her help regarding dynamic mechanical analyses and stress-strain measurements of thermoplastic elastomers.

....R. Würfel and Dr. I. G. Voigt-Martin for their help regarding TEM analyses of thermoplastic elastomers.

....Dr. H. Much for his advice regarding HPLC under critical conditions.

....J. Ludwig for his help when new glass equipment was needed and for the repair of broken glass apparatus.

....P. Blumers and N. Gilbert for their experimental help during this project.

....all the present and former colleagues in the working group for helpful discussions and a pleasant time at the university.

Curriculum Vitae

Name: Jesper Feldthusen Jensen
Born: 24.05. 1970
Location: Torsted, Horsens in Denmark.
Nationality: Danish

Address:

Hans-Boeckler Str. 7A, D-55128 Mainz, Germany
(*Permanent address*: Jupitervej 11 Brejning, DK-7080 Boerkop, Denmark)

Education:

1976 - 1986: Primary school (Gauerslund, Denmark)
1986 - 1989: High school (Vejle, Denmark)
Oct. 1989: Technical University of Denmark (Lyngby), Studies in chemistry
Sept. 1994: Master in Chemical Engineering. Title of Master Thesis: "Polymers for biomedical applications prepared by a combination of living cationic and living anionic polymerization". The experimental work for the thesis was performed in Mainz at the Institute of Physical Chemistry.
Instructors: Professor Béla Iván, Professor Jørgen Kops, and Professor Axel H. E. Müller.
Oct. 1994 - June 1998: University of Mainz: Ph.D. study. Title of thesis: "Synthesis of tailored polymer structures by living cationic and living anionic polymerizations".
Instructors: Professor Axel H. E. Müller and Professor Béla Iván.